CONF-7805211--

COO-3904-1

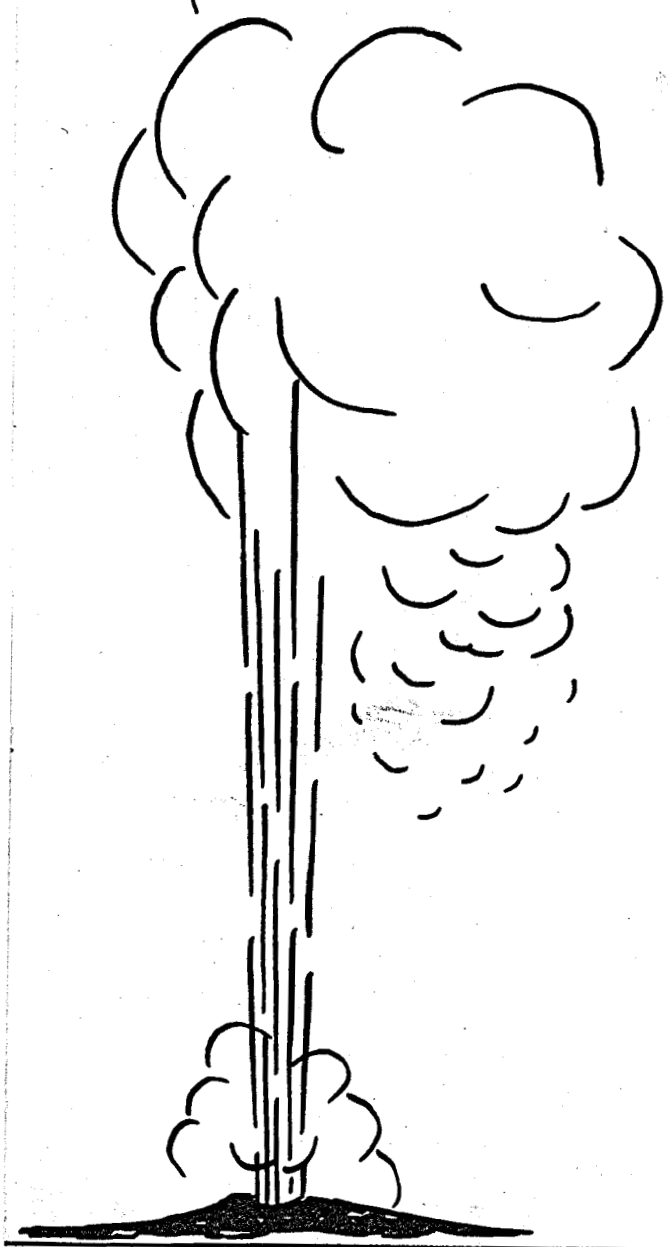

# GEOTHERMAL SYSTEMS MATERIALS: A WORKSHOP/SYMPOSIUM

Proceedings, May 23—25, 1978

Work Performed Under Contract No. EG-77-C-04-3904

Radian Corporation
Austin, Texas



U. S. DEPARTMENT OF ENERGY
Geothermal Energy

## DISCLAIMER



Available from the National Technical Information Service, U. S. Department of Commerce, Springfield, Virginia 22161.

Price: Paper Copy $18.00
Microfiche $3.50

COO-3904-1
Distribution Categories UC-66 and UC-66d

# GEOTHERMAL SYSTEMS MATERIALS: A WORKSHOP/SYMPOSIUM

# PROCEEDINGS

Arranged by:

RADIAN CORPORATION
8500 Shoal Creek Blvd.
Austin, Texas 78766

Under Contract EG-77-C-04-3904

Lakeway Inn, Austin, Texas
23-25 May 1978

## DISCLAIMER

# INTRODUCTION

The Workshop/Symposium on Materials in Geothermal Energy Systems was held at Lakeway Inn, Austin, Texas, during May 23-25, 1978. It was sponsored by the U.S. Department of Energy, Division of Geothermal Energy (DOE-DGE) as a part of DOE's continuing technology transfer program. The meeting was organized and conducted by Radian Corporation, under DOE Contract No. EG-77-C-04-3904.

The purpose of the Workshop/Symposium was to provide a forum for the exchange of ideas and information on recent developments affecting the reliability and applicability of materials for energy extraction from geothermal fluids. More than 60 participants from government, industry, and academia used the meeting to discuss the development status of geothermal energy efforts and the direction of long- and short-term geothermal energy goals.

During the course of the meeting, 15 technical papers were presented on a variety of topics pertaining to geothermal materials problems. Attendees rotated among five discussion groups, whose topics included corrosion, failure analysis, fluid chemistry, non-metallic materials, and materials selection. Discussion emphasis centered on identification of materials problems, research results and newly found solutions, development status, and identification of areas requiring work.

These Proceedings are comprised of copies of the participating authors' papers (as received) and summaries of topics discussed in each of the five discussion groups. A list of attendees is also included.

TABLE OF CONTENTS

TABLE OF CONTENTS (Continued)

# WORKSHOP/SYMPOSIUM ON MATERIALS IN GEOTHERMAL ENERGY SYSTEMS

## Symposium Schedule

Monday Afternoon, May 22
Registration

Tuesday Morning, May 23
Registration

Welcome, W. N. KOCUREK, Radian Corporation

DOE-DGE Welcome, ROBERT R. REEBER, DOE

Keynote Address: Materials Progress at Cerro Prieto, Mexico - ALFREDO MAÑON MERCADO, Comision Federal de Electricidad

Materials Selection for Sealed and Unsealed Rolling Cone Geothermal Bits - R. R. HENDRICKSON,* A. H. Jones, and R. W. Winzenried, Terra Tek, Inc.

A Nondestructive Evaluation Technique for Detecting the Incipient Failure of Drill Pipes Used in Geothermal Well Drilling - L. L. YEAGER and A. A. Hochrein, Jr., Daedalean Associates, Inc.

Tuesday Afternoon, May 23

Materials Problems Encountered in Sperry's Down Hole Geothermal Pump Program - H. B. MATTHEWS and W. D. McBee, Sperry Rand Corporation

Materials Selection for Geothermal Steam Turbines - JOSEPH A. CAMERON, Elliott Company

*Speaker indicated in all capitals

Summary of First 12 Months Progress on Geothermal Elastomeric Materials Program, A. R. HIRASUNA, L'Garde, Inc.

Workshop 1

- Corrosion
  Discussion Leader: R. L. Miller, EG&G Idaho, Inc., INEL
- Failure Analysis
  Discussion Leader: A. D. Thomas, Radian Corporation
- Fluid Chemistry
  Discussion Leader: D. W. Shannon, Batelle Pacific Northwest Laboratory
- Non-Metallic Materials
  Discussion Leader: P. E. Cassidy, Texas Research Institute, Inc.

Wednesday Morning, May 24

Development of a Cavitating Descaling Technique for Geothermal Scale Removal - F. Graham and A. A. HOCHREIN, JR., Daedalean Associates, Inc.

Corrosion Research on Geothermal Systems at SRI International - D. D. MACDONALD and B. C. Syrett, SRI International

Corrosion Testing in a Multiple-Stage Flash System - R. D. McCRIGHT and R. E. Garrison, Lawrence Livermore Laboratory

Hydrogen Sulphide Stress Corrosion Cracking in Materials for Geothermal Power - A. R. TROIANO and R. F. Hehemann, Case Western Reserve University

Workshop 2

Today's Workshop topics are the same as Tuesday's.

Wednesday Evening, May 24

Workshops 3 and 4

These Workshop topics are the same as Tuesday's.

Thursday Morning, May 25

East Mesa Geothermal Component Test Facility - K. L. NEWMAN, Westec Services, Inc.

Materials for Use in Corrosive Geothermal Brine Environments - F. X. McCAWLEY, J. P. Carter, and S. D. Cramer, U. S. Bureau of Mines

In-Situ Protection of Metals Against Corrosion and Scaling in Hot Brines - S. B. BRUMMER, EIC Corporation

Workshop 5

- Materials Selection

  Discussion Leader: R. R. Reeber, DOE-DGE

Thursday Afternoon, May 25

Polymer Concrete Materials for Geothermal Processes - L. E. Kukacka and MEYER STEINBERG, Brookhaven National Laboratory

Some Observations on Materials Problems in Nonelectric Utilization of Geothermal Energy - GENE CULVER, Geo-Heat Utilization Center, Oregon Institute of Technology

Panel Discussion by Workshop Leaders

Closing Comments - MARSHALL CONOVER, Radian Corporation

# SYMPOSIUM PAPERS

# MATERIAL PROGRESS AT CERRO PRIETO, MEXICO

by

Alfredo Manon Mercado
Comision Federal de Electricidad
Coordinadora Ejecutiva de Cerro Prieto

## SUMMARY

A brief general description is presented about the principal problems observed on the materials used in the Cerro Prieto geothermal project. These include those problems that have been observed in drill pipes, well casing separation equipment and conduction pipes for geothermal water and steam as well as the problems observed in geothermal power plant materials.

## OBSERVED MATERIAL PROBLEMS DURING DRILLING OF GEOTHERMAL WELLS

The main material failure problem that occurs during drilling of geothermal wells has been the breakage of drill pipes. This can have various explanations such as tubing fatigue, excessive strain during drilling and probably intergranular corrosion. Heavy economic losses and in some cases the partial loss of the well, have occurred because of the failures observed. In some cases it has been necessary to deviate the well in order to continue drilling.

These failures necessitate fishing operations. The cost of these is around $4,000 per day, with a variation on the fishing period of from 2 to 30 days.

The effects on the constructive characteristics and final well quality are revealed during the heating, development, and production stages.

The formation alterations due to physical and chemical effects caused by long periods of contact between drilling mud and certain type of formations (shales), produces nonuniform holes. This makes cementation difficult or leaves the well in bad condition, so that after the heating and elongation of the casing, tube-cement separation can easily occur. This leaves the tubing in contact with the geological formation. The possibility for corrosion and mechanical failures due to stress corrosion during heating and cooling are higher.

Regular inspections of the drill pipe are recommended in order to lessen fracture possibilities and to detect microfractures or intergranular corrosion. These can be produced during material exposure to an environment with a high content of $H_2S$ under elevated tension efforts and high stress.

## OBSERVED MATERIAL PROBLEMS IN SURFACE AND PRODUCTION CASING

One of the first problems observed in well casings was found on the surface where surface casing and production casing are in contact. It is important to pack and try to avoid any air admission and salty water into the annular space of both tubings. Corrosion could have been galvanic or crevice, or a combination of these two. After such experience, we have avoided any surface contact of these tubings, thus solving the problem.

Other important problems detected in the Cerro Prieto geothermal wells was the frequent failure in casing. Three principal types of failures have occurred: collapses, casing or joint failure and wall thinning due to corrosion, (interior and exterior, or both).

The following explanation about casing collapse has been one of the most accepted: During the cement-water mixture for cementation, certain water amount remains without mixing, remaining trapped in the annular space, between surface casing and production casing. When cement hardening is complete and the well comes into production, the trapped water heats, producing high pressure and causing collapse.

This problem has been solved by using higher resistance well casing and by improving the cement-water conditions during cementation. Casing breakage detected in some wells was explained by the combination of a poor cementation job, and a low resistance of the casing used.

Solutions to this problem have included using higher grades such as N-80, changing the joint type to Hydrill, and improving the cementation job. In some cases where difficient cementation is present, sand instead of cement has to be used between production and surface casing; it has been observed that squeezing operations were not satisfactory. This procedure has shown good results, but further testing is necessary.

Two methods have been used to detect the presence of failures and corrosion in production casing. The first method uses lead seals that allow us to observe the kind of failures occurring (collapse, joint breakage or failure). The other method uses depth caliper electric logs to detect thinning in the production casing due to corrosion effects. Such corrosion has been confirmed in the well reworking operations, during which samples have been recovered from small parts of casings that suffered thinning by corrosive effects.

This problem has not yet been totally solved, and it is considered to be the one of greatest importance in Cerro Prieto. It is known that good cementation operations help avoid excessive rates of external corrosion.

Interior corrosion can be reduced by putting the well in production as soon as it is completed, since at low temperatures the corrosive effects of $H_2S$ are higher. In order to solve corrosion problems, it is also recommended that the feasibility of utilizing cathodic protection in the geothermal wells be evaluated.

## OBSERVED MATERIAL PROBLEMS IN THE CONDUCTION OF GEOTHERMAL FLUIDS

One of the most common material problems discovered in the early stages of the exploitation of the Cerro Prieto geothermal field, was erosion. This occurred in the pipe elbows between each well and the water steam separator. It is attributed to high fluid velocities and to the presence of sand in small quantities. The problem was solved using "T" shaped fittings instead of elbows. This produced a hydraulic cushion in the solid particles, thus minimizing erosion. Before connecting a new well to the water steam separator, the well flows freely in the atmosphere for a period that varies from 5 to 10 days in normal cases. This allows time for the mixture contents of sand to decrease to low values and allows the sending of the mixture to the water steam separator.

For protection of the water steam separator against overpressure, safety valves were used in the first stage. Small vapor leakage occurred in the seats, causing corrosion problems in the protective s.s. 316 elbow that ruined the valves. It was decided to use rupture disks instead of safety valves. These are protected from the atmospheric environment (saline), and have given good results up to this date.

The formation of deposits on the interior of the casing on the Cerro Prieto wells has previously been described by Mercado and Guiza (7). The formation incrustations in the casing produce a gradual reduction of the well capacity. Faster incrustation has been observed in wells with lower enthalpies, where $CaCO_3$ is predominant. However, in wells with high quality enthalpy, lower incrustation velocities, $S_iO_2$ predominates in the composition of the scale.

In general, a well with a low enthalpy of 320 cal/g reduces its production to 50% in 5 years (M-5) due to scaling. However, wells with 260 to 280 cal/g enthalpies reduce their production to 50% in a period of 6 months. Various methods have been tested to clean these incrustations. We are currently using only mechanical cleaning with conventional drilling equipment, though with less capacity of those used in drilling works. In order to perform this work, the well must be "killed." This is done by cooling it slowly to avoid fractures in the tubing caused by tension. The cooling process consists of reducing the flow to zero and subsequently further cooling by water injection. Periodic temperature logs monitor the thermic charges. In 1978 the average cost to clean a well was $35,000.00.

Another very common problem at Cerro Prieto is the formation of silica scale in the seats of the control water valves. These are installed in piping that conduct hot brine. This scale does not permit the valves' operation. It is frequently necessary to stop the operation. This permits a consequent corrosion problem in the separators caused by air admission.

In order to solve or lessen this problem, another type of valve is presently being tested.

Another corrosion problem exists in piping stems that show small leaks due to a poor seal in the gasket system. This problem has been avoided by using valves with a more efficient gasket system, and an adequate maintenance program.

In general terms, scale formation in the interior piping and its cleaning does not represent a serious problem, nor does it significantly increase the cost of the Cerro Prieto wells. However, piping failures in fact has been a serious problem. In the last 5 years that the field has been in operation, repairs due to fractures or collapses in seven wells have been made with an average cost of $180,000 per well.

Scale in water-steam separators has not been a serious problem. Cleaning is carried out when one of the turbines is stopped for maintenance. This is done on the average of once every 18 months. Cleaning is done mechanically, using common hand tools.

In line pipes to the evaporation pond, a slow but gradual scaling incrustation has occurred. The thickness increases in proportion to pressure and temperature drops, to maximum values of 2 cm. in 5 years.

In order to perform cleaning in piping, tests have been carried out with water blasting at high pressure, by chemical methods using sodium hydroxide and cavitation cleaning methods and cleaning bullets. Results from oil addition tests are also being evaluated as a means of scale prevention.

The estimated costs to apply these methods vary from $6 to $12 per meter in an 8" diameter pipe, assuming cleaning is required every three to five years.

Another materials problem observed during the first four years of well operation was wood deformation and degradation in the silencer chimney installed for each well. After testing the endurance of fiber glass resin polyester, it was decided to replace the wood chimney with polyester. Good results after two years of operation have been obtained.

## OBSERVED PROBLEMS AT THE GEOTHERMAL POWER PLANT (2 Units - 37.5 MW)

During 1968 and 1969 a large number of corrosion tests were performed in order to choose the materials for the first geothermal plant to operate in America under a liqui-dominated geothermal field. The results that were obtained have been published by various authors. The materials that were chosen were reliable enough, with the exception of the aluminium selected for the heat exchanger. This was used to cool the oil and hydrogen at the power plant. It showed a high degree of pitting in condensed steam.

### Turbine Deposits

It was observed during the plant's first years of operation (1973, 1974) that deposits were formed in the first stages of the turbine blades, which produced a gradual reduction of the turbine capacity. Due to this, it was necessary to clean the blades every year and carry out a general maintenance of the plant.

After modifications were made to the water-steam separators, this step of the process improved and the maintenance interval was extended to 18 months. This increased the plant operation factor up to a 1977 value of 90%.

## Circulation Channel of Cooling Water

Since plant operation was initiated, it has been observed that the reinforced concrete used in the circulation channels of cooling water to the cooling tower has suffered damage that occurs primarily in the upper part of the channel. At this point there is no water contact with the surface, only steam and gas.

A partial solution to this problem has been to apply a coal tar epoxy coating to the surface of the concrete.

## Cooling Water

It was observed during the first months of the plant operation that the cooling water pH was decreasing rapidly, and at the same time the sulfate content was increased because of the presence of bacteria*. Biocides have given good results for controlling these pH changes.

## Cooling Tower

Slight degradation has been observed in the wood of the cooling tower, mainly in the upper part of the spray zone, and in the zone where the water level varies. During maintenance shutdowns, the wood is treated with bactericides and algacides.

## Carbon Steel Valves and Barometric Legs

The carbon steel valves used in cooling water line pipes showed an excessive amount of corrosion as well as carbon steel piping on their last stage of intercondensers. This has been corrected using stainless and epoxy resin reinforced with fiber glass.

*Acromobacter, Acrobacter, Bacillus, Proteus, Desulfovibrio, Pseudomonas, Flavobacteria

REFERENCES

1. Manon M. Alfredo - "Corrosion Problems at the Cerro Prieto Geothermal Project". Workshop on materials problems associated with de development of geothermal energy. El Centro, California. 16-18 May 1977.

2. Toney S., Cohen M., Mercado S., Manon A. - "Observations on materials exposed to geothermal steam at Cerro Prieto". Corrosion/78, Nat'l Assoc. of Corrosion Engrs Symposium, Houston, Texas, March 6-10, 1978.

3. Mercado G. Sergo - "Cerro Prieto Geothermoelectric Project: Pollution and Basic Protection". Second United Nations Symposium on the Development and Use of Geothermal Resources. San Francisco, California, USA. 20-29 May, 1975.

4. Tolivia M.E., "Corrosion Measurements in a Geothermal Environment" 1970, U.N. Symposium on the Development and Utilization of Geothermal Resources, Pisa.

5. Tolivia M.E. - "Corrosion of Turbine Materials in Geothermal Steam Environment in Cerro Prieto, Mexico". Second U.N. Symposium on the Development and Use of Geothermal Resources. San Francisco, California, USA. 20-29 May, 1975.

6. Mercado G. Sergio - "Corrosion by Geothermal Fluids in Cerro Prieto, B.C.N. Mexico". Corrosion/78. National Association of Corrosion Engineers Symposium, Houston, Texas. March 6-10, 1978.

7. Mercado G. Sergio and Guiza J. - "Problems of Silica Scaling at Cerro Prieto Geothermal Power Station" Scale Management in Geothermal Energy Development. San Diego, Calif. USA. 1976.

8. Harco Corp. "Detailed Corrosion Survey" Comisión Energía Geotérmica - Six Geothermal Well Casings. El Campo Geotermico de Cerro Prieto - March 1969". A Study prepared for C.F.E. - C.F.E. Files.

# MATERIALS SELECTION FOR SEALED AND UNSEALED ROLLING CONE GEOTHERMAL BITS

by

R. R. Hendrickson, A. H. Jones,
and
R. W. Winzenried
Terra Tek, Incorporated
420 Wahara Way
Salt Lake City, Utah 84108

Geothermal drilling is done almost exclusively with rolling-cutter bits and other conventional drilling equipment developed for oil and gas recovery. The objective of Terra Tek's program with the Department of Energy/Division of Geothermal Energy is the hastening of the commercial availability of geothermal drill bits having significantly longer life in severe applications such as the Geysers.

## AIR DRILLING WITH UNSEALED BITS

The life of conventional unsealed bits may or may not be shortened when drilling with mud or water in a geothermal reservoir, depending on the bottom-hole (not formation) temperature. Air drilling usually results in a comparatively short life due to inadequate cooling and higher detritus velocities, but does not quench steam vents, plug the producing formation, nor alter the formation temperature. The predominant bit failure modes at the Geysers are bearing wear and loss of gage, i.e., diameter. Bearing life is shortened by frictional heat, which acts in concert with the high bottom-hole temperature to cause annealing of the races, cones, and balls; reduced bit weighting is employed to extend bearing life. Detritus erosion of the gage-cutting area of the cones is increased by the use of lighter bit weighting, because more particles are generated per foot of hole drilled. Thus, gage wear is partially a result of the bearing life problem.

## EXPERIMENTAL UNSEALED BITS

It was the consensus of the drillers and bit manufacturers that there was no significant temperature-induced alteration of the drillability of the Franciscan graywacke, thus, no bit geometry changes were contemplated. The unsealed bit program was structured to:

1. Characterize essential materials properties for each bit component (Table 1).
2. Locate materials and select carburizing and heat treating specifications to maintain these properties in the geothermal environment (Figure 1).
3. Construct experimental bits and conduct full-scale drilling tests in the laboratory and field (Figures 2, 3 and 4) to verify materials performance.

Figure 2 details the Drilling Research Laboratory, used to evaluate experimental bits. Figure 3 depicts the Geothermal Wellbore Simulator, a large 5000 psi pressure vessel capable of temperatures to 350°C, which was used to evaluate conventional bits and two generations of experimental bits.

The air-drilling test facility (Figure 4) will be used to test the third-generation bits; this system provides a circulating fluid (air) to purge the bearings and remove cuttings.

## RESEARCH FOR SEALED AND LUBRICATED BITS

Sealed bits offer better overall economy in non-geothermal situations, but the lack of a high-temperature seal and lubricant has limited their usefulness in geothermal drilling. They can be used for mud drilling into hot formations with limited

TABLE 1. Minimal Materials Property Requirements for Geothermal Bit Components Capable of 20°C to 300°C Operation.

| COMPONENT | SURFACE HARDNESS | CORE 0.2% YIELD KSI | FRACTURE TOUGHNESS $K_{Ic}$ MPa$\sqrt{m}$ |
|---|---|---|---|
| Lug | $R_C$56 | 150 | 95 |
| Friction-Pin Facing | $R_C$59 | - | - |
| Cones | $R_C$42 | 80 | 90 |
| Rollers | $R_C$50† | 250 | 30, 21* |
| Balls | $R_C$50† | 250 | 30, 21* |
| Nose Bushing | $R_A$89† | 450** | 10 |
| Driver Inserts | $R_A$87.5† | 400** | 13 |
| Gage Inserts | $R_A$89† | 350** | 13, 11* |

*Indicates best attainable with MK-III Materials
†Indicates homogeneous material
**Transverse rupture strength

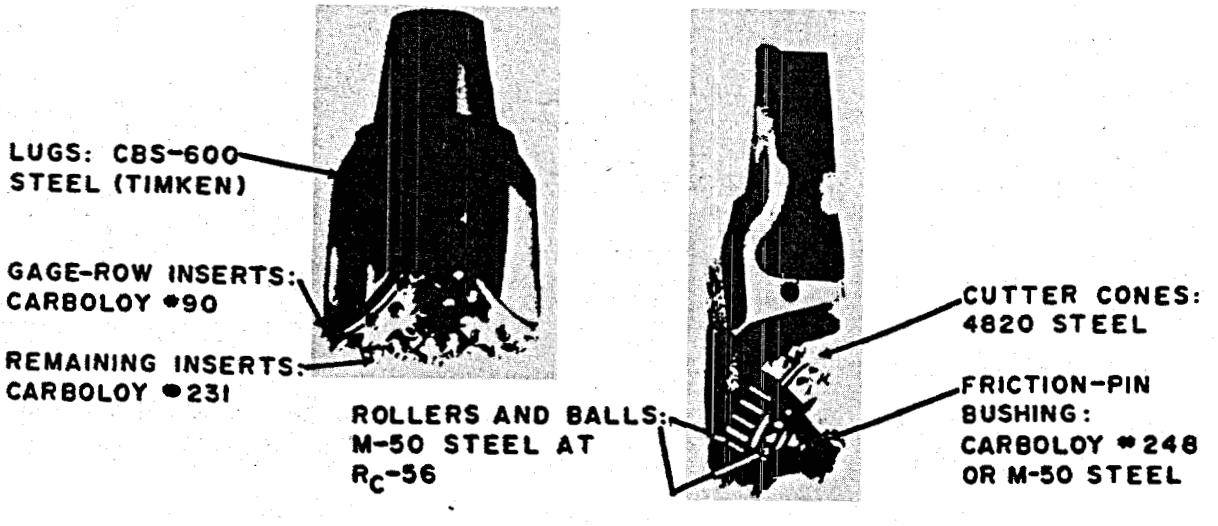


FIGURE 1. Materials Selected for Third Generation of Experimental Unsealed Bits.

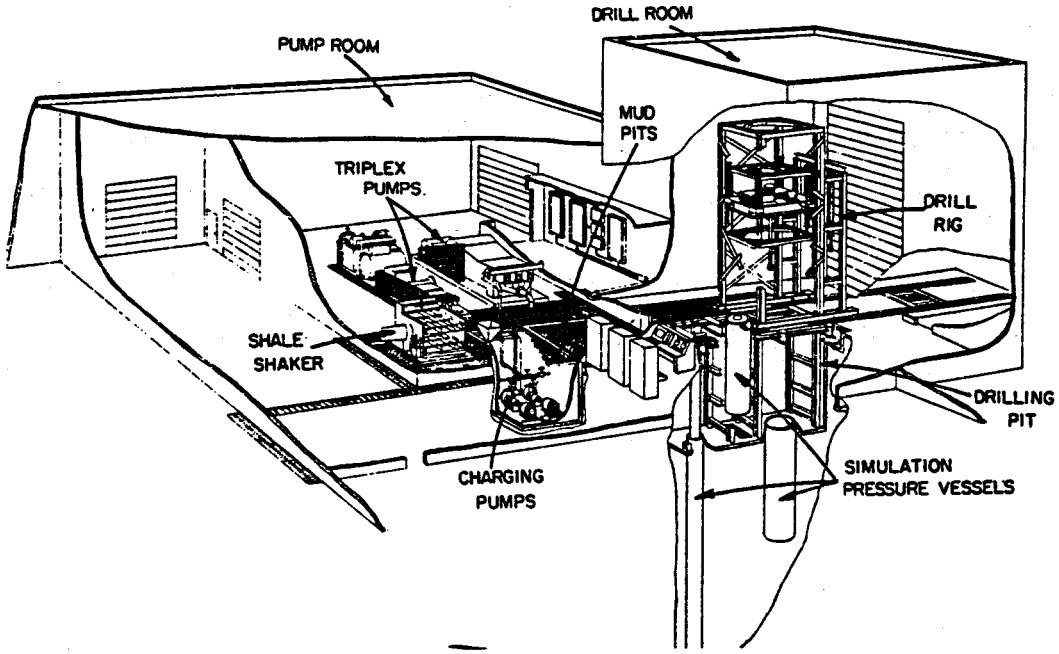


FIGURE 2. Drilling Research Laboratory

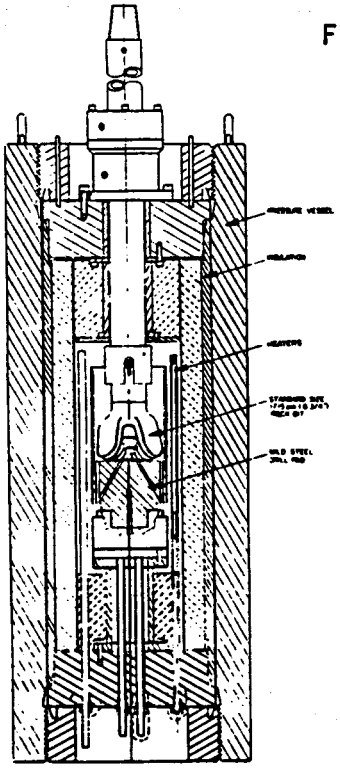

FIGURE 3. Geothermal Wellbore Simulator

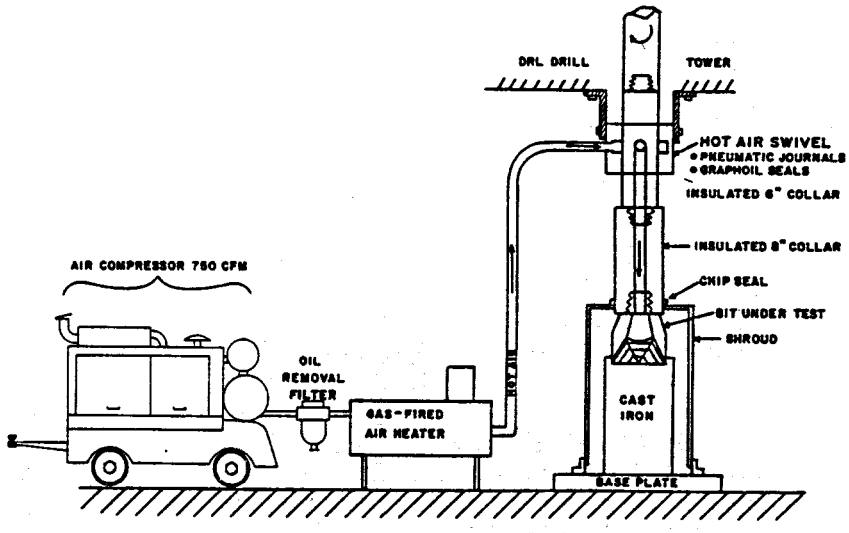


FIGURE 4. Geothermal Air-Drilling Test Facility

life, and are seldom used in air drilling. The sealed bit effort was therefore directed at development of an improved seal and at the testing of lubricants under simulated geothermal drilling conditions. The seal testing machine (Figures 5 and 6) duplicates the temperature, pressures, mechanical eccentricities and abrasiveness experienced in drill bit cones. Typical test conditions include ±0.03 inches of stroke, ±0.007 inches of wobble, Geysers abrasives, 2,500 psi absolute and ±50 psi differential.

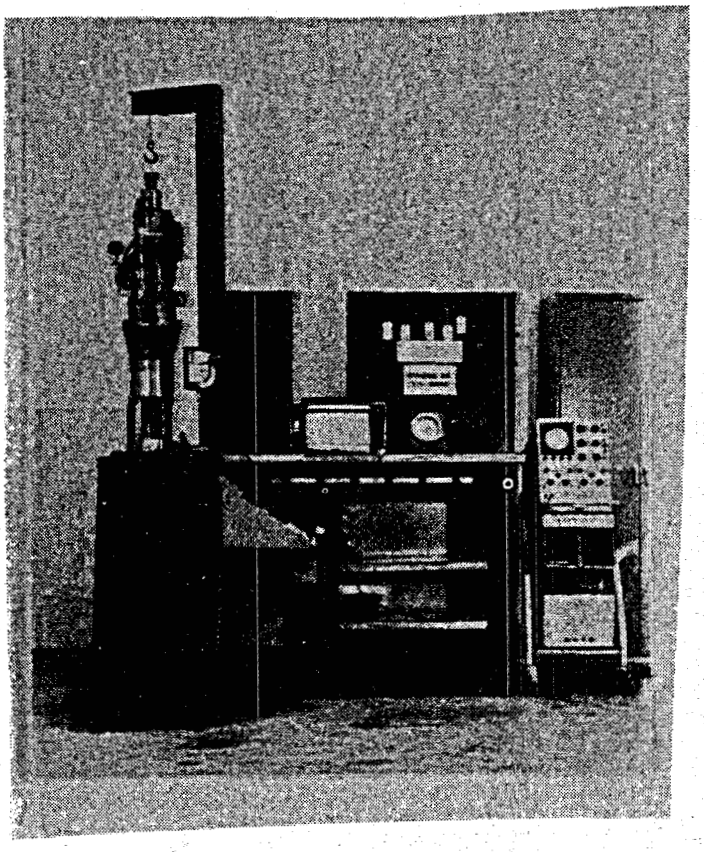

FIGURE 5. Seal Test Facility

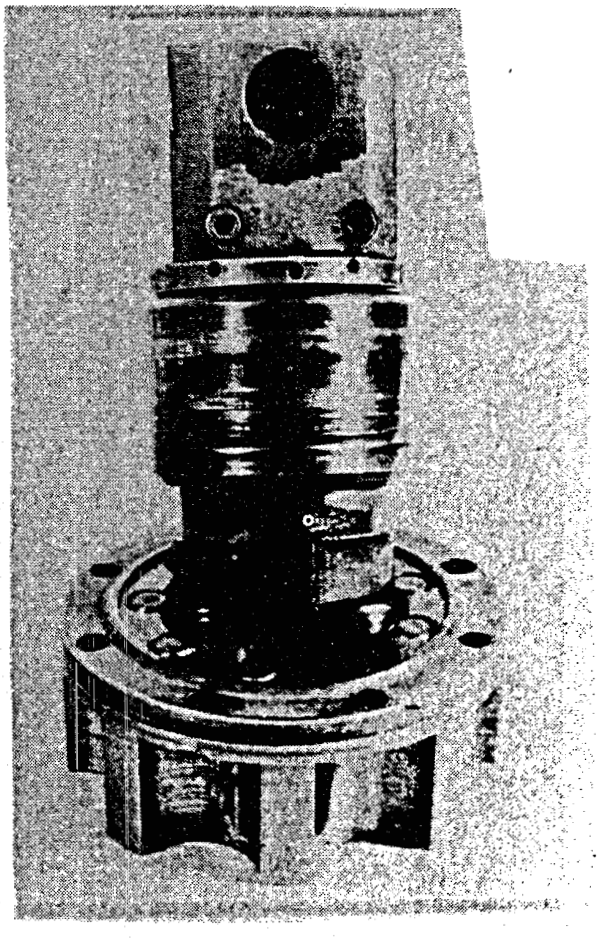

FIGURE 6. Bit Lug Simulator and Pin Cup Assembly

The lubricant tester (Figures 7 and 8) features a 200 psi nitrogen purge atmosphere and temperatures to 400°C, but is otherwise similar to the Alpha LFW-1, run per ASTM D27140-68. Lubrication is evaluated by measuring the width of the scar left on the friction block. Testing has not yet commenced.

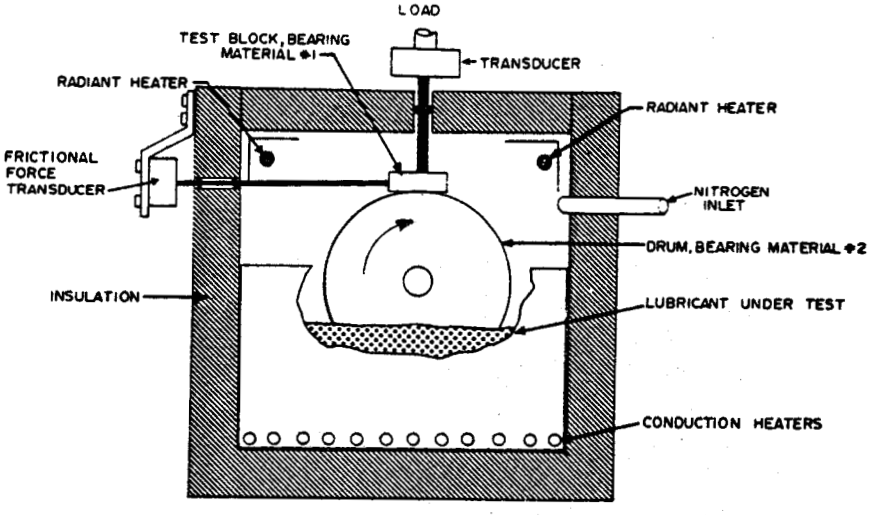


FIGURE 7. Lubricant Tester Schematic

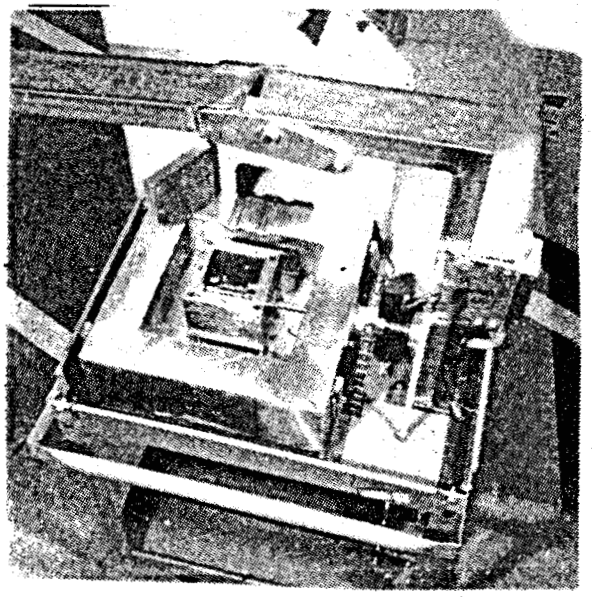

FIGURE 8.
Lubricant Tester Load Frame, Insulation box, Pressure Vessel, and Ring Assembly.

## SEAL TEST RESULTS

Extensive screening tests have been run on elastomeric seals: Fluorocarbon elastomer (Viton or Fluorel), Buna-N, Kalrez, peroxide-cured Viton, two fluorosilicone rubbers, and PNF-200. Several experimental mechanical seals have also been tested; over 155 tests have been run overall. Figure 9 illustrates several findings for the leading elastomer, Viton.

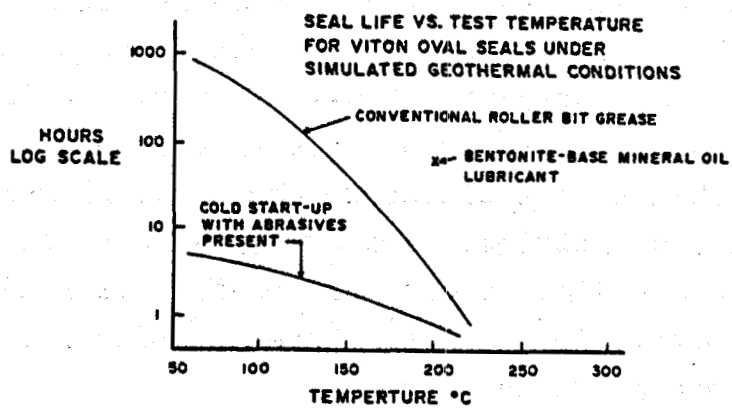


FIGURE 9. Fluorocarbon Elastomer (Viton) Tests

Significant program findings to date are as follows:

1. Cold (20°C) startups induce rapid attack by abrasives. Rotation is now started at 50°C or greater.

2. Conventional bit greases are detrimental to high-temperature seal life, possible due to a lack of lubricity of the base oil, or due to an abrasive effect of one or more of the EP additives such as $Mo_2S$.

3. A high-flash-point mineral oil grease with a bentonite base gave exceptional seal life, but probably cannot support the bearing loads of a journal-type bit.

4. Mechanical seals tend to be too large, but have exhibited some success; new designs have been initiated to reduce the size.

## CONCLUSIONS

Field and laboratory testing of the final generation of unsealed bits (MK-III) should allow the unsealed bit program to enter the commercialization phase. Extensive seal testing has shown that conventional bit seals are near the state-of-the-art for high-temperature service. However, it may be possible to raise the seal's temperature limitations by the use of a more compatible lubricant. Non-elastomeric seals may provide a much greater improvement, but face size limitations and corrosion problems in addition to the heat, abrasiveness and mechanical eccentricities. Improvements in seal, or seal/lubricant temperature limitations can benefit all sealed bit applications by permitting higher RPM/penetration rate as well as the higher temperature ceiling.

# A NONDESTRUCTIVE EVALUATION TECHNIQUE FOR DETECTING THE INCIPIENT FAILURE OF DRILL PIPES USED IN GEOTHERMAL WELL DRILLING

by

A. A. Hochrein, Jr.
and
L. L. Yeager
DAEDALEAN ASSOCIATES, Inc.
Springlake Research Center
15110 Frederich Road
Woodbine, Maryland 21797

Detecting incipient failure modes in materials and determining the structural integrity of complex forms in order to assure component safety and reliability have been the major impetus in developing nondestructive evaluation techniques.

DAEDALEAN engineers have developed a unique nondestructive evaluation technique which utilizes the phenomenon of internal friction in materials and identifies changes in the specific damping capacity as a function of the integrity of the material being tested.

Specifically, geothermal drill pipes used in well drilling have been tested utilizing the internal friction nondestructive evaluation (IF-NDE) technique. Various conditional operating parameters such as hydrogen sulfide embrittlement, corrosion fatigue, and stress corrosion cracking were correlated to the useful life of drill pipes as identified by the IF-NDE technique. The analysis of data derived from numerous tests conducted in the field indicate that the different failure mechanisms each have their own characteristic decay associated with failure in the drill pipe. Further, the internal

friction measurement which is identified as the specific damping capacity of the various drill pipes increases as the drill pipes progress toward ultimate failure. The identification of the various failure modes could be associated with a characteristic internal friction measurement and enable the user to drill pipes to immediately assess the integrity of his sample pipe.

The savings associated with the IF-NDC technique would be realized as the drill pipes are used more efficiently. The elimination of questionable drill pipes from the drill string would reduce the number of downhole failures which would in turn reduce the drilling costs. The cost associated with the purchase of the equipment or rental of a service would be offset by reduced drilling costs.

The ability to identify certain parameters that affect the useful life of drill pipe which would result in an early incipient failure prediction technique would benefit the drilling industry. The IF-NDE technique would enable the drill pipe user to control the various failure mechanisms to his advantage.

## SCOPE

The scope of this technical feasibility program includes utilization of previous investigations and engineering design data of the specific damping capacity as a nondestructive evaluation technique for testing 4-1/2-inch diameter, Grade "E", drill string pipe. The pipes varied from the as-received condition with no applied service loads to failed sections of drill pipe that have undergone numerous applications of torsional fatigue and associated environmentally-assisted failure. The field data is presented for form of design curves for various failure mechanisms. An analytical model has been developed for the field data. Moreover, a field inspection technique has been developed for field measurements.

It has been well known for over a century that materials manifest deviations from perfect elastic behavior even at small stress levels. Zener (1)* calls this behavior "anelasticity" of materials. Since real solids are never perfectly elastic some of their mechanical energy is always converted into heat. The various mechanisms by which this occurs are collectively termed as internal damping.

The most direct method for defining internal damping is by the specific damping capacity. Precisely, the specific damping capacity, D, is given by:

$$D = \frac{\Delta W}{W} \qquad (1)$$

where:

$\Delta W$ is the energy dissipated in one cycle and

W is the total energy of the cycle.

The mechanism by which the energy is dissipated may be any one of the following (2):

1. Relaxation by thermal diffusion,
2. Relaxation by atomic diffusion,
3. Relaxation by magnetic diffusion,
4. Relaxation by ordered distribution,
5. Relaxation of preferential distributions,
6. Stress relaxation along previously formed slip bands,
7. Stress relaxation across grain boundaries, and
8. Stress relaxation across twin interfaces.

*Numbers in parentheses refer to references at the end of this report.

The phenomenon of internal damping of materials is used throughout the world to test authenticity of coins, the soundness of castings, the operating condition of railroad wheels, and the quality of musical instruments and glassware by listening to the tone and duration of sound (3). The study of internal damping has been very useful as a research tool in physical metallurgy; in vibration control of high-speed missiles, planes, and vehicles; in fatigue of materials; and in the study of properties of metals and alloys from the standpoint of theoretical and academic considerations. There are various technical terms to characterize this phenomenon: internal friction, logarithmic decrement, hysteretic constant, viscosity, elastic-phase constant, damping capacity, and so on.

The data reduction procedure and calculation of specific damping capacity that characterizes the dynamic response of the test components after a specific loading history are outlined in this section. Furthermore, the following relationships would be useful in data reduction and interpretation of results obtained on various components.

The dynamic response of the material is characterized by the damping coefficient or logarithmic decrement which can be expressed as:

$$\alpha = \left(\frac{1}{N}\right) \left(\ln \frac{A_o}{A_n}\right) \qquad (2)$$

where $\alpha$ is the damping coefficient, $A_o$ is the vibrational amplitude of the reference cycle, and $A_n$ is the vibrational amplitude after N cycles. From the determination of , the specific damping capacity ($\Delta W/W$) for materials is calculated from the following equation:

$$\frac{\Delta W}{W} = 1-e^{-2\alpha} \qquad (3)$$

where $\Delta W$ is the energy dissipated in one cycle, and W is the total energy of the cycle.

The damping coefficient ($\alpha$) is determined by plotting on semi-logarithmic axes several points of the equation:

$$N_i = \ln \frac{A_o}{An_i} \tag{4}$$

A linear relationship is established from the experimental points on the graph and the damping coefficient is determined from the linear relationship for the appropriate number of cycles. From the determination of $\alpha$, the specific damping capacity ($\Delta W/W$) can be determined.

Where the level recorder is used, the output signal ($A = f\ [t]$) is automatically translated into the function:

$$\frac{A_o}{A_n}\ (dB) = f\ (N) \tag{5}$$

The determination of $\alpha$ is made by measuring the slope of the recorded curve. The damping coefficient is proportional to the natural logarithm of the ratio of the amplitudes. On the level recorder output, the slope of the curve is proportional to the common logarithm of the ratio of the amplitude.

## EXPERIMENTAL APPARATUS, TECHNIQUES, AND PROCEDURES

The internal friction technique requires an input pulse and an associated output signal. The specific damping capacity is determined from the resultant decay curve of the output signal. In application, the technique uses the input of periodic excitation pulses. The input pulses are generated by a beat

frequency oscillator gated through a tone burst generator to a permanent magnet vibration exciter. The beat frequency oscillator supplies a continuous periodic signal at a specific frequency, and a tone burst generator is used to gate the signal from the oscillator into a series of discreet pulses. The generator controls the pulse duration and the time interval between pulses. The permanent magnet vibration exciter converts the electrical pulses from the generator into mechanical vibrations.

The vibrational response is measured by an output accelerometer. The signal from the accelerometer is filtered by a frequency analyzer and displayed on a storage oscilloscope. The specific damping capacity is determined from the decay curve of the input pulse. The accelerometer converts the vibrational response of the specific component to an electrical signal. The output signal from the accelerometer is filtered by an Audio Frequency Analyzer and the output decay curve is displayed on a storage oscilloscope which is externally triggered by the sync output from the tone burst generator.

Measurements of the vibration decay are made between pulses with a pick-up transducer. The generation of these pulses require an oscillator coupled to a tone burst generator. On the pick-up side, the unit measures a wide range of damping levels and various degrees of amplification in time and in amplitude. The amplification units will consist of a voltage amplifier for the amplitude of the received signal and an oscilloscope for the spread in time of the received signal.

Thus, the selection of the major components has to satisfy practical requirements to allow meaningful interpretation of results. Such design criteria consists of:

1. Frequency range: 20- 20,000 Hz
2. High pick-up sensitivity
3. High signal/noise ratio
4. High accuracy of measurements
5. High amplification (100 dB)
6. Minimum harmonic distortion

A comparison of available off-the-shelf equipment led to the selection of several commercially available instruments. A description of the components and of the test apparatus is given in the next section. A schematic representation of the equipment including the microprocessor technology is included in Figure 1.

The measured values of specific damping capacity during the load cycle history of the drill string pipe indicated in feet of use are used in a point-by-point determination of a base line equation for $\frac{\Delta W}{W}$. Using a preassigned probability level, $\alpha$, an upper confidence limit for the calculated values of $\frac{\Delta W}{W}$ is determined. The equation for $\frac{\Delta W}{W}$ in conjunction with the upper confidence limit is used to predict the interval in which the next measured value of $\frac{\Delta W}{W}$ will be found. When succeeding measured values of $\frac{\Delta W}{W}$ fall below the calculated upper confidence limit, these values are used to refine the equations for $\frac{\Delta W}{W}$ and the upper confidence limit prior to prediction of the next measured value. The probability level, $\alpha$, used in determining the upper confidence limit is chosen so that should the next measured value of $\frac{\Delta W}{W}$ be found above the confidence limit, there is a high probability that crack propagation is in progress (5). Standard statistical techniques were used for data evaluation.

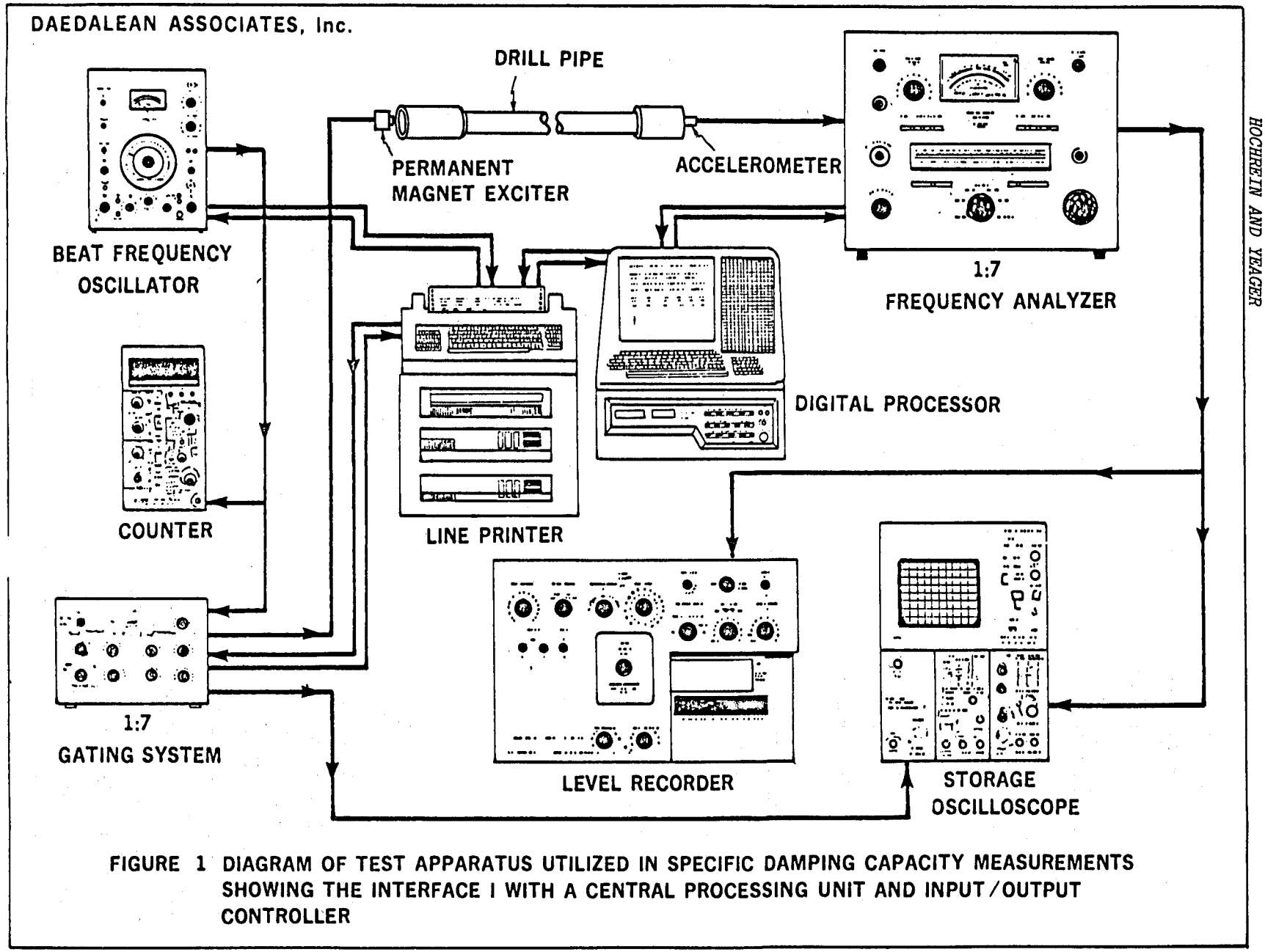


FIGURE 1 DIAGRAM OF TEST APPARATUS UTILIZED IN SPECIFIC DAMPING CAPACITY MEASUREMENTS SHOWING THE INTERFACE I WITH A CENTRAL PROCESSING UNIT AND INPUT/OUTPUT CONTROLLER

Drill pipe failures occur with a connection failure at the joints and couplings or with a body failure in the stem of the drill pipe. Figure 2A shows a typical connection failure at the joints and couplings. Transverse cracks are produced primarily in the end areas of the tube during the upsetting operation. These cracks may occur on either the inside or the outside surface. High strength steels and special upset tubular steels are particularly subject to this type of failure. A typical body failure is shown in Figure 2B. These cracks, especially those located in the bottom of plug scores, are usually longitudinal in direction. Moreover, they result from residual stresses left in the pipe by the manufacturing process and from gouges on the inside surface of the pipe produced in the piercing operation. In recent years, body failures have dominated drill string failures in contrast to connection failures.

The causes for drill pipe failures result from overloads, fatigue loading, corrosion fatigue, stress corrosion cracking, hydrogen sulfide embrittlement, corrosion, erosion, wear, galling, and handling damage. Fatigue failures, assisted by corrosion and hydrogen sulfide embrittlement, constitute the dominent mechanism for drill pipe failures. Examples of various types of failures by these mechanisms are readily available in the literature. Fatigue failures are easily identified after the fact by the half-moon rings on the face of the characteristic flat break. The fatigue nucleation sites are easily visible at the center of the half-moon cracks. These nucleation sites are generally located at niches, bends, abrasion marks, gouges, or corrosion pits. Similarly, the description and photograph record for other types of drill pipe failures are fully documented in the literature. Tens of thousands of feet of drill pipe are lost annually to various failure mechanisms. During a 12-month period, a major independent oil company had 11 drill string failures in

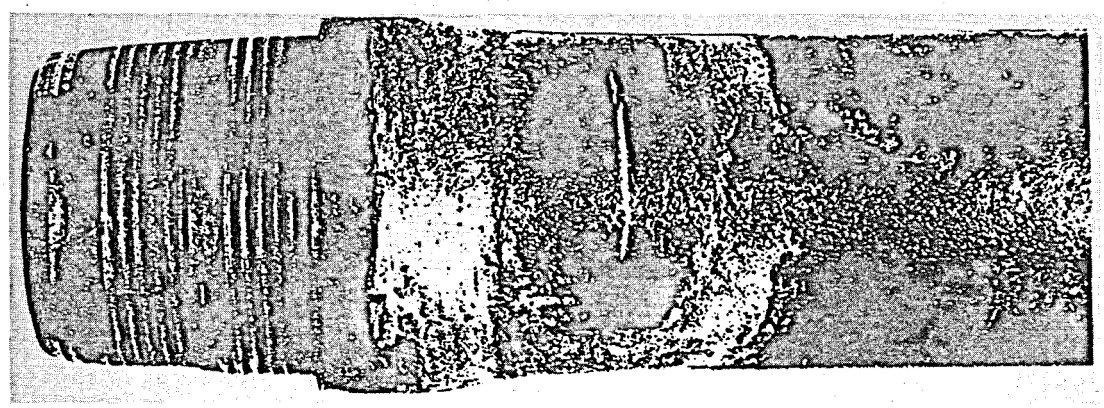

FIGURE 2A TYPICAL EXAMPLE OF CONNECTION FAILURE CRACKS IN DRILL PIPE

TRANSVERSE CRACKS ARE PRODUCED PRIMARILY IN THE END AREAS OF THE TUBE DURING THE UPSETTING OPERATION. THESE CRACKS MAY OCCUR IN EITHER THE INSIDE OR OUTSIDE SURFACE. HIGH STRENGTH STEELS AND SPECIAL UPSET TUBULAR STEELS ARE SUSCEPTIBLE TO THIS TYPE OF FAILURE.

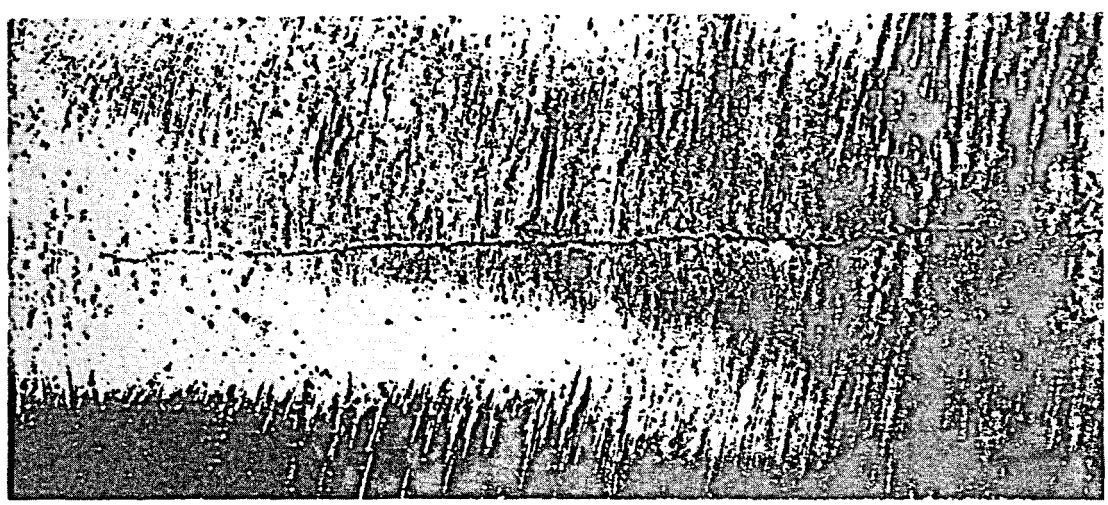

FIGURE 2B TYPICAL EXAMPLE OF BODY FAILURE CRACKS IN DRILL PIPE

THESE CRACKS, ESPECIALLY THOSE LOCATED IN THE BOTTOM OF PLUG SCORES, ARE GENERALLY LONGITUDINAL IN DIRECTION. MOREOVER, THEY RESULT FROM RESIDUAL STRESSES LEFT IN THE PIPE BY THE MANUFACTURING PROCESS AND FROM GAUGES ON THE INSIDE SURFACE OF THE PIPE PRODUCED DURING THE PIERCING OPERATION.

its Permian basin wells. It is estimated that one drill string in ten fails during the drilling operation.

Drill pipes have been tested and evaluated at the Tom Brown, Inc. yard in Midland, Texas. Groups of drill pipe tested include new Grade "E" pipe produced by three different manufacturers as well as seven different categories of used Grade "E" pipe. The used pipe categories are slightly used, incipient cracks, corrosion fatigued, stress corrosion cracks, heavily used, $H_2S$ embrittled (20,000 feet of use) and $H_2S$ embrittled with 30,000 feet of use.

The categorization of drill pipes into the groups listed above was accomplished using the extensive and complete records of use kept by the driller along with the results of testing by AMF Tubescope which had been carried out on samples from each group. The pipes categorized as having incipient cracks were pulled from a drill string because of a pressure loss. Of the 15 pipes in the group, only one had an abnormally high specific damping capacity. Upon eddy current testing by a local testing company, this pipe was found to be cracked. The rest of the group were structurally sound.

Figure 3 shows the feet of use versus the average specific damping capacity for all 12 groups of pipe tested. The data are shown to define four curves. Two of the curves are for pipe subjected essentially to fatigue. One curve is defined by the data for pipes subjected to an $H_2S$ environment. The fourth curve consists of the data for pipes believed to have experienced a combination of fatigue and environment related deterioration.

Figures 4 through 7 show each curve individually along with the upper confidence limit for the pipes. The confidence

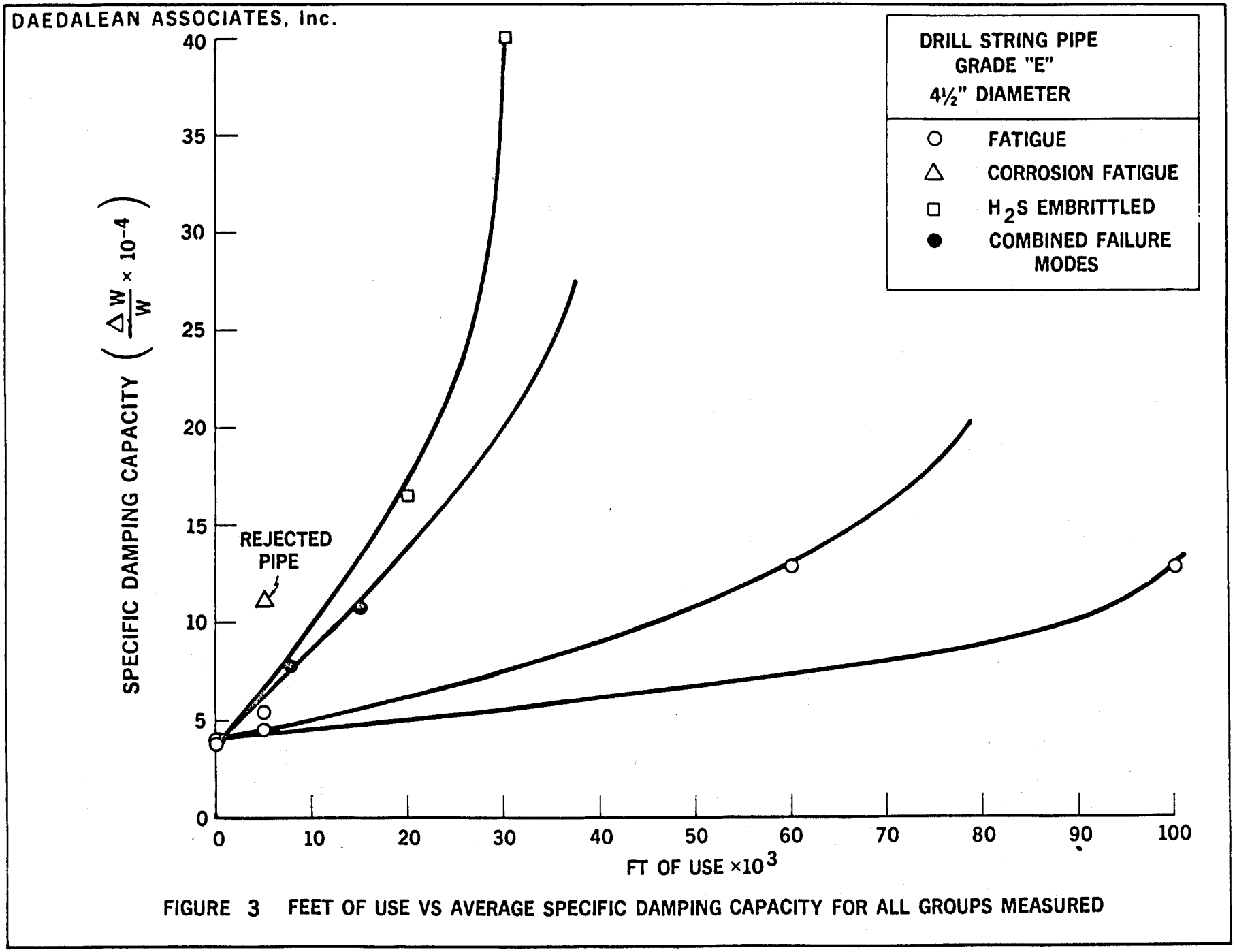


FIGURE 3 FEET OF USE VS AVERAGE SPECIFIC DAMPING CAPACITY FOR ALL GROUPS MEASURED

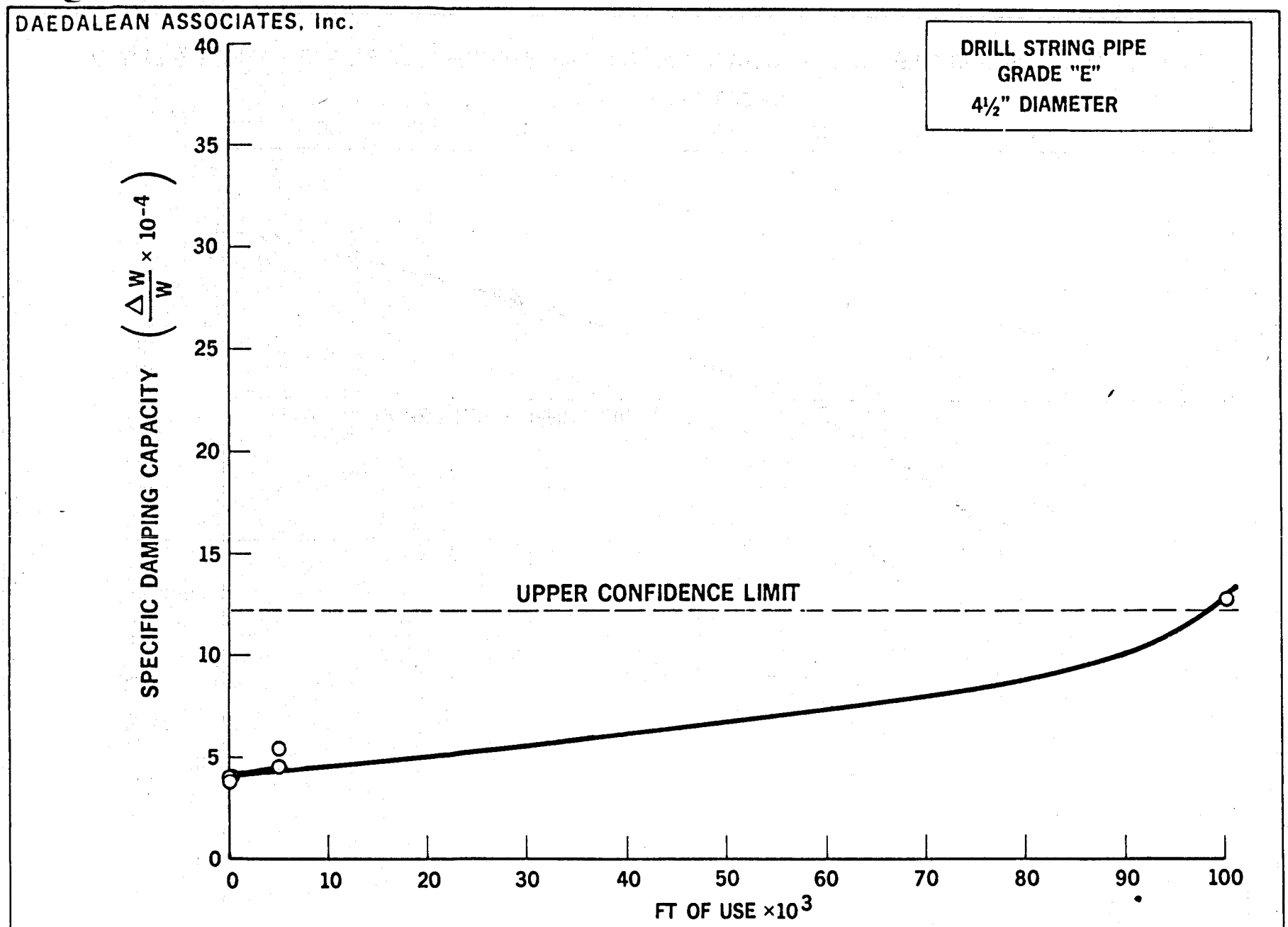


FIGURE 4 FEET OF USE VS AVERAGE SPECIFIC DAMPING CAPACITY FOR PIPES SUBJECTED TO FATIGUE

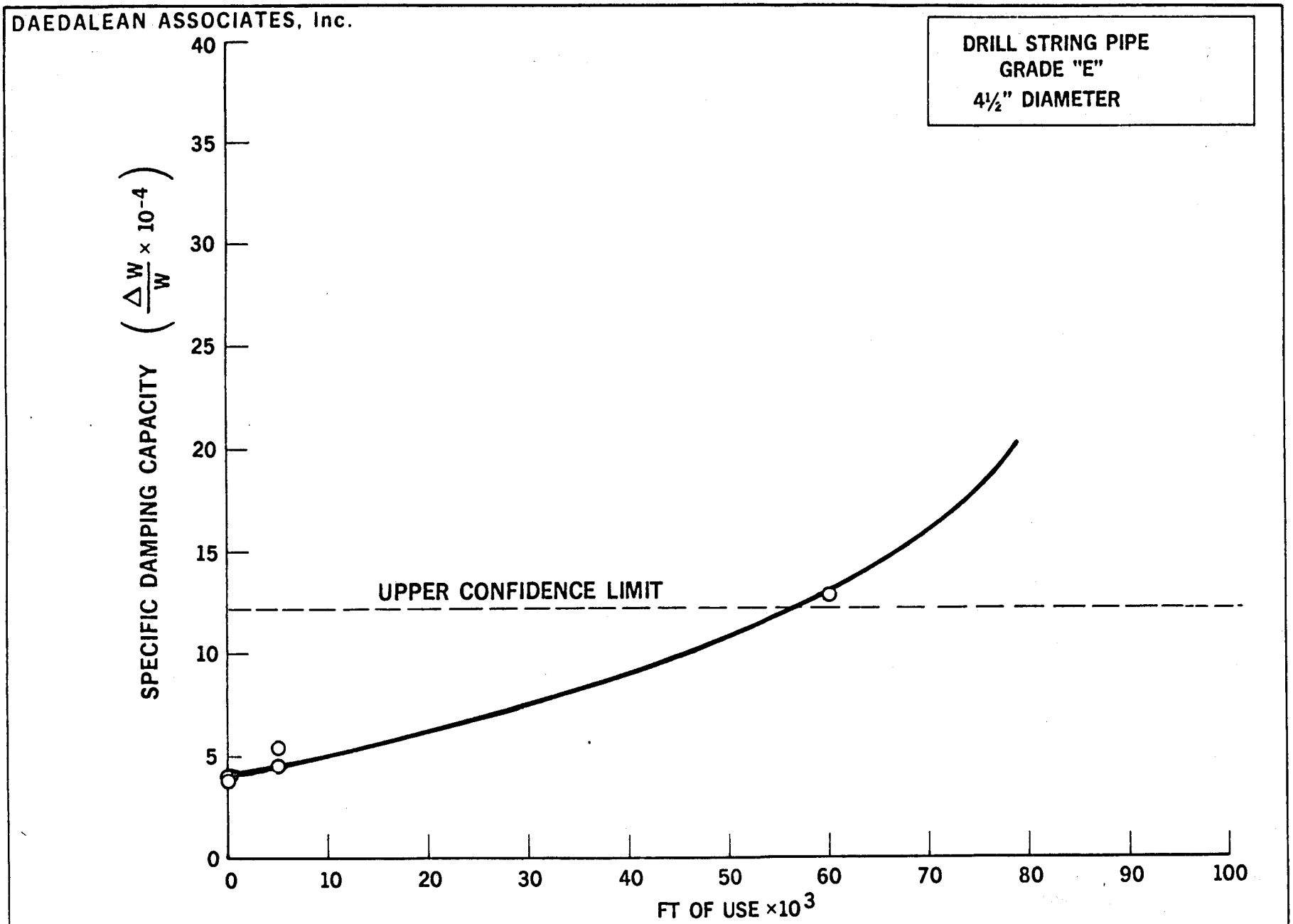


FIGURE 5 FEET OF USE VS AVERAGE SPECIFIC DAMPING CAPACITY FOR PIPES SUBJECTED TO FATIGUE

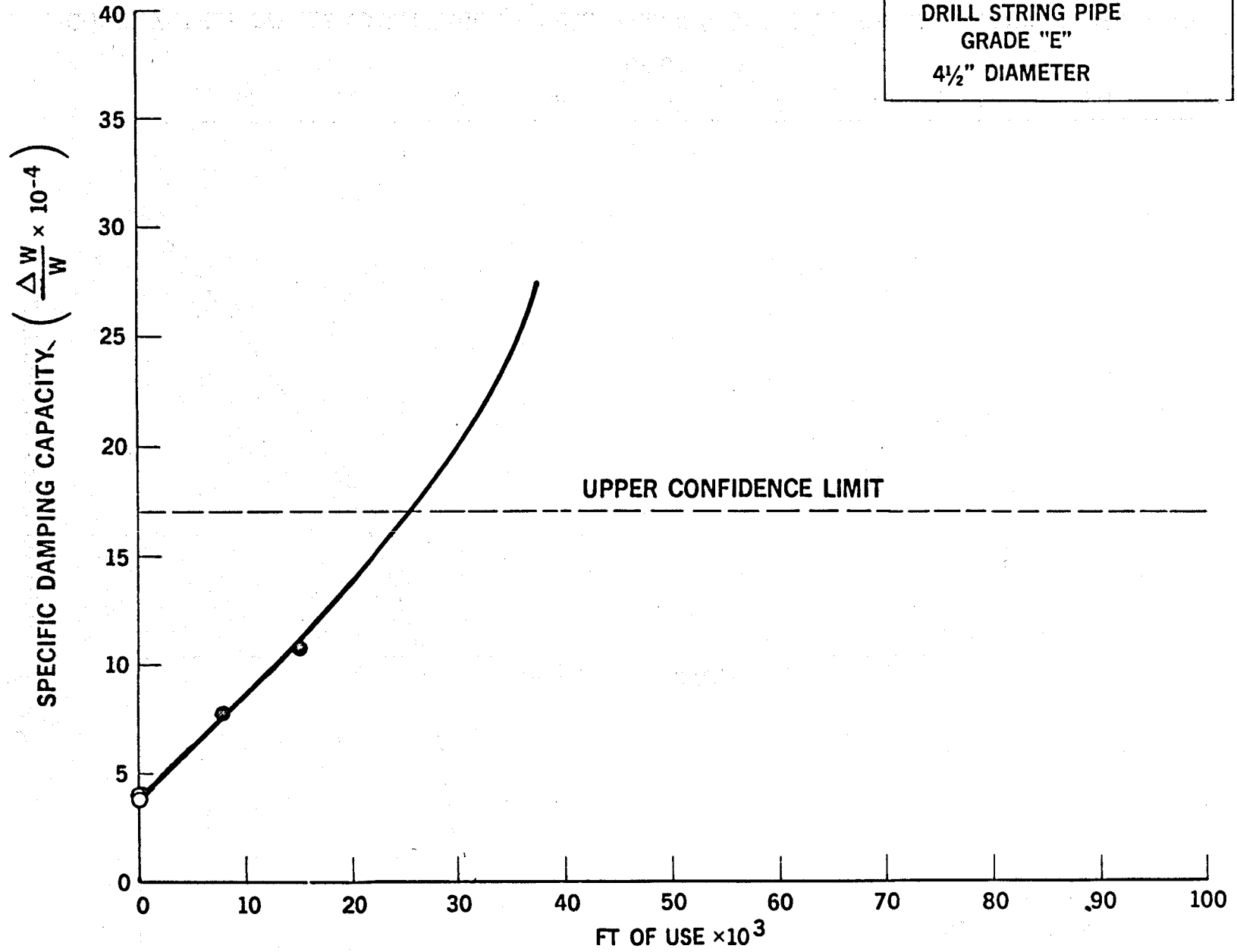


FIGURE 6 FEET OF USE VS AVERAGE SPECIFIC DAMPING CAPACITY FOR PIPES SUBJECTED TO COMBINED FAILURE MODES

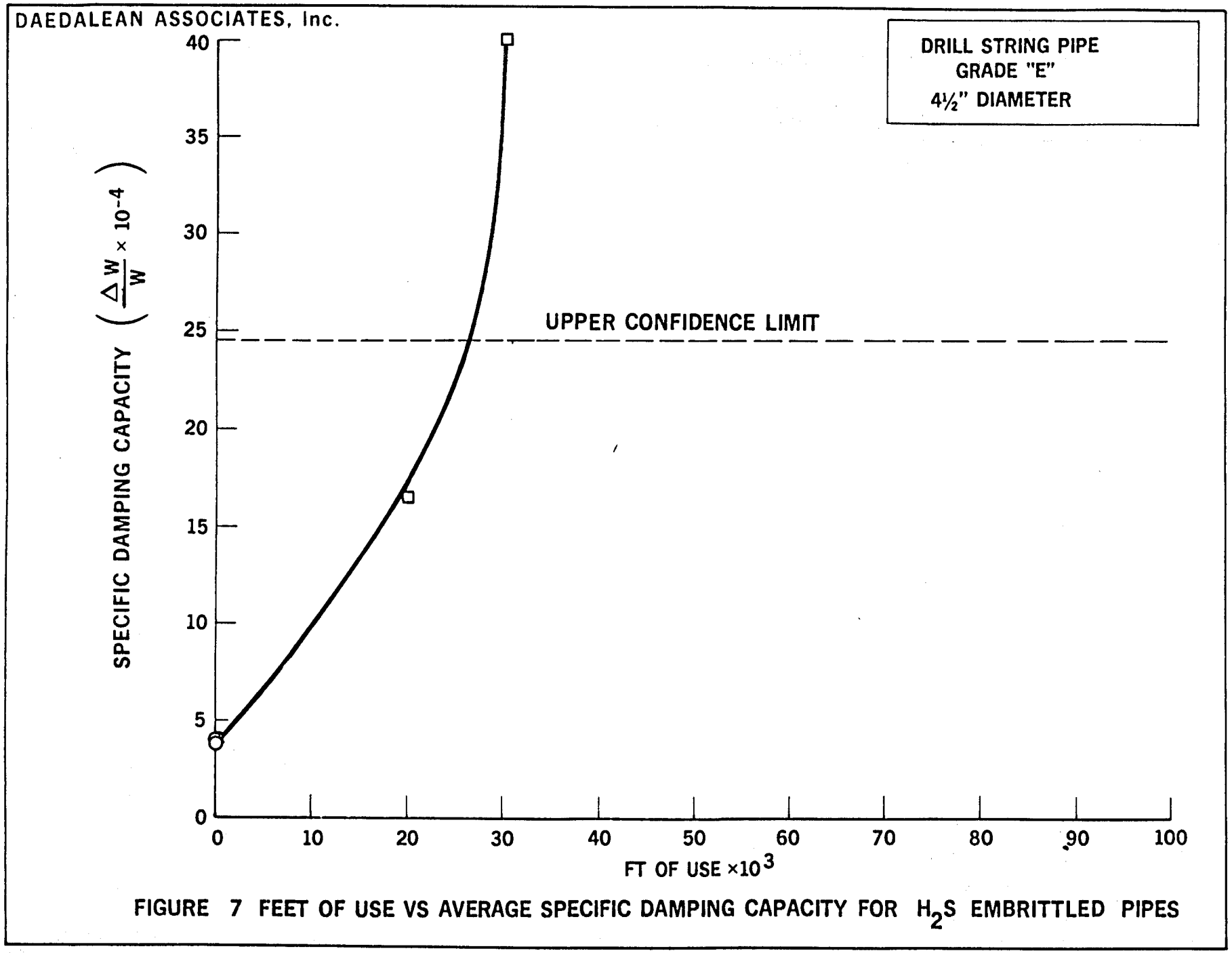


FIGURE 7 FEET OF USE VS AVERAGE SPECIFIC DAMPING CAPACITY FOR $H_2S$ EMBRITTLED PIPES

limit is based on the limited data presently available and would be refined as more data is obtained from the next phase of the work.

Within the scope of this program, the reliability of the specific damping capacity measurements was assessed utilizing numerous 4-1/2-inch O.D., Grade "E" steel drill pipe with 0.337 wall thickness. The dimensions of the pipe included 4-1/2-inch diameter by 32 feet nominal length with welded end caps on the tube section. Various specific damping capacity measurements taken on the drill pipe sections were reliable at the 98.5% confidence level. Improved test conditions and refinement of the test procedure increased the reliability to 99.7%.

In each case, the reproducibility of the data was verified by the trend of each set of data giving the clear indication of a large change in $\frac{\Delta W}{W}$ toward the end of the useful life of the drill string pipe. An indication of the failure was evidenced in each frequency of interest. The geometry of the drill pipes did not alter the ease of applying the NDE technique to detect incipient failure. The reliability of measurements has been established at 98.5% for the level of confidence chosen in tests performed for various failure modes of drill pipe.

Figures 4 through 7 illustrate the change in $\frac{\Delta W}{W}$ versus feet of use for each of the drill pipes. Certain variations are evident in the $\frac{\Delta W}{W}$ versus feet of use plot that include:

1. An increase in $\frac{\Delta W}{W}$ as the feet of use increase.
2. An increase in $\frac{\Delta W}{W}$ versus feet of use as the drill experience more severe environmentally-assisted failure mechanisms.

For the drill pipes tested in this program, complete failure was defined as that time in the feet of use history for the drill pipe where one or a combination of the following criteria was met:

1. Drill mud exhausted through a crack in the drill pipe section pressure,
2. Plastic deformation of the drill pipe was evident,
3. Pressure drop was caused by crack propagation, and
4. Microscopic detection of a crack was evident.

In all cases sufficient data was obtained to determine the base line value of $\frac{\Delta W}{W}$ (specific damping capacity). The analysis program accurately determined the critical point when the value of $\frac{\Delta W}{W}$ increased beyond the normal expected value within the chosen confidence level. A least-squares fit of the $\frac{\Delta W}{W}$ versus feet of use established the base line equation. The confidence interval at a specific probability level is also calculated. Using these functions, a predicted value of $\frac{\Delta W}{W}$ for a specific additional period (1,000 feet of use, 5,000 feet of use, etc.) was calculated and compared with an actual measured value. Whenever the value remained within the predicted envelope, the data point was added to those already being used in the analysis. Whenever two consecutive points were located outside the predicted envelope, the specific damping capacity of the drill string was increased significantly. This change was related to other base line data obtained, and a prediction of incipient failure was ascertained. This process was utilized on 4-1/2-inch Grade "E" drill string pipes with results that predicted failure (as defined earlier in this section) in all cases defined before the crack was detectable using other methods.

Figures 4 through 7 illustrate: 1) the specific damping capacity as a function of the total feet of use, and 2) also indicate the point during the feet of use history wherein the data analysis program first predicted that the actual measured value of $\frac{\Delta W}{W}$ was actually beyond the confidence limit of the predicted average value of $\frac{\Delta W}{W}$ for the same point. This point may be located on Figures 4 through 7 by following the solid line to its intersection with the dashed line of the upper confidence interval.

The prediction program based on engineering data and analytical models was used to further classify flaws into specific and definitive categories. Such categories included $H_2S$ embrittlement corrosion fatigue and stress corrosion cracking to mention a few. The ability to predict incipient failure and to include the probable failure mechanism provides the incentive for further development of the internal friction nondestructive evaluation technique for field use. Figures 4 through 7 indicate the base line data necessary for the development of field design charts that could be used to predict incipient failure of drill pipe as a function of time in feet of use for the various failure modes.

## CONCLUSIONS AND RECOMMENDATIONS

Conclusions from current technology data indicate that the internal friction damping nondestructive evaluation technique can be a viable method for classification of drill pipe and for predicting impending failure caused by various failure mechanisms. Current data indicates that various stages of degradation of drill pipes and impending failure of drill pipes can be identified by the measured specific damping capacity as a function of feet of use history.

The present data is inadequate to define specific mathematical models. Obtaining complete data for different environments by monitoring drill string pipes over their useful life will enable specific models to be defined and make possible the prediction of impending failure. Once sufficient data is available, it will be possible, knowing the specific damping capacity and the feet of use a pipe has seen, to define the failure mechanism acting on the pipe and the percentage of useful life remaining.

It is recommended that the end result of the program be a field-mobile NDE system which will evaluate pipes at the drill site and classify them based on the specific damping capacity measurement and length of service. The rejection criteria contained in Table B6-1, "Classification of Used Drill Pipe" of the API Drilling Manual will be correlated to the specific damping capacity results.

A qualitative example of the correlations to be obtained would be the reduction in cross-sectional area due to wear. For Premium Class and Class 2 pipe, the cross-sectional area must not be less than the area calculated for a 20% reduction in wall thickness. For Class 3 and Class 4 pipe, the cross-sectional area must not be less than the area calculated for a 37.5% reduction in wall thickness. It is anticipated that the data curves shown in Figures 4 through 7 will be refined by the amount of data collected with the field system, and a specific point on each curve will be correlated with the physical wear units for each class of pipe.

Furthermore, it is recommended that the field system contain the necessary signal generation, signal analysis, and digital processing equipment to conduct immediate, on-site evaluation of drill pipe.

REFERENCES

1. Zener, C., "Internal Friction in Solids, Theory of Internal Friction in Reeds," Physical Review, Vol. 52, p. 230, 1937.

2. Zener, C., "Elasticity and Anelasticity of Metals," The University of Chicago Press, Chicago, 1948.

3. Jenson, J.W., "Damping Capacity - Its Measurements and Significance," Bureau of Mines Report of Investigation 5441. United States Department of Interior, 1959.

4. Hochrein, A.A., Jr., Envent, F., Cavanaugh, J., and Thiruvengadam, A.P., "An Exploratory Study of Specific Damping Capacity Measurements as a Nondestructive Acceptance Test for Deep Ocean Submersible Pressure Hulls," DAI Report No. PR-7441-03B, 31 October 1974.

5. Envent, F., Thiruvengadam, A.P., and Hochrein, A.A., Jr., "A Feasibility Study of Applying Internal Friction Measurements as a Nondestructive Acceptance Test for Deep Ocean Submersible Pressure Hulls," DAI Report No. FE-7447-FR, July 1975.

6. Yeager, L.L., Thiruvengadam, A.P., and Hochrein, A.A. Jr., "The Application of a Nondestructive Evaluation Technique for Hyperbaric Pressure Vessels Utilizing the Phenomenon of Internal Friction in Materials." DAI Report No. LY-7639-02-TA, October 1977.

# MATERIALS PROBLEMS ENCOUNTERED IN SPERRY'S DOWNHOLE GEOTHERMAL PUMP PROGRAM

H. B. Matthews and W. D. McBee
Sperry Research Center, Sudbury, MA 01776

January 1979
SCRC-RP-79-2



SPERRY RESEARCH CENTER

## INTRODUCTION

Since 1972 the Sperry Research Center has been actively engaged in the development of a down-well pumping system for liquid-dominated geothermal resources. As the literature points out, this has been one of the key technical problems in the exploitation of hot water geothermal energy resources. Down-well pumping (vs. free-flowing) of geothermal hot water wells offers several potential benefits:

- Inhibition of precipitation and scaling by prevention of flashing and $CO_2$ release.
- Higher wellhead brine temperature and, hence, conversion efficiency.
- Enhanced flow.

To achieve these benefits, a down-well pumping system must have the following features:

- Highest possible efficiency (Hydraulic Output/Brine Thermal Input).
- Deep setting (at least 2,000 feet as a maximum).
- Compatibility with geothermal temperature, chemistry, installation, and operating environment.
- Cost effectiveness in terms of initial installation, operation, and maintenance costs.

Between 1972 and 1974 effort was conducted by the Research Center, under its own research and development program, on the analysis and design of this pumping system. This system, granted Patents 3,967,448; 3,938,334; 3,824,793; 3,898,020; 3,988,896; 3,910,050; 3,939,659; 3,905,196; 3,908,381; 3,961,866; 3,908,380; and others pending, is based on direct transfer of the

small fraction of the available thermal energy in the pumped brine that is required for pumping by means of a down-well boiler-turbine pump assembly.

Since 1974 the conversion of this concept into demonstration hardware has been funded by government agencies principally concerned with the development of alternate energy resources. This funding has as its objective a successful feasibility demonstration of this system in a typical hot brine well. The work content of the program was separated into three consecutive phases to allow for periodic reviews and changes in scope as the work progressed. Phase I was concerned with the design, fabrication, and laboratory testing of a 20,000-barrel-per-day (BPD) turbine pump unit (TPU) and the dissemination of information to the geothermal community. Phase IIA, as a result of industry inputs, was concerned with the design, fabrication, and laboratory testing of a 30,000 BPD TPU, the design and fabrication of the associated support system, and the selection of a field test site. Phase IIB in turn covered the laboratory testing of the associated support equipment, the specification and purchase of field support hardware, and the actual field site testing of the pumping system.

In July 1974 the National Science Foundation (NSF) awarded Grant No. AER-74-08874 to the Sperry Research Center to pursue Phase I of this feasibility demonstration program. Phase I effort was successfully completed in February 1975. In March of that year, the funding of the NSF grant was increased to cover Phase IIA activity. This work effort was completed in May 1976. In October 1975 responsibility for the program was transferred to the Energy Research and Development Administration (ERDA) and a Contract No. EY-76-C-02-2838 was awarded for Phase IIB activity. This last phase of the program saw the termination of the field testing in December 1976.

The program was structured to allow the participation of several organizations and consultants under the project management responsibility of the Sperry Research Center. The principal contributors to this program were:

- Barber-Nichols Engineering Company
- Chevron Resources Company
- Sperry Research Center.

# SECTION 1

# THE SPERRY GEOTHERMAL DOWN-WELL PUMPING SYSTEM

## 1.1 SPERRY PUMPING SYSTEM CONCEPT

Geothermal energy is the natural heat of the earth, which, if recoverable, can be made to do useful work. The basis of the Sperry down-well pumping concept is that the down-hole pump obtains its energy to pressurize the brine directly from the heat of the brine itself. The principle involved is shown in Fig. 1. A small quantity of working fluid (less than 2 percent of the brine flow) is pumped from a surface system down to the pumping unit through a down-hole heat exchanger, which consists of two annuli formed by the well casing and two concentric lengths of standard oil field casing. The working fluid flows down the inner annulus, and the hot brine flows up the outside annulus. The intimacy of these streams results in heat being transferred from the brine across the boiler wall and into the working fluid, resulting in its vaporization.

The working fluid vapor is used to drive a turbine, which in turn drives the pump impeller. Upon exiting the turbine, the steam exhaust is returned through the exhaust casing to the surface, where it is condensed and then sent back down-hole for another cycle. Thus the working fluid is contained in its own closed loop, and the brine is excluded from this subsystem. In this manner some of the thermal energy (heat) of the brine is used to drive the down-hole pump.

Figure 1 also shows how a small portion of the working fluid is conveyed down to the turbine-pump unit under pressure and in the liquid state to lubricate the turbine bearings. Since this liquid is at a higher pressure than the brine, the contaminated brine is excluded from the turbine cavity. A small continuous flow of the lubricant is permitted into the turbine exhaust to carry away heat from the turbine bearings.

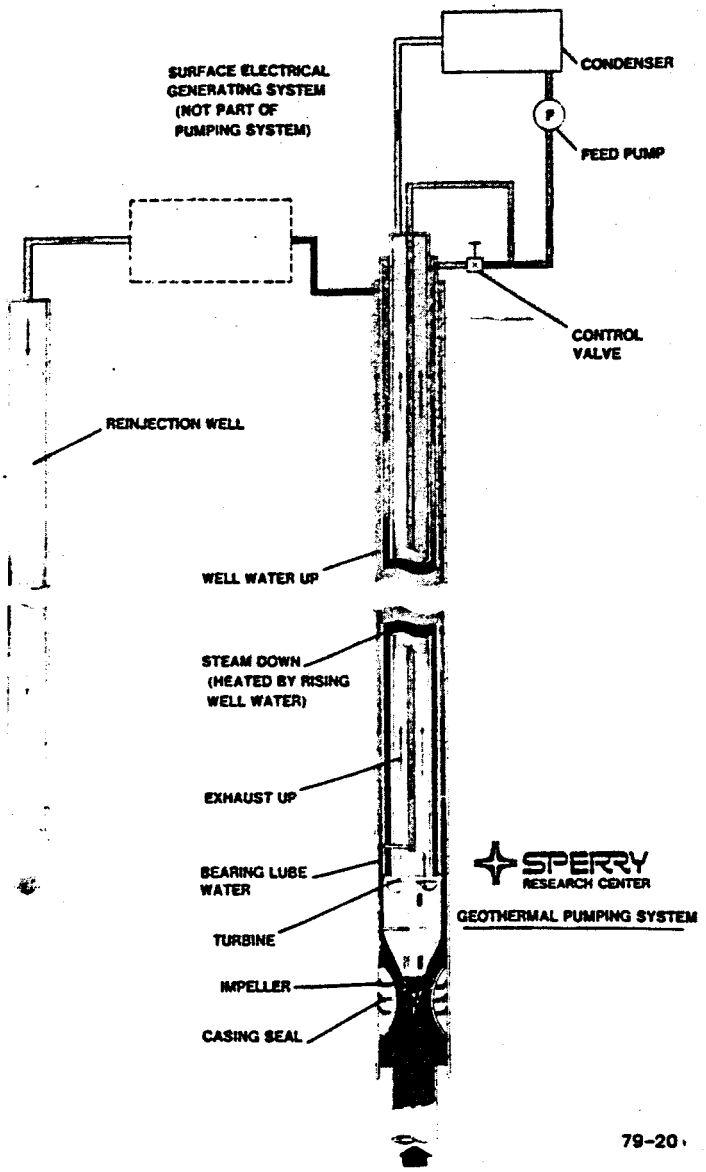


FIG. 1 Schematic of Sperry pumping system for geothermal well.

This extraction of thermal energy from the hot well water down-hole at the site of the pump minimizes the number of energy conversions necessary to power a pump. Only two energy conversions are required--heat to shaft work and work to head and flow. All other pumping systems involve a larger number of energy conversions from the primary energy source (i.e., the brine heat). Since any energy conversion involves loss in efficiency, the Sperry system has inherent potential for higher efficiency than alternative approaches. At first glance, there would seem to be a penalty on the efficiency of the subsequent system for conversion of the remaining brine thermal energy (e.g., to electricity) as demonstrated by the Carnot principle, since energy for pumping is taken from the top of the cycle. However, careful analysis shows that for roughly equivalent thermal efficiencies for the pumping and power plant cycles, the penalty is negligible.

An additional energy saving accrues from this system. The energy for pumping must come from the brine heat in any system. Removing this energy down-hole lowers the temperature of the brine down-well, and it arrives at the surface with a correspondingly lower saturation pressure, requiring less pressure added. In a 400°F well, this typically could amount to an additional 12-percent saving in energy required for pumping.

## 1.2 TPU (TURBINE-PUMP-UNIT)

Figure 2 is a schematic of the turbine pump unit (TPU). The TPU consists of a mixed flow pump and a two-stage axial-flow turbine configured on a common shaft. The shaft is supported by two, three-element ceramic radial bearing assemblies located near the turbine and pump impeller. The shaft thrust load is carried by a six-element ceramic thrust bearing near the middle of the shaft. A ball bearing was provided to carry the reverse thrust that exists at low pump speeds during start-up and shut-down. The bearing cavity is sealed from the brine flow by a face seal located behind the pump impeller. Excess bearing leakage is controlled by a similar seal located at the turbine end of the TPU. A detailed description of these components is provided in the following sections.

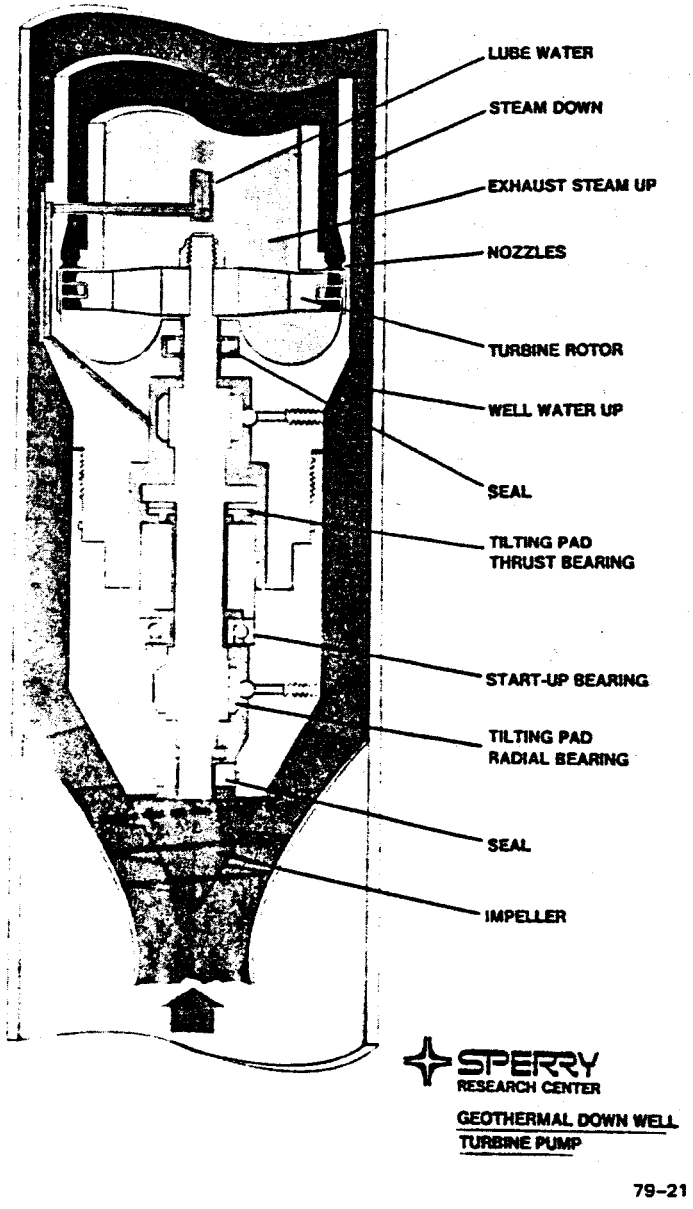


FIG. 2 Schematic of the turbine pump unit (TPU).

1.2.1 Pump

Two basic pump configurations were designed and fabricated, one for 600 and one for 900 gallon per minute (GPM) brine flow, i.e., 20,000 and 30,000 BPD respectively. Both units were laboratory tested, but only the 900 GPM pump was used in the down-hole testing. Design specifications common to both units are as follows:

| | |
|---|---|
| Depth | 850 ft. |
| Speed | 17,000 rpm |
| $\Delta P$ | 216.4 psid (576.5 ft. head) |
| NPSH | 202.5 ft. (76.0 psi) |
| Minimum Pump Efficiency | 0.70 |

The two major elements of these pumps, the impeller and diffuser, are discussed below in separate sections.

1.2.1.1 Impeller. Six hundred and 900 GPM impeller configurations were designed, built, and tested. Both models are conceptually similar. The dimensional differences are shown in Table 1 and Fig. 3.

The impeller blade angle is a constant $20^{\circ}$ throughout the impeller measured at the RMS diameter. This low blade angle was chosen to minimize pump cavitation. An open impeller design was selected to simplify manufacturing. Reasonable blade strength and stiffness were achieved using six impeller vanes. Thrust balance was accomplished by using an increased hub diameter and venting the back side of the impeller to pump inlet pressure as shown in Fig. 3. The hub diameter, the location of the labyrinth seal, and hub venting were designed to reduce axial thrust to approximately 320 pounds, which is suitable for the selected bearing configuration.

1.2.1.2 Diffuser. The high kinetic energy of brine leaving the impeller is partly converted into pressure head by removing swirl and by diffusion through vanes. The fluid velocity diffusion and straightening takes place as the fluid flows through three distinct regions: stator vanes, vaneless space,

TABLE 1

Impeller Dimensional Comparison

| | 600 GPM Impeller | 900 GPM Impeller |
|---|---|---|
| Impeller Eye Diameter (inches) | 2.52 | 2.70 |
| Impeller RMS Exit Diameter (inches) | 3.238 | 3.50 |
| Impeller Exit Blade Height (inches) | 0.60 | 0.59 |

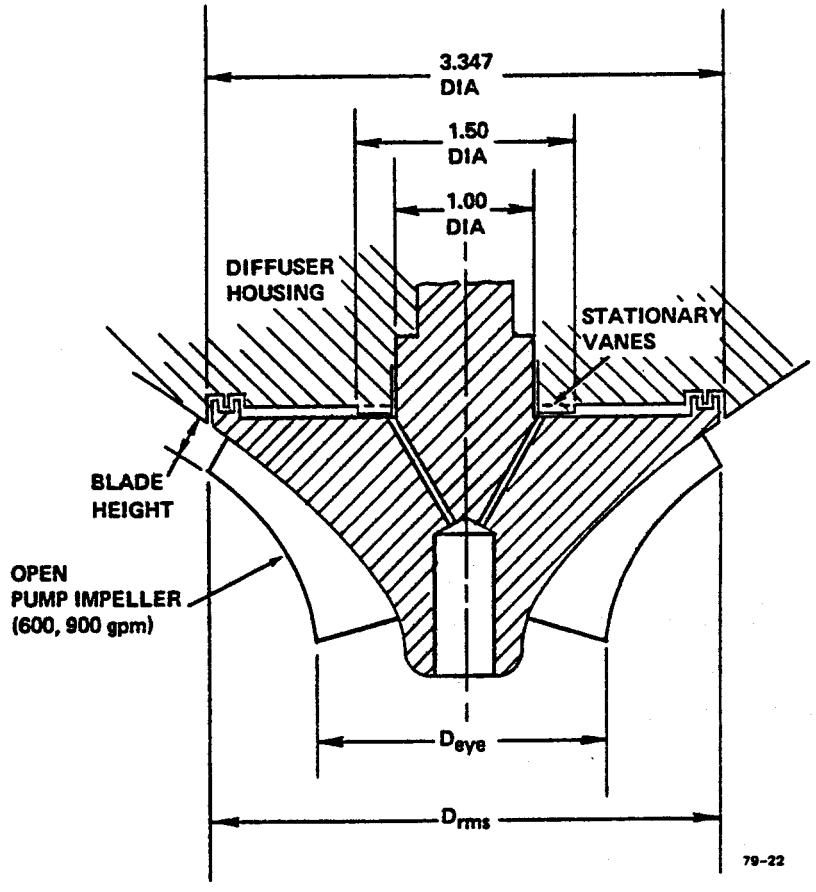


FIG. 3 Impeller dimensional schematic comparing 600 and 900 GPM designs.

and turning vanes. The design and function of these regions are described below.

1) Stator Vanes - The stator vanes are contained in a conical passage with the hub surface making an angle of $54.2^{\circ}$ with the axis of the pump. The vanes have a blade angle of $21^{\circ}$ at the inlet and $40^{\circ}$ at the exit. The seven stator vanes are designed to yield a uniform reduction in velocity and rotation. These stator vanes were cut back for the 900 GPM version to an angle of $27^{\circ}$ at the inlet, allowing for the higher brine velocities associated with the greater flow rate.

2) Vaneless Space - This region is also a conical passage making a smooth transition to an annular passage at its termination. Thus the flow is turned to an axial direction in the meridional plane. More diffusion is achieved here mainly because of the radius change. Fluid leaves the vaneless space at an angle of $45.16^{\circ}$.

3) Turning Vanes - This region is an annular passage with long vanes to take out the remaining swirl so that the flow leaves in an axial direction. Fourteen vanes have an inlet blade angle of $47^{\circ}$ and an exit blade angle of $90^{\circ}$.

### 1.2.2 Thrust Balance

Mixed flow pump impellers can produce very significant axial thrust levels. For example, an unbalanced version of the geothermal pump would produce approximately 1,100 pounds thrust. Since this value exceeds thrust bearing limitations (based on the limited package size and power loss requirements) some means of thrust balance must be provided. Also it is

imperative to maintain axial thrust in the direction of the pump over the full operating speed range to avoid unloading the axial thrust bearing. A design value for pump axial thrust (of 320 pounds) was selected using the best available estimate of well pressure as a function of flow to estimate the force due to shaft unbalanced area.

The approach chosen to control impeller thrust was to provide a labyrinth seal near the O.D. of the impeller and vent the back side of the impeller to inlet pressure as shown in Fig. 3. In addition, short stationary vanes are employed. In this fashion, the static pressures can be controlled on the back side of the pump impeller, thereby maintaining the desired value of axial thrust load.

1.2.3 Turbine

A turbine prime mover was selected to drive the geothermal pump for several reasons. Among these were life, performance, and the inherent performance matching of a turbine and pump. Several turbine design approaches were examined, including a single impulse stage, re-entry, and multi-row velocity compounded staging. For this application the turbine type offering the best potential performance was the multi-row velocity compounded configuration. A two-row stage was selected for the final design.

The turbine stage consists of an inlet nozzle block, two rotating blade rows, and a stator located between the moving blade rows. After expansion through the turbine, exhaust steam must be turned and sent back to the surface. To accomplish this within the available package size, the steam is routed back through the center of the turbine hub section. To minimize the losses of passing the flow through the hub, it was designed with air foil section spokes which act as a fan. Steam flow was assumed to enter the blades axially, and the blade angle was chosen to provide an angle of attack of a positive $3^{\circ}$. At this design condition the fan head rise is equal to the total pressure loss of flow through the fan.

The design criteria used stressed maximum power and efficiency within the constraints of restricted turbine diameter and speed. Again, two turbine configurations were designed, fabricated, and tested. The first, the "A" configuration, was designed to match the power requirements of the 600 GPM pump. Figure 4 is a schematic showing the design geometry. The second, the "B" configuration, was designed for a higher flow rate and output power level corresponding to the 900 GPM pump. Figure 5 is a schematic showing the design geometry for the higher power turbine.

### 1.2.4 Design Parameters

To maximize power capability, an exit isentropic expansion wetness of 5.0 percent was selected with inlet conditions corresponding to saturated steam vapor. From an efficiency standpoint, data is available on velocity compounded turbines operating with 15-20 percent wetness which shows little reduction in efficiency due to the high wetness. Erosion or life data are not available from these high wetness tests. Data on reaction turbines indicates that 10-12 percent wetness can be run with good life characteristics.

A maximum turbine diameter of 6.25 inches was established to match the well casing used in the selected well. The TPU design speed of 17,000 rpm was selected after a trade study of pump NPSH requirements vs. turbine efficiency. The turbine would achieve higher efficiency at higher shaft speed, but the probability of pump cavitation would increase. A 10-percent design stator reaction fraction was then chosen based on a parametric study which examined the effect of stator reaction on overall efficiency. The stator or turning vanes between the first and second rotor were sized based on continuity of flow at this station. Exit angle and height were determined using standard techniques. The remainder of the design geometry was based on continuity and incidence-free operation at the design point.

### 1.2.5 TPU Mechanical Design

The main objective in the mechanical design of the TPU was to obtain a configuration and materials that would provide long unattended life. The major controlling factors were the casing diameter limitation and the need to use surface supplied water for bearing lubrication. The following

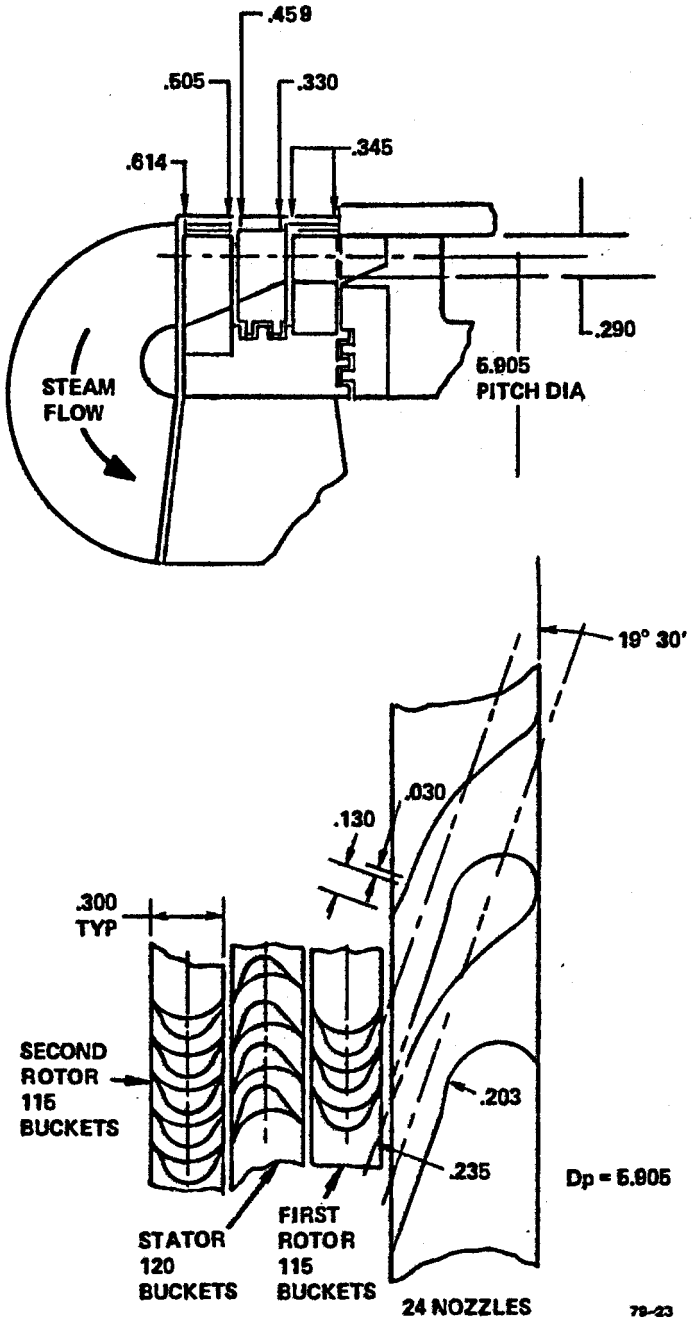


FIG. 4 Turbine design geometry for 20,000 BPD TPU

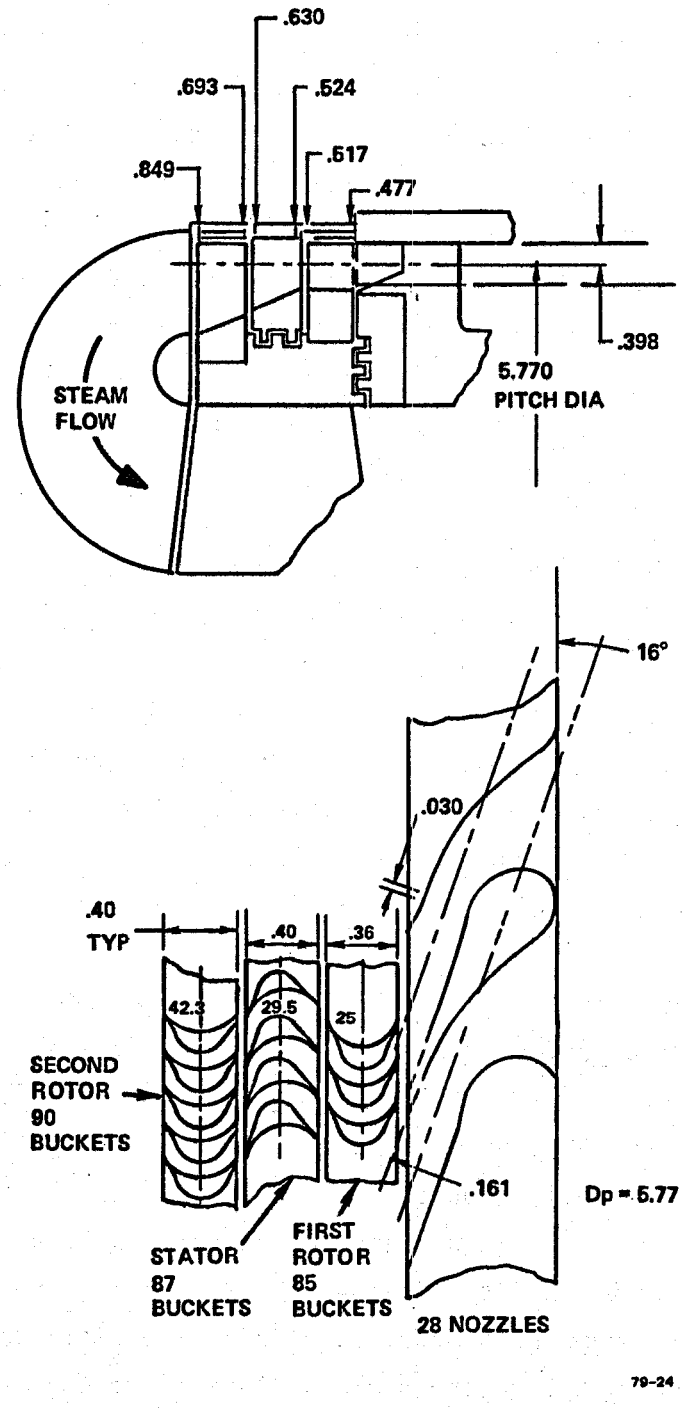


FIG. 5 Turbine design geometry for 30,000 BPD TPU.

sections outline the configuration and selected design factors.

The basic TPU configuration was established early in the preliminary design phase. The rotating assembly utilizes front and back bearing housings to support the thrust and radial bearings. The pump inlet and outer wall structure is a brazed assembly which includes the straightening vanes and vaneless diffuser sections. This assembly is tied to the bearing housings through a threaded joint. The pump assembly is suspended in the well by a 10-3/8 inch pipe, which is threaded to the rear bearing housing and provides the isolation between the well water and the steam supply to the turbine. The steam supply, bearing water, and steam exhaust are brought in at the turbine end with three concentric pipes.

A single shaft supports both the pump impeller and the two-row turbine in a cantilever configuration. The three-element ceramic radial bearing assemblies are located at either end, close to the turbine and close to the pump impeller. A ceramic, six-element hydrodynamic thrust bearing in the middle of the shaft supports the thrust load. For the short periods during startup or shutdown when the thrust load can reverse, a ball bearing is incorporated to handle these reverse loads. Clean water is supplied to the bearings for lubrication and cooling.

The primary rotating shaft seals for the turbine and the pump consist of pressure-balanced face seals. The rubbing parts of these seals are made of silicon carbide ceramic. The face configurations of these seals are designed with wear pads to provide high stiffness and long life. The secondary seals consist of ethylene-propylene "O" rings. The turbine shaft is drilled with bleed holes to allow a small cooling flow to be expelled through the center of the turbine shaft. During pump operation, the bearing cavity is pressurized above pump inlet pressure. This eliminates the possibility of well brine entering through the seal and thus corroding or contaminating the bearing system.

TABLE 2

DOWN-HOLE SYSTEM COMPONENT MATERIALS

| Component | Material |
|---|---|
| Impeller | 15-5 PH |
| Turbine | 15-5 PH |
| Shaft | 15-5 PH |
| Diffuser | 15-5 PH (High Flow), Monel 400 (Low Flow) |
| Secondary Diffuser | Monel 400 |
| Main Pump Housing | Monel 400 |
| Radial Bearing | Alumina Ceramic (99.9%) |
| Thrust Bearing | Alumina Ceramic (99.9%) |
| Seals | Silicon Carbide |
| Elastomer Seals (Static) | Modified Ethylene-Propylene |
| Piping & Tubing | API J-55 Low Carbon Steel |

A static seal has been incorporated to seal between the pump and the I.D. of the protective housing. This housing has a nominal 7.921-inch I.D. The seal subassembly is mounted over the inlet nose of the pump housing. The sealing members consist of five John Crane V-rings locked in place by a sleeve. A steel sealing ring is located on either end of the V-ring.

### 1.2.6 Materials

The primary material choice was monel because of its low susceptibility to corrosion, cracking, and heavy pitting in brine liquids. Like most of the materials exhibiting the greatest corrosion resistance in the geothermal regime, its mechanical strength properties are low. Laboratory tests of the higher strength metals, such as vanadium alloys, stellites, and super alloys (Rene 41), have revealed their susceptibility to various forms of corrosive attack, or stress cracking, rendering them unsuitable for highly stressed applications. High purity titanium has shown promise, but it is of borderline mechanical capability. Higher strength alloyed titanium may require expensive, corrosion-resistant coatings.

An extensive material study showed the material best suited for highly stressed duty in a non-oxidizing chloride environment to be 15-5 PH stainless steel. Thus the turbine wheel, the pump impeller, and their common shaft are made from this material. The selected material for the highly stressed components, 15-5 PH, is a precipitation-hardened alloy exhibiting good strength capability and acceptable corrosion resistance. Its cost, formability, weldability, and brazing compatibility are good, and it requires non-complex thermal treatment processes. Table 2 shows the selected materials for major down-hole system components.

## 1.3 SURFACE SYSTEM

The above ground support hardware which closes the pumping system loop is referred to as the surface system. The surface system is a skid-mounted assembly for condensing the turbine exhaust steam and for supplying boiler and bearing water. It also serves as a means to start, control, and stop the down-hole turbine pump unit. The skid assembly weighs approximately 10,000 pounds and is transportable aboard a flat-bed trailer. All hardware that was installed on the surface system is commercially available.

## 1.4 DOWN-HOLE PIPE STRING

The importance and complexity of the design and operation of the down-hole pipe string was recognized early in the program. This aspect of the system, encompassing the general field of 2-phase flow, was and still is the least understood part of the whole loop. Pertinent research data, let alone reliable design guidelines, were not available for this program.

The approach taken therefore was not to attempt to optimize the performance of the down-hole pipe string, but rather to select a configuration that seemed to have a good chance of working and was relatively easy to implement. Experimental results and parametric trade-off studies conducted during this program indicated that further progress in this area would be a major contribution to improved pumping system performance.

### 1.4.1 Geometry

The down-hole boiler consists of a liquid preheater annulus and an evaporator annulus with the preheater beginning at the wellhead and being separated from the evaporator by a circular plate with carefully sized orifices. The pipe sizes for the down-hole boiler were selected on the basis of pressure drop calculations using minimum wall thicknesses suitable for flush joint low-pressure-drop couplings. The boiler was formed by the pipe sizes shown in Fig. 6, with the hot brine flowing upward between the 12.615-inch I.D. well casing and the boiler pipe. The figure shows the

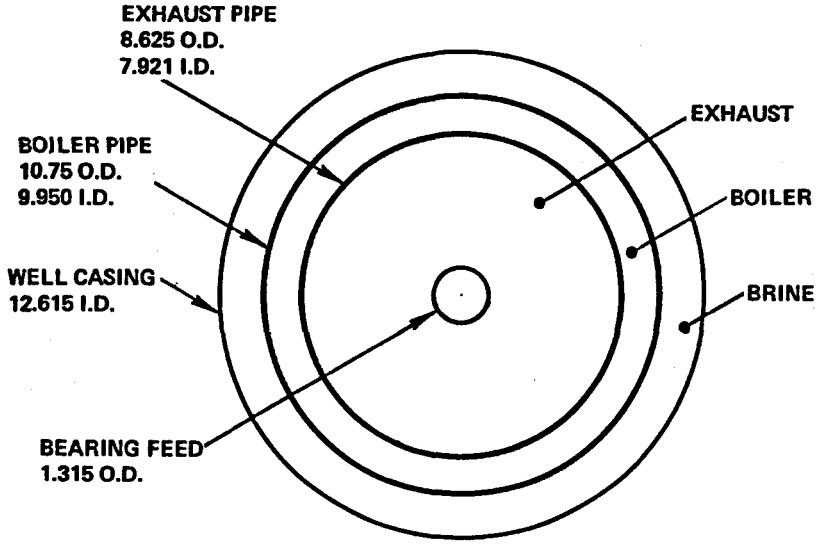


FIG. 6 Downhole boiler geometry.

10.75-inch O.D. evaporator pipe which is located below the 9.625-inch O.D. preheater pipe. The outer pipe size is reduced in the preheater to increase the water velocity and heat transfer coefficient. The preheater is approximately 42 feet long, and the evaporator section is 808 feet long, for a total boiler length of 850 feet.

### 1.4.2 Evaporator Concept and Heat Transfer

The first portion of the evaporator (boiling until 80 percent quality) was designed as a falling film evaporator. This type of heat exchanger was chosen because it is characterized by large heat transfer coefficients and low pressure drops, since the fluid does not fill the tube but rather flows in a thin film down the tube wall. Normally, these devices are built as a tube or multiple tubes rather than an annulus, as is the case being analyzed here. The major problems associated with falling film evaporators are insuring proper distribution of the liquid film around the pipe at the top and maintaining complete wetability of the tube. Normally, falling film evaporators are not used to boil a fluid to 100 percent vapor, but they have been designed to do so. The literature indicated that vapor qualities of 80 percent should be readily achievable with a falling film evaporator. Heat transfer coefficients were calculated using relations found in the literature for a falling film evaporator for qualities less than 80 percent. The heat transfer film coefficients used in the analysis were weighted averages of the calculated local coefficients. The total required boiler length is the sum of the length of its four sections, and the heat transfer calculations predicted its length to be 600 feet, which is 71 percent of the available 850 feet.

At the bottom of the evaporator where the boiler quality is approximately 100 percent, the evaporator film coefficient approaches 48 Btu/hr-ft$^2$-$^o$F. The larger coefficient of the turbine exhaust flow (because of the 90 percent quality) and the larger available temperature difference between the evaporator and the exhaust could result in more heat being transferred from the evaporator to the turbine exhaust than is transferred into it from the brine. This would

result in liquid water running down the turbine inlet pipe and entering the turbine, thereby reducing efficiency. Condensation of the turbine inlet steam on the cold exhaust pipe was minimized by insulating the lowest 100 feet of the exhaust pipe. Above this level the evaporator film coefficient is large enough to allow net heat transfer into the evaporator. Insulating the full length of the turbine exhaust pipe is not justified because the large heat transfer area and temperature differences will result in approximately the same heat leak into the turbine exhaust with any reasonable insulation or with no insulation at all. Although spray-on insulation was investigated, it did not appear reasonable to use it on the lower exhaust pipe because it cannot be applied thickly enough to produce an adequate thermal barrier. The selected approach was to use a 1/16-inch thick dead steam space on the inside of the exhaust pipe to provide the required insulation. This dead steam space was provided by installing 19-foot-long sleeves into the lowest five joints of 8-5/8 inch casing and welding them shut at the top.

### 1.4.3 Lube Pipe String

The TPU bearings are lubricated with filtered, demineralized water supplied from the surface system. Water is pumped down the center 1-1/4 inch pipe of the three concentric pipes shown in Fig. 6. The turbine exhaust steam cools the lube water as it approaches the TPU. Immediately above the TPU the center pipe is terminated, and the water is ducted to the center cavity. In addition to carrying water, the lube pipe serves a secondary function as an acoustic and electromagnetic (EM) signal transmission channel from the down-hole instrumentation to the surface. However, being lightweight, it is very flexible and will tend to lie along the surface of the 8-5/8 inch casing. To avoid shorting the EM signal to the exhaust pipe, rubber insulators were installed on the lube pipe approximately every 10 feet.

### 1.4.4 Turbine Exhaust

The turbine exhaust steam is ducted to the surface through the annulus formed by the I.D. of the exhaust pipe string (7.921 inches) and the O.D. of the bearing lube line (1.315 inches). The calculated pressure drop of the exhaust steam at a turbine flow of 2.0 pounds and 1.0 GPM of bearing leakage is 10.0 psid. The calculation assumes a surface condensing pressure of 15 psia.

## 1.5 TEST WELLHEAD EQUIPMENT

Connection of the downhole pipe string to the surface system and brine handling system was achieved by the installation of a specially manufactured wellhead usually referred to as the Christmas tree. Fig. 7 is an assembly drawing of the three-section wellhead designed for these tests. The lower 6-inch ANSI flange provides an outlet for the brine, while the upper 6-inch ANSI flange provides an outlet for the turbine steam exhaust. The boiler feedwater entry is in Sec. B and is a 2-inch NPT threaded port. The bearing lubrication water enters through the top of Sec. C via a 1-inch NPT threaded port in the bearing line hanger which is located in this section.

The wellhead schematic also shows how the concentric pipe strings are located in the wellhead bore. The entire string is hung from a 9-5/8 inch casing hanger which is located in the lowest section. The hanger fits into a tapered recess, and the dog nuts are tightened to prevent the string from being blown out of the hole.

## 1.6 BRINE TRANSPORT SYSTEM

To better understand the brine transport system, refer to Fig. 8, which traces the path of the brine from the producing well to the re-injection well. As discussed previously, the hot brine flows or is pumped up the annulus formed by the well casing and the boiler pipe. At the surface of the well, the produced brine exits the well via an 8-inch flanged connection on the lower spool of the three-spool wellhead (Christmas tree) assembly.

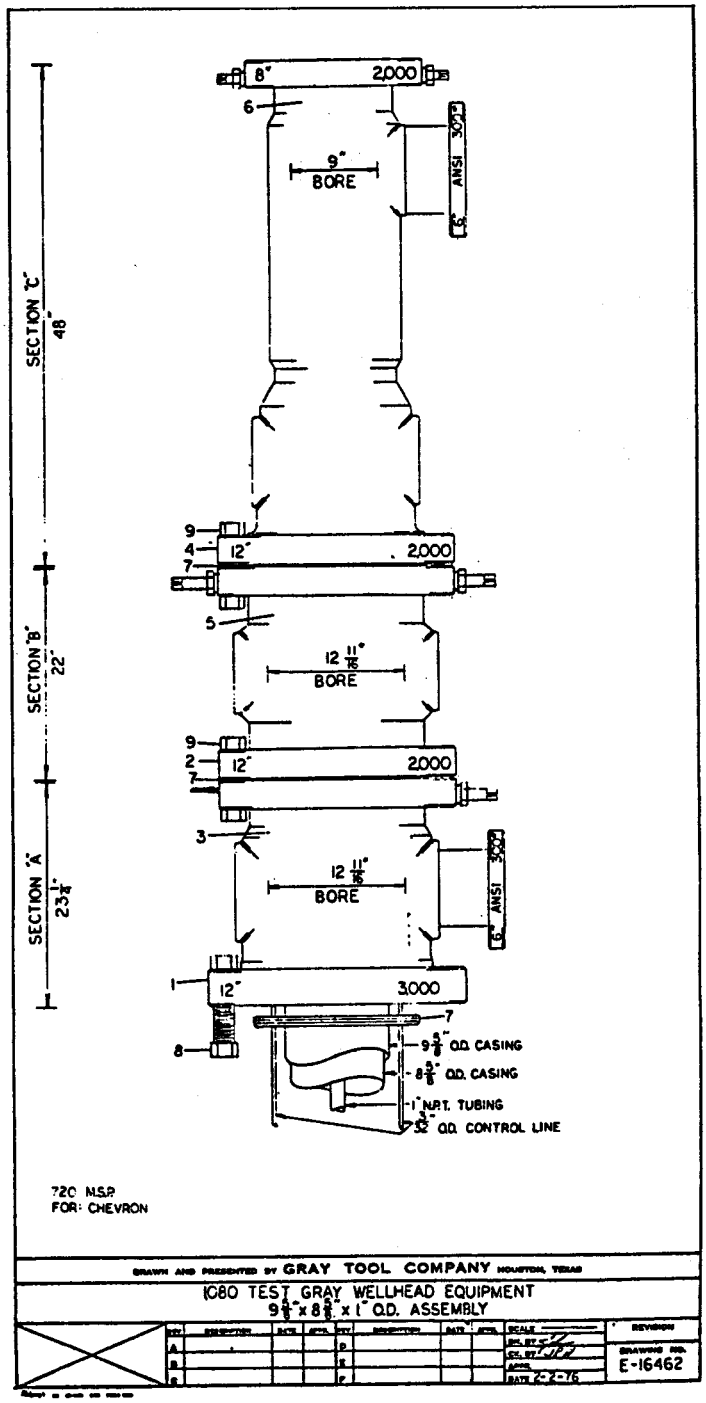


FIG. 7 Test wellhead assembly.

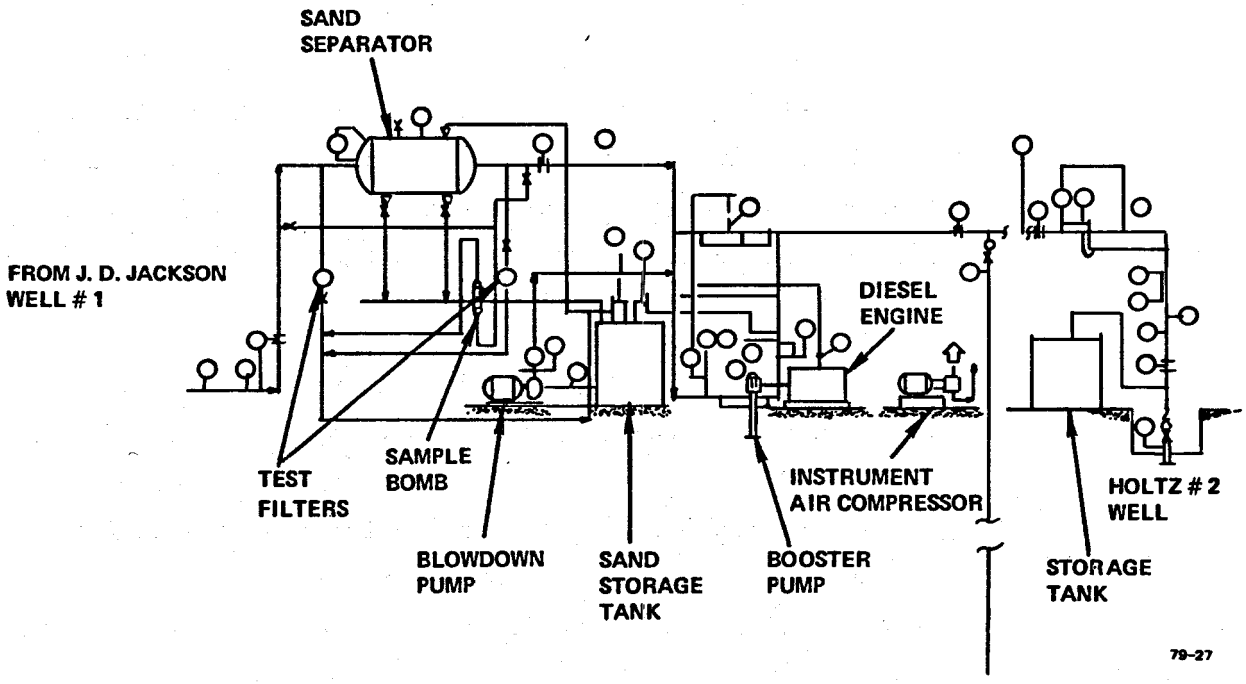


FIG. 8 Surface piping and instrumentation layout.

The brine flows through two 8-inch valves before it is directed into a 1,000 gallon baffled cylindrical vessel. The first valve, as is usual in brine field practice, is simply a shut-off valve with flow control being handled by the second valve. In our tests, the second valve was usually left fully opened and the controller at the re-injection well or the well itself was used to control flow. This valve was only used to throttle flow when data for a head-flow characteristic curve was being run. Located between these two valves were various pressure and temperature instruments used in monitoring brine parameters.

The large volume of the baffled cylinder slows down the fluid velocity and encourages sand deposition to occur therein. The "clean" brine exits the de-sander and is directed through a conventional sharp-edged orifice with flanged taps before being routed to the inlet of the surface booster. The booster pump is a 10-stage, 1,200 GPM vertical centrifugal pump driven by a diesel through a right-angle drive and a manually operated clutch.

In addition to this hardware, two 500-barrel portable storage tanks were rented and installed. One tank was used for storage of canal water which was used to "kill" the well. The other tank served a multitude of purposes, among the most important being holding weighted water (with either calcium chloride or sodium chloride added) used to "kill" the well during workover. It was used as an evacuation tank when the pipe strings were being cleared of water, and as a sand holding tank when the de-sander was blown down or sand samples were taken.

The brine leaving the booster pump is then directed out of the test site through 1,500 feet of 6-inch line which terminates in a tee. From here it flows another 3,000 feet through 6-inch and 10-inch pipe to the re-injection well where it can either be directed through a flow controller or bypassed around it. Expansion loops are provided at regular intervals along the pipe route to minimize pipe stresses. Only the pipe within the test site is insulated to protect employees and visitors from being burned. The pipe outside the test site has warnings painted in both English and Spanish at regular intervals informing of the potential hazard.

# SECTION 2

# FIELD TEST

## 2.1 FIELD TEST CONDITIONS

The field test was conducted during 1976 in the Heber KGRA on a site jointly controlled by Chevron Resources, San Diego Gas and Electric, and Magma Power, with Chevron acting as the field operator.

The brine temperature at the pump setting depth of 850 feet was approximately 350°F. The total dissolved solids content was approximately 15,000 parts per million, consisting principally of chloride salts.

During the field test phase, system operating time exceeded 1000 hours, with one continuous run of nearly one month. The emphasis of the test was to prove operational feasibility and, by using the geothermal well itself as the only acceptable test arena for equipment and materials, uncover problems that could then be investigated in a more conventional laboratory environment.

## 2.2 MATERIAL & MECHANICAL PROBLEMS DURING FIELD TEST

Problems encountered during the tests were principally those of materials or material-related mechanics.

The turbine-pump unit and the surface systems, which were developed and engineered for the geothermal environment, showed few problems of this nature, and there were rather obvious solutions to the one or two that did occur. However, severe and continuous problems were encountered with

standard down-hole oil field equipment used in the geothermal well - virtually every piece of it failed in one way or another. This is not an indictment of the equipment, since it was not designed for the purpose; but it does illustrate that the technology of the oil field is in many cases unsuitable for geothermal energy.

### 2.2.1 Threaded Down-hole Pipe Connections

Although we used the most expensive and reputedly the best available, pipe connections were our single worst problem. Not only were leaks epidemic, but uncoupling of the pipes after being immersed in the brine was difficult and time consuming. As a final expedient we welded the pipes together as we inserted the string in the well.

### 2.2.2 Fixed Packer

To establish a seal between the pump and well casing, a device known as a fixed packer was used. The packer is anchored vertically to the well casing by serrated wedges called slips, and an ethylene propylene element seals the packer structure to the casing. A smooth vertical bore at the center of the packer receives a sliding tube that is attached to the pump and contains Viton "A" seals that seal to the packer bore. This arrangement permits an up and down movement of the pump due to expansion and contraction of the pipe string suspending the pump.

Two problems surfaced with this packer:

- Some two months after setting, it slipped fifty feet down the casing and came to rest at the elevation where the well casing reduces in size. This same malfunction had previously occurred with the design of packer in a nearby geothermal well. In our case, the sealing element continued to be effective.

- The Viton "A" seals became hard and brittle within a few days exposure to the brine and were frequently found broken upon removal from the well.

### 2.2.3 Elastomers

Two elastomer types were used downhole; a peroxide cured ethylene propylene, and Viton A. When trapped in a proper "O" ring groove and left undisturbed, no failures were experienced, although Viton lost its resiliency in a short time and ethylene propylene had little physical strength at 350°F. When subjected to abrasion or abuse, both compounds suffered considerable damage. It was our conclusion that at the time of the test two years ago, no dependable elastomer for 350°F. or above existed.

### 2.2.4 Pump Impeller

The impeller, made of 15-5 heat treated stainless steel, experienced some erosion of its leading edges. Even though this probably occurred during the early hours of operation while the well was producing large amounts of sand, and although performance was not affected, we believe that a harder alloy should be selected. No corrosion of the impeller was observed.

### 2.2.5 Corrosion

No significant corrosion of any of the metals exposed to the brine was observed, including the mild steel pipes. This was probably the favorable result of keeping the brine under pressure and preventing it from flashing.

### 2.2.6 Fouling

Fouling was noticeably absent on all down-hole surfaces during regular operations. The use of an improper kill fluid did cause one incident of deposits on the boiler surface, however.

## 2.3 CONCLUSIONS

- Keeping the brine under pressure to prevent flashing is an effective way of reducing down-hole corrosion and fouling, at least in the Heber reservoir.

- Silicon carbide is a good face seal material where contamination is present.
- 99.9 percent purity alumina is an excellent material for hydrodynamic bearings.
- Ethylene propylene is an acceptable material only for non-sliding "O" rings at this temperature in brine or steam. Viton A is not acceptable.
- Off-the-shelf oil well hardware is generally unsatisfactory without alterations.
- A hardened material is needed on the leading edge of the impeller.
- Except for the impeller, no wear-out syndrome in the turbine-pump was observed, and a down-well lifetime of a year seems a safe prediction under the conditions of a Heber-type resource.

# Materials Selection for Geothermal Steam Turbines

Joseph A. Cameron
Manager, Materials Engineering
Elliott Company
Division of Carrier Corporation
Jeannette, PA 15644

# Materials Selection for Geothermal Steam Turbines

Selection of materials for steam turbines using geothermal steam is fundamentally similar to the selection of materials for turbines operating on steam from fossil fuel fired boilers with some modification in importance attached to certain properties and characteristics of these materials. For example, geothermal steam turbines do not operate in the range where long time high temperature properties of materials need to be considered. Conversely, resistance to sulfide stress cracking and stress corrosion cracking may be more important in the case of geothermal steam than with more conventional boiler generated steam.

In the evaluation and selection of materials for geothermal steam turbines it is necessary to consider the following properties and characteristics:

1. Tensile properties
2. Modulus of elasticity
3. Corrosion resistance
4. Erosion resistance
5. Fatigue strength
6. Coefficient of thermal expansion
7. Susceptibility to brittle fracture (toughness)
8. Material damping
9. Specific heat
10. Thermal Conductivity
11. Hardenability
12. Weldability

Each of the above items will be discussed separately using the same identifying numbers as above:

1. Tensile properties, especially the yield strength, must be known to select materials having adequate strength to withstand the stresses that will be imposed in service. Generally the operating stress is higher for rotating parts than for stationary components.

2. The modulus of elasticity must be known in order to compute operating stresses and to determine the deflection that will be encountered when a given stress is applied.

3. Corrosion resistance, including resistance to sulfide stress cracking and stress corrosion cracking, is very important in the case of geothermal steam turbines. These problems are considered carefully in conventional steam turbines, but need to be even further emphasized in the case of geothermal steam. While geothermal steams do not often contain caustic soda, they can be high in hydrogen sulfide, chloride, and other corrosive agents which might give rise to premature and unexpected failures. These same contaminants can cause corrosion in the wet regions of a turbine or during the time the turbine is on standby operation if it is not blocked in such a way that steam cannot enter.

4. Erosion resistance is a factor in the selection of materials and protection systems in the wet regions of steam turbines. Since virtually the entire turbine is wet in geothermal steam turbines, it is important to use materials of adequate resistance to erosion. Erosion of turbine parts may also be accelerated in geothermal steam due to the presence of contaminants which make the moisture more aggressive.

5. Fatigue problems due to resonance are less likely in turbines driving constant speed generators than in mechanical drive turbines which may be called upon to operate over a wide range of speed. Nevertheless, in geothermal steam where pitting corrosion is more likely to be encountered than in steam from fossil fuel fired boilers, fatigue is quite important.

6. The coefficient of expansion determines the dimensional change which will take place in a turbine as the temperature increases from ambient to operating. The changes are less for geothermal steam turbines than for other turbines operating at higher temperatures, but this effect must still be taken into account.

7. Susceptibility to brittle failure, (toughness) does not usually present a problem in geothermal steam turbines. It should, however, be examined, especially for new materials to avoid possible problems.

8. Damping is considered in stress calculations, particularly with regard to vibration which may take place in turbine buckets. Conventional turbine bucket materials are good in this respect.

9. Specific heat and thermal conductivity like the coefficient of
10. thermal expansion are used in the computation of dimensional changes and thermal stresses.

11. Hardenability is important to the turbine manufacturer in selecting materials that will respond to heat treatment in the section thicknesses involved. This property is not ordinarily of interest to the turbine user.

12. Weldability is considered in selecting materials for parts which may be fabricated by welding or where repair welding may be performed as a field operation.

Turbines for use on geothermal steam which have been built to date have been made from the same materials as would be used in turbines using steam from fossil fuel fired boilers. The compositions of the materials referred to in the following paragraphs are listed in Table 1:

1. Rotating buckets have been made from 12% chromium steel, AISI Type 403 or 410. The standard analysis is frequently modified slightly to minimize the occurrence of ferrite in the microstructure. The buckets of stages operating where there are substantial amounts of moisture are sometimes fitted with Stellite strips on the back side of the leading edge to minimize erosion by the moisture.

2. Diafram blades have been made from a 12% chromium steel, AISI Type 405. Usually this non-hardening grade of 12% chromium steel is used to improve weldability of fabricated diaframs or castability where the diafram centers and outer rings are made from cast iron.

3. Turbine rotors and disks have been made from carbon steel and low alloy steel such as AISI 4340, ASTM A517 Type B or F, and ASTM A470 Class 4, 6, or 8.

4. Sleeves on the shaft between disks have been made from either a medium carbon steel or a medium carbon alloy steel such as AISI 4140 or 4340.

5. Shafts seals have been made in at least two ways. One method involves the use of thin strips (0.012" thick) of 12% chromium steel (AISI Type 410). The other method utilizes austenitic nickel alloy cast iron (D2C Ni Resist) seals.

6. Casings operate at low temperatures and low pressures. Cast or fabricated carbon steel has been used. In some cases AISI Type 304 stainless steel liner strips have been used in the casing to protect from erosion due to moisture being thrown off the rotating buckets.

Even in the case of fossil fuel fired boilers there may be a considerable difference in the quality of steam from one plant to another. Steam quality varies with such things as composition of the raw water, feed water treatment employed, percentage of make-up required, mode of operation, etc. In the case of geothermal steam, the variations are much greater. Variations in geothermal wells occur with time and from one location to another. To illustrate the substantial differences, Table 2 shows the range of impurity concentrations in domestic goethermal waters. The acidity of these geothermal waters can be very high, the pH can be as low as 1.8.

Variations in separated geothermal steam are much less extreme than those in geothermal waters because the solids in solutions in the water which cause the greatest variations should not be present in the steam. Efficiency of separation has a substantial influence on steam quality. Non-condensible gases may raise or lower the pH. The greatest variations will occur in the first condensate to form where the concentrations of dissolved gases will be greater than when more of the steam has condensed.

As pointed out previously, corrosion and erosion resistance are important properties of steam turbine bucket materials. It is usual in conventional turbines to provide erosion shields on turbine buckets operating over about 1000 feet per second and with moisture contents above 6-8%. It may be necessary in aggressive geothermal service to adopt more conservative criteria and use moisture catchers. It has also been suggested that erosion may be reduced by limiting the tip speed. This is a solution which, while effective, could limit performance and increase the cost of turbines.

Because of the aggressive nature of the steam and water, general or pitting corrosion may occur on turbine buckets under conditions of temperature and pressure where these problems would not ordinarily be encountered.

A phenomenon usually called stand-by corrosion occurs in turbines when steam is allowed to leak into a machine which is not in service. The steam then condenses and pitting corrosion results. This problem will undoubtedly be more acute with geothermal turbines because of the contaminants which will make the condensate more aggressive than is generally the case with steam from conventional fossil fuel fired boilers. These contaminants, for example hydrogen sulfide, are even more aggressive in the presence of oxygen. Geothermal steams usually do not contain oxygen. It is possible, however, that air containing oxygen may leak into a turbine during periods of standby. If there is condensate from a hydrogen sulfide bearing geothermal steam in a turbine and this leakage of air occurs corrosion will be accelerated. This problem may be avoided by arranging the piping (Figure 1) to prevent the leakage of steam into the turbine when it is not in operation and by purging the turbine when it is shut down with a non-reactive gas such as nitrogen.

Fatigue failures of rotating buckets in geothermal steam turbines have occurred due to fatigue cracks propagating from corrosion pits. Pits on one such bucket are shown in Figure 2. With the exception of standby attack, pitting corrosion rarely occurs in conventional turbines. This problem, like that of moisture erosion, could be alleviated by limiting the tip speed, but it would be preferable to find other solutions.

Fouling due to deposition of solids can occur in nozzles with loss of performance. Fouling, which causes an accumulation of solids under the shroud of steam turbine buckets, can also cause unbalance. This problem may be reduced by the use of lashing wires rather than shrouds. Where it is possible to design around the use of these damping devices their elimination will further reduce the fouling problem.

It has been reported that there have been failures in geothermal steam turbine buckets protected with Stellite strips due to the poor resistance to corrosion of the silver brazing alloy used

to attach the strip. This material would have poor resistance to corrosion in geothermal steam in bulk, but the access of the brazing alloy to the steam is very limited, and there may be an alternate explanation.

Attaching the Stellite strip by brazing requires heating the material locally to about 1400°F. This is enough to cause some degree of hardening in the material immediately underlying the strip. Many thousands of buckets have been protected in this manner without difficulty when operating on conventional steam. In the case of many geothermal steams, however, the steam is contaminated with hydrogen sulfide, and conditions at the location of the attachment of the Stellite strip to the turbine bucket may favor sulfide stress cracking. This problem may be avoided by using a post brazing heat treatment at 1100-1150°F to reduce the hardness of the heat affected zone.

In order to avoid sulfide stress cracking due to hydrogen sulfide it is frequently recommended that materials be used having a maximum yield strength of 90,000 psi and/or a maximum hardness of Rockwell C22. Both buckets and disks, especially the latter, have been used successfully in geothermal steam turbines with yield strengths well above this figure. The yield strength of some of the disks has been about 120,000 psi. It is apparent that the conditions of operation in these turbines have been less severe than in applications such as casings in sour crude oil wells where the more restrictive limits may be needed.

Materials Selection for
Geothermal Steam Turbines

Table 1

Chemical Analysis of Materials Used in Turbines

| Grade | C | Mn | Ni | Cr | Mo | V | Others |
|---|---|---|---|---|---|---|---|
| Type 403/410 | 0.10 | 0.6 | 0.2 | 12.0 | 0.1 | ---- | ---- |
| Type 405 | 0.06 | 0.6 | 0.2 | 12.0 | 0.1 | ---- | 0.2 Al |
| AISI 4140 | 0.40 | 0.8 | ---- | 1.0 | 0.2 | ---- | ---- |
| AISI 4340 | 0.40 | 0.8 | 1.8 | 0.8 | 0.25 | ---- | ---- |
| ASTM A470 Cl. 4 | 0.24 | 0.4 | 2.8 | 0.6 | 0.3 | 0.04 | ---- |
| ASTM A470 Cl. 6 | 0.24 | 0.4 | 3.5 | 1.5 | 0.4 | 0.08 | ---- |
| ASTM A470 Cl. 8 | 0.30 | 0.8 | 0.5 | 1.2 | 1.3 | 0.25 | ---- |
| ASTM A517 Type B | 0.18 | 0.8 | ---- | 0.5 | 0.2 | 0.05 | 0.02 Ti, 0.002B |
| ASTM A517 Type F | 0.15 | 0.8 | 0.8 | 0.5 | 0.5 | 0.05 | 0.3 Cu, 0.002B |
| D2C NiResist | 2.6 | 1.8 | 22.5 | ---- | ---- | ---- | ---- |
| Type 304 | 0.05 | 1.2 | 9.0 | 19.0 | ---- | ---- | ---- |
| Carbon Steel | 0.25 | 0.7 | ---- | ---- | ---- | ---- | ---- |

Table 2

Variations in U.S. Domestic Geothermal Waters

| Contaminant | Range of Concentration (ppm) |
|---|---|
| Silica ($SiO_2$) | 16-96 |
| Sodium (Na) | 9-6500 |
| Ammonia ($NH_3$) | 1-1400 |
| Calcium | 2-9200 |
| Chloride (Cl) | 1-124000 |
| Sulfate ($SO_4$) | 3-5700 |

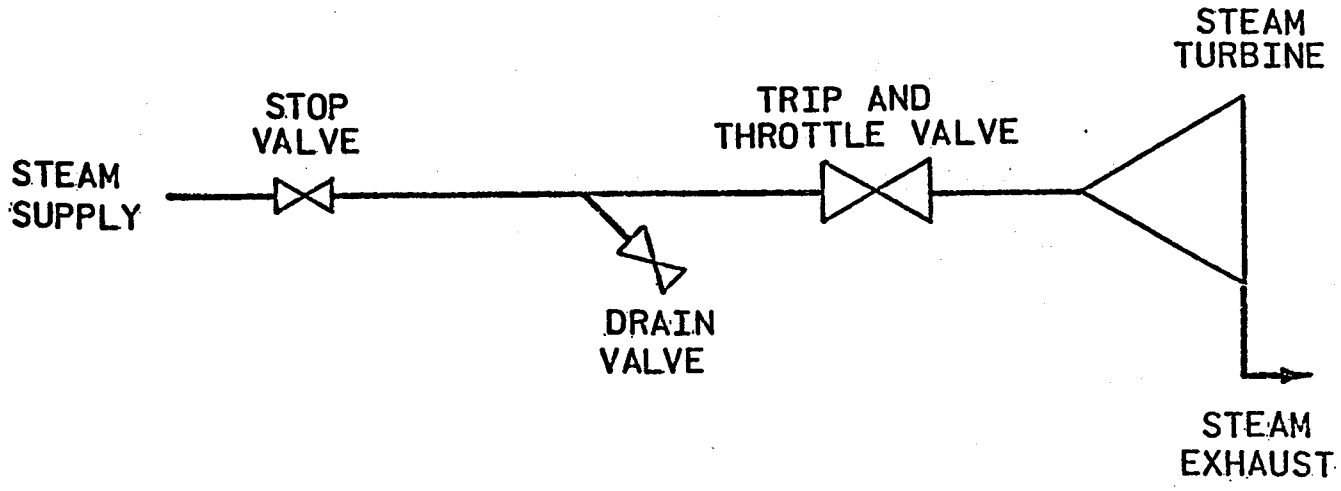


Figure 1

Example of piping arrangement used to avoid standby corrosion in steam turbines.

Materials Selection for
Geothermal Steam Turbines

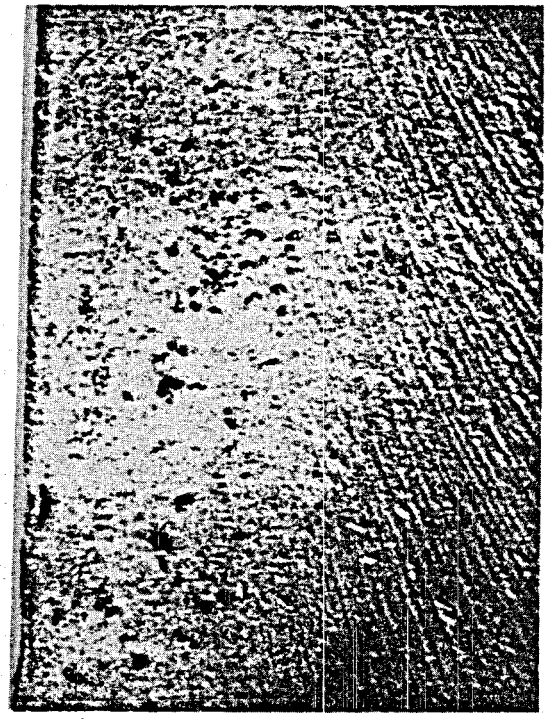

Figure 2

Corrosion pits in bucket from turbine operating on geothermal steam. In service 2-3 years. Also shows mechanical damage on leading edge (on left).

## Bibliography


1. Toney, S., Cohen, M. and Cron, C. J. "Metallurgical Evaluation of Materials for Geothermal Power Plant Applications" Geothermal Energy September (1977), pp. 8-38.

2. Marshall, T. and Hugill, A. J. "Corrosion by Low Pressure Geothermal Steam", Corrosion, Vol. 19, (1957), pp. 329t- 365.

3. Yoshida, H. "Corrosion Control in Geothermal Steam Turbines", Tokyo Shibaura Electric Company publications.

4. Dodd, F. J., Johnson, A. E., and Ham, W. C., "Material and Corrosion Testing at The Geysers Geothermal Power Plant", Second U. N. Symposium on the Development and Use of Geothermal Resources, San Francisco, CA., May, 20-30, 1975.

5. Dodd, J. F. and Ham, W. C., "Corrosion Studies on The Geysers Geothermal Steam Power Plant", Golden Gate Materials Conference, San Francisco, CA., January 22, 1975.

6. Tolivia, E. M., Hoashi, J. M., and Miyazaki, M. "Corrosion of Turbine Materials in Geothermal Steam in Cerro Prieto, Mexico", Second U. N. Symposium on the Development and Use of Geothermal Resources, San Francisco, CA., May 20-30, (1975)

7. Tokyo Shibaura Electric Co., "Toshiba Geothermal Power Plant", Sept., 1969.

8. Curran, R. M., Seguin, B. R. Quinlan, J. F., and Toney, S. "Stress Corrosion Cracking of Steam Turbine Materials", Southeastern Electric Exchange Conference, April 21-22, 1969.

9. McCord, T. G., Bussert, B. W., Curran, R. M., and Gould, G. C. "Stress Cracking of Steam Turbine Materials". NACE Paper No. 107 (1975).

10. Greer, J. B. "Factors Affecting the Sulfide Stress Cracking Performance of High Strength Steel". NACE Paper No. 55 (1973).

11. Keller, H. F. and Cameron, J. A. "Laboratory Evaluation of Susceptibility to Sulfide Cracking". NACE Paper No. 99 (1974).

12. Warren, D. and Beckman, G. W. "Sulfide Corrosion Cracking of High Strength Bolting Material". Corrosion, 13, pp. 631t - 641t (October, 1957).

13. Splittgerber, A., "An Interesting Case of Corrosion of Steam Turbines". Vom Wasser, Vol. 17 (1949), pp. 146-149, Brutcher Translation 2925.

14. Highley, L., and Schnarrenberger, W. R. "Prevention of Standby Corrosion in Power Plants". Corrosion, Vol. 8, No. 5, (1952) pp. 171-177.

# SUMMARY OF FIRST 12 MONTHS PROGRESS ON GEOTHERMAL ELASTOMERIC MATERIALS PROGRAM DOE CONTRACT EG-77-03-1308

by

A. R. Hirasuna
L'Garde, Inc.
1555 Placentia Avenue
Newport Beach, California 92663

The following is a summary of the technology developed by L'Garde, Inc., during the first 12 months effort under the Geothermal Elastomeric Materials (GEM) Program, Contract Number EG-77-03-1308.[1] The fundamental objective of the program is to develop elastomers for the downhole geothermal seal application. Figure 1 shows the overall flowchart of the Program. The crosshatched box indicates where future candidates will enter the evaluation system.

Seals are most commonly made from elastomers because it is the most practical seal material. They are economical, relatively very inexpensive except for a minority made from exotic polymers and are reuseable except for very severe environments. They are very reliable and forgiving with respect to installation and manufacturing tolerances of the mating parts to be sealed. Because of the forgiving nature of elastomeric seals, they can be successfully installed by unskilled mechanics and they can be installed in field environments. On the other hand, metal seals are extremely sensitive to contamination and handling. L'Garde's experience with gold plated metal K-seals on the Simulation Test indelibly imprinted on application for elastomeric seals. Extreme care is required for the metal

[1] Hirasuna, A. R., et al, "Geothermal Elastomeric Materials, Twelve-Months Progress Report for Period 1 October 1976-30 September 1977," December 1977, SAN/1308-1, L'Garde, Inc., Newport Beach, California 92663.

FIGURE 1 -- PROGRAM FLOWCHART

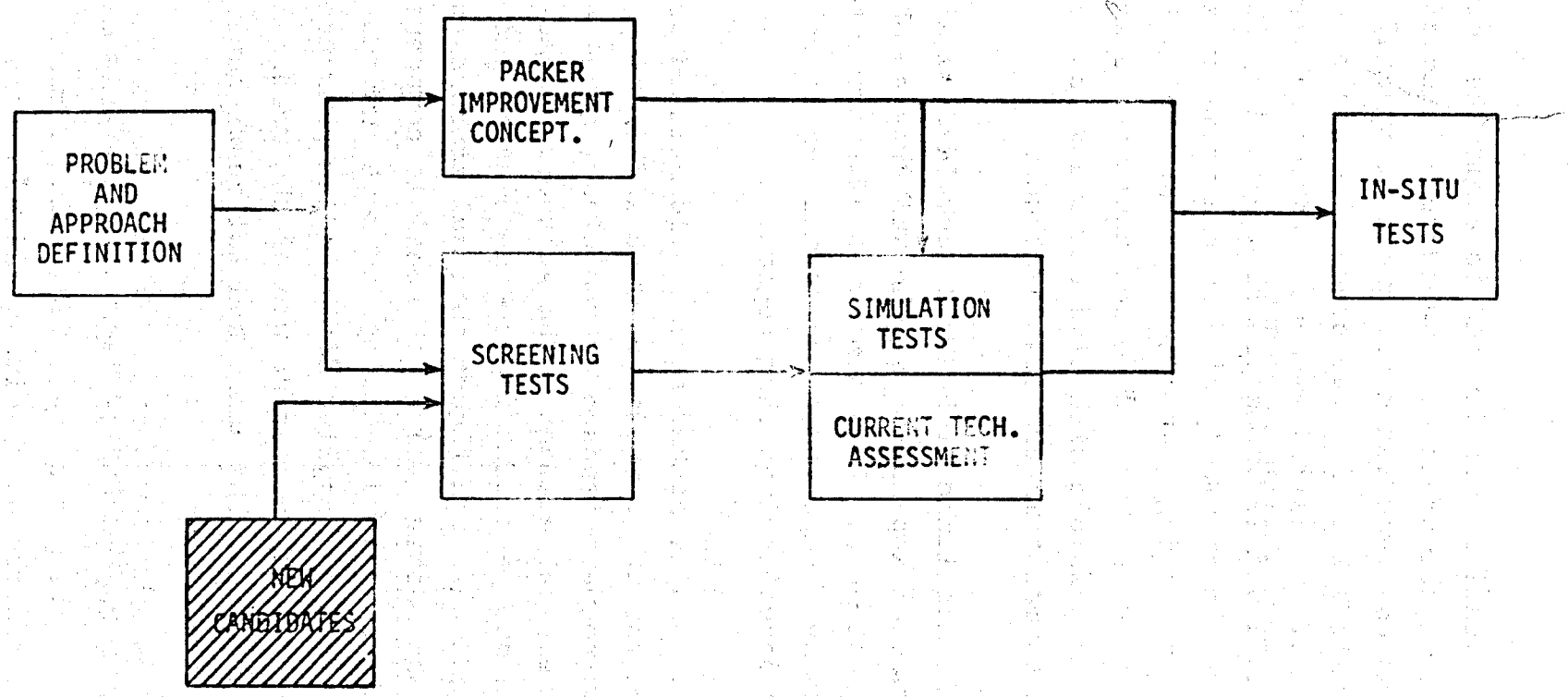

seals to clean the sealing surfaces and to apply the correct and evenly distribute the preload. Furthermore, each of the three seal applications required development of special procedures for each unique set of circumstances to assure that the seal is delicately installed without abrasion or bumping. Elastomers have the added advantage of flowing and conforming to irregularities while providing elastomeric resistance to continued flow after seating. On the other hand, plastic seals continue to flow after seating and do not achieve the stable equilibrium which is possible with elastomers and must be constantly recinched to maintain the sealing force.

In view of the multitude of benefits provided by elastomeric materials in seal applications, the GEM Program objective fulfills an important need. Development of elastomers to meet requirements of higher temperature geothermal environments will extend their benefits into that regime.

The geothermal casing packer seal was identified as the target application for the current research and development. The geothermal environment imposes extraordinary requirements on the casing packer seal element. The geothermal temperature and chemistry both substantially reduce the elastomeric seals ability to withstand the significant internal stresses which are generated in the rubber: 1) as the seal is compressed endwise to cause it to expand radially and seat against its OD and ID, and 2) from the applied differential pressure. Because of the severe and complex nature of the materials and structural requirements of the seal, special tests have been designed and developed.

A three-step graduated testing and evaluation of material candidates is used. The first step, "Screening Tests," is a battery of tests performed on specimens made from sheet stock. The tests include standard ASTM tests and a special test de-

veloped by L'Garde, the Extrusion Resistometer or Punch Test. It tests the extrusion resistance of the candidate materials, a key property for geothermal packer seals. The purpose of the Screening Tests is to quickly and efficiently filter out the less qualified materials candidates to maximize coverage of potential materials and minimize the amount of more expensive subsequent testing and evaluation.

The second step, "Simulation Tests," is a laboratory equivalent of downhole operational conditions. Under the Screening Tests chemically aged flat samples are run through the battery of tests after they have been thermohydrochemically aged in the autoclave. In contrast, the Simulation Test uses a fullscale, 4-inch packer seal as the test specimen and simultaneously submits it to the operational chemistry, temperature, pressure, differential pressure, and the seating forces for the required duration of the test. Based on comments from oil tool personnel regarding the post mortem specimens, the fixture is providing a good simulation of the actual packer.

The third step is to test the most promising candidates from the SIM Test downhole in a geothermal well. At operational depths the specimen will be exposed to the unaltered fluid and no questions exist as to whether the specimen exposure is representative. Any possibilities of fluid modifications which may occur because of temperature or pressure changes or dilution or contamination of the fluid from other strata are eliminated. A testing module was designed which operates much as the laboratory SIM test fixture except down in the geothermal well. The design of the module is such that it is not necessary for it to interface with the well casing. This enables preservation of the post mortem specimen and minimization of the potential for becoming lodged in the well. Minimization of the risk to the well will result in wider access to test wells and, hence, a wider variety of test chemistries. In addition, the module uses

a wire-line hoist as opposed to the more complex and expensive tubing string.

The elastomer formulation effort was concentrated on the peroxide cured fluoroelastomer family during this contract period as candidates to improve geothermal packer seals. Because the peroxide cured fluoroelastomer results were not overwhelmingly promising some effort was also spent investigating EPDM, butyl, and resin cured fluoroelastomers. The SIM tests revealed that an important contributor to the failure of the packer seal is the substantial internal stresses which are generated within the seal as it is seated and the differential pressure is applied. A critical balance is required to be struck between modulus, ultimate elongation, and ultimate tensile strength of the material to allow it to be deformed while seating and during pressurization without breakage, yet to be stiff and strong enough to bridge gaps. Striking this balance becomes increasingly difficult if not impossible as the temperature increases.

The following is prefaced with the fact that insufficient data exists to make firm conclusions and any conclusions are preliminary and tentative. At this point it appears that EPDM holds the most promise of the elastomer formulations developed and tested thus far. The peroxide-cured fluoroelastomer also holds promise, but is more extensively degraded by the synthetic geothermal fluid. Both are recommended for further development. Table 1 shows the typical effect of chemically aging EPDM, peroxide-cured fluoroelastomer and perfluoroelastomer in synthetic geothermal fluid for 24 hours at 260°C.

A minor task under the GEM Program was evaluation of the current commercially available elastomers in the SIM Test to provide a reference for the DOE developed elastomers. Five

TABLE 1 -- EFFECT OF CHEMICAL AGEING IN SYNTHETIC GEOTHERMAL FLUID

| ELASTOMER | APPEARANCE | TENSILE @ RT | ULTIMATE ELONGATION @ RT | EXTRUSION RESISTANCE @ 260C | SHORE A @ 260C |
|---|---|---|---|---|---|
| EPDM (E263) | FAIR | 75%* | N/A | 57% | 85% |
| FLUOROELASTOMER (201) | POOR | 48% | 73% | 77% | 80% |
| PERFLUOROELASTOMER (3073)** | GOOD | 53% | 230% | 94% | 84% |

* Exceeds capability of tester, 840% elongation, maximum tensile stress recorded.

** No development of perfluoroelastomer for this specific application was performed; cured test sheets were obtained directly from du Pont to get "a data point".

materials were received from five different companies. The elastomers included two nitriles, one EPDM, one epichlorohydrin, and one non-peroxide-cured fluoroelastomer.

Separate from the elastomer development, another minor task was performed. L'Garde developed a conceptual design of a casing packer improved to provide better potential in the geothermal environment. The design serves as a model providing guidance for development of current elastomers which may have potential, and new polymers synthesized under the sister efforts being performed by Jet Propulsion Laboratory and Hughes Aircraft Company.

An important message is indicated from the development test results which has far reaching implications. SIM tests were run on compounds from 6 base polymer families and all seals tested at about 260°C failed catastrophically in the SIM test which is more severe in certain aspects than some packer systems. The seals with ultimate elongation of less than 200% tended to crack and only seal for a short time, if at all. The seals with higher elongations, suffered substantial deformation and breakage. Of these, however, the nitrile and EPDM seals did hold differential pressure for the full 24 hours even though they extruded and were substantially and permanently deformed.

Efforts to improve the formulations to alleviate the gross failure modes are in progress, however, an underlying indication from the general failure of the multitude of compounds SIM tested exists. 260°C aggravated by the geothermal chemistry is indicated to be, at a minimum, a very difficult performance level to achieve with state-of-the-art elastomers and probably impossible at temperatures greater than say 316°C (600°F) with

current day packer systems. Consequently, there exists a long range requirement to develop basically different packer concepts which accommodate the elastomeric seal better by preventing the inducement of excessive stresses.

Invaluable information was obtained through the cooperation of several Government laboratories and commercial companies in the oil and gas, and chemical products industries. Mr. J. K. Sieron, Chief of the Elastomers and Coatings Branch, Air Force Materials Laboratory; Mssrs. J. D. Foster and M. B. Jett of Dresser Industries/Guiberson Division; and Mssrs. E. H. Bigelow, W. W. Henslee, Jr., J. H. Oden, D. C. Preston, Jr., and H. K. Todee and Dr. D. M. McStravick of Baker Division Baker Oil Tools, Inc., were especially helpful.

PUNCH TEST FIXTURE

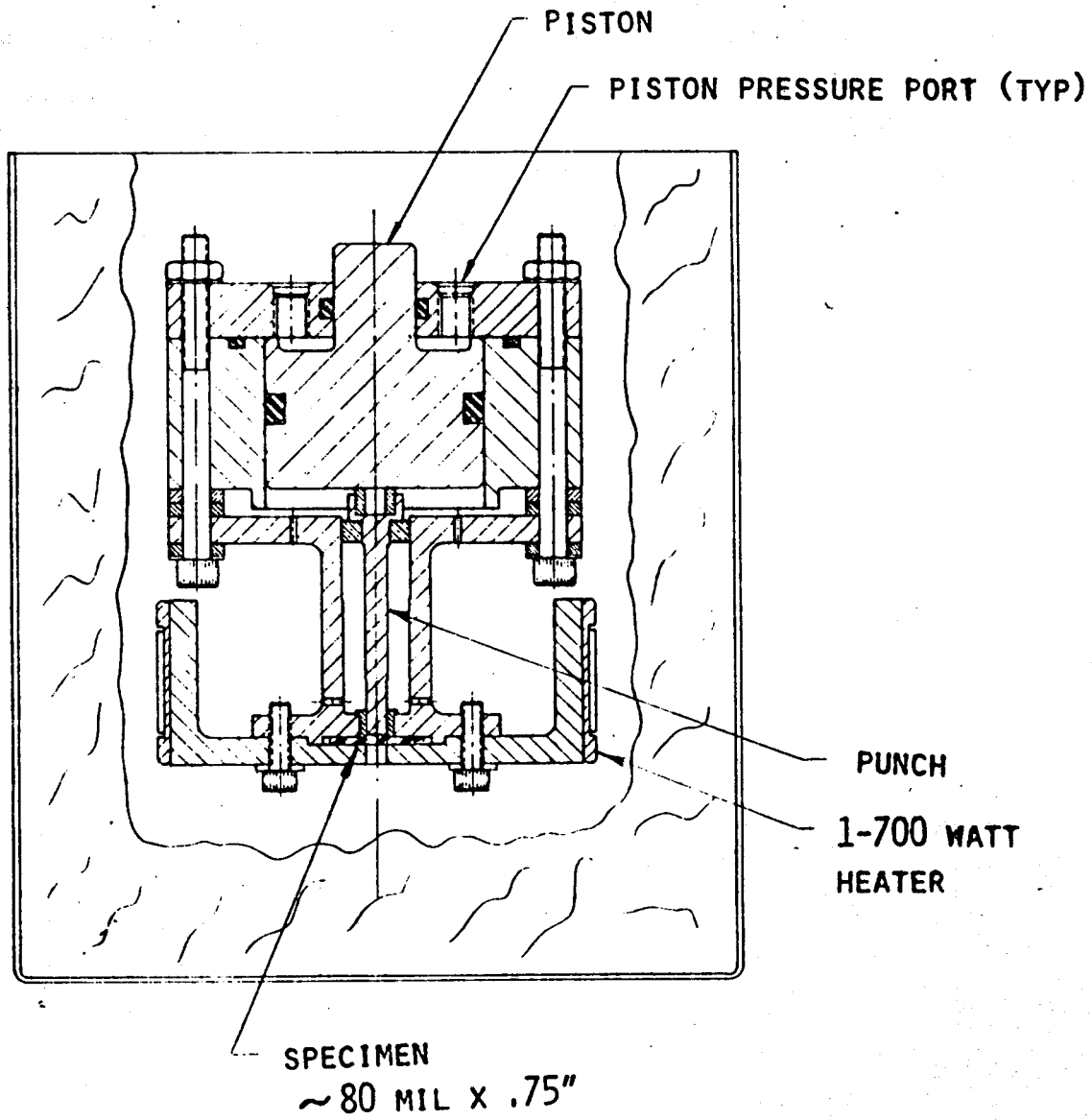

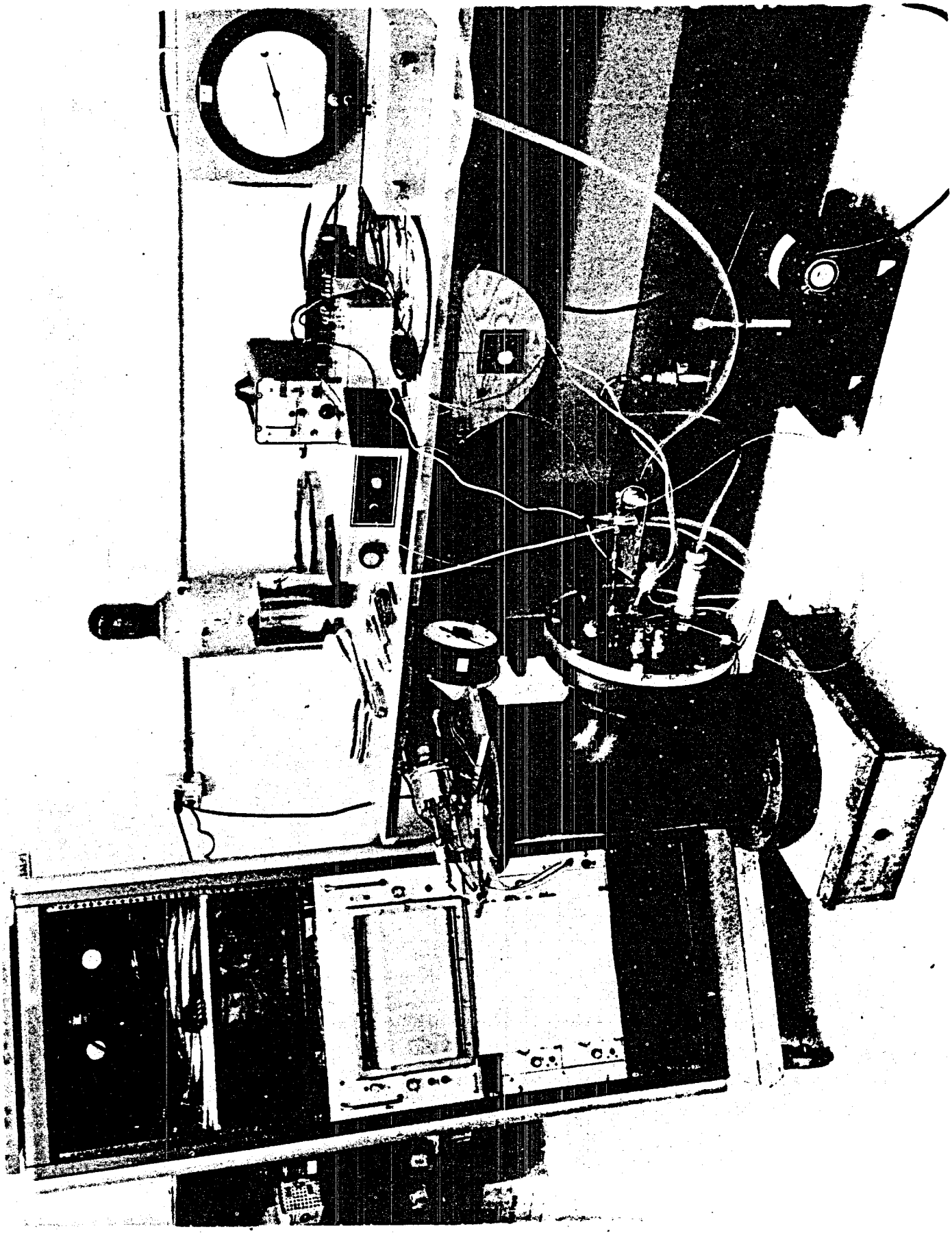

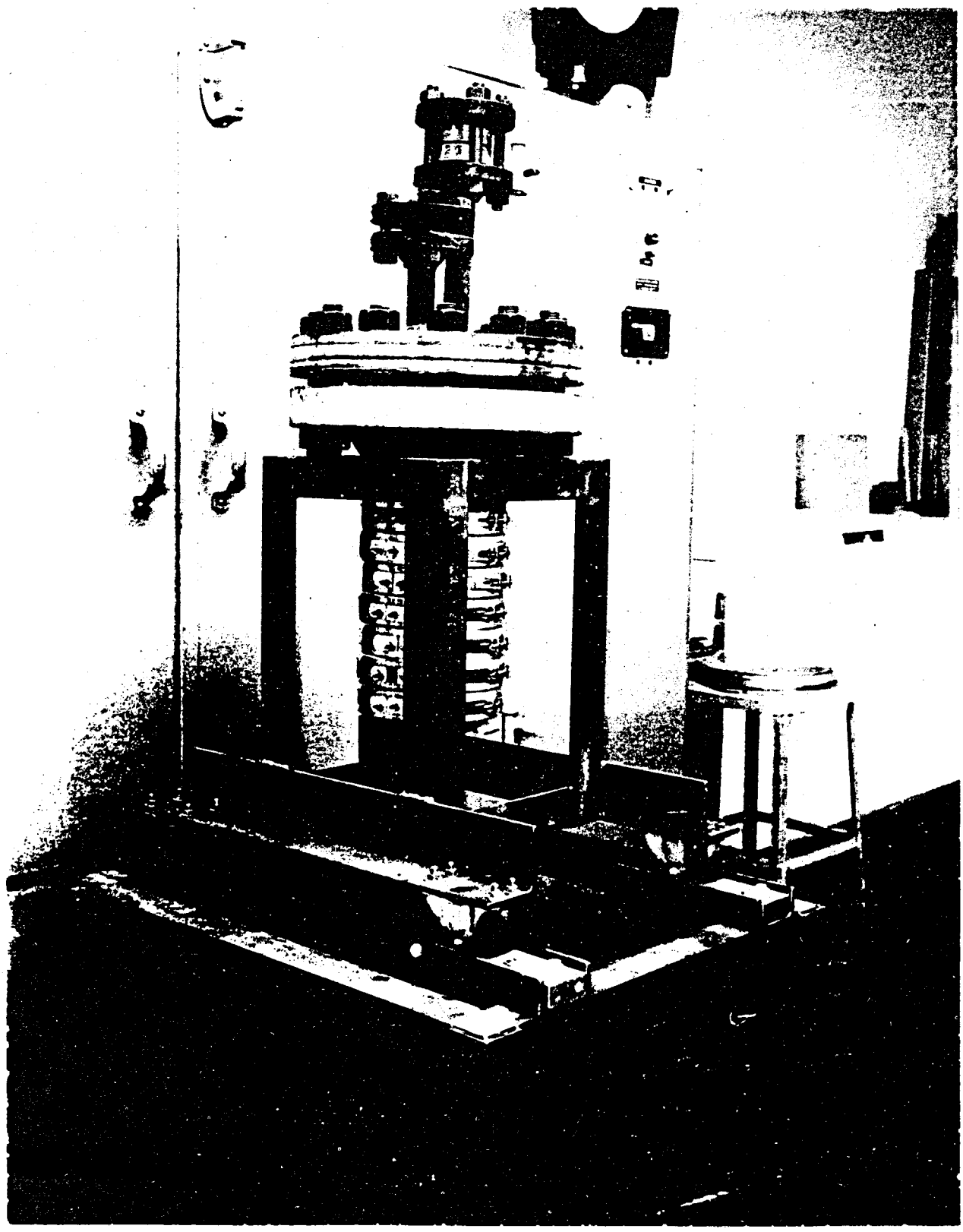

# STATISTICAL EVALUATION OF PUNCH TEST

- 3 FORMULATIONS, 8 SPECIMENS EACH, TESTED RANDOMLY.

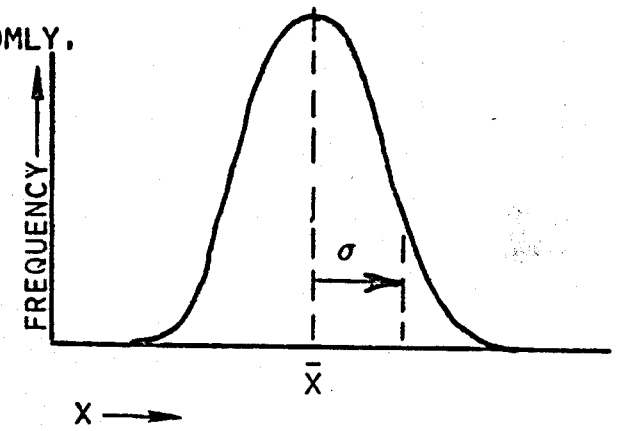


| COEFF. OF VARIATION | DIRECT READING | SHEAR STRESS |
|---|---|---|
| $\sigma/\bar{x}$ | .0519 | .0895 |

| NO. SPECIMENS | 95% CONFIDENCE THAT THE TRUE MEAN FALLS WITHIN |
|---|---|
| 1 | ± 3.5 DIVISIONS |
| 2 | ± 2.5 |
| 3 | ± 2.0 |
| 4 | ± 1.8 |

- NO CORRELATION WITH SPECIMEN THICKNESS.

SIMULATION TEST APPARATUS
P & I DIAGRAM

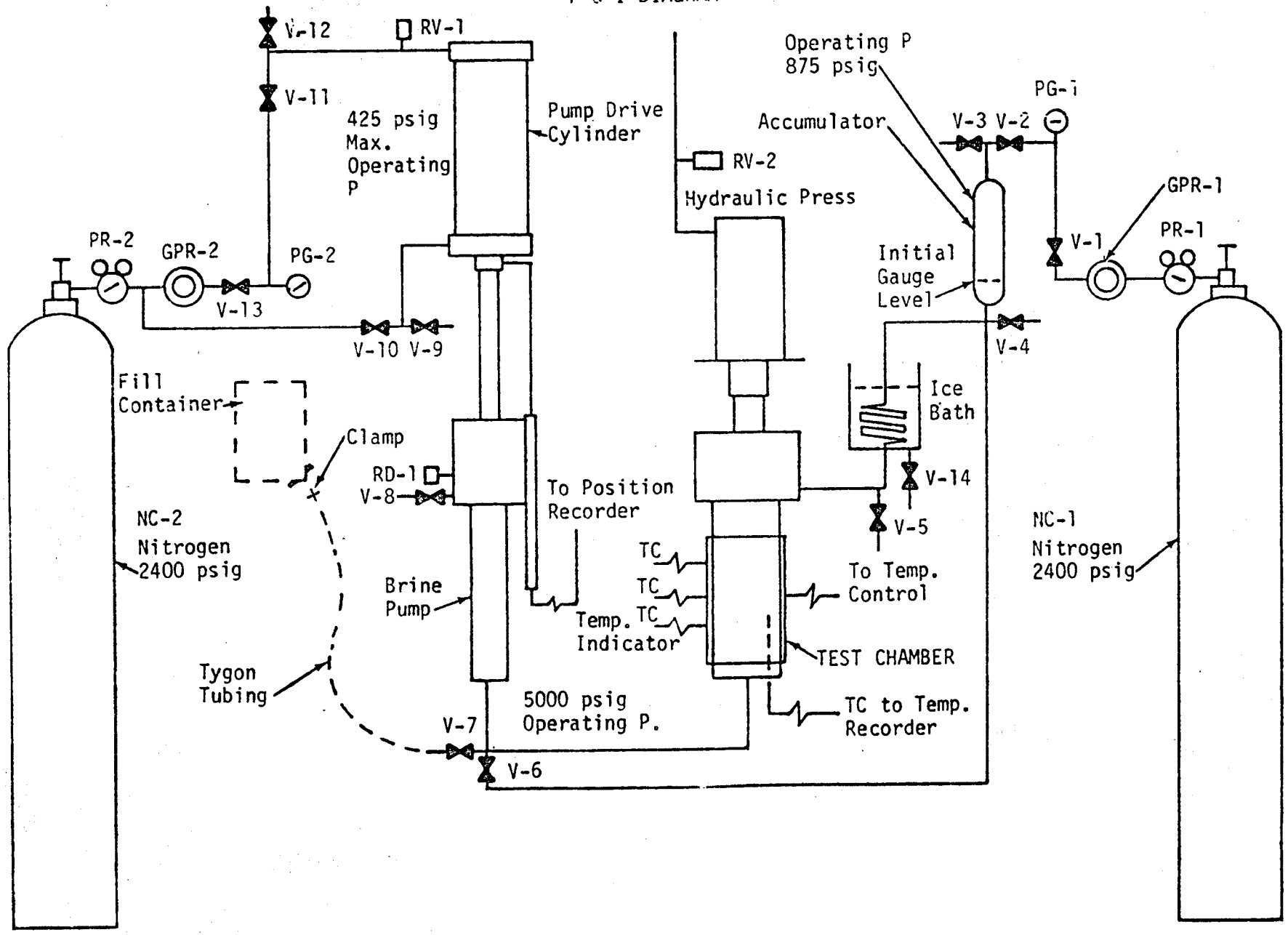

FIGURE 7 -- SIMULATION TEST

Close-up of Control Panel & Test Section

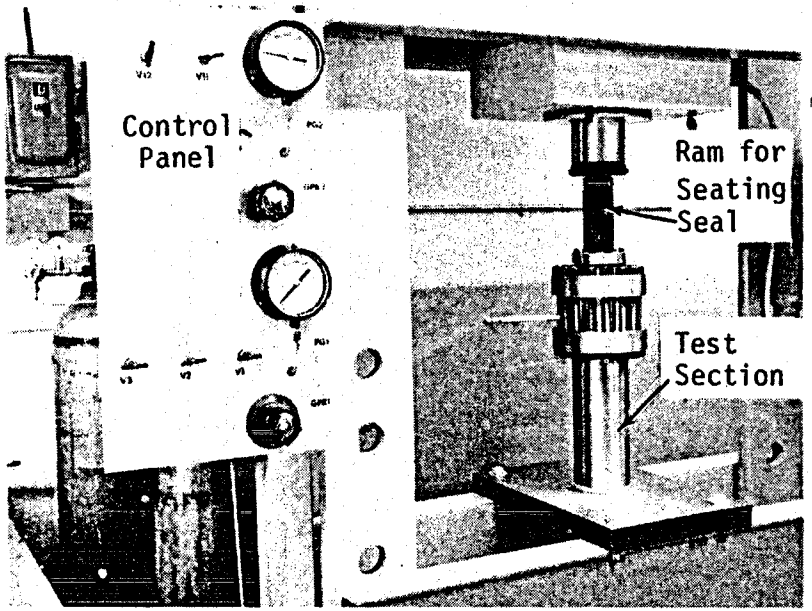


Close-up of Positive Displacement Fluid Pump

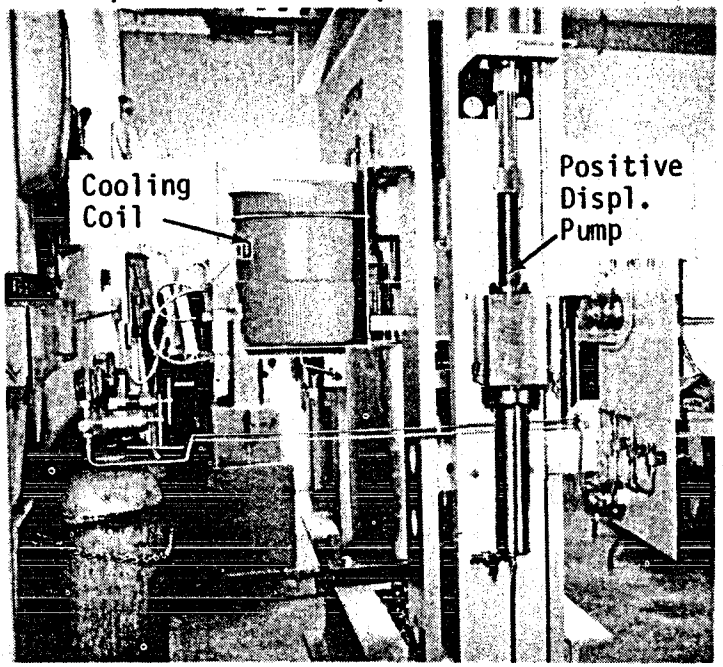


General View of SIM Test

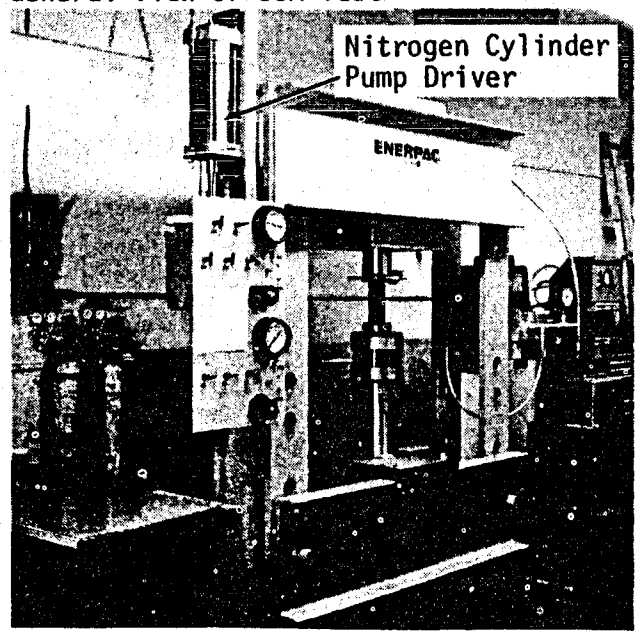

# PRELIMINARY CONCEPT GEOTHERMAL IN SITU TEST FIXTURE

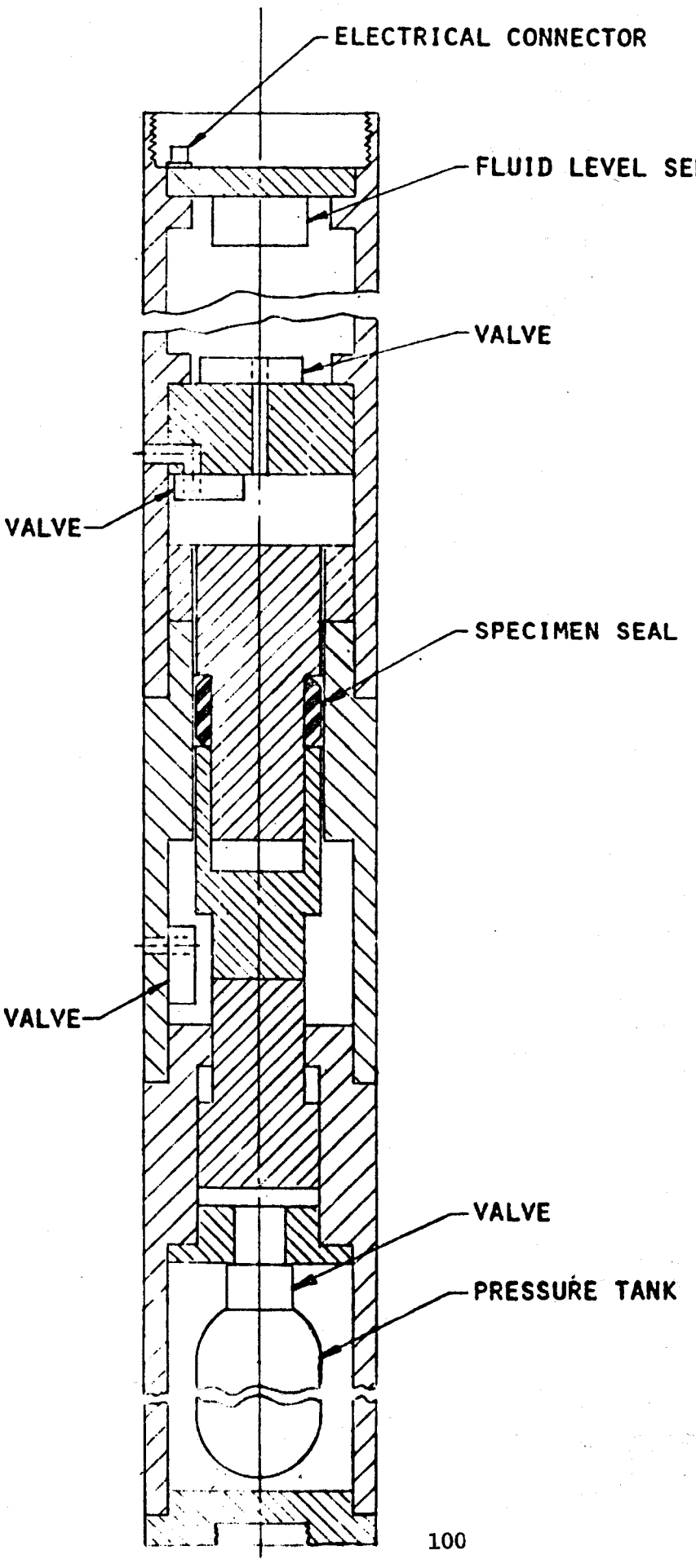

## SEAL DEFORMATION

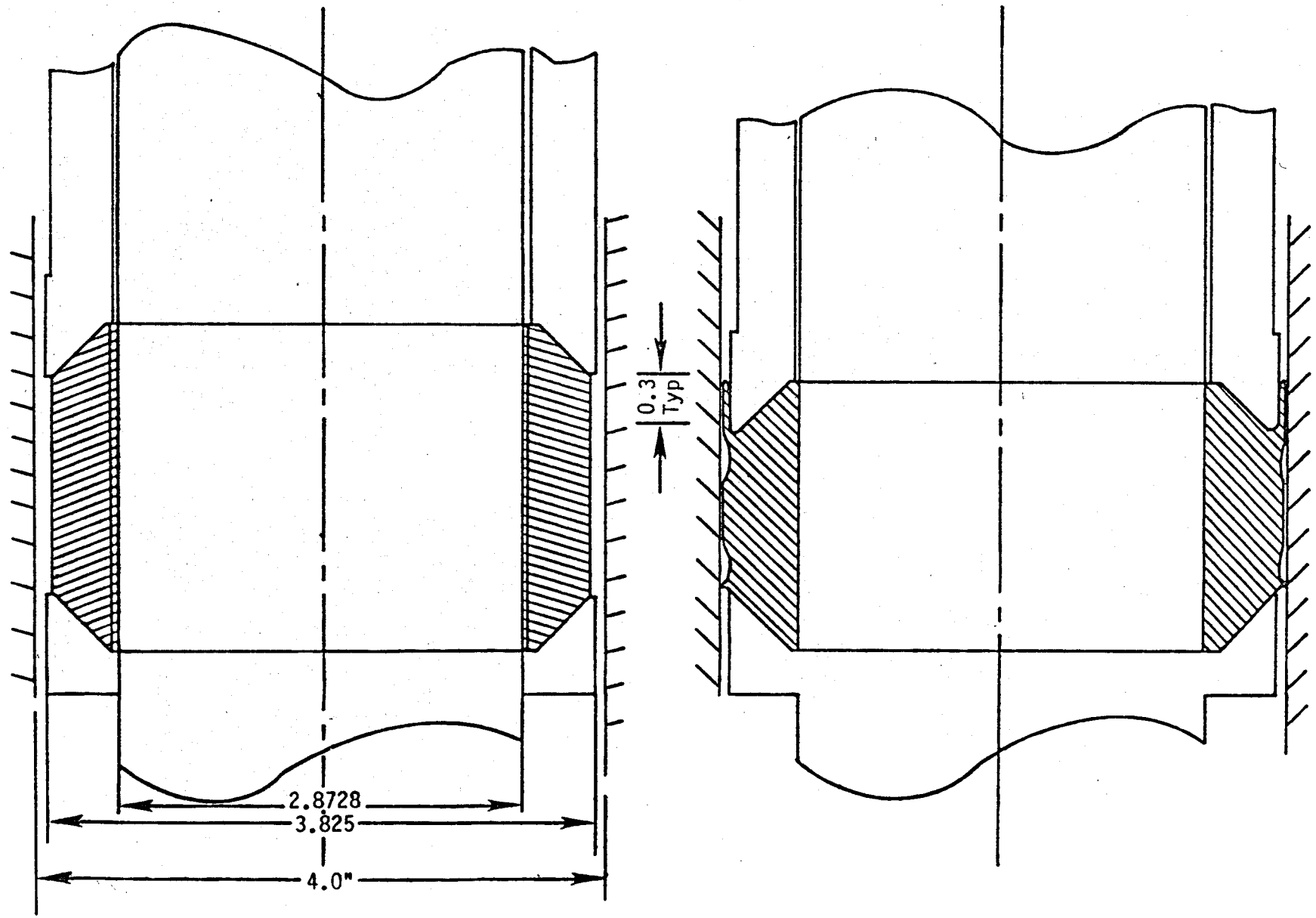

## SEAL COMPRESSION RESULTING IN PRESTRESSES

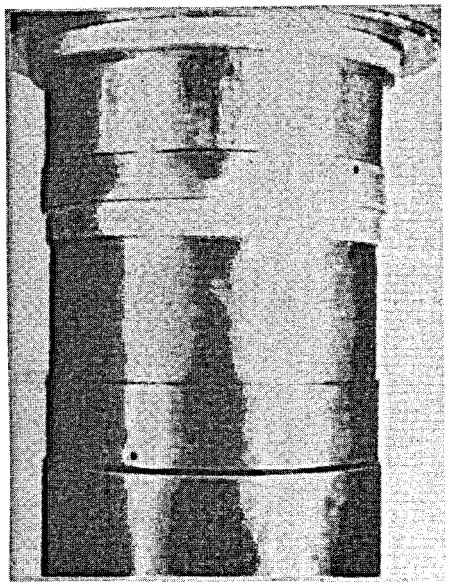

SEAL UNCOMPRESSED

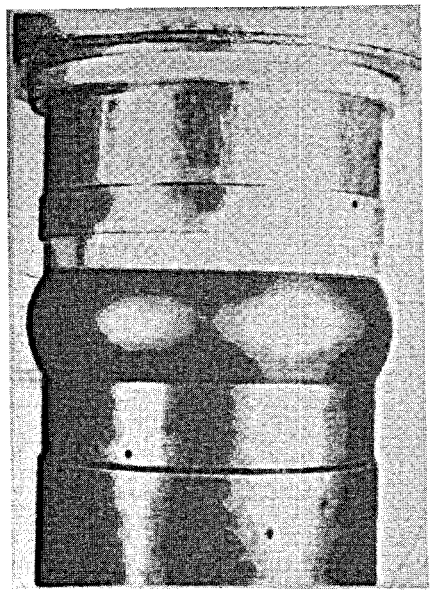

SEAL COMPRESSED TO
4.167 INCH DIAMETER

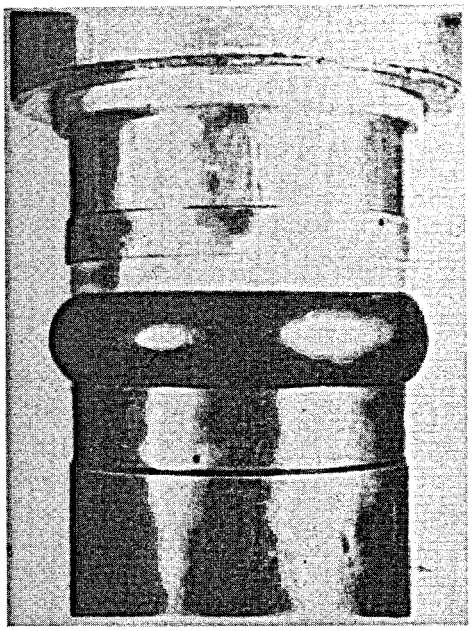

SEAL COMPRESSED TO
4.327 INCH DIAMETER

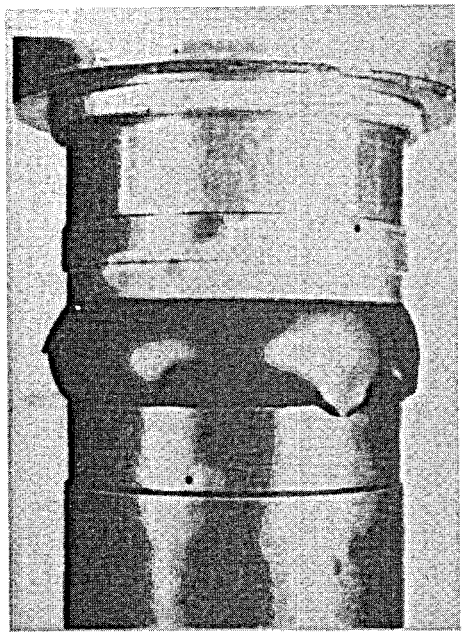

COMPRESSION REVEALS NO-
KNIT DEFECTS ON SEAL

NON-REPRO COLOR

VIEWGRAPH OF

SIM TEST SEAL FIXTURE

## SIM TEST SUMMARY

| Sequence No. | Specimen No. | Compound | Duration Hrs:Min | Inches Extrusion | Set Temp. °C | Diamet. Gap, Mils | Configuration |
|---|---|---|---|---|---|---|---|
| 1 | 215-3 | VT-R-4590,Austin 70 phr | 5:52 | Nil | 260 | 13 | Flat |
| 2 | 215-2 | VT-R-4590,Austin 70 phr | :07 | Nil | 260 | 13 | Flat |
| 3 | A-3 | Nitrile | 24: | Nil | 149 | 13 | Flat |
| 4 | A-2 | Nitrile | 24: | Nil | 149 | 25 | Flat |
| 5 | A-6 | Nitrile | 11: | 0.5 | 260 | 175 | Flat |
| 6 | 213-3 | VT-R-4590,Asbestine 3X | :00 | Nil | 260 | 175 | Flat |
| 7 | 220-3 | VT-R-4590,Austin 65 phr | :00 | Nil | 260 | 175 | Flat |
| 8 | 216-2 | VT-R-4590,Kevlar | :00 | Nil | 260 | 175 | Flat |
| 9 | 105-II-1 | Viton GH, Austin/MT | :05 | Nil | 260 | 175 | Flat |
| 10 | 216-1 | VT-R-4590, Kevlar | :00 | <0.1 | 260 | 175 | Chamfered |
| 11 | A-5 | Nitrile | 24: | 1.75 | 260 | 175 | Chamfered |
| 12 | 105-II-2 | Viton GH, Austin/MT | :47 | Nil | 260 | 175 | Chamfered |
| 13 | B-3 | EPDM | 24: | 3.75 | 260 | 175 | Chamfered |
| 14 | 217-2 | EPDM | 24: | 2.5 | 260 | 175 | Chamfered |
| 15 | C-4 | Nitrile | 1:13 | 4.5 | 260 | 175 | Chamfered |
| 16 | D-3 | Epichlorohydrin | :00 | N/A | 260 | 175 | Chamfered |
| 17 | E-3 | Viton | 3:44 | No Meas. | 260 | 175 | Chamfered |
| 18 | 222-3 | VT-R-4590,Austin 40 phr | :03 | 0.75 | 260 | 175 | Chamfered |
| 19 | 221-2 | VT-R-4590, Maglite K | :38 | 0.75 | 260 | 175 | Chamfered |

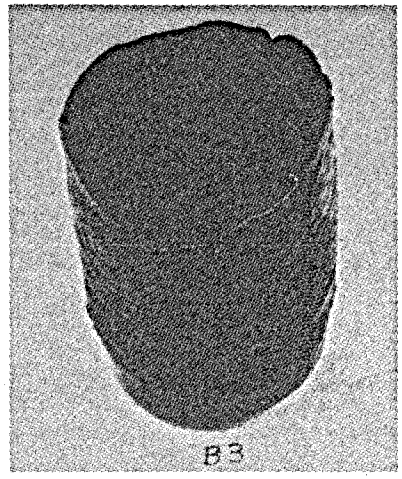


COMPANY B EPDM -- THIS AND L'GARDE EPDM REMAINED ELASTOMERIC AND SURVIVED FULL 24 HRS. ONLY DIFFERENCE L'GARDE EPDM EXTRUDED 2.5 INCHES VS COMPANY B'S 4.0 INCHES.

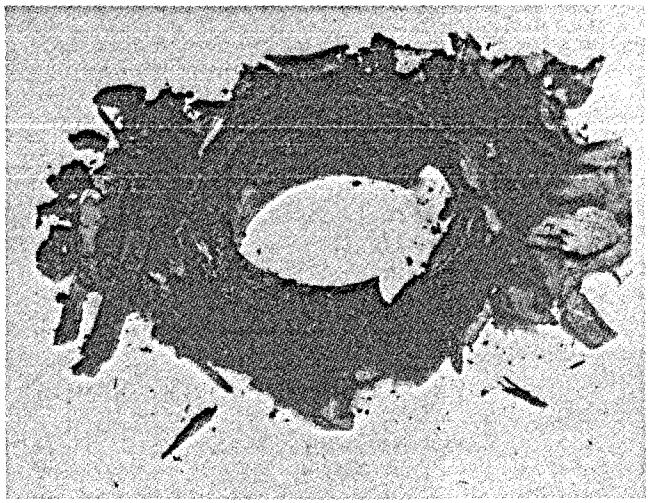

COMPANY D EPOCHLOROHYDRIN -- LOST ALL STRUCTURAL STRENGTH AND BECAME SOFT, AND CRUMBLY BEFORE SEATING.

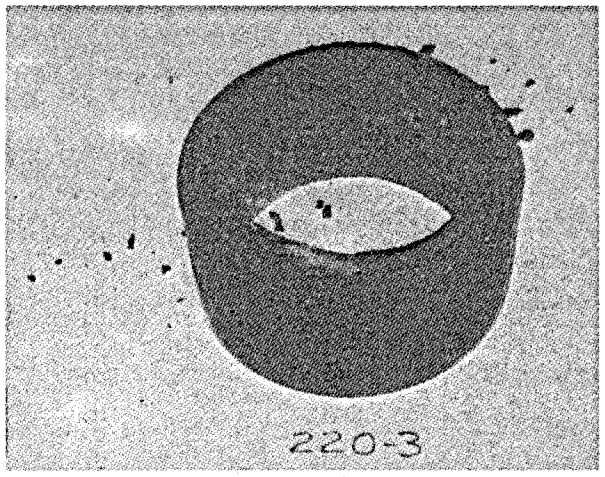


L'GARDE VITON -- FAILED BECAUSE OF INABILITY TO ELONGATE SUFFICIENTLY DURING SEATING.

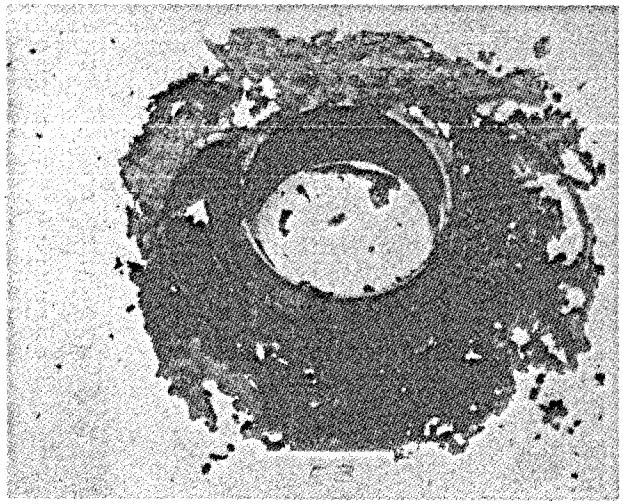

COMPANY E VITON -- FAILED BY BREAKING IN THE HIGH STRESS REGION. SURVIVED 3.75H WITH SLOW LEAK, THEN FAILED.

## TENTATIVE CONCLUSIONS & LONG-RANGE IMPLICATIONS

- CONCLUSIONS ARE TENTATIVE -- NOT ENOUGH DATA.
- CASING PACKER ELEMENTS ARE HIGHLY STRESSED WHEN SEATED.
- APPEARS TO BE A GENERAL PROBLEM OF STRESSES EXCEEDING THE STRENGTH AT 260°C.
- BECAUSE ELASTOMERIC SEALS ARE SO MUCH SUPERIOR TO METAL OR PLASTIC SEALS ESPECIALLY IN THE FIELD ENVIRONMENT, SIGNIFICANT RETURN AND BENEFIT WILL BE DERIVED FROM DEVELOPING AN ELASTOMERIC SYSTEM.
- PRESENT CASING PACKER COMPRESSION DESIGNS WHICH WORK AT 120°C HAVE MUCH REDUCED PROBABILITY OF PERFORMING AT 260°C.
- NEW HIGH TEMPERATURE DESIGNS (NON-COMPRESSION TYPES) MUST BE DEVELOPED FOR THE GEOTHERMAL ENVIRONMENT.

# DESIGN GOALS

- HIGH TEMPERATURE APPLICATION (260°C)
- HIGH EXPANSION RATIO
- RESETTABLE

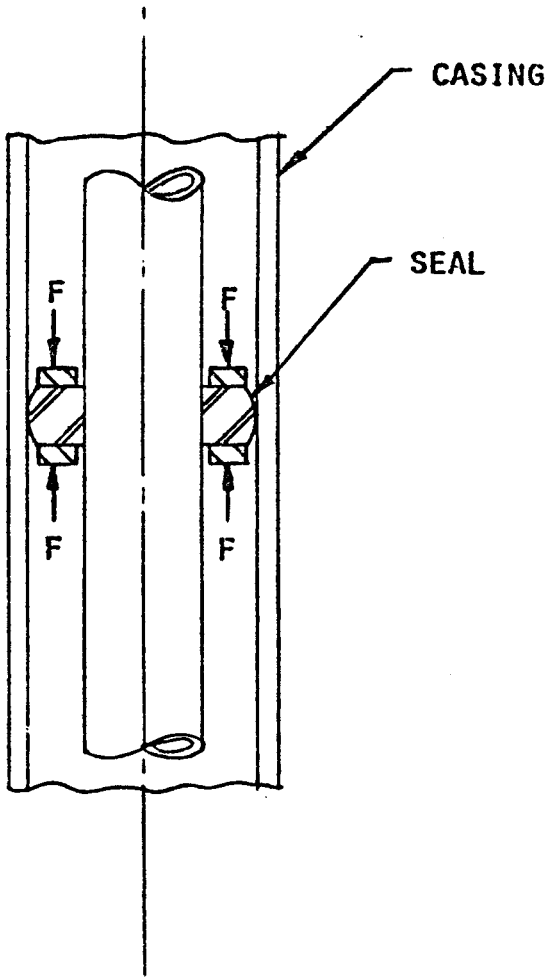


MECHANICAL "SQUEEZE"
TYPE PACKER
EXPANSION OF
8 TO 10%

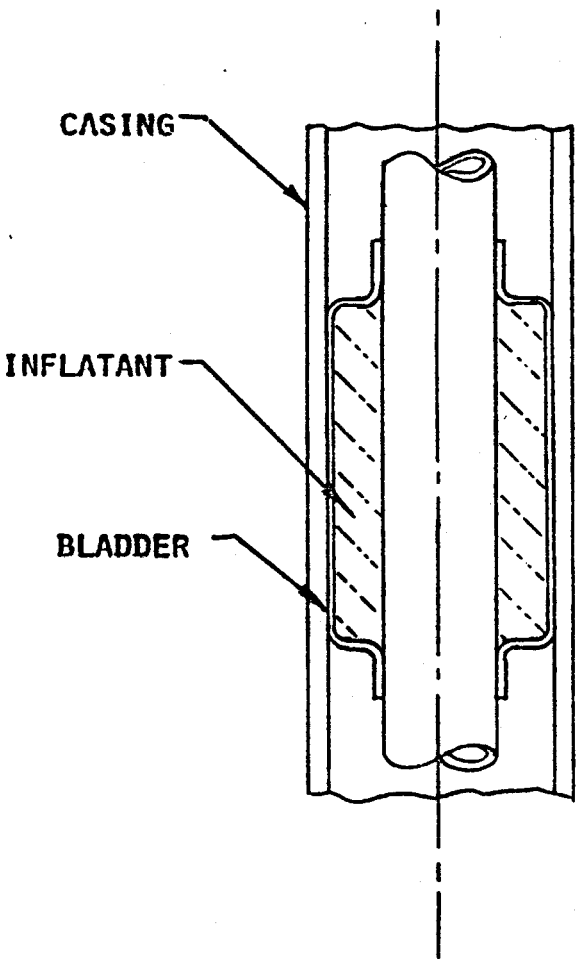


INFLATABLE
TYPE PACKER
EXPANSION OF
30 TO 60%

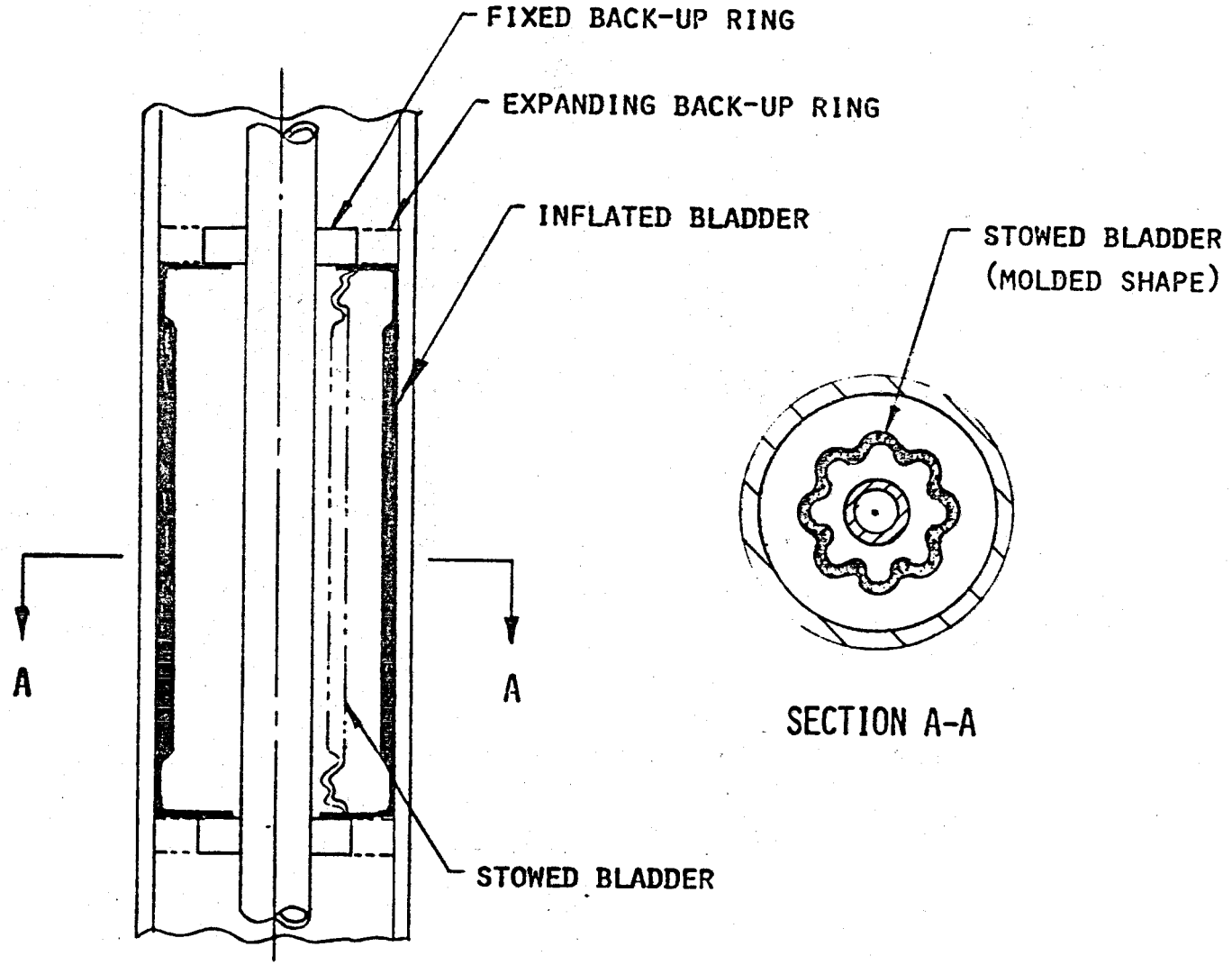


PACKER CONCEPT

# INFLATABLE PACKER CONCEPT

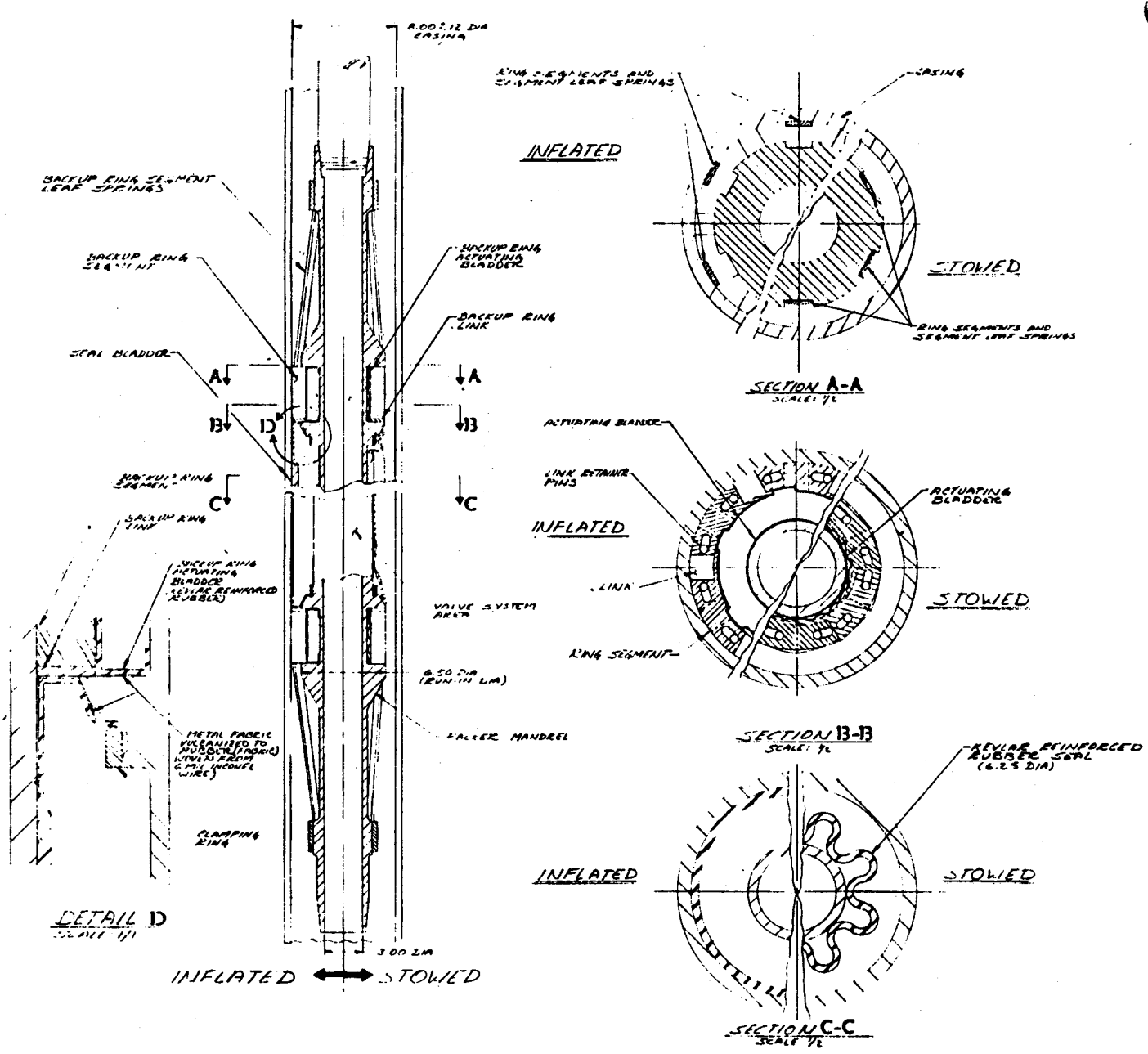


| QTY REQD | CODE IDENT | PART OR IDENTIFYING NO. | NOMENCLATURE OR DESCRIPTION |
|---|---|---|---|
| | | | PARTS LIST |

UNLESS OTHERWISE SPECIFIED DIMENSIONS ARE IN INCHES TOLERANCES ARE:
FRACTIONS DECIMALS ANGLES
.X ±
.XXX ±

CONTRACT NO.

| APPROVALS | DATE |
|---|---|
| DRAWN Tom C | 9/1/93 |
| CHECKED | |

MATERIAL

FINISH

NEXT ASSY USED ON

APPLICATION

DO NOT SCALE DRAWING

BARDE INC.

INFLATABLE THERMAL CASING PACKER CONCEPT

| SIZE | CODE IDENT NO. | DRAWING NO |
|---|---|---|
| D | 1F888 | SK0052 |

SCALE 1/4 SIZED SHEET 1 OF 1

# L'GARDE GEOTHERMAL PACKER ELASTOMERS DEVELOPMENT PROGRAM

## RECENT DEVELOPMENTS -- OCTOBER 1978

Significant progress was made during the second 12-month period of elapsed time of geothermal packer elastomer compound development. Compounds are being developed to withstand the unusually severe geothermal environment for 24 hours at 260°C (500°F) with the following chemistry:

| | |
|---|---|
| $H_2S$ | 300 ppm |
| $CO_2$ | 1,000 |
| NaCl | 25,000 |
| $H_2O$ | balance |

Figure 1, specimens B3 and 220-3 on the upper half of the page, shows the typical results L'Garde was experiencing about August 1977. The EPDM compounds were extruding excessively and the Viton compounds were hardening and cracking preventing successful sealing. General thermohydrochemical instability was also being experienced with all compounds. The unusually severe environment, especially the 260°C temperature, was proving to be too much for the capability of the elastomers at that time, by degrading the elastomer and reducing its mechanical properties to unacceptably low levels.

During the previous four months, significant improvements were experienced. Table I shows a comparison of the thermohydrochemical stability of present versus early values as represented by four characteristics which are critical to packer elastomers. The four parameters are ultimate tensile strength and elongation measured at room temperature, and Shore A hardness and extrusion resistance measured at 260°C. The percentage values represent the level of each characteristic which is retained after chemically ageing the specimen in synthetic geothermal brine at 260°C for 22 hours. In other words if the value is 100%, the virgin and chem aged values are identical, and therefore, the characteristic unaffected by the brine.

Company B EPDM -- This and L'Garde EPDM remained elastomeric and survived full 24 hours. Only difference L'Garde EPDM extruded 2.5 in. vs company B's 4.0 in.

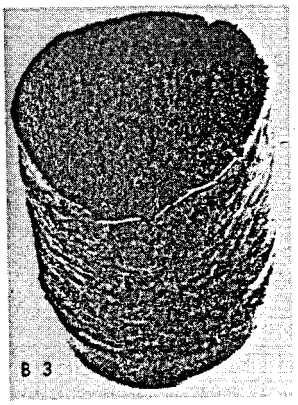


L'Garde Peroxide-Cured Fluoroelastomer -- Failed because of inability to elongate sufficiently during seating.

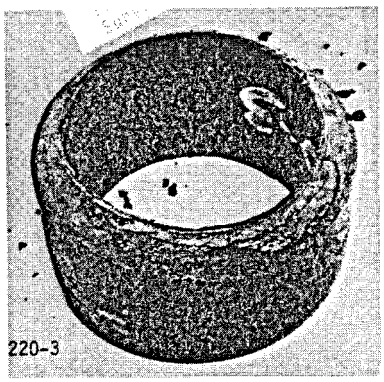


Company D Epichlorohydrin -- Lost all structural strength and became soft and crumbly before seating.

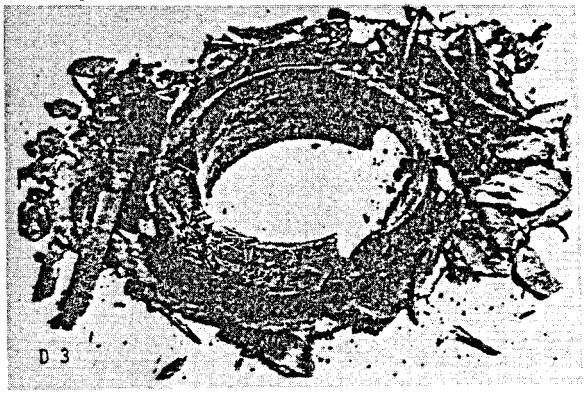


Company E Non-Peroxide-Cured Fluoroelastomer -- Failed by breaking in the high stress region. Survived 3.75H with slow leak, then failed.

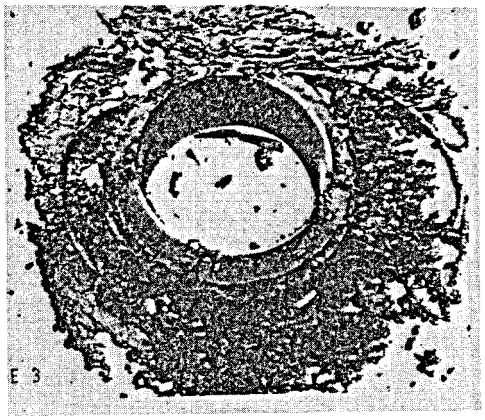


Figure 1 -- SIM TEST POST MORTEM SPECIMENS, TYPICAL RESULTS

TABLE I

THERMOHYDROCHEMICAL STABILITY OF GEOTHERMAL ELASTOMERS

CURRENT STATUS - OCTOBER 1978

| Elastomer | Ult. Tensile @ RT | | Ult. Elong. @ RT | | Shore A Hard. @ 260°C | | Extrusion Resist. @ 260°C | |
|---|---|---|---|---|---|---|---|---|
| | Early | Present | Early | Present | Early | Present | Early | Present |
| EPDM<br>Early-E263<br>Present-267 | 75% | 97% | --- | 98% | 85% | 100% | 57% | 103% |
| Viton<br>Early-115<br>Present-255 | 14% | 72% | 46% | 101% | 73% | 100% | 32% | 55% |
| EPDM/Viton<br>Early-235<br>Present-266 | 80% | 96% | 63% | 84% | 110% | 101% | 128% | 96% |

As is apparent, the present EPDM compound 267 is showing excellent stability and all four characteristics are unchanged by the exposure to the synthetic geothermal brine. The earlier compounds were fair but the present compounds have achieved the ultimate from the standpoint of hydrothermochemical stability. The Viton compound 255 shows substantial progress. Major difficulty was encountered with the early compounds becoming brittle to the extreme, note the severe falloff of the ultimate elongation. Compound 255 shows excellent stability of the ultimate elongation and Shore A hardness and good retention of ultimate tensile strength and extrusion resistance. 255 is a viable packer seal elastomer as shown by the Simulation Tests discussed below. Finally the EPDM/Viton blends show good stability. Minor reduction of the ultimate elongation is experienced after chem ageing.

Table II shows the actual values of the characteristics represented by the percentages of Table I. The development procedure consisted of determining first what compounding provided good hydrothermochemical stability and then the mechanical properties were developed to provide improved extrusion resistance. The lower ultimate elongations and higher hardnesses of the later EPDM and blend compounds indicate the trend towards higher modulus and more extrusion resistance compounds. The primary feat accomplished with the Vitons was to develop compounds which did not become brittle and which could withstand the significant deformation required without cracking of the elastomer when the packer seal is compressed for seating.

The data generated which is most meaningful is from L'Garde's Simulation Test. This test subjects a full-scale casing packer seal to simulated downhole conditions in the laboratory. The seal specimen is immersed and seated in 260°C synthetic geothermal brine with all the attendant forces simultaneously applied, i.e., seating compressive force, pressure, and differential pressure forces. The clearance gap between the elastomer backup rings and the vessel (simulated casing) was set at 150 mils on the

TABLE II

## GEOTHERMAL ELASTOMERS PROGRESS

### CURRENT STATUS - OCTOBER 1978

| ELASTOMER | ULT. TENSILE @ RT, PSI | | ULT. ELONG. @ RT, % | | SHORE A HARD @ 260°C | | EXTRUSION RESIST @ 260°C, PSIA | |
|---|---|---|---|---|---|---|---|---|
| | V | CA | V | CA | V | CA | V | CA |
| EPDM | | | | | | | | |
| EARLY - E263 | >1363 | >1020 | >840 | >840 | 61 | 52 | 9.6 | 9.5 |
| PRESENT - 267 | 1610 | 1554 | 141 | 148 | 92 | 92 | 17.1 | 17.6 |
| VITON | | | | | | | | |
| EARLY - 115 | 1699 | 244 | 162 | 74 | 80 | 58 | 11.2 | 3.6 |
| PRESENT - 255 | 2195 | 1591 | 224 | 226 | 79 | 79 | 11.4 | 6.3 |
| EPDM/VITON | | | | | | | | |
| EARLY - 235 | 1882 | 1506 | 681 | 431 | 67 | 74 | 8.3 | 10.6 |
| PRESENT - 266 | 1596 | 1531 | 193 | 163 | 88 | 89 | ~18 | 17.3 |

diameter for the early tests and narrowed to 50 mils on the diameter for the later tests. The 50 mil gap is still conservative with respect to typical operational thermal packer conditions.

Table III shows a qualitative description of the amount of extrusion experienced at various temperatures for each base elastomer. All seals were tested for 22 hours with a differential pressure from 3,000 to 4,000 psi. The EPDM suffered only minor extrusion at the 260°C. The EPDM extruded less than the Viton, something considered highly improbable during the earlier phases of compound development. The Viton suffered moderate extrusion at 260°C and very minor extrusion at 204°C. The EPDM/Viton blend did not suffer any extrusion although there was a very minor amount of permanent deformation at the gap.

TABLE III
PACKER SEAL SIM TEST EXTRUSION SUMMARY
CURRENT STATUS - OCTOBER 1978

| Elastomer | 260°C (500°F) | 204°C (400°F) | 149°C (300°F) |
|---|---|---|---|
| EPDM | very minor | none | none |
| Viton | moderate | very minor | none |
| EPDM/Viton | none | none | none |

Figure 2 is a composite photograph of the post mortem specimens represented in the 260°C column of Table III. The differential test pressures were 4,000 psi, 3,000 psi, and 3,500 psi for the EPDM, Viton, and EPDM/Viton respectively.

It would be premature to conclude from these data that one elastomer is better than the other as further development will probably result in further improvements of each. However, if choices were required based on these present compounds, the EPDM

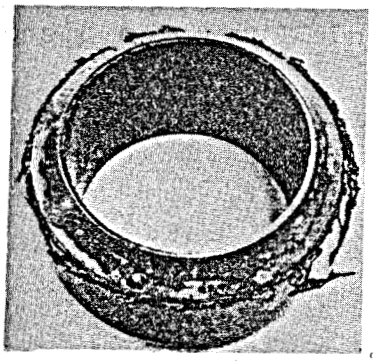


EPDM
4000 psi ΔP

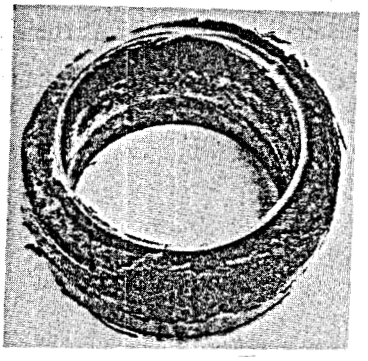


Viton
3000 psi ΔP

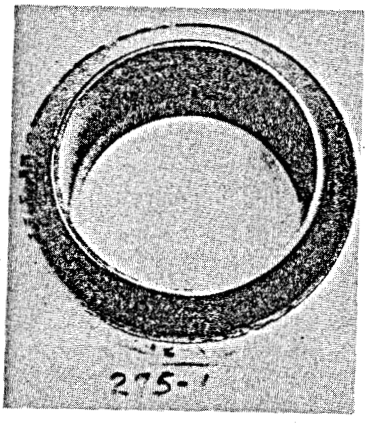


EPDM/Viton
3500 psi ΔP


Close-up of minor
permanent deformation

Figure 2 -- POST SIM TEST SPECIMENS FOR CURRENT FAVORED COMPOUNDS TESTED AT 260°C - OCTOBER 1978

would be recommended where hydrothermochemical stability is important, e.g. long sustained usage or higher temperatures, the EPDM/Viton blend would be recommended where extrusion resistance is of utmost importance and hydrothermochemical stability secondary, and the Viton would be recommended for hydrocarbon environments if the EPDM and EPDM/Viton blend compounds were too severely affected.

# DEVELOPMENT OF A CAVITATING DESCALING TECHNIQUE FOR GEOTHERMAL SCALE REMOVAL

by

A. A. Hochrein, Jr.
and
F. Graham
DAEDALEAN ASSOCIATES, Inc.
Springlake Research Center
15110 Frederich Road
Woodbine, Maryland 21797

DAEDALEAN ASSOCIATES, Incorporated has conducted extensive research in the field of cavitation erosion. Data has been gathered concerning the cause, prevention, control and damage resulting from this cavitation phenomena. Resulting from this research has been: 1) an understanding of the damaging effects of cavitation erosion and 2) an understanding of the conditions necessary to develop and control cavitation. From this understanding of the development and control of cavitation erosion DAI has developed a high pressure water jet system (CONCAVER®) utilizing the phenomena of controlled cavitation erosion as a working tool for cleaning and cutting applications.

The conversion of geothermal energy into usable electrical power has become increasingly important to the overall national energy needs and requirements. A major problem area which has resulted from the initial development of geothermal power plants is the scale formation in downhole wells, piping systems, flash tanks, injection lines and other system components. The scale formation is due to the concentration of minerals in the geothermal water and steam. Silica scale initiates in the geothermal well and continues throughout the system. The current cleaning methods (waterblasting, acid soaking, sandblasting and "pigging") utilized by the Geothermal

Loop Experimental Facility (GLEF) at Niland, California requires lengthy periods of facility shutdown and extensive disassembly of the facility pipe and components. Because the GLEF can operate only about 1,000 hours before scale buildup necessitates shutdown, the required cleaning operation has become an important factor in determination of facility operating costs.

DAI has developed and field demonstrated, at the GLEF, a CONCAVER cleaning system utilizing the phenomenon of cavitation for cleaning and removing geothermal scale from pipes and system components. Using this technique, water is pumped under high pressure through a properly designed pump/motor/nozzle system. The high speed jet emerging from the nozzle, pump and motor combination, produces a large number of cavitation bubbles. These bubbles are carried by the jet to the hard mineral scale wherein they collapse with a predetermined intensity of erosion which is tailored for the type of scale occurring in geothermal pipes and system components. Since the size and intensity of the cavitating envelope can be accurately controlled, the geothermal scale is removed with no damage or deterioration to the facility components or pipes.

The CONCAVER system assembled for the field demonstration contained two cleaning assemblies. The first was a hand-held unit used for external descaling and the second was a winch propelled rotating cleaning head for pipe descaling. Figure 1 is a photo of the CONCAVER model developed for pipe descaling. The areas descaled were selected by GLEF personnel and were determined to be the areas producing the hardest scale. During the demonstration scale was removed at a rate of 60 to 90 square inches per second. Figure 2 shows geothermal pipe before and after cavitation.

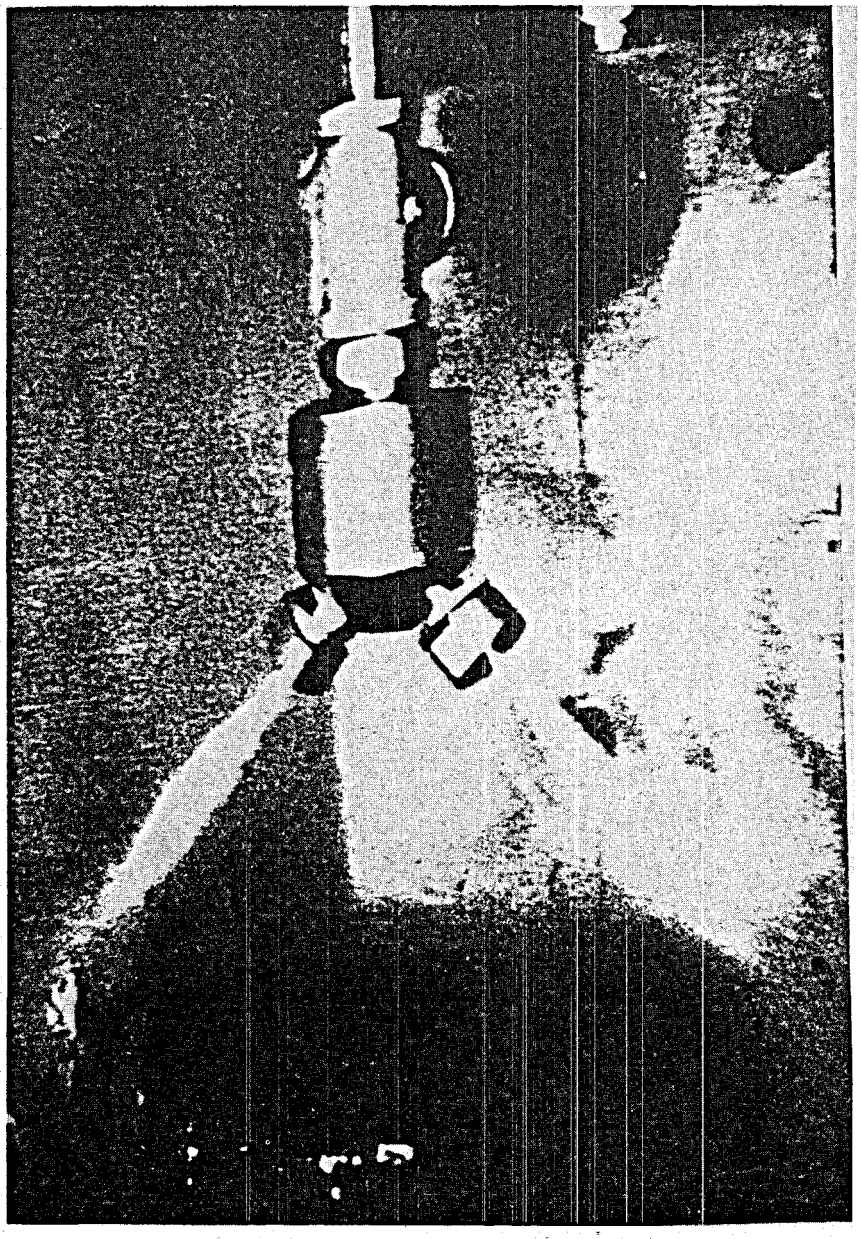

FIGURE 1

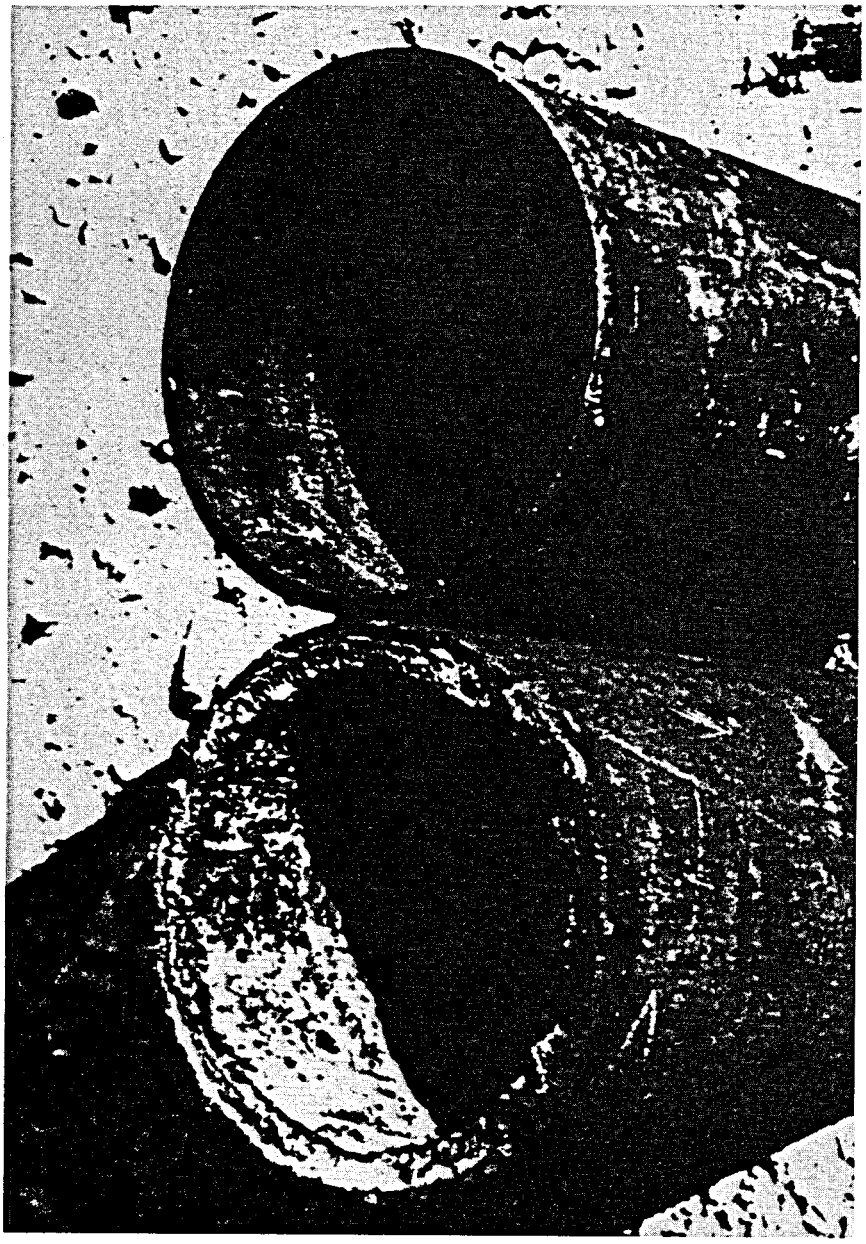

FIGURE 2

The field demonstration has proven the capability of the CONCAVER system to be superior to the methods of scale removal presently utilized in the geothermal industry. DAI is currently involved in refining and improving the design of the CONCAVER system hardware and cleaning heads to further improve and expand cleaning capabilities related to the geothermal energy industry.

# A THERMODYNAMIC ANALYSIS OF CORROSION PHENOMENA IN HIGH SALINITY GEOTHERMAL BRINES

By

**Digby D. Macdonald and Barry C. Syrett**

**Materials Research Center**
**SRI International**
**Menlo Park, California 94025**

## INTRODUCTION

It is well recognized that high-salinity geothermal environments are corrosive to many metals and alloys.[1-4] The high corrosiveness of the environment arises from the combination of elevated temperature (e.g., up to 350 C), and the presence of a high concentration of chloride ion (typically up to 4 m). Hydrogen sulfide is also frequently present, although usually only in the parts-per-million concentration range. Nevertheless, sulfide attack might be expected on many of the materials of technical interest. Furthermore, the related sulfide-induced failure mechanisms may also impose severe limits on the use of high strength alloys in geothermal systems, as has been the case in the sour natural gas industry. Accordingly, a major factor in the economic exploitation of geothermal resources will be the cost-effective selection of materials that have sufficient resistance to corrosion to maintain component integrity.

In this paper we review our recent studies[2-4] of the corrosion potential and cyclic voltammetric behavior of AISI 1010 carbon steel, E-Brite 26-1 stainless steel, AISI 316L stainless steel, Haynes Alloy 20 Mod, Carpenter 20 Cb-3, Inconel Alloy 625, Hastelloy Alloy G, Hastelloy Alloy C-276, Titanium 50A (ASTM B265 Gr. 2), and TiCode 21 in a sulfide-free high-salinity geothermal brine taken from a producing well located in the

Imperial Valley in Southern California. Potential-pH diagrams for the component metal (Fe, Ni, Cr, Ti)-brine systems[2,3] at temperatures of 25°C and 250°C are used to rationalize the corrosion potentials and the oxidation and reduction peak potentials for the alloys observed by cyclic voltammetry.[5] Previous work[6-8] has shown that comparison of experimental corrosion and cyclic voltammetric peak potentials with calculated equilibrium potentials is a useful method for analyzing the corrosion behavior of metals and alloys in aqueous systems at elevated temperature.

We also report potential-pH diagrams for iron and nickel in high salinity brine at 25°C and 250°C containing 10 ppm of total dissolved sulfide.[2,4] These diagrams are used to analyze the general features of the thermodynamic behavior of iron and nickel in high temperature sulfide-containing geothermal systems.[4]

## EXPERIMENTAL

Corrosion potentials and cyclic voltammograms were measured using a conventional once-through flow line containing a 2-liter pressure vessel manufactured from Hastelooy Alloy C-276. The design and operation of the apparatus have been fully described elsewhere.[2]

The brine used was taken from the Magmamax No. 1 well near Niland, California, and was reconstituted by sparging with a $N_2$ + 2 vol% $CO_2$

gas mixture to adjust the pH to the wellhead value (at ambient temperature) of 5.2. The chemical composition of the brine used for the experimental work in this study is given in Table 1.[2] In spite of our attempts[2] to maintain the chemical stability of the brine during transportation and storage, a sludge precipitated over a period of time. Energy dispersive X-ray (EDX) analysis showed that this precipitate contained Fe, Si, Al, Cl, and some Ca, Na, and K. Only NaCl was identified by X-ray diffraction analysis, although two additional, but unindexed, lines were also observed. The halite (NaCl) phase presumably precipitated during drying of the sludge. Further precipitation occurred when the filtrate was stored in a polyethylene bottle that remained open to the atmosphere.

Specimens (1 cm x 1 cm x 0.16 cm) of each alloy were exposed simultaneously to the brine for the determination of the corrosion potentials and acquisition of cyclic voltammograms. The chemical compositions of the alloys are given in Table 2. Each specimen was given an abraded finish with 120-grit SiC paper, and was degreased with acetone, washed with distilled water, and air-dried before exposure to the brine environment.

Cyclic voltammograms[5] were recorded by linearly sweeping the potential for each alloy between the limits given in Table 3. A single sweep rate of 0.010 V/s was used, and the voltammograms were recorded over at least

Table 1

CHEMICAL COMPOSITION OF THE MAGMAMAX No. 1 BRINE USED IN THE LABORATORY TESTS
(Total Dissolved Solids = 215.8 mg/l)

| Element | Method | Concentration mg/l |
|---|---|---|
| Cl | XRF | 129,000 |
| Na | AA | 52,000 |
| Ca | XRF | 25,000 |
| K | XRF | 6,250 |
| Mg | XRF | 1,100 |
| P | C | ~ 500 |
| Mn | XRF | 450 |
| Sr | XRF | 360 |
| Zn | XRF | 240 |
| Si | AA | 190 |
| Fe | XRF | 180 |
| Br | XRF | 100 |
| Rb | XRF | 65 |
| Pb | XRF | 46 |
| V | XRF | 30 |
| B | PT | 25 |
| Al | AA | 25 |
| Li | PT | ≤ 25 |
| Ba | XRF | < 10 |
| I | XRF | < 10 |
| Ti | XRF | < 10 |
| As | XRF | 6.2 |
| F | ISE | < 5.0 |
| Cr | XRF | < 5.0 |
| Cd | XRF | 3.7 |
| Co | XRF | < 2.0 |
| Ni | XRF | < 1.5 |
| Cu | XRF | 1.4 |
| Sn | XRF | < 1.0 |
| Hg | XRF | < 0.50 |
| Se | XRF | < 0.50 |
| Ag | XRF | 0.35 |

XRF = X-ray fluorescence; AA = atomic absorption; C = colorimetry, PT = potentiometric titration; ISE = ion selective electrode; <5.0 = not detected (limit of detectability is 5.0 mg/l).

## Table 2

### CHEMICAL COMPOSITIONS OF TEST MATERIALS

(Weight Percent)

| Alloy | Fe | Ni | Cr | Co | Mo | W | Si | Mn | C | Cu | Ti | P | S | Other |
|---|---|---|---|---|---|---|---|---|---|---|---|---|---|---|
| AISI 1010 Carbon Steel | Bal | - | - | - | - | - | 0.01 | 0.31 | 0.061 | - | - | 0.009 | 0.012 | |
| E-Brite 26-1 Stainless Steel[a] | Bal | 0.11 | 26.01 | - | 1.01 | - | 0.22 | 0.02 | < 0.001 | 0.02 | - | 0.012 | 0.011 | 0.010 N |
| AISI 316L Stainless Steel[b] | Bal | 13.29 | 17.39 | - | 2.31 | - | 0.63 | 1.79 | 0.021 | - | - | 0.021 | 0.007 | |
| Haynes Alloy 20 Mod[c] | Bal | 25.87 | 21.85 | - | 4.23 | - | 0.58 | 0.84 | 0.03 | - | 0.36 | 0.013 | 0.010 | |
| Carpenter 20 Cb-3[b] | Bal | 33.13 | 19.35 | 0.33 | 2.20 | - | 0.43 | 0.26 | 0.03 | 3.22 | - | 0.02 | 0.002 | 0.78 Cb + Ta |
| Inconel Alloy 625[d] | 3.10 | Bal | 21.41 | - | 8.82 | - | 0.30 | 0.11 | 0.03 | - | 0.31 | 0.013 | 0.002 | 3.47 Cb + Ta, 0.18 Al |
| Hastelloy Alloy G[c] | 18.98 | Bal | 21.99 | 1.82 | 6.47 | 0.51 | 0.32 | 1.34 | .0.03 | 1.77 | - | 0.025 | 0.010 | 2.11 Cb + Ta |
| Hastelloy Alloy C-276[c] | 5.94 | Bal | 15.15 | 2.04 | 15.48 | 3.37 | 0.03 | 0.40 | 0.004 | - | - | 0.013 | 0.009 | 0.19 V |
| Titanium 50A (ASTM B265 Gr.2)[e] | 0.13 | - | - | - | - | - | - | - | 0.013 | - | Bal | - | - | 0.008 N, 0.004 H, 0.11 O |
| TiCode 12[e] | 0.11 | 0.84 | - | - | 0.29 | - | - | - | 0.012 | - | Bal | - | - | 0.009 N, 0.14 O |

[a]Donated by Airco Vacuum Metals.
[b]Donated by Carpenter Technology Corporation.
[c]Donated by Stellite Division of Cabot Corporation.
[d]Donated by Huntington Alloys Inc.
[e]Donated by Timet.

Table 3

CORROSION POTENTIAL AND CYCLIC VOLTAMMETRIC DATA FOR THE ALLOYS IN HIGH SALINITY BRINE AT 250°C

| | $E_{corr}$ | $E_{ff}$ | Polar. Limits | $E_p$ (Oxidation) | $E_p$ (Reduction) |
|---|---|---|---|---|---|
| AISI No. 1010 Carbon Steel | -0.66 to -0.45 | -0.71 to -0.69 | -1.06 to 0.11 | (-0.41), -0.36, -0.18 | -0.73 |
| E-Brite 26-1 | -0.47 to -0.35 | -0.89 to -0.80 | -1.97 to 1.03 | -0.72, -0.62, (-0.48), (-0.05), 0.44 | -1.32 |
| 316L SS | -0.44 to -0.34 | -0.89 to -0.87 | -1.99 to 0.46 | -0.67, -0.61 | |
| Haynes Alloy 20 Mod | -0.44 to -0.33 | -0.95 to -0.80 | -1.98 to 0.14 | (-0.85), -0.73, -0.55, (-0.42) | |
| Carpenter 20 Cb-3 | -0.42 to -0.32 | -0.95 to -0.88 | -1.97 to 0.23 | -0.88, -0.72, -0.55 | |
| Inconel Alloy 625 | -0.44 to -0.33 | -0.99 to -0.77 | -1.99 to 0.22 | -0.95, -0.74, -0.53 | -1.20 |
| Hastelloy Alloy G | -0.47 to -0.33 | -0.99 to -0.78 | -1.97 to 0.13 | -0.95, -0.74, -0.57, -0.41 (-0.11) | |
| Hastelloy Alloy C-276 | -0.45 to -0.32 | -0.99 to -0.81 | -1.98 to 0.31 | -0.90, -0.70, -0.52, -0.38 | -1.32,-0.97, (-0.79) |
| Titanium 50A | -0.47 to -0.34 | -0.56 to -0.40 | -1.99 to 1.04 | -0.87, -0.50, -0.22, 0.14, 0.29, 0.56 | |
| TiCode 12 | -0.48 to -0.38 | -0.73 to -0.45 | -1.99 to 1.03 | -0.67, -0.61, -0.42, -0.34, -0.17, 0.36, 0.50, 0.85 | -1.78 |

All potentials are in volts versus the standard hydrogen electrode at 250 C.
$E_{corr}$ - Corrosion Potential. $E_{ff}$ - zero current potential after reduction. (-0.41) - brackets around a potential indicate a point of inflection rather than a peak.

three successive cycles. The cyclic voltammograms were measured during the last 50 hours of the test. The specific time of aquisition for each alloy is given in the caption of the appropriate figure (Figs. 3-12). All experiments were carried out at a temperature of 250°C and at a pressure of 5.52 MPa. The pressure, which was sufficiently high to prevent boiling, was maintained by use of a metering pump and a pressure release valve in the outlet leg of the system.

All potential measurements were made with respect to internal silver-silver chloride electrodes[9] (0.1 m KCl or 3.6 m KCl) operating at the temperature of interest, as previously described.[2,3] The higher KCl concentration in one of the reference electrodes was used to minimize the liquid junction potential between the brine (~ 3.6 m KCl) and the electrode contents. In general, the 0.1 m KCl electrode gave more reliable service than that with the 3.6 m KCl electrolyte; a behavior that we attribute to a lower tendency in the dilute system to form soluble silver chloride anionic complexes of the type $AgCl_{n+1}^{2-}$ or possibly due to a lower susceptibility to reduction of silver chloride by dissolved hydrogen.[8,10]

## RESULTS

### Corrosion Potential

The variation of corrosion potential for each alloy with time from startup at 22°C to termination of the experiment after 150 hours exposure at 250°C is shown in Figs. 1 and 2. For all materials studied,

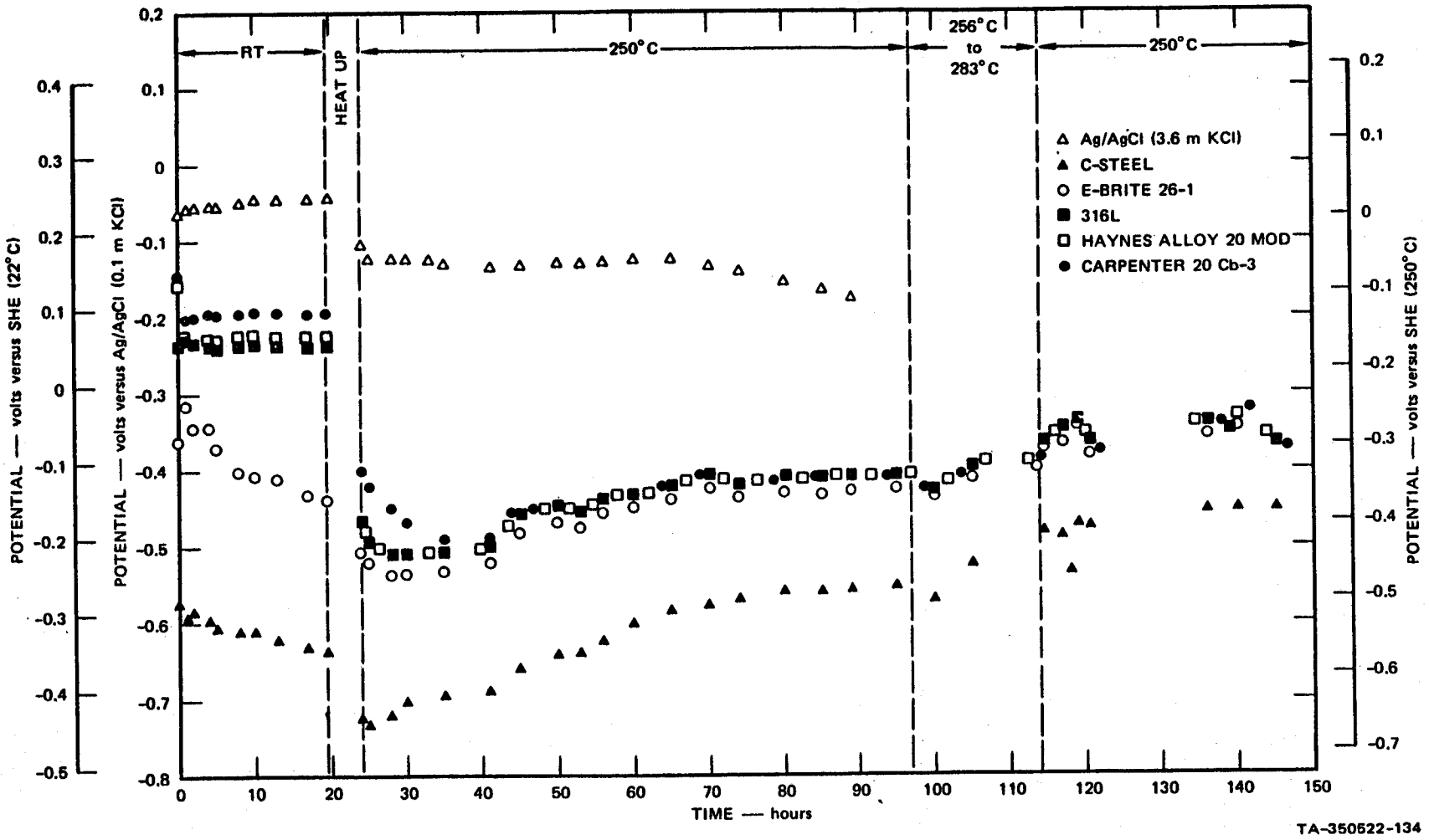


FIGURE 1 CORROSION POTENTIAL-TIME CURVES FOR IRON-BASED MATERIALS IN HIGH-SALINITY BRINE (pH 5.36 AT 25°C)
RT — room temperature

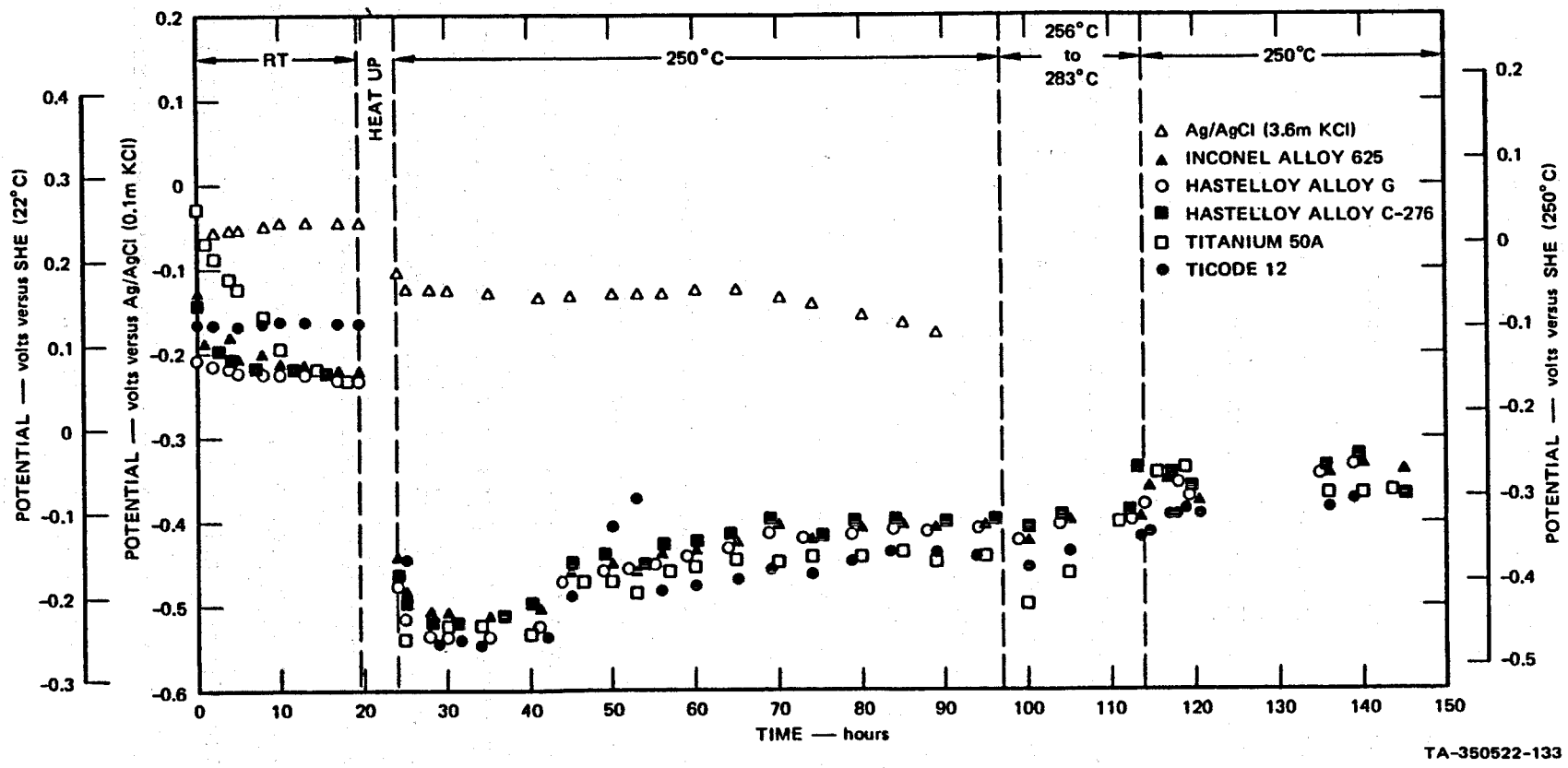


FIGURE 2 CORROSION POTENTIAL-TIME CURVES FOR NICKEL- AND TITANIUM-BASED MATERIALS IN HIGH-SALINITY BRINE (pH 5.36 AT 25°C)

RT — room temperature

the corrosion potential was found to shift sharply to more active values when the temperature of the system was changed from 22°C to 250°C. A gradual drift of $E_{corr}$ with time to more noble values was then observed over the 130-hour exposure period at elevated temperatures. The corrosion potential was not significantly affected by the temperature excursion to 283°C that occurred between 97 and 113 hours after initiation of the test. The sudden change to more active values that occurred when the system was heated parallels the behavior previously observed for carbon steel in lithium hydroxide solution at elevated temperatures.[11] This sudden shift probably reflects the consumption of trace amounts of oxygen in the system as the temperature is changed, and also the tendency for many metals and alloys to corrode in the "active" state in aqueous systems at elevated temperatures.[6-8]

The more negative corrosion potential for carbon steel suggests that this alloy corrodes in a more active mode than the other alloys in both the ambient and elevated temperature environments. This observation is in keeping with previous work on the behavior of metals and alloys in high temperature aqueous systems.[6-8,11-13] The gradual shift in $E_{corr}$ to more noble values with time at elevated temperature is consistent with the formation of a surface film that progressively inhibits the anodic partial reaction. Accordingly, the corrosion potential is expected to shift towards the equilibrium potential for the cathodic partial reaction (hydrogen evolution) as observed in Figs. 1 and 2.

## Cyclic Voltammetry

Typical cyclic voltammograms for the ten alloys studied in this work at a temperature of 250°C and after exposure for at least 115 hours are shown in Figs. 3 to 12. For clarity, only the first and third cycles are shown. All voltammograms were recorded by initially sweeping the potential in the noble to active direction from $E_{corr}$, followed by reversal of the sweep once the potential had been displaced well into the hydrogen evolution region. The active to noble sweep was continued until oxygen evolution occurred, or until the current exceeded 300-400 mA. The sweep was then reversed to complete the cycle.

Of principal interest in this work was the appearance of oxidation and reduction peaks when the potential was cycled between the selected upper and lower limits. The observed current can be expressed in general form as[5]

$$i = C(E)_{dl} \cdot \left(\frac{dE}{dt}\right) + i_F \qquad (1)$$

where $C(E)_{dl}$ is the potential-dependent double-layer capacitance, and $i_F$ is the current due to faradaic (including pseudocapacitive) processes. Peaks in cyclic voltammograms do not necessarily reflect active-to-passive transitions, as is commonly assumed, but may also arise from any charge-transfer process that experiences acceleration, followed by inhibition, as the potential of the metal is varied linearly with time. Examples of such processes include reversible and irreversible reactions involving

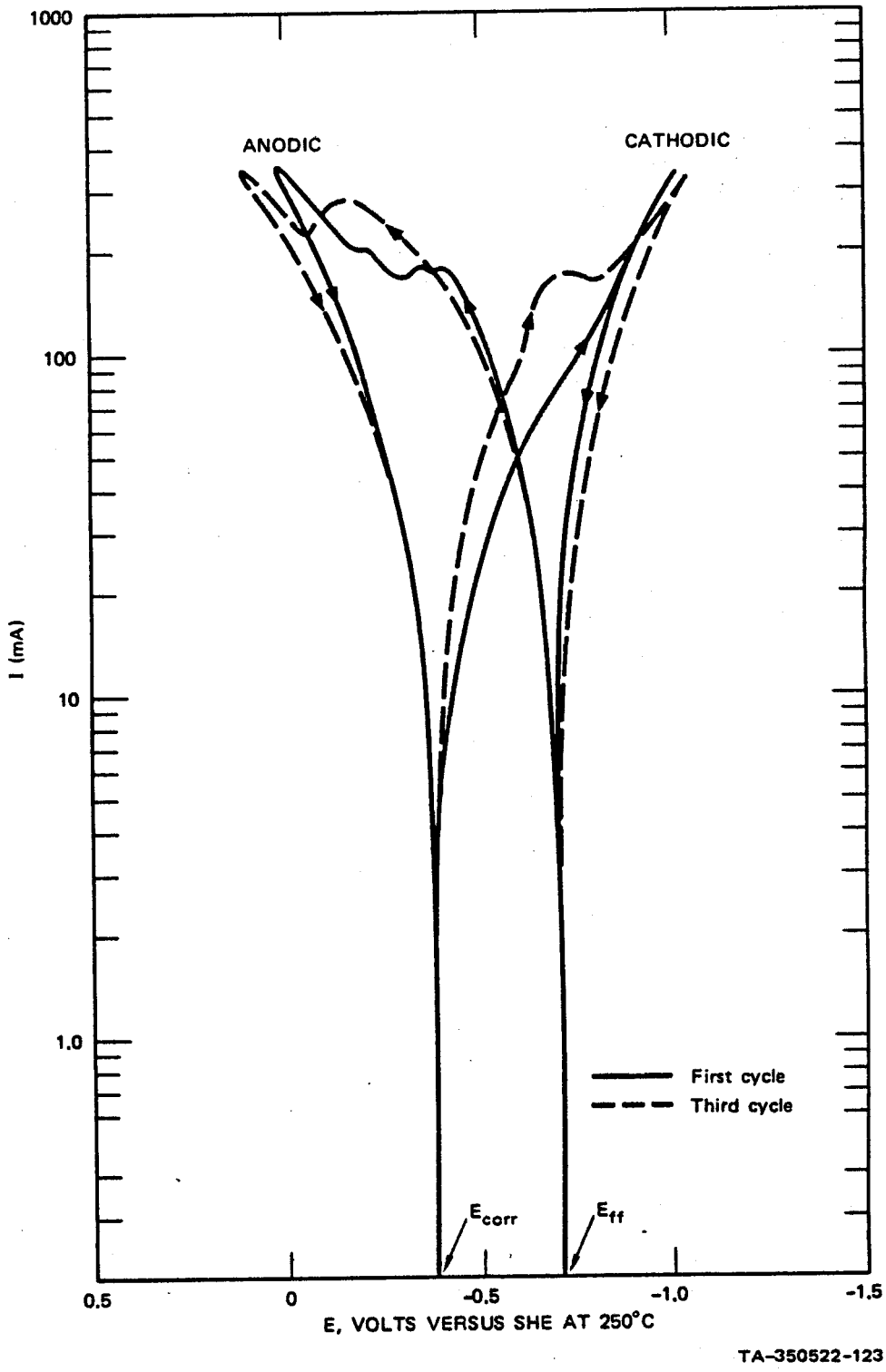


FIGURE 3 CYCLIC VOLTAMMOGRAM FOR AISI TYPE 1010 CARBON STEEL IN HIGH-SALINITY BRINE AT 250°C AFTER 117.5 HOURS EXPOSURE

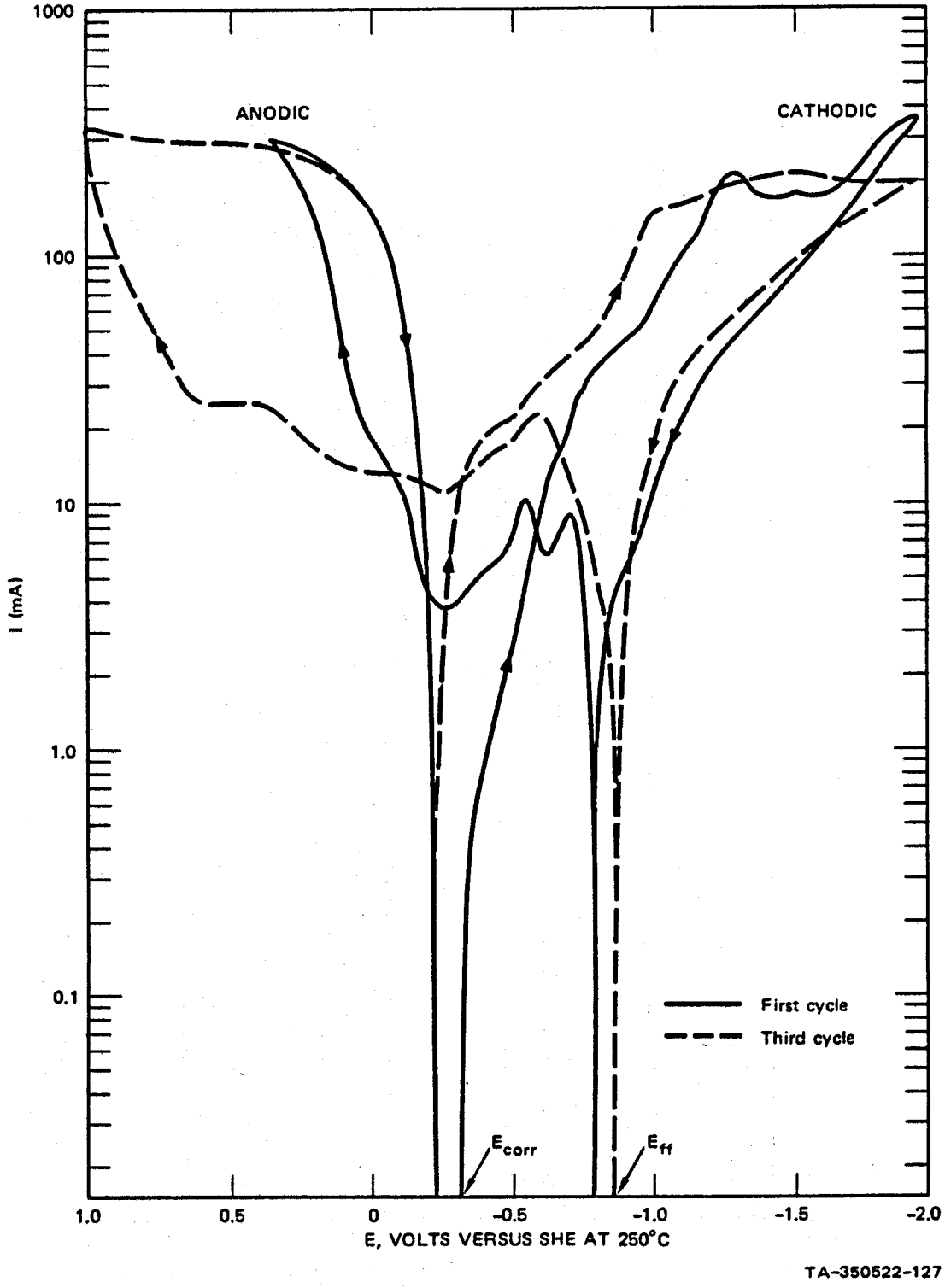


FIGURE 4 CYCLIC VOLTAMMOGRAM FOR E-BRITE 26-1 SS IN HIGH-SALINITY BRINE AT 250°C AFTER 145 HOURS EXPOSURE

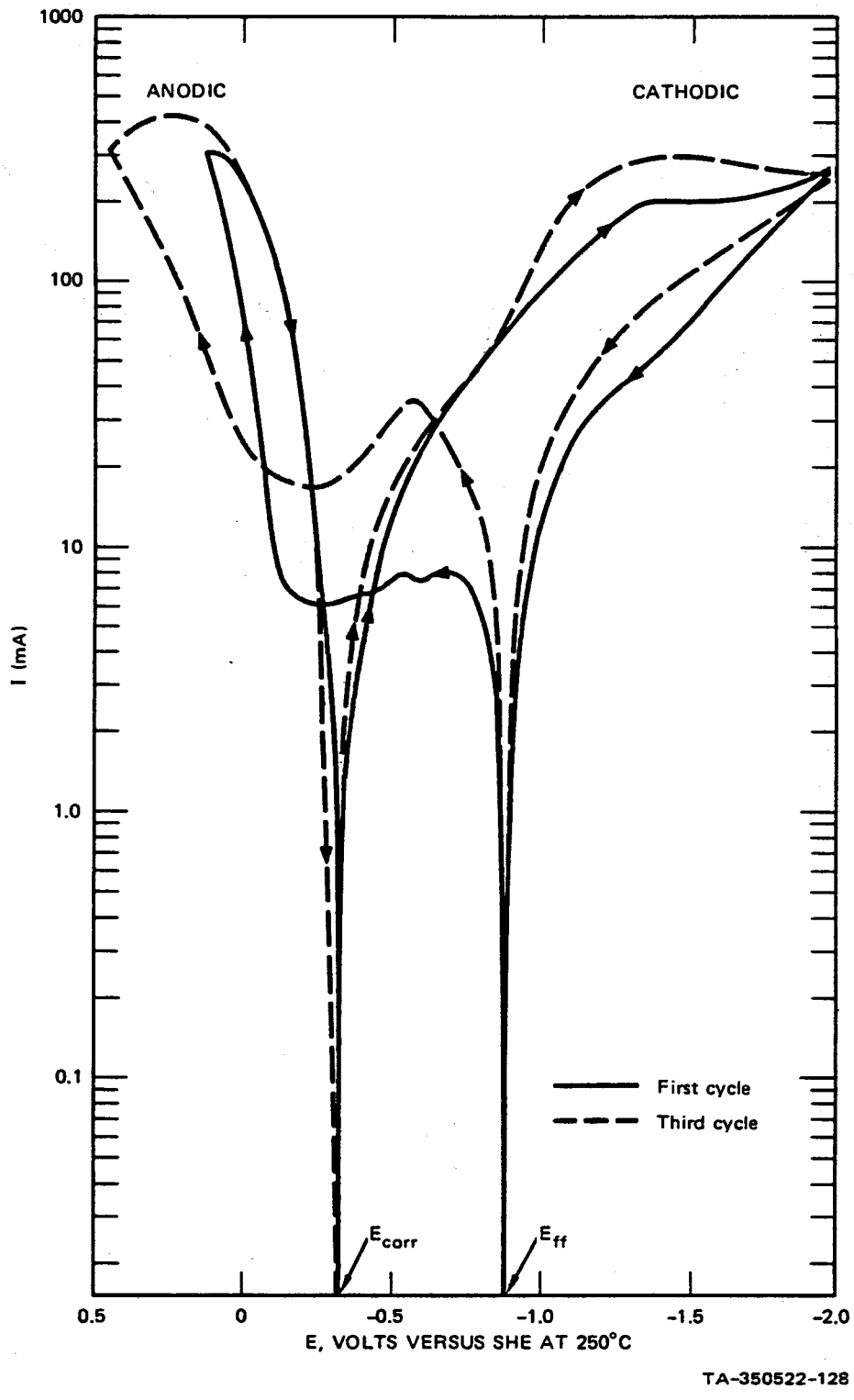


FIGURE 5 CYCLIC VOLTAMMOGRAM FOR 316L SS IN HIGH-SALINITY BRINE AT 250°C AFTER 143.5 HOURS EXPOSURE

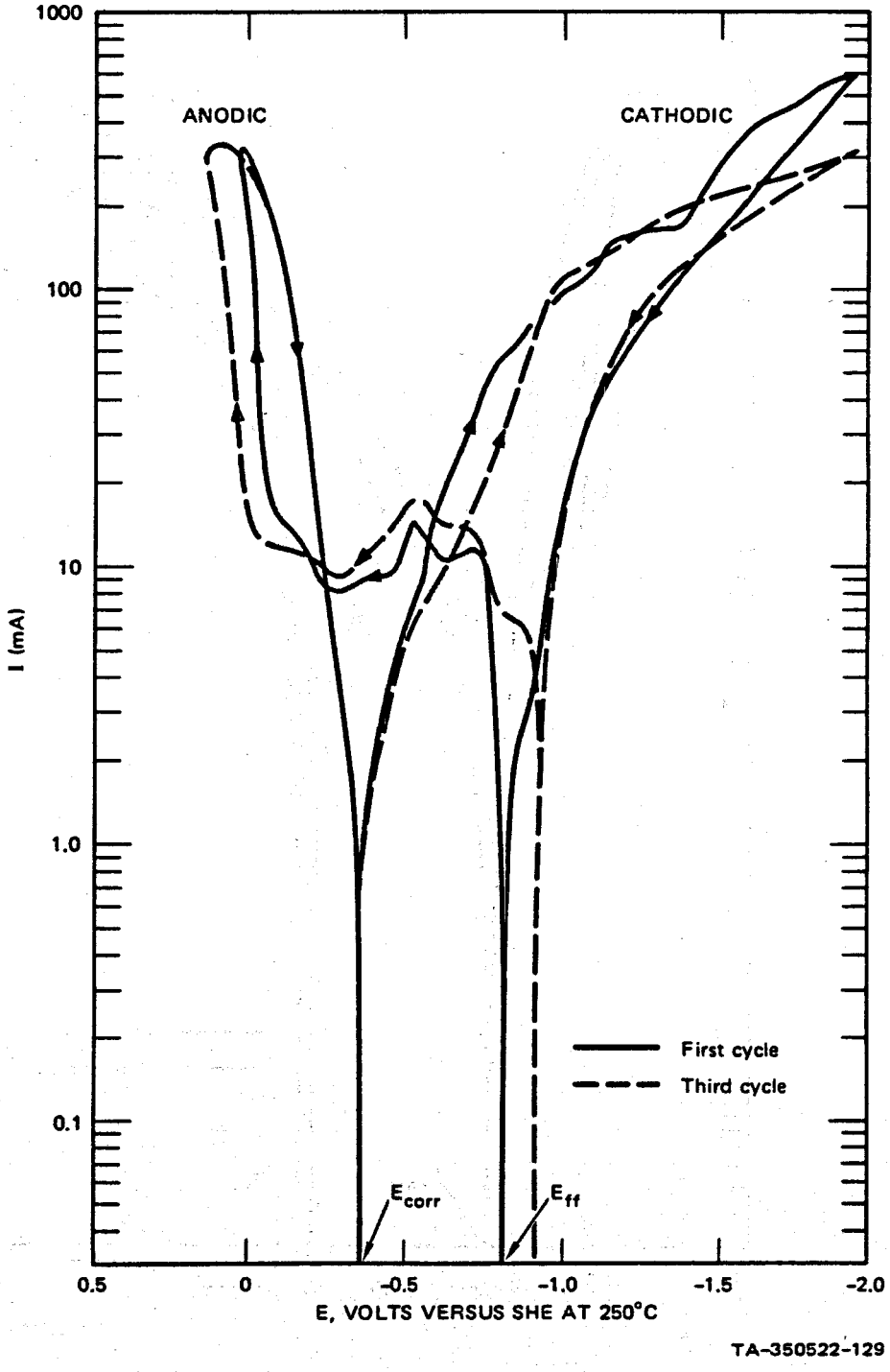


FIGURE 6 CYCLIC VOLTAMMOGRAM FOR HAYNES ALLOY 20 MOD. IN HIGH-SALINITY BRINE AT 250°C AFTER 143 HOURS EXPOSURE

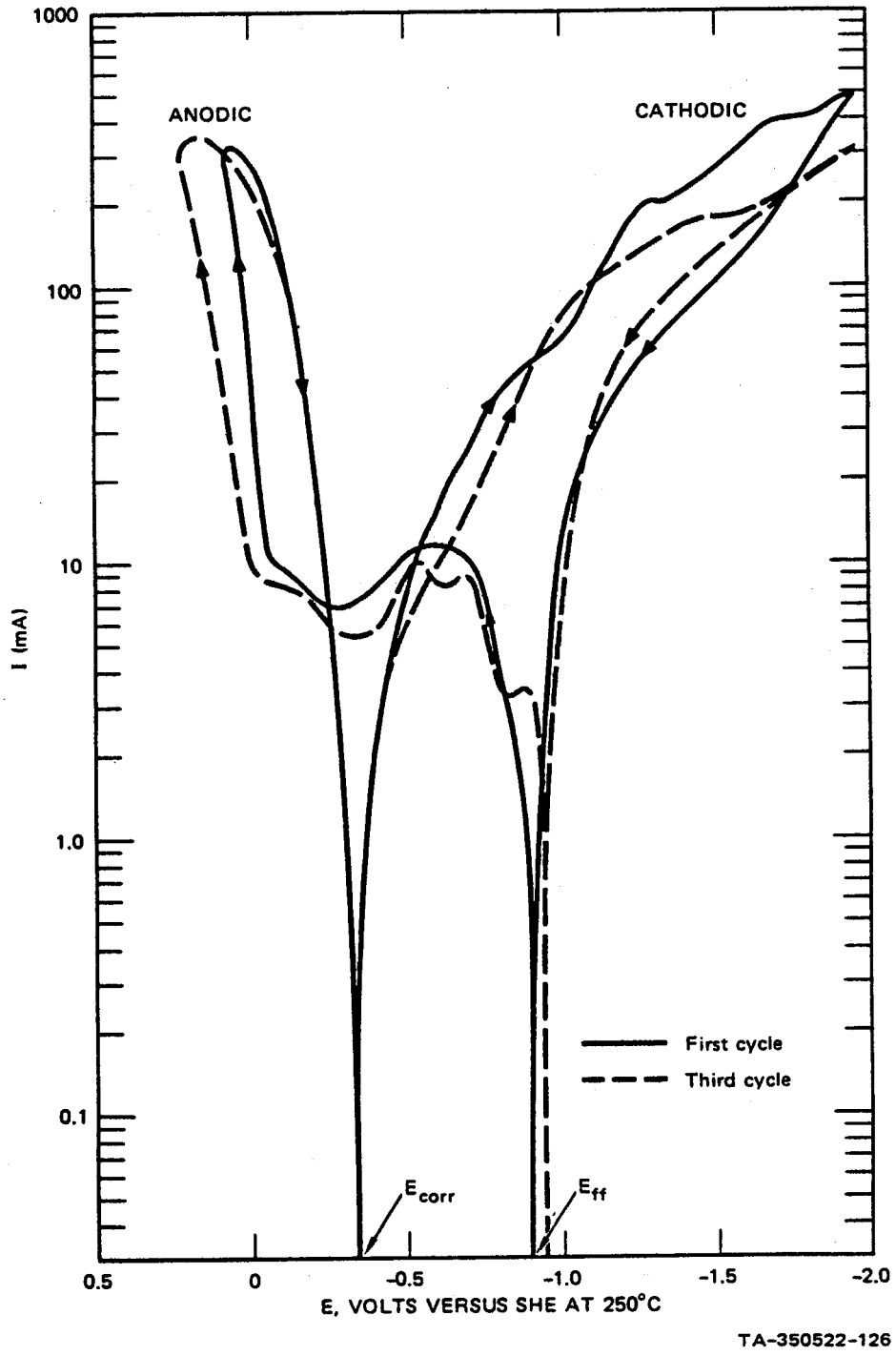


FIGURE 7 CYCLIC VOLTAMMOGRAM FOR CARPENTER 20Cb-3 IN HIGH-SALINITY BRINE AT 250°C AFTER 144 HOURS EXPOSURE

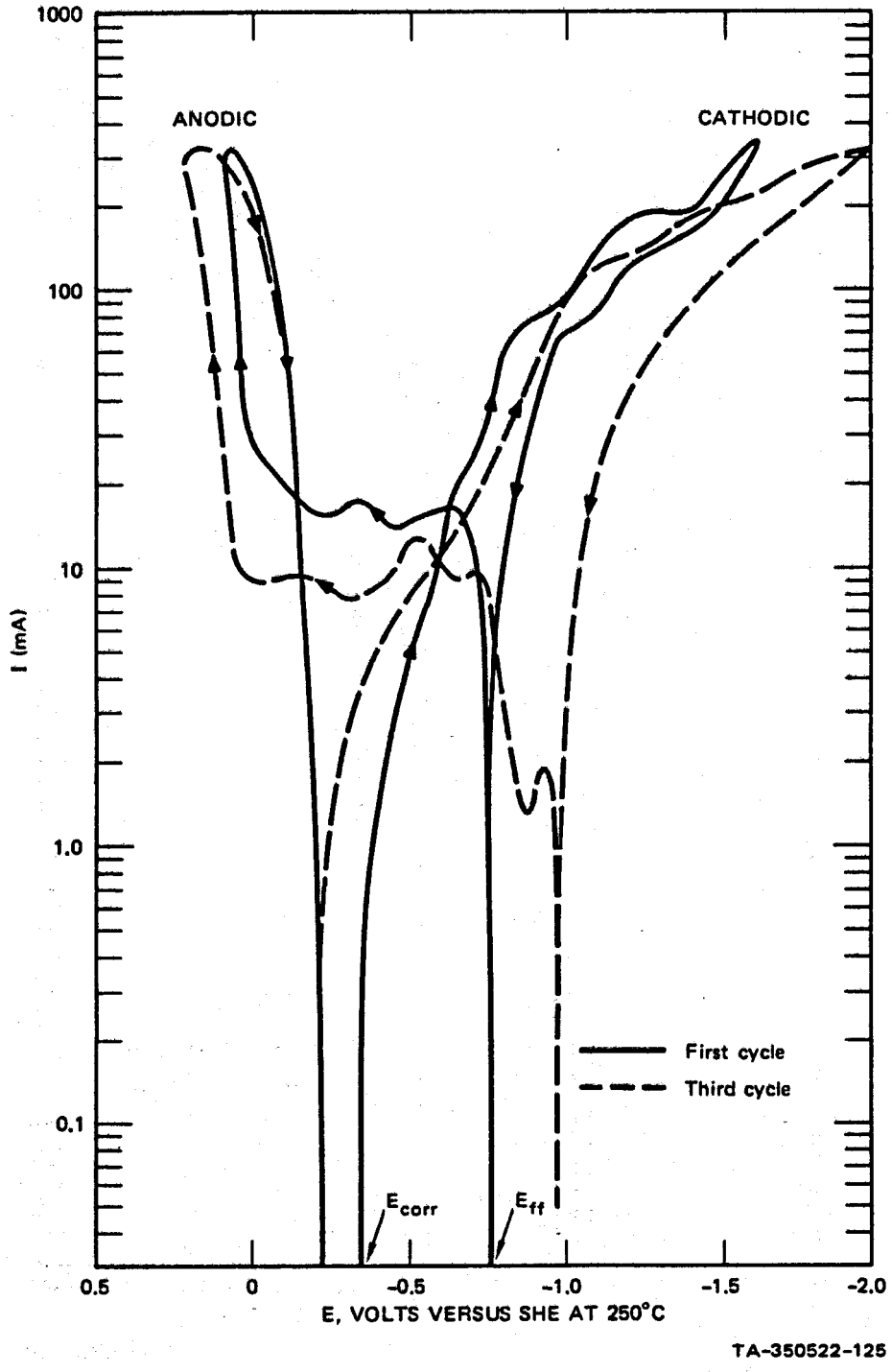


FIGURE 8 CYCLIC VOLTAMMOGRAM FOR INCONEL ALLOY 625 IN HIGH-SALINITY BRINE AT 250°C AFTER 118.5 HOURS EXPOSURE

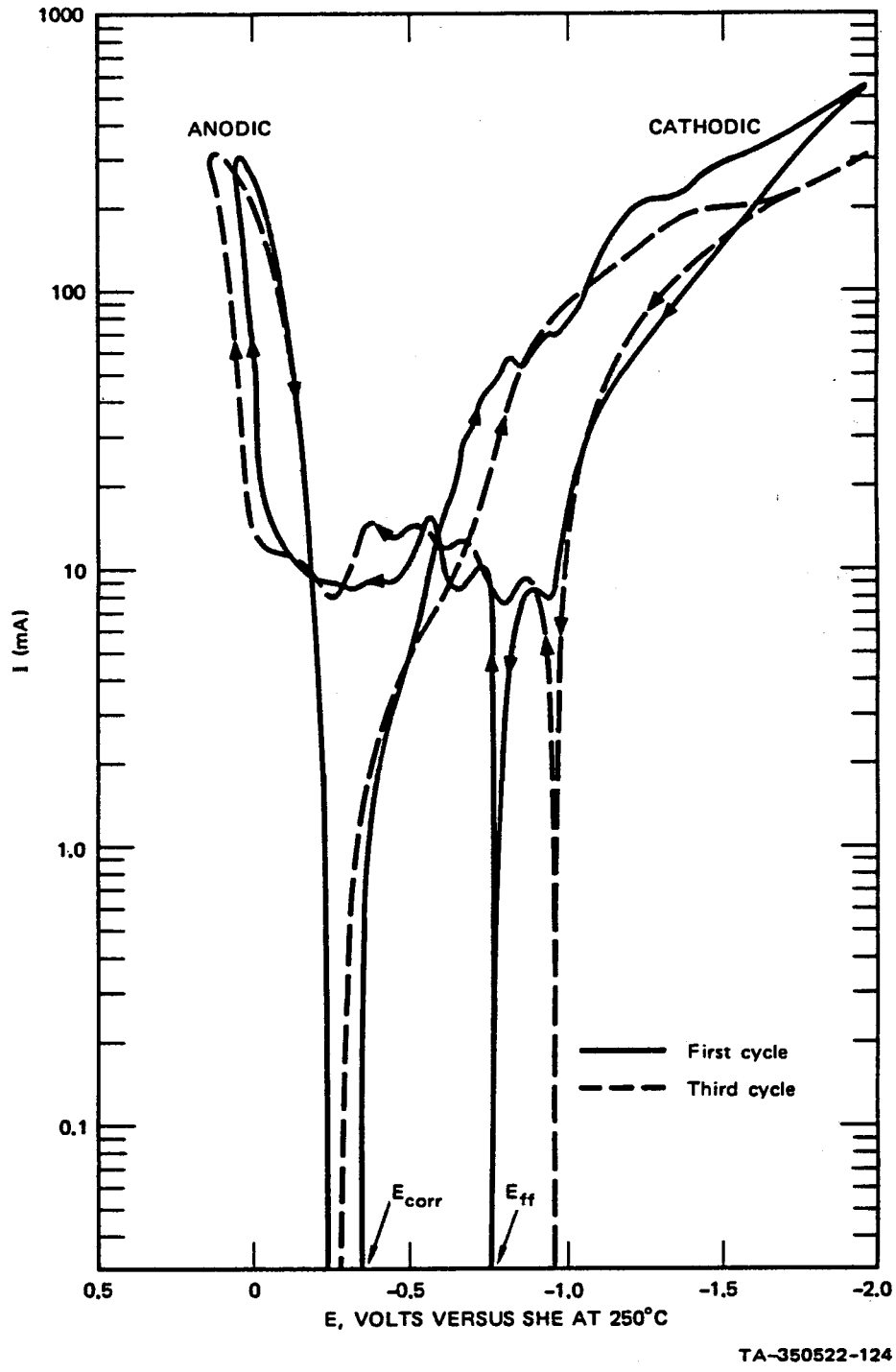


FIGURE 9 CYCLIC VOLTAMMOGRAM FOR HASTELLOY ALLOY G IN HIGH-SALINITY BRINE AT 250°C AFTER 145.5 HOURS EXPOSURE

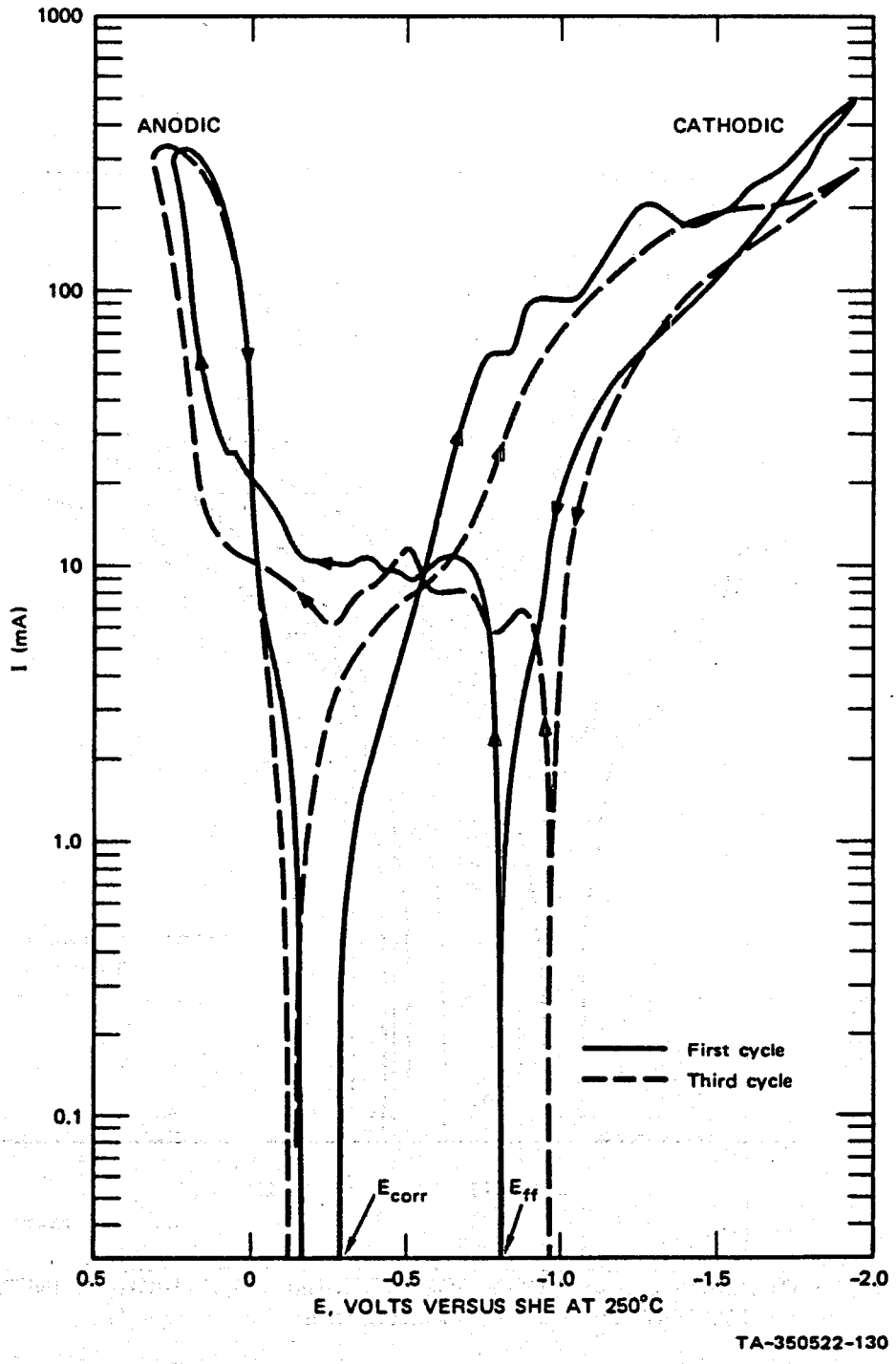


FIGURE 10 CYCLIC VOLTAMMOGRAM FOR HASTELLOY ALLOY C-276 IN HIGH-SALINITY BRINE AT 250°C AFTER 144.5 HOURS EXPOSURE

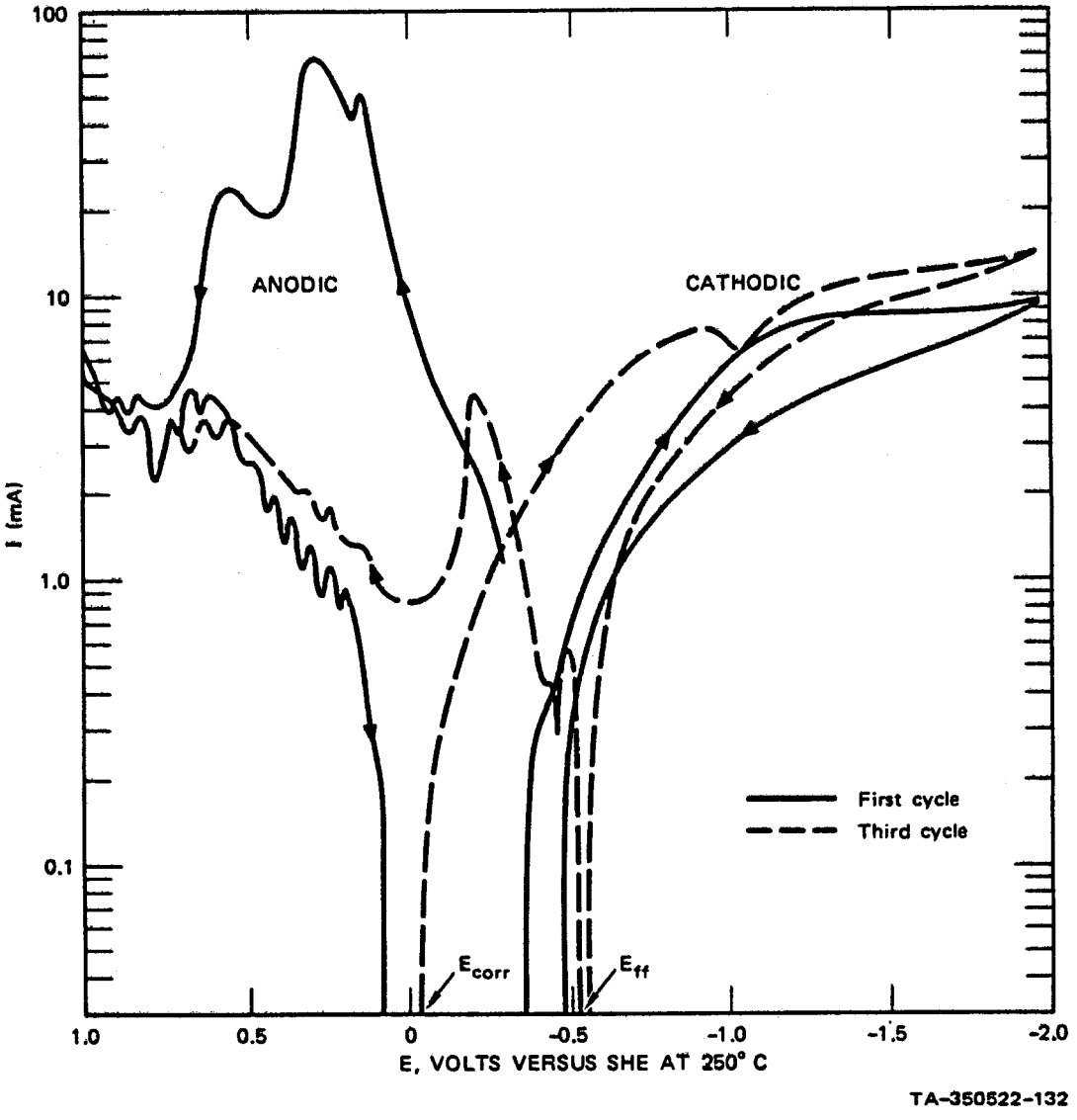


FIGURE 11 CYCLIC VOLTAMMOGRAM FOR TITANIUM 50A IN HIGH-SALINITY BRINE AT 250°C AFTER 120 HOURS EXPOSURE

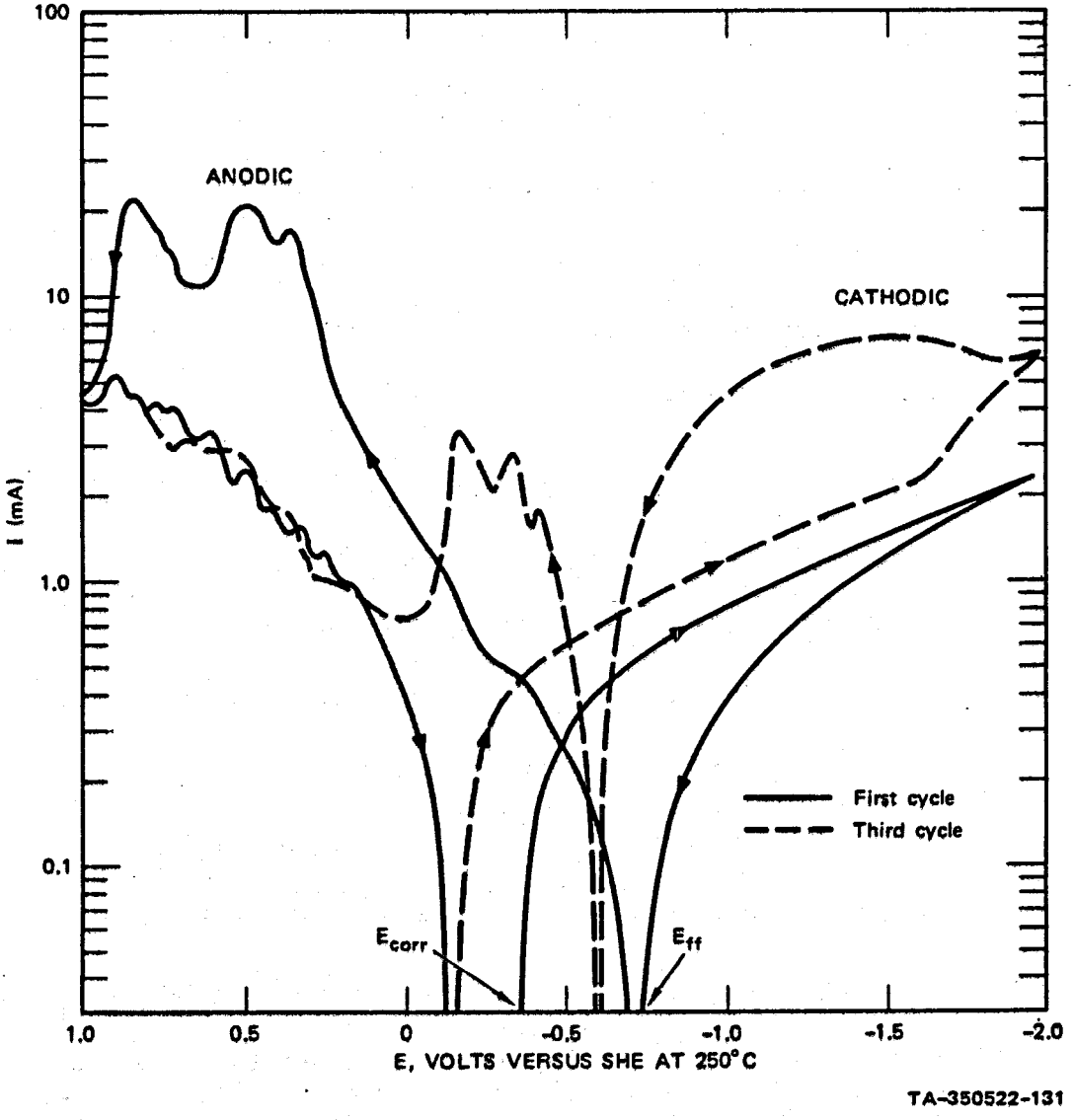


FIGURE 12 CYCLIC VOLTAMMOGRAM FOR TiCODE 12 IN HIGH-SALINITY BRINE AT 250°C AFTER 146 HOURS EXPOSURE

diffusion of dissolved reactants and products, and the formation of surface films via electrochemical adsorption of oxide or other ions onto the alloy surface,[5] in addition to the commonly assumed active-to-passive transitions. In principal, it is possible to differentiate between these various processes by analyzing the peak potential and current as a function of sweep-rate.[5,14] However, few of the transition metals and their alloys exhibit sufficiently reproducible voltammograms to make this type of analysis possible. This problem is well illustrated in the present work by a comparison of the first and third cycles for each alloy. Thus, for most of the materials studied, multiple cycling not only seriously affects the peak currents and potentials, but also leads to a change in the number of peaks observed. In view of the complex nature of cyclic voltammetric response, no attempt was made in this work to determine the sweep-rate dependencies of the peak currents and peak potentials. Instead, equivalent peaks in the three potential cycles were compared, and the most active oxidation peak potentials and the most noble reduction peak potentials were used for comparison with calculated equilibrium potentials for selected reactions involving pure components of the alloys.

For most of the materials studied (with the possible exception of the titanium alloys), the initial sweep of the potential in the noble-to-active direction from $E_{corr}$ probably reduced the surface films. Accordingly, the potential ($E_{ff}$) at which the current changes from cathodic to anodic on the subsequent active-to-noble sweep defines a

pseudo-corrosion state (i.e., $i_a + i_c = 0$, where $i_a$ and $i_c$ are the partial anodic and cathodic currents, respectively) in which inhibition of the partial anodic process by a surface film has been eliminated, or at least greatly reduced. Simple argument on the basis of the Wagner-Traud mechanism for electrochemical corrosion shows that $E_{ff}$ should be more active than the true, spontaneous, corrosion potential $E_{corr}$, as observed in Table 3.

All of the high-nickel and high-chromium alloys studied in this work exhibit a region of inverse hysteresis when the sweep is reversed at high noble potentials, with the current on the noble-to-active sweep exceeding that observed on the active-to-noble sweep. This behavior is characteristic of localized attack, such as pitting, and will be discussed in detail in a following paper.[15]

## DISCUSSION

### Potential-pH Diagrams For Sulfide-Free Systems

Potential-pH diagrams for iron (Figs. 13 and 14), nickel (Figs. 15 and 16), chromium (Figs. 17 and 18) and titanium (Figs. 19 and 20) in sulfide-free high salinity brine (3.6-m NaCl) at 25°C and 250°C were derived using previously described techniques.[16-20] A detailed discussion of the computational methods employed is given elsewhere,[2-4,20] and a listing of the species considered, together with the thermodynamic parameters used, may be found in Ref. 2. Briefly, equilibrium potentials and solubility relationships for

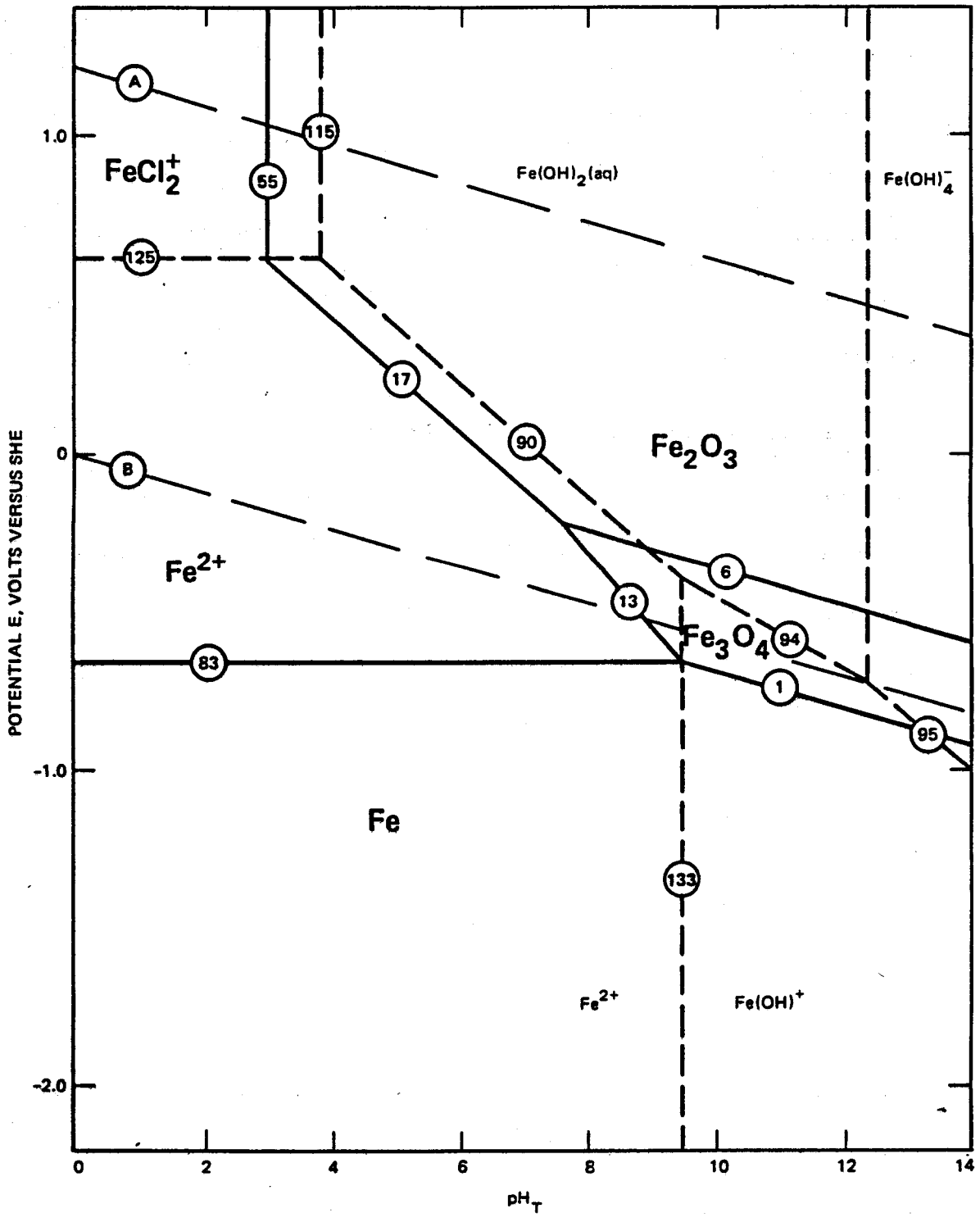


NOTE: (aq) designates soluble molecular species.

SA-5308-33

FIGURE 13 POTENTIAL-pH DIAGRAM FOR IRON IN HIGH-SALINITY BRINE AT 25°C

Activities of dissolved iron species = $10^{-6}$ molal.

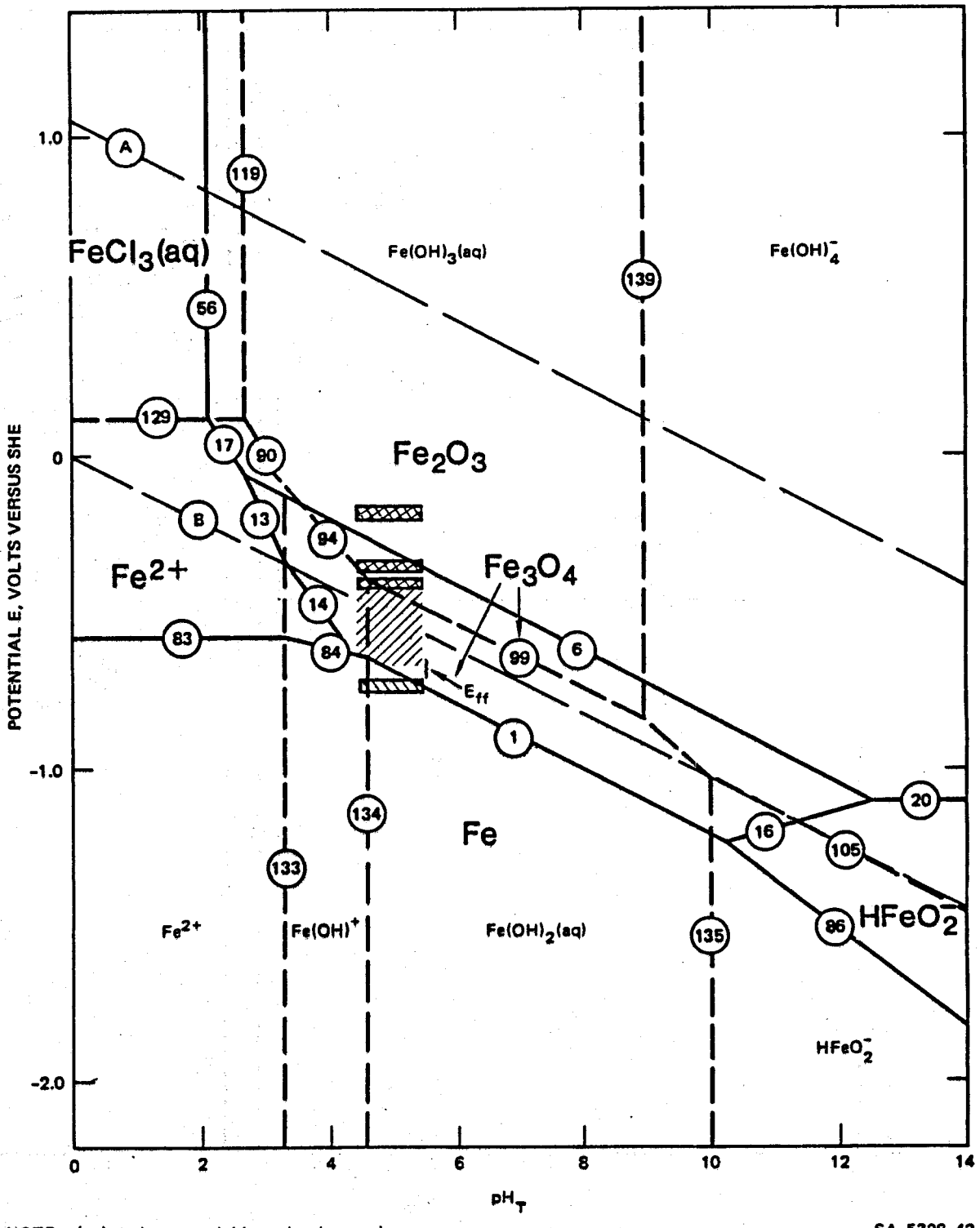


FIGURE 14 POTENTIAL-pH DIAGRAM FOR IRON IN HIGH-SALINITY BRINE AT 250°C

Activities of dissolved iron species = $10^{-4}$ molal. //// – $E_{corr}$ for carbon steel, ▨ – oxidation peak potential for carbon steel, ▧ – reduction peak potentials for carbon steel (see Table 3).

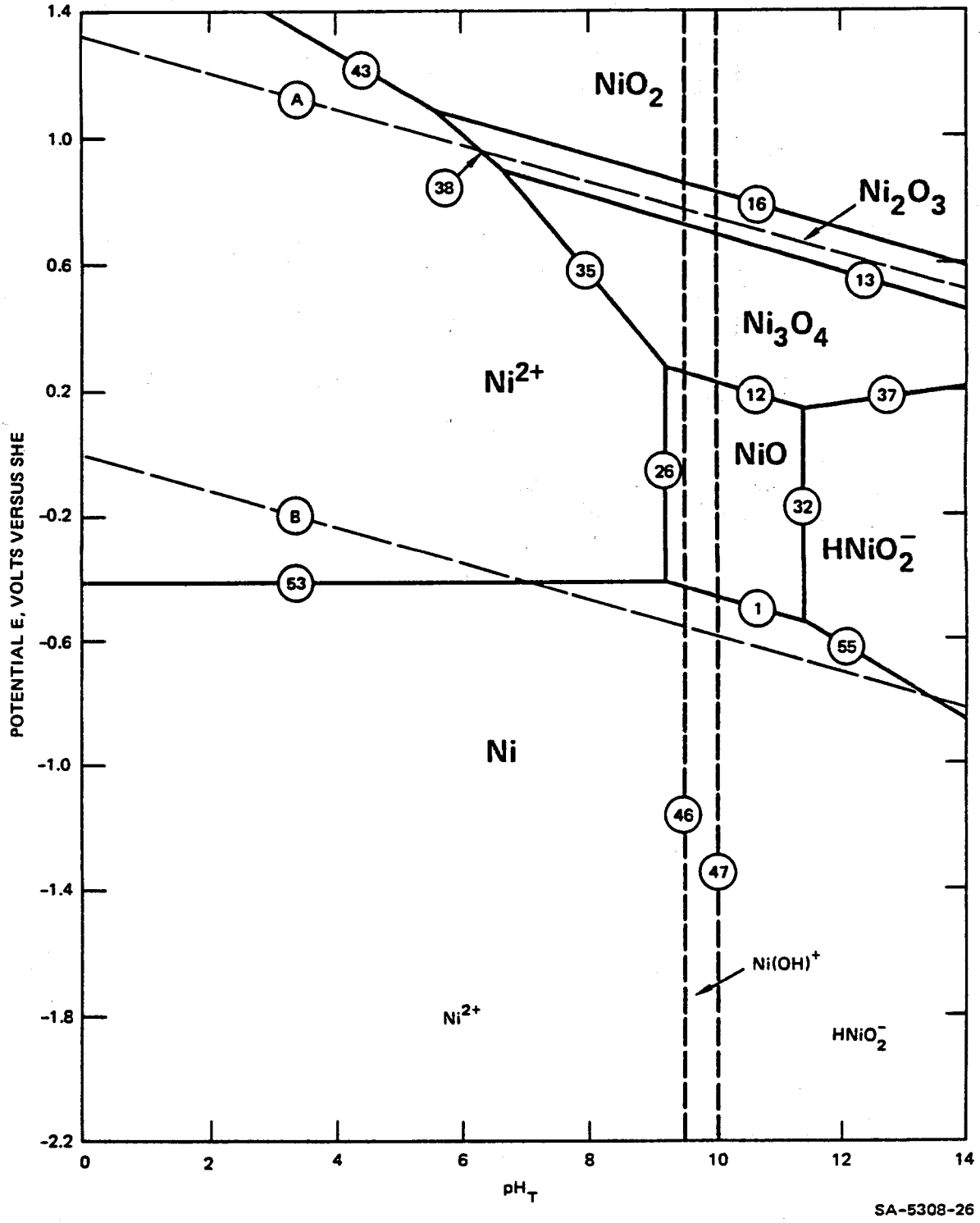


FIGURE 15 POTENTIAL-pH DIAGRAM FOR NICKEL IN HIGH-SALINITY BRINE AT 25°C

Activities of dissolved nickel species = $10^{-6}$ molal.

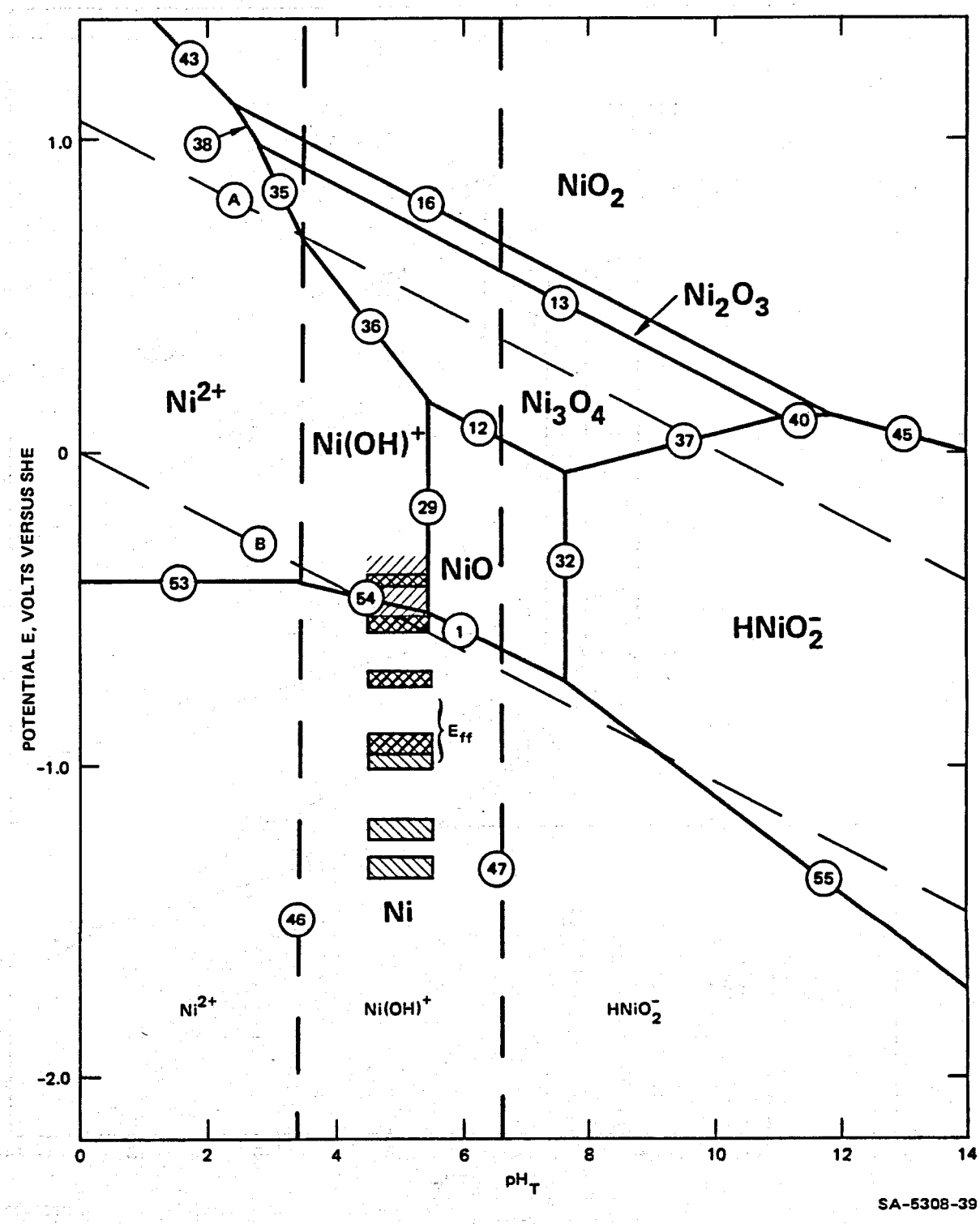


FIGURE 16 POTENTIAL-pH DIAGRAM FOR NICKEL IN HIGH-SALINITY BRINE AT 250°C

Activities of dissolved nickel species = $10^{-6}$ molal. //// – $E_{corr}$ for nickel-based alloys, ▨ – oxidation peak potentials for nickel-based alloys, ▨ – reduction peak potentials for nickel-based alloys (see Table 3).

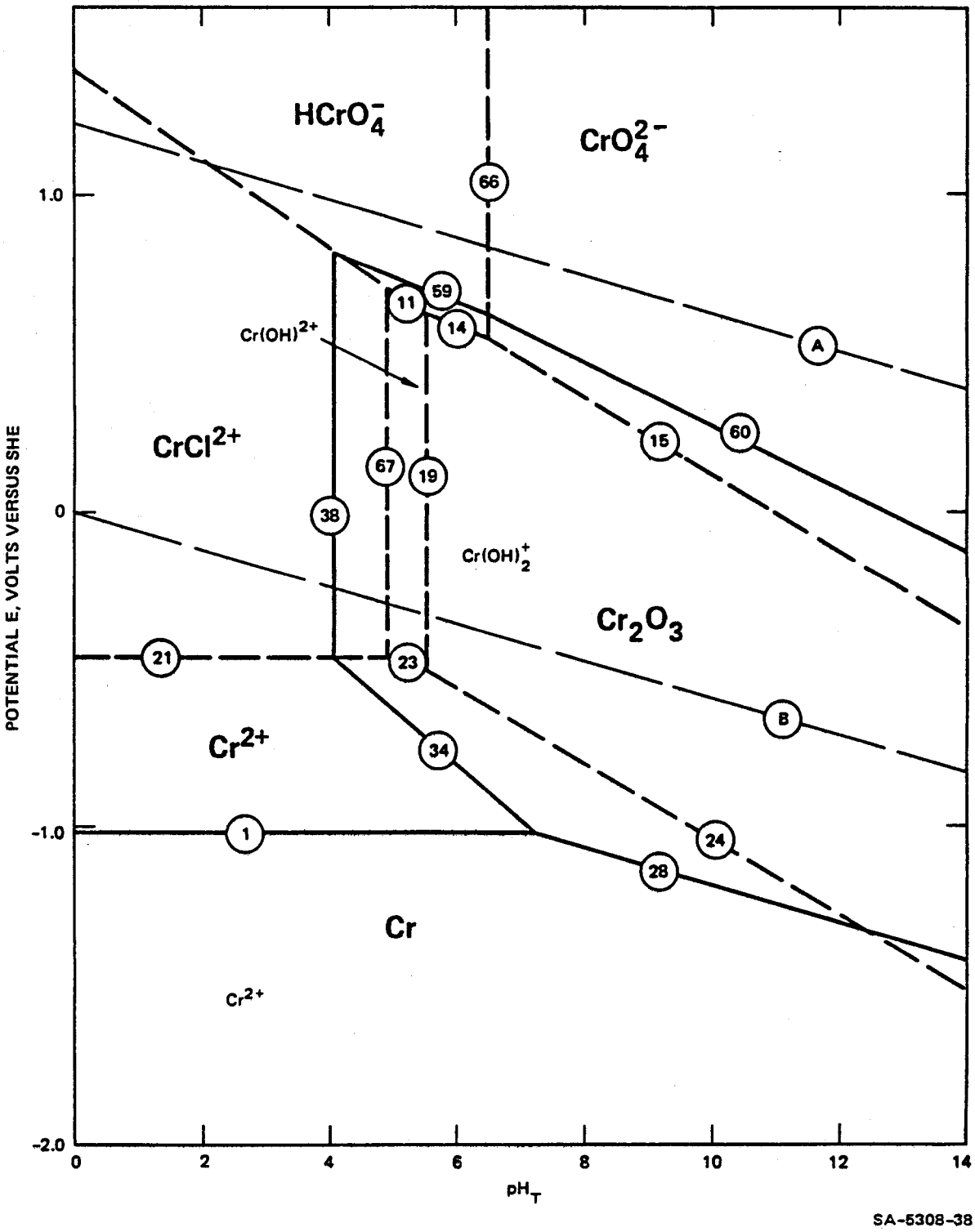


FIGURE 17 POTENTIAL-pH DIAGRAM FOR CHROMIUM IN HIGH-SALINITY BRINE AT 25°C

Activities of dissolved chromium species = $10^{-6}$ molal.

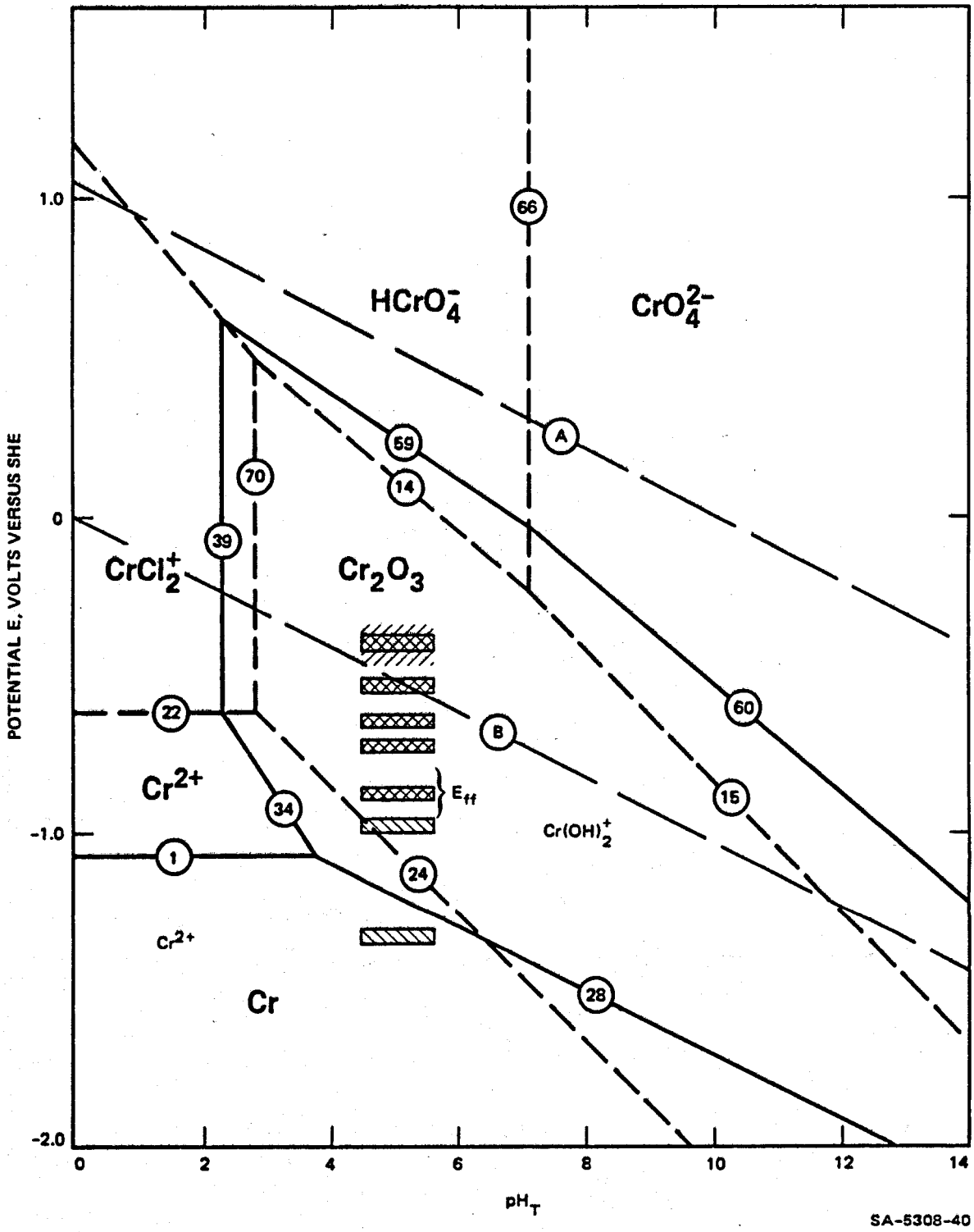


FIGURE 18 POTENTIAL-pH DIAGRAM FOR CHROMIUM IN HIGH-SALINITY BRINE AT 250°C

Activities of dissolved chronium species = $10^{-6}$ molal. //// – $E_{corr}$ for high chromium alloys (>15 wt%), ▨ – oxidation peak potential for high chromium alloy, ▨ – reduction peak potential for high chromium alloy.

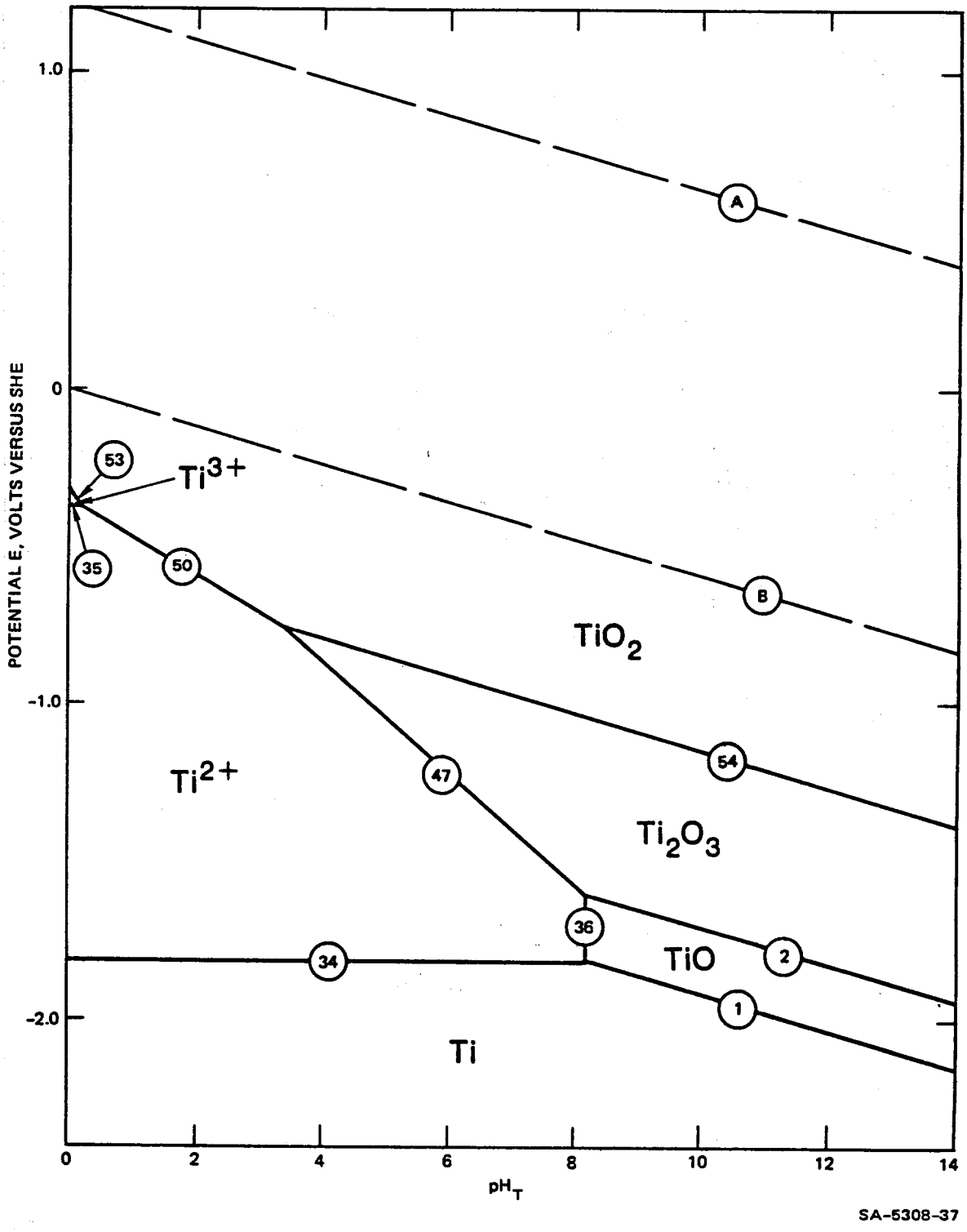


FIGURE 19 POTENTIAL-pH DIAGRAM FOR TITANIUM IN HIGH-SALINITY BRINE AT 25°C

Activities of dissolved titanium species = $10^{-6}$ molal.

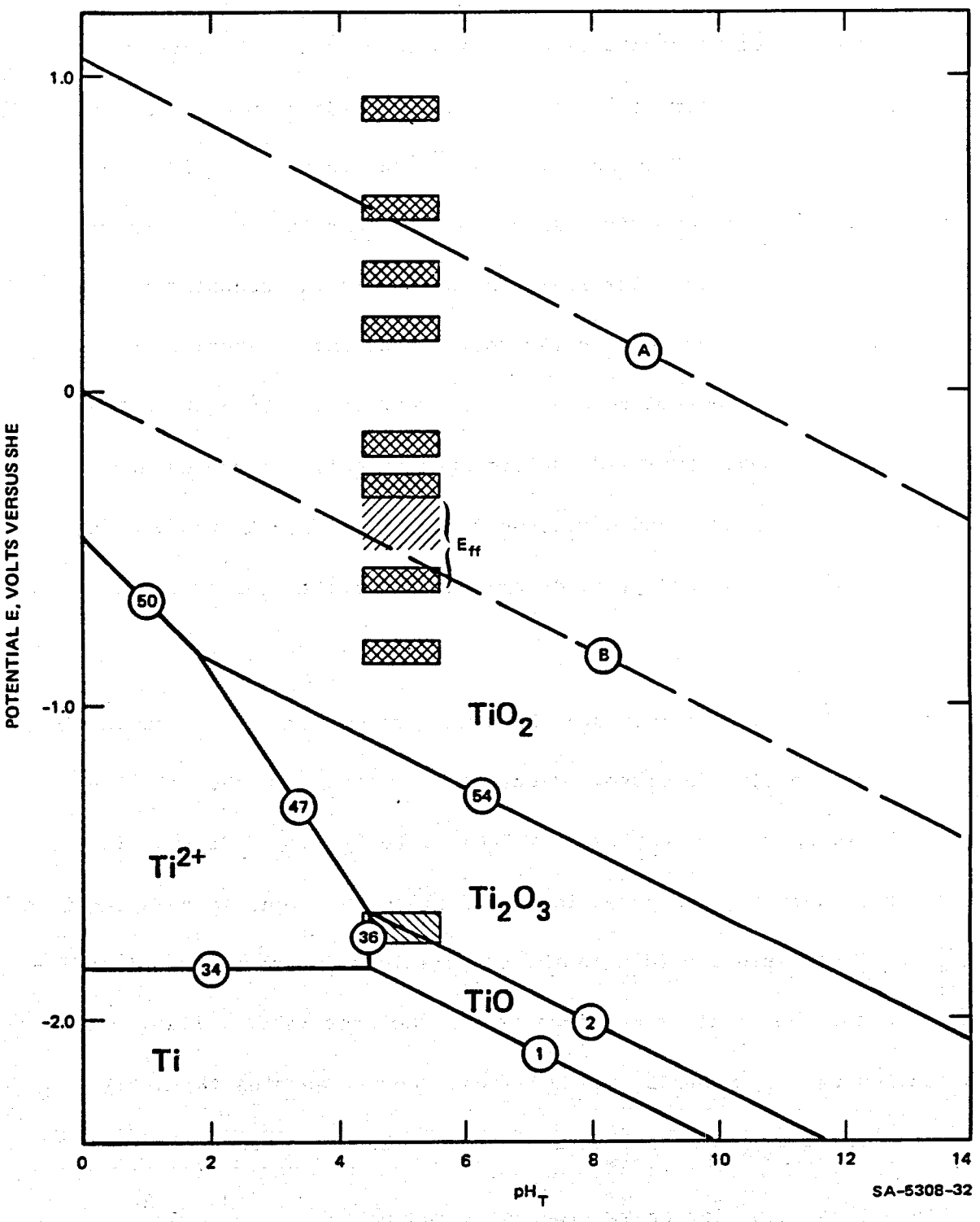


FIGURE 20 POTENTIAL-pH DIAGRAM FOR TITANIUM IN HIGH-SALINITY BRINE AT 250°C

Activities of dissolved titanium species = $10^{-6}$ molal. //// – $E_{corr}$ for titanium-based alloys, ▨ – oxidation peak potential for titanium-based alloys, ▨ – reduction peak potentials for titanium-based alloys.

reactions at elevated temperatures were calculated using the linear heat capacity approximation for dissolved components as developed by Naumov et al.[21] and subsequently used by Macdonald and Hyne[20] and later by Taylor.[22] The thermodynamic data were taken from a single compilation,[21] whenever possible, so as to maintain internal consistency in the computations. Equilibrium relationships between two solid components or between a solid component and a dissolved species are represented by solid lines, whereas reactions that involve dissolved species only are represented by broken lines. Lines A and B represent the limits for thermodynamic stability of water, and are plotted for unit fugacities for hydrogen and oxygen.

Only in the cases of iron and chromium were sufficient thermodynamic data available to include dissolved chloride complexes in the calculations. Accordingly, the complex ions $FeCl^{2+}$, $FeCl_2^+$, and $FeCl_3(aq)$ were considered in deriving the potential-pH diagrams for iron, whereas the ions $CrCl^{2+}$ and $CrCl_2^+$ were included in the computations for chromium. Insufficient data for the divalent metal-chloride complexes were available, so that species of the type $MCl^+$ and $MCl_2(aq)$, where M denotes the metal under consideration, could not be included in the derivations.

Since ions with high charge-to-radius ratios (e.g., $Fe^{3+}$, $Cr^{3+}$, $Ti^{4+}$) tend to hydrolyze at elevated temperatures,[23,24] we attempted to include hydrolyzed ions in the calculations. Thus, hydrolyzed species such as $Ni(OH)^+$, $HNiO_2^-$, $TiO_2^{2+}$, $Cr(OH)_2^+$, $Cr(OH)_2^+$, $H_2CrO_4(aq)$,

$HCrO_4^-$, $CrO_4^{2-}$, $Fe(OH)^+$, $Fe(OH)_2(aq)$, $HFeO_2^-$, $Fe(OH)^{2+}$, $Fe(OH)_2^+$, $Fe(OH)_3(aq)$ and $Fe(OH)_4^-$ have been considered. Only those ions that exhibit fields of predominance appear in the potential-pH diagrams. However, a complete listing of the equilibrium properties of reactions that involve all of the species listed above is given in Reference 2.

Only metal oxide and oxyhydroxides (e.g., FeOOH) solid phases were considered in this work for three reasons. First, only sparse heat capacity data are available for metal hydroxides such as $Ni(OH)_2$ and $Ni(OH)_3$. Second, the crystallographic states of the hydroxides for which data are available are frequently ill-defined, so that it is not always possible to decide if the phase considered is the most stable. Finally, many of the hydroxides are thermodynamically unstable with respect to the oxides at evelated temperatures, so that only the latter should be considered in the derivations. It should be noted, however, that the hydroxides are frequently stable with respect to the oxides at ambient temperature, and their omission from the diagrams reported here for 25°C is due to lack of data.

The effect of temperature on the thermodynamic behavior of each metal in sulfide-free brine may be ascertained by comparing the diagrams at 25°C and 250°C. Thus, in the cases of iron (Figs. 13 and 14) and chromium (Figs. 17 and 18), a principal effect of temperature in the acid region is to change the identity of the predominant dissolved species under oxidizing conditions from $FeCl_2^+$ and $CrCl^{2+}$ at 25°C to $FeCl_3(aq)$ and $CrCl_2^+$ at 250°C.

This change is expected, because it is known that the dielectric constant for water decreases as the temperature is increased. Thus, the higher complexes with lower charge-to-radius ratios become more stable due to the more favorable electrostatic energy of the ion in the aqueous medium at elevated temperatures.

An increase in temperature also decreases the stability regions for dissolved cationic species at low pH, but leads to an increase in the stability regions for anionic species at high pH. In the latter case, the increased stability of ions of the type $HMO_2^-$ is due to a shift in the equilibrium line for the $HMO_2^-/M$ couple to lower potentials, as well as a shift in the oxide dissolution reactions (e.g., $NiO \rightarrow HNiO_2^-$) to lower pH values. These predicted relationships indicate that both iron and nickel may be more susceptible to corrosion in alkaline systems at elevated temperatures. Experimental data[6,11] support this contention. The calculated behavior of chromium at 25°C (Fig. 17) and 250°C (Fig. 18) shows that the equilibrium lines for the oxidative dissolution of chromic oxide ($Cr_2O_3$) to form the Cr(VI) species $HCrO_4^-$ and $CrO_4^{2-}$ shift to more negative potentials as the temperature is increased. The consequences of this shift for the pitting tendencies of alloys containing chromium in high-salinity geothermal brines at elevated temperatures are discussed elsewhere.[15]

## Thermodynamic Analyses of the Corrosion and Cyclic Voltammetric Peak Potentials

In analyzing the corrosion potential behavior and the cyclic voltammograms for the various alloys in terms of the predicted thermodynamic behavior of the component metals, it is necessary first to establish expected relationships between the observed cyclic voltammetric peak potentials, the corrosion potentials, and the equilibrium potentials plotted in the diagrams. Theoretical arguments[6,11] dictate that since the overpotentials for anodic (oxidation) and cathodic (reduction) processes are positive and negative, respectively, the following inequalities should be obeyed:

$$E_p^a > E_{eq} \tag{2}$$

$$E_p^c < E_{eq} \tag{3}$$

where subscripts p and eq denote peak and equilibrium properties, and superscripts a and c denote anodic and cathodic processes. For conjugate oxidation/reduction peaks--that is, for peaks that arise from the same electrochemical process--the inequalities become more restrictive:

$$E_p^c < E_{eq} < E_p^a \tag{4}$$

Similarly, the Wagner-Traud hypothesis for electrochemical corrosion predicts that the corrosion potential will lie between the equilibrium

potentials for the anodic and cathodic partial reactions contributing to the overall corrosion reaction:

$$E^{a}_{eq} < E_{corr} < E^{c}_{eq} \tag{5}$$

Furthermore, the corrosion potential is predicted to lie closest to the equilibrium potential for the process with the highest exchange current density--that is, to the equilibrium potential for the "fastest" of the two partial processes. Exceptions to this last generalization do occur, particularly with passive systems, but nevertheless the generalization frequently serves as a convenient rule of thumb for the interpretation of corrosion processes.

Both theoretical calculations and experimental data indicate that the pH of the brine used in this work at 250°C lies within the range of 4.5 to 5.5.[2] A more exact estimate is not possible because of the complex nature of the brine, particularly with respect to the presence of ill-defined mineral buffering components. Nevertheless, the estimated value above is sufficiently precise to permit a meaningful comparison to be made between the observed corrosion potentials and cyclic voltammetric peak potentials, and the calculated equilibrium potentials as plotted in the potential-pH diagrams (Figs. 13-20). To aid the analysis presented below, we have plotted the corrosion potentials and the potentials of the principal oxidation and reduction peaks (see Table 3) as the hatched and cross-hatched areas, respectively, on the diagrams

for each element at 250°C. The ranges given for the corrosion potential correspond to those observed over the period of exposure of the alloys to the brine at the elevated temperature.

The corrosion potentials observed for carbon steel in high-salinity brine at 250°C straddle the region between the equilibrium lines for the formation of magnetite from iron and the reduction of hydrogen ion to form molecular hydrogen. Accordingly, the observed corrosion potential behavior is consistent (see Eq. 5) for the operation of these anodic and cathodic partial processes. Two of the observed oxidation peaks occur at potentials that are more positive than that for the $Fe_3O_4/Fe$ couple, but they lie on the negative side of the equilibrium line for the $Fe_2O_3/Fe_3O_4$ couple. These peak potentials are also more positive than the extrapolated lines for the $Fe^{2+}/Fe$ and $Fe(OH)^{+}/Fe$ couples in the pH region of interest as required by Eq. (2) for viable anodic processes. Accordingly, we tentatively attribute these two peaks to dissolution and film formation phenomena. The third clearly defined anodic peak occurs at a potential that is slightly positive to the $Fe_2O_3/Fe_3O_4$ equilibrium line (Fig. 14), and it may arise from the oxidation of magnetite (or iron) to an Fe(III) surface oxide phase.

Only one clearly defined reduction peak was observed when the potential was swept in the noble-to-active direction (Fig. 3). This peak lies just on the negative side of the $Fe_3O_4/Fe$ equilibrium line,

and therefore satisfies Eq. (3) for the reduction of magnetite to iron. The general consistency of the arguments presented above is also supported by the experimental data for the "film-free" pseudo-corrosion potential, $E_{ff}$. Thus, prior sweeping of the potential to a highly active value (-1.06 V vs. SHE) is expected to reduce the surface oxide films back to metallic iron. The current on the reverse sweep (i.e., active-to-noble direction) is expected to be zero when the anodic current due to the dissolution of the metal or due to the formation of a thin film of magnetite balances that due to hydrogen evolution. Since the potential drop across any film formed under these conditions is expected to be less than that across the massive corrosion film that forms under freshly corroding conditions, it is expected that $E_{ff}$ will more closely reflect the equilibrium potential of the anodic partial reaction than does $E_{corr}$. The observed close agreement between $E_{ff}$ and equilibrium potentials for the $Fe_3O_4/Fe$, $Fe^{2+}/Fe$, or $Fe(OH)^{+}/Fe$ couples is in keeping with this expectation. Finally, the overpotentials for the oxidation and reduction peaks (i.e., $E_p - E_{eq}$) are quite small for carbon steel in the high salinity sulfide-free brine at 250°C compared with those observed for the other alloys (see Figs. 16, 18, and 20). The low overpotentials suggest that the charge transfer reactions (dissolution, oxidation, reduction) involving carbon steel are much faster (i.e., higher exchange current densities) than those for the other alloys studied in this work. This hypothesis is supported by the much higher corrosion rate for carbon steel compared with the other alloys in this high temperature geothermal brine.[2,15]

The other alloys that consist of essentially one component are titanium 50A and TiCode 12 (Table 2). Figure 20 shows a comparison of the corrosion potential and the oxidation and reduction peak potentials for these alloys with the calculated equilibrium potentials for titanium in sulfide-free high-salinity brine at 250°C. The free corrosion potential is found to straddle the equilibrium line for hydrogen evolution and lies within the stability region for rutile ($TiO_2$). Even if a much lower hydrogen fugacity than the 1 atm used for the calculations is assumed (e.g., $10^{-4}$ atm), the corrosion potential still lies within a few tenths of a volt below the hydrogen evolution line. In view of the highly resistive nature of the corrosion product films on titanium alloys in brine,[2] we suggest that $E_{corr}$ is determined principally by the $H^+/H_2$ couple; that is, the alloys tend to act as hydrogen electrodes in high salinity brine at 250 C. This clearly implies that the exchange current density for the hydrogen evolution reaction is much greater than that for the formation of an oxide on the surface, as expected.

The observed oxidation peak potentials for titanium 50 A and TiCode 12 do not correlate well with any of the equilibrium lines for the phases chosen for construction of the titanium potential-pH diagram. Although Eq. (2) is satisfied, it is difficult to reconcile the large number of anodic peaks observed with the relative simplicity of the potential-pH diagram. It is possible that the peaks arise from redox processes that involve electroactive components of the brine or, more

likely, from localized dissolution-repassivation phenomena at the surface. This latter hypothesis is consistent with the frequently observed (see Figs. 11 and 12, third cycle), current fluctuations that occur when the potential is swept in both directions between 0 V and 1.0 V versus SHE (250°C). The localized dissolution sites apparently were not sufficiently stable to produce macroscopic pitting.[2,15]

It is more difficult to compare the kinetic behavior and the predicted thermodynamic properties for those alloys that do not contain a large excess of one component. Thus, for the stainless steels (E-Brite 26-1, 316L, Haynes Alloy 20 Mod, and Carpenter 20 Cb-3), all of which contain iron as the principal component, but also contain large amounts of chromium and nickel (except E-Brite 26-1, see Table 2), the corrosion potential tends to be more positive than that observed for carbon steel. In these cases, the $E_{corr}$ values tend to correlate with equilibrium lines in the nickel diagram [e.g., $Ni(OH)^{+}/Ni$, NiO/Ni in Fig. 16] and also lie in the stability region for chromic oxide ($Cr_2O_3$) in the chromium-brine diagram (Fig. 18). This clearly demonstrates the influence of minor components on the corrosion behavior of Fe-Ni-Cr alloys, and also illustrates the difficulties inherent in using the potential-pH diagram for only the major component when analyzing the corrosion behavior of an alloy. The same general considerations apply to the nickel-based alloys (Inconel Alloy 625, Hastelloy Alloy G, and Hastelloy Alloy C-276--see Table 2). In these cases, however, there appears to be a much better

correlation between $E_{corr}$ and equilibrium lines in the nickel -brine diagram (Fig. 16).

The difficulties outlined above for the interpretation of corrosion potentials for high alloy systems also apply when attempts are made to rationalize the cyclic voltammetric peak potentials and the $E_{ff}$ values in terms of the potential-pH diagrams for the component metals. Thus, for the nickel-based alloys, $E_{ff}$ is more negative than the lowest-lying equilibrium line in the nickel-brine diagram (Fig. 16), and therefore is not consistent with Eq. (5) for processes that involve phases containing nickel only. Instead, the $E_{ff}$ values for these alloys (and for the stainless steels) appear to correlate much better with processes that involve phases containing chromium (Fig. 18); this suggests that the initial process that occurs on the surface of an Fe-Ni-Cr alloy is the dissolution of chromium from the matrix to form $Cr^{2+}$ in solution or to form a thin $Cr_2O_3$ (or possibly chromium-containing spinel) layer on the surface. Likewise, many of the anodic peaks observed by cyclic voltammetry for nickel-based alloys lie below the equilibrium lines for reactions that involve phases containing nickel only (Fig. 16). These peak potentials are therefore in conflict with Eq. (2) if it is assumed that the peaks arise from oxidation of the nickel component of the alloys. The same consideration also applies to the stainless steels (Table 3), where some of the anodic peaks lie below all of the equilibrium lines in both the iron-brine and nickel-brine diagrams. In these cases, Eq. (2)

is satisfied only if it is assumed that the peaks arise from oxidation of the chromium component of the alloy. Thus, chromium appears to play a major role in determining the electrochemical, and hence corrosion behavior of Fe-Ni-Cr alloys in sulfide-free high salinity brine at elevated temperatures.

## Potential-pH Diagrams for Sulfide-Containing Systems

Although few systematic studies of corrosion phenomena in sulfide-containing brines have been reported, the presence of dissolved sulfide is expected to exert a major influence over the corrosion behavior of metals and alloys in high temperature geothermal systems. In anticipation of future work in this field, we discuss here potential-pH diagrams[4] for iron and nickel in sulfide-containing ($[H_2S] + [HS^-] + [S^{2-}] = 10$ ppm) high salinity brine at 25°C and 250°C (Figs 21-24).

A total constant sulfide concentration has been assumed in the derivation of the diagrams. This constraint results in nonlinear potential-pH relationships for those reactions that involve solid sulfide phases and dissolved sulfide species (e.g., lines 5 and 11, Fig. 21), as previously shown.[4] Because the total sulfide content in a closed system is fixed, we considered that this constraint was reasonably realistic for the present purpose. Other constraints can be used for the derivation of potential-pH diagrams for complex systems. For example, Macdonald and Hyne[20] employed a constant $H_2S$ partial pressure constraint

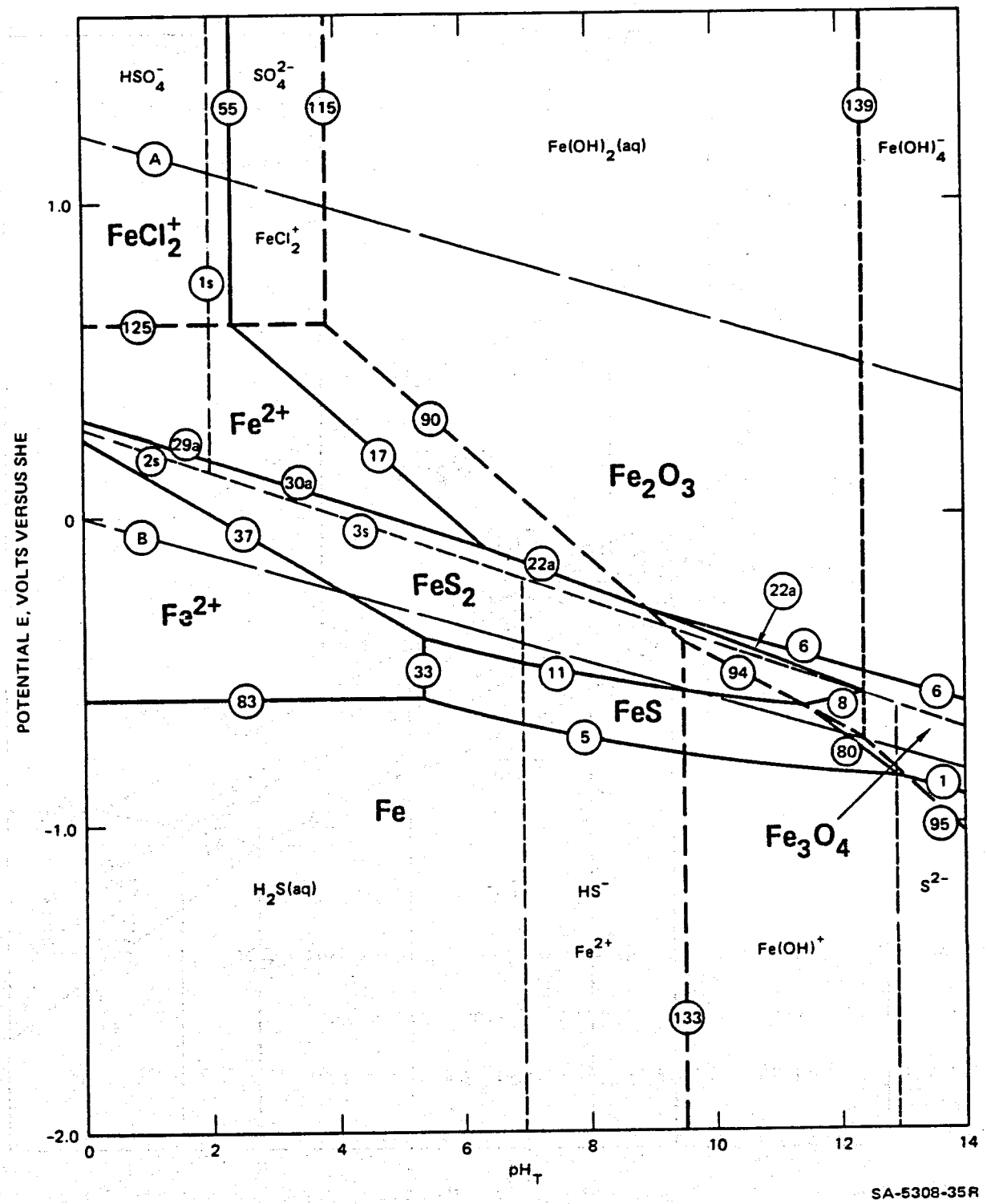


FIGURE 21 POTENTIAL-pH DIAGRAM FOR IRON IN HIGH-SALINITY BRINE AT 25°C IN THE PRESENCE OF 10 ppm TOTAL DISSOLVED SULFIDE ($H_2S + HS^- + S^{2-}$)

Activities of $HSO_4^-$ and $SO_4^{2-}$ = $10^{-6}$ molal. Activities of dissolved iron species = $10^{-4}$ molal.

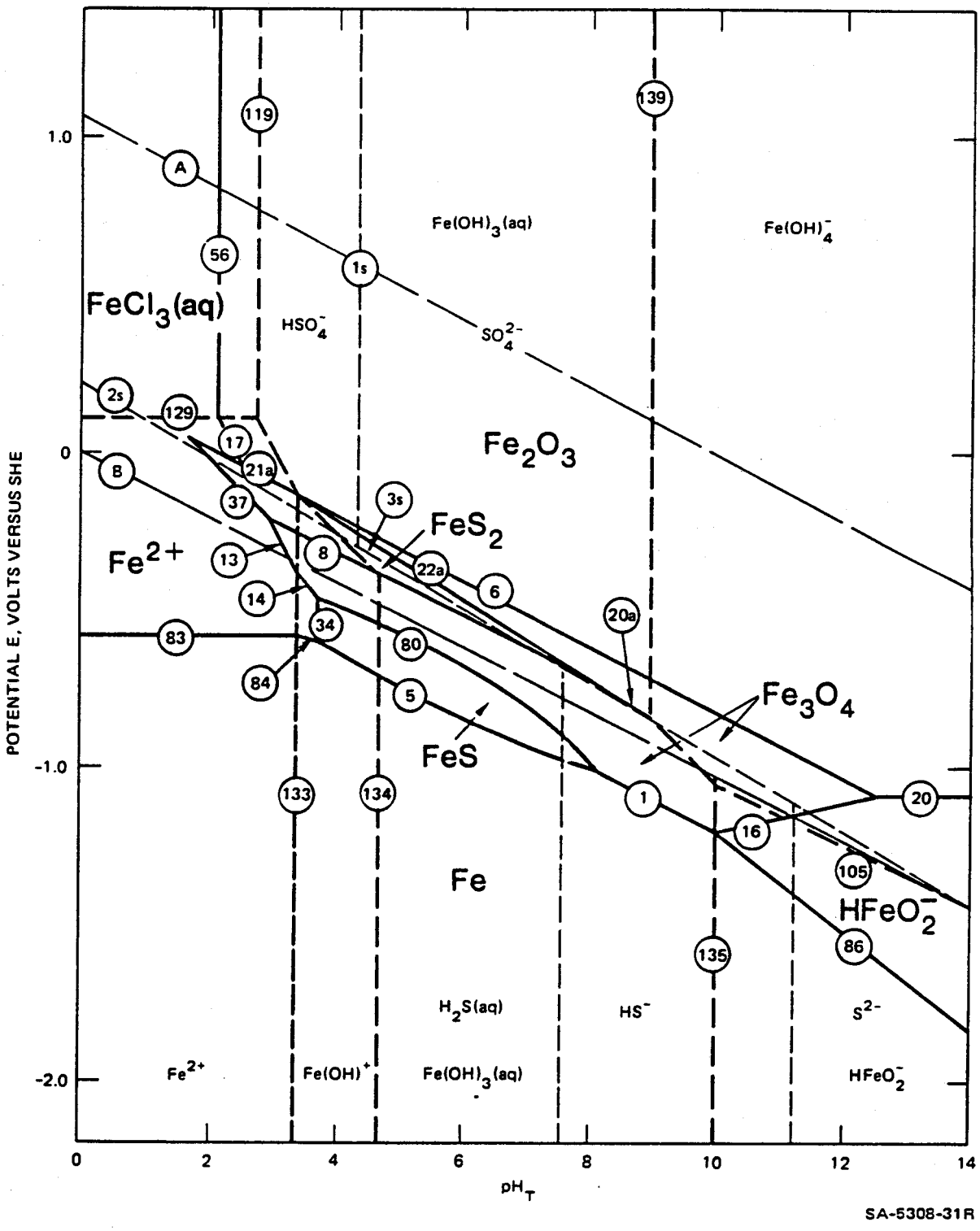


FIGURE 22 POTENTIAL-pH DIAGRAM FOR IRON IN HIGH-SALINITY BRINE AT 250°C IN THE PRESENCE OF 10 ppm TOTAL DISSOLVED SULFIDE ($H_2S + HS^- + S^{2-}$)

Activities of $HSO_4^-$ and $SO_4^{2-}$ = $10^{-6}$ molal. Activities of dissolved iron species = $10^{-4}$ molal.

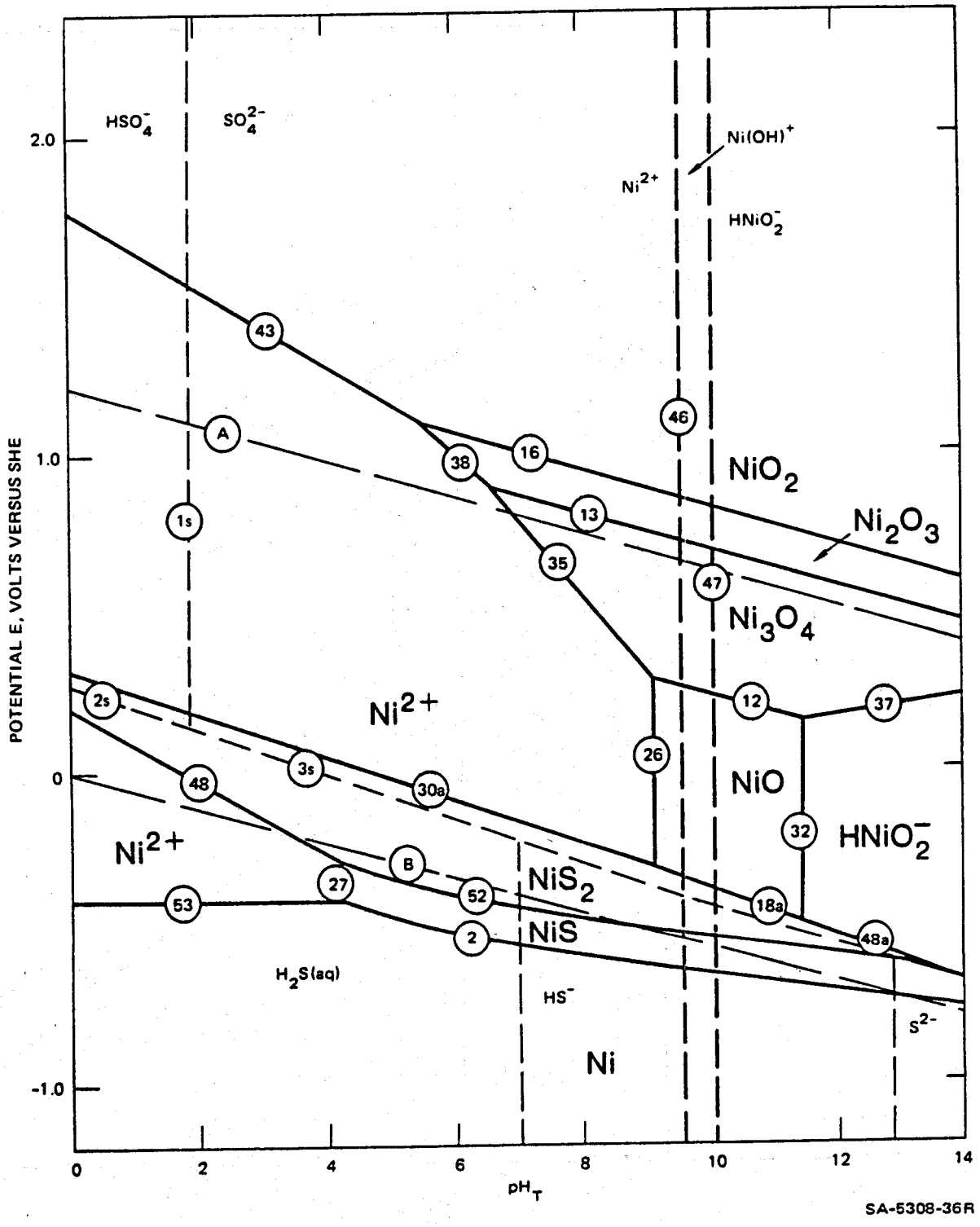


FIGURE 23 POTENTIAL-pH DIAGRAM FOR NICKEL IN HIGH-SALINITY BRINE AT 25°C IN THE PRESENCE OF 10 ppm TOTAL DISSOLVED SULFIDE ($H_2S + HS^- + S^{2-}$)
Activities of $HSO_4^-$, $SO_4^{2-}$, and dissolved nickel species = $10^{-6}$ molal.

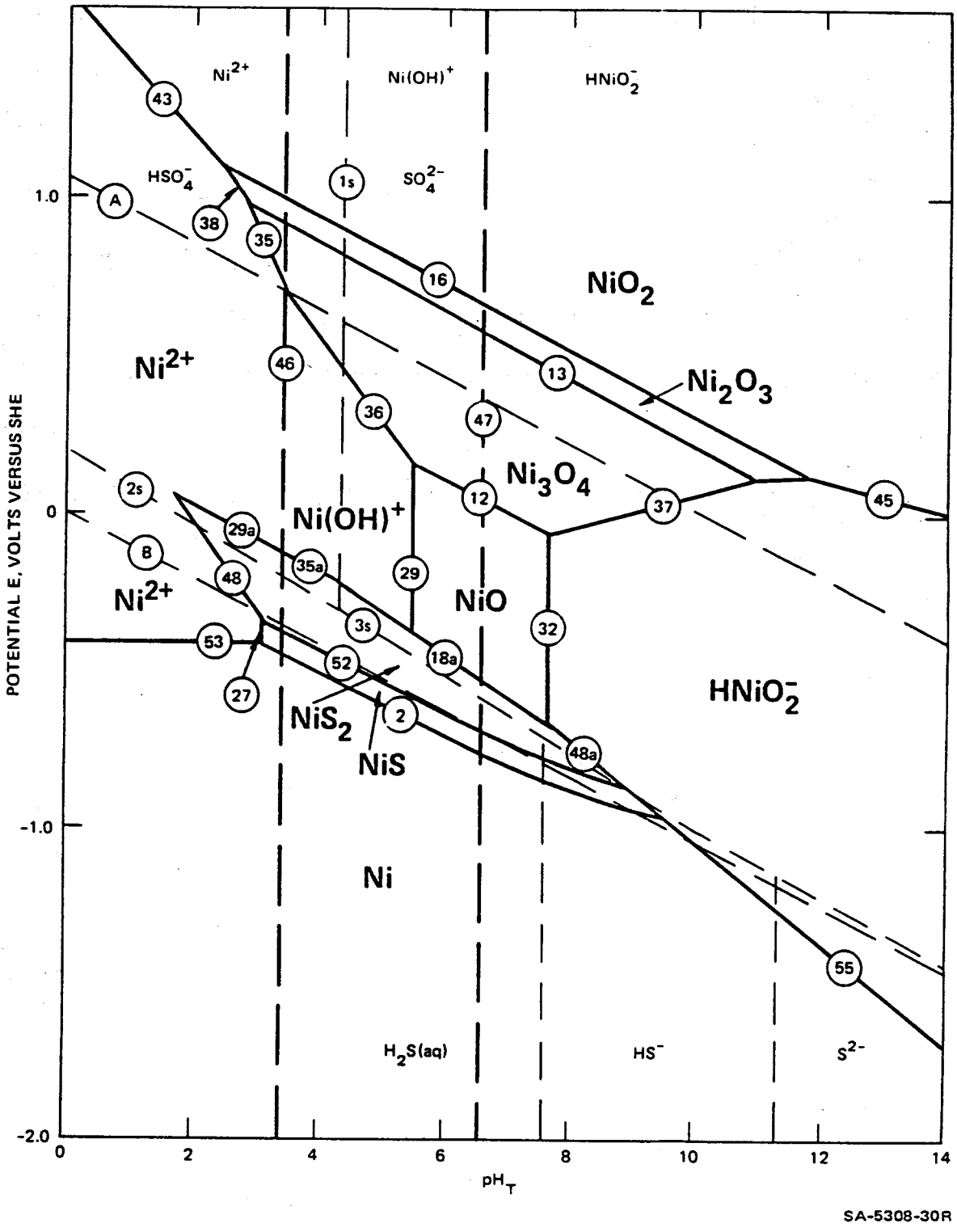


FIGURE 24 POTENTIAL-pH DIAGRAM FOR NICKEL IN HIGH-SALINITY BRINE AT 250°C IN THE PRESENCE OF 10 ppm TOTAL DISSOLVED SULFIDE ($H_2S + HS^- + S^{2-}$)

Activities of $HSO_4^-$, $SO_4^{2-}$, and dissolved nickel species = $10^{-6}$ molal.

in their thermodynamic analyses of the $Fe/H_2S/H_2O$ system at elevated temperatures as related to the production of heavy water (deuterium oxide) by the Girdler-Sulfide process.

Also plotted in Figs 21-24 are the potential-pH diagrams for the sulfur-water system, whose equilibrium relationships are designated by the light broken lines and by number ending with the letters (1s, 2s, etc). The sulfur-water equilibria are used to define the regions of predominance of various dissolved sulfide and sulfur oxyanion species which are subsequently employed for constructing the potential-pH diagrams for the metal/$H_2S/H_2O$ systems. Elemental sulfur and dissolved polysulfide species were not considered in the present work, although they were taken into account in the more detailed analysis by Macdonald and Hyne[20] of the $Fe/H_2S/H_2O$ system. Because sulfur-containing species are present in the system of interest at very low concentrations, we do not believe that omission of elemental sulfur and the polysulfide ions materially affects the structure of the diagrams. All four diagrams were derived for constant activities for $HSO_4^-$ and $SO_4^{2-}$ equal to $10^{-4}$ m. In the case of the iron-brine system, the activities of dissolved metal-containing species were arbitrarily set equal to $10^{-4}$ m, whereas for the nickel-brine system dissolved species activities of $10^{-6}$ m were assumed. The higher activities for the iron-brine system were required so as to exceed the calculated minimum solubilities of the oxide phases at

elevated temperatures. Had the lower activity been assumed, the oxide phases would not have appeared as stable phases on the diagrams.[2]

In the case of both iron and nickel at 25°C, the most stable solid oxidation phase is the M(II) sulfide. Only troilite (stoichiometric FeS) was considered in the derivation of the diagram for iron, although it is recognized that other sulfide phases such as mackinawite ($Fe_{1+x}S$) and pyrrhotite ($FeS_{1+x}$) exist, and indeed mackinawite may form at lower potentials than troilite under certain conditions.[20] As the potential is increased, oxidation of MS to $MS_2$ is predicted to occur over almost the entire pH range. Note that Both $FeS_2$ and $NiS_2$ are Fe(II) and Ni(II) phases, respectively; the change in oxidation state is associated with the sulfur anions in the lattices. Thus $FeS_2$ and $NiS_2$ are best described as iron and nickel disulfides in which the average oxidation state of sulfur is -1. Note also that the conversion of MS to $MS_2$ involves reaction with $H_2S$ (or its anions $HS^-$ and $S^{2-}$) as shown by the location of the equilibrium lines 11 (Fig. 21) and 52 (Figs 23 and 24) in the stability region for sulfide ($H_2S$ and $HS^-$) in the potential-pH diagram for the sulfur water system. On the other hand, equilibrium between $MS_2$ and the oxides $Fe_3O_4$, $Fe_2O_3$, and NiO involves sulfur oxyanions as demonstrated the potentials for these processes lying within the stability regions for $HSO_4^-$ and $SO_4^{2-}$.

Increasing the temperature from 25°C to 250°C proved to have several important consequences for the thermodynamic equilibrium behavior of iron, nickel, and sulfur in sulfide-containing geothermal brine. Thus, the stable iron III complex at 25°C ($FeCl_2^+$) is no longer the predominant species at 250°C; the decrease in the dielectric constant of the medium favors the formation of the neutral complex $FeCl_3$ as previously noted in this paper. Similarly, $pK_a$ for the dissociation of bisulfate ion ($HSO_4^-$) increases from approximately 1.98 at 25°C to 4.39 at 250°C. Increasing the temperature also has a marked effect on the stability regions for the dissolved metal-containing ions in geothermal brine. For example, as noted previously for the sulfide-free systems, the stability regions for cations at low pH values become more restricted as the temperature increases, whereas those for the anions $HFeO_2^-$ and $HNiO_2^-$ [or equivalently $Fe(OH)_3^-$ and $Ni(OH)_3^-$, respectively] increase. In the case of the anions the shifts in the lines for equilibrium between the ions and the oxides (e.g., line 32, Fig. 23) appear to be greater than can be accounted for by the change in the dissociation constant of water alone.[16-19] This observation suggests that the anions become stabilized with respect to the cations at elevated temperatures.

Probably the most important change in the diagrams for the $Fe/H_2S/H_2O/Cl^-$ and $Ni/H_2S/H_2O/Cl^-$ systems due to increasing temperature occurs in the relative stabilities of the sulfides and oxides. Thus, in both cases the disulfides, $FeS_2$ and $NiS_2$ are predicted to exhibit domains of

stability at 25°C that extend to very low pH values into the cation stability regions. The lower boundaries of these regions are determined by equilibrium between $MS_2$ and dissolved $M^{2+}$ and $H_2S$, whereas the upper boundaries represent equilibrium between $MS_2$ and dissolved $M^{2+}$ and the oxyanions $HSO_4^-$ or $SO_4^{2-}$. Thus, if the potential is first increased from within the lower stability region for $M^{2+}$, at some point the formation of solid $FeS_2$ (line 37, Fig. 21) or $NiS_2$ (line 48, Fig. 23) becomes spontaneous by oxidative deposition. However, if the potential is increased still further, oxidative dissolution of the disulfides can occur. These relationships are of considerable importance in the mining and geothermal industries because they provide the thermodynamic boundaries for the oxidative and reductive dissolution of pyrite ores (for example) and pyrite-rich scales in geothermal systems. At elevated temperatures, however, the stability domains for the sulfides, and particularly for the disulfides $FeS_2$ and $NiS_2$, are reduced sharply in size, thereby indicating much more restrictive conditions for the formation of these phases in high-temperature geothermal systems. Nevertheless, Seward[25] has argued that the down-hole redox potential and pH in the Broadlands geothermal field south of Reporoa in New Zealand lie within the stability region for $FeS_2$, and indeed pyrite is observed in core samples from the steam-producing formation.

## SUMMARY

The use of potential-pH diagrams for the interpretation of corrosion phenomena in geothermal bines has been discussed. Although considerable care must be exercised when comparing kinetic parameters with equilibrium properties, we have shown that the diagrams are valuable for the rationalization of corrosion phenomena in terms of proposed partial anodic and cathodic reactions. Furthermore, the diagrams conveniently summarize the equilibrium properties of metal-brine systems in general, and are therefore of considerable value for the interpretation of non-corrosion processes such as scaling.

## ACKNOWLEDGMENTS

Financial support of this work by NSF(RANN) under Grant No. AER 76-00713 is gratefully acknowledged.

## REFERENCES


1. J. F. Carter and F. X. McCawley, J. Metals, 30, 11 (1978).

2. B. C. Syrett, D. D. Macdonald, H. Shih, and S. S. Wing, "Corrosion Chemistry of Geothermal Brines. Part 1: Low Salinity Brines, Part 2: High Salinity Brine," Final report to NSF(RANN) and Dept. of Energy, Washington, D.C. NSF(RANN) Grant No. AER 76-00713 (1977).

3. D. D. Macdonald and B. C. Syrett, "The Use of Potential-pH Diagrams for the Interpretation of Corrosion Phenomena in High Salinity Geothermal Brines," Corrosion, in press (1978).

4. D. D. Macdonald and B. C. Syrett, "Potential-pH Diagrams for Iron and Nickel in High Salinity Geothermal Brine Containing Low Levels of Hydrogen Sulfide," Corrosion, Submitted for publication (1978).

5. D. D. Macdonald, Transient Techniques in Electrochemistry, Plenum Press, New York (197).

6. D. D. Macdonald and D. Owen, In High Temperature High Pressure Electrochemistry in Aqueous Solutions, Ed. by R. W. Staehle, D. de G. Jones, and J. E. Slater, NACE-4, Houston, Texas (1976), p. 513.

7. R. L. Cowan and R. W. Staehle, J. Electrochem. Soc., Vol. 118, p. 557 (1971).

8. D. D. Macdonald, in Modern Aspects of Electrochemistry, Ed. by J. O'M. Brockris and B. E. Conway, Vol. 11, Plenum Press, New York (1975), p. 141.

9. D. D. Macdonald, Corrosion, Vol. 34, p. 75 (1978).

10. D. D. Macdonald, P. Butler, and D. Owen, Can. J. Chem., Vol. 51, p. 2590 (1973).

11. D. D. Macdonald and D. Owen, J. Electrochem. Soc., Vol. 120 p. 317 (1973).

12 J. Postlethwaite, Electrochim. Acta, Vol. 12, p. 337 (1962).

13. D. de Jones and R. W. Staehle, eds., High Temperature High Pressure Electrochemistry in Aqueous Solutions, NACE-4, Houston, Texas (1976).

14. D. D. Macdonald and B. Roberts, Electrochim. Acta, Vol. 23, p. 781 (1978).

15. B. C. Syrett, D. D. Macdonald, H. Shih, and S. S. Wing, to be published.

16. D. D. Macdonald, G. Shierman, and P. Butler, "The Thermodynamics of Metal-Water Systems at Elevated Temperatures. I The Water and Copper-Water Systems," Atomic Energy of Canada Ltd. report, AECL-4136 (1972).

17. D. D. Macdonald, G. Shierman, and P. Butler, "The Thermodynamics of Metal-Water Systems at Elevated Temperatures II The Iron-Water System," Atomic Energy of Canada, Ltd. report, AECL-4137 (1972).

18. D. D. Macdonald, G. Shierman, and P. Butler, "The Thermodynamics of Metal-Water Systems at Elevated Temperatures. III The Cobalt-Water System," Atomic Energy of Canada Ltd. report, AECL-4138 (1972).

19. D. D. Macdonald, "The Thermodynamics of Metal-Water Systems at Elevated Temperatures. IV. The Nickel-Water System," Atomic Energy of Canada Ltd. report, AECL-4139 (1972).

20. D. D. Macdonald and J. B. Hyne, "The Thermodynamics of the Iron/Sulfur/Water System," Final report to Atomic Energy of Canada Ltd., Pinawa, Manitoba (1976).

21. G. B. Naumov, B. N. Ryzhenko, and I. L. Khodakovsky, Handbook of Thermodynamic Data, Transl. U.S. Geological Survey USGS-WRD-74-001 (1974).

22. D. G. Taylor, "Thermodynamic Properties of Metal-Water Systems at Elevated Temperatures," Report No. 77CRD213, General Electric Co., Schenectady, New York (1977).

23. R. E. Mesmer and C. F. Baes, Inorg. Chem., Vol. 10, p. 2290 (1971).

24. D. D. Macdonald, P. Butler, and D. Owen, J. Phys. Chem., Vol. 77. p. 2474 (1973).

25. T. M. Seward, Am. J. Sci., Vol. 274, 190 (1974).

# CORROSION TESTING IN A MULTIPLE-STAGE FLASH SYSTEM

by

R. D. McCright
and
R. E. Garrison
University of California
Lawrence Livermore Laboratory
P. O. Box 808
Livermore, Calfornia 94550

Corrosion rate results from a 720-hour exposure period to geothermal brine acidified to pH4 are discussed in this paper. The corrosion tests were performed in a four-stage flash system so that results obtained at different temperatures could be compared. Carbon steel and alternate construction materials were used as test specimens. Results indicate that carbon steel corrodes excessively (more than 50 mils/year) at temperatures above 150°C. Alternate construction materials (alloy steels) may be utilized under these conditions.

Work performed under the auspices of the Department of Energy, Contract No. W-7405-Eng-48.

One of the major concerns of acidification to control scale in geothermal power plants is the expected increase in corrosion rate of the plant construction materials. Therefore, the Lawrence Livermore Laboratory (LLL) has initiated a program for measuring the corrosion rate and evaluating other aspects of materials performance in acidified geothermal brines. The principal material of interest is carbon steel, of course, but alternate construction materials include alloy steels with chrominum and molybdenum as the alloy additions. Further, in the most severe conditions highly corrosion resistant alloys may have to be used as cladding or liners

or for construction of limited size but high performance items such as valve trim.

In order to evaluate the performance of a wide variety of candidate materials under operating conditions, a four-stage flash system was construction at the LLL Field Test Site in the Imperial Valley. The system was designed to accomodate corrosion test specimens of two kinds: 1) direct exposure flat coupons for weight loss determinations, and 2) cylindrical electrodes for electrochemical determination of the corrosion rate by the linear polarization resistance technique (LPR). The LLL four-stage flash system replicates the San Diego Gas and Electric Co. Geothermal Loop Experimental Facility (GLEF). Both installations have been supplied with geothermal brine from Magmamax Well No. 1.

A schematic diagram showing the location of corrosion specimens in the LLL Four-stage flash system is shown in Figure 1. Racks containing the direct exposure coupons were installed in the second, third, and fourth stage flash units. The nominal operating temperatures and pressures in these units were: second stage, 150°C and 50 psig; third stage, 125°C and 15 psig; fourth stage 110°C and 3 psig. Racks were located in the top (stream phase) and bottom (brine phase) of the second and third stage units and in the brine phase of the sourth stage unit. Thus, corrosion weight loss data were obtained at five locations in the system.

The individual corrosion coupons were nominally two inches by one inch. Thickness varied from about 1/16 to 1/8 inch according to the available stock of the alloy. The coupons were glass bead blasted (25-80μm particles) and bolted onto a carbon steel support bar. Care was taken to

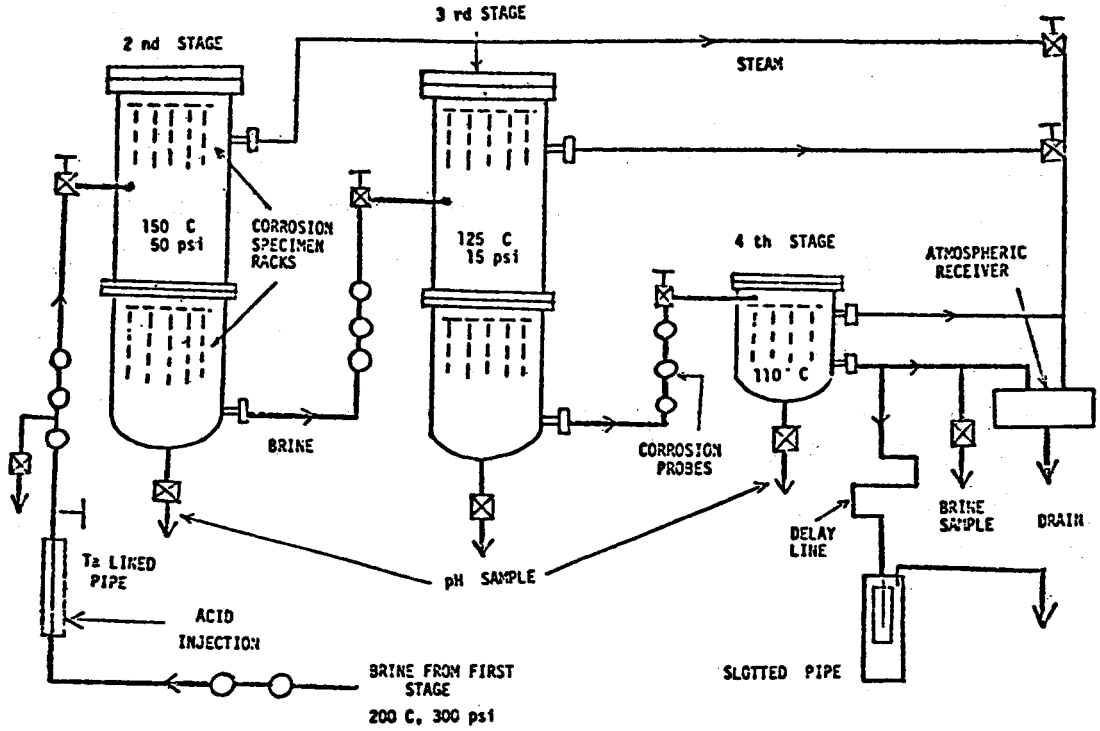


Figure 1. Schematic of Four-Stage Flash System Showing Location of Corrosion Probes (LPR Technique) and Corrosion Test Racks.

electrically insulate the test coupon from the bar by means of Teflon washers and sleeves. The bars, each holding four to six specimens, were fixed to a steel ring which rested inside the flash unit. Overall dimension of the test rack was 13 inch diameter ring by 16 inch height.

The electrochemical specimens were placed in four locations in the system, as indicated in Figure 1. Specimens were exposed to untreated brine at 210°C (Station A), acidified brine at 210°C (Station B), acidified brine at 150°C (Station C), and acidified brine at 125°C (Station D). Three identical specimens of each alloy tested were mounted in probe holders manufactured by Petrolite Corporation. Briefly, the principle of corrosion measurement by the LPR technique is to apply a small potential difference (10 mV) between a pair of the three electrodes (reference and test) and measure the current which flows between another pair (test and auxiliary). This technique was described in our previous paper.[1]

The corrosion test period occurred during December 1977, January 1978 and February 1978. The test schedule is indicated in Table 1. The emphasis of the test procedure was to simulate real operating conditions. Therefore, during the first 36 hours of exposure, the system was operated with unmodified brine as would probably be the case in plant start-up. The test was interrupted because of the Christmas holidays. Also, short interruptions occurred because of planned or inadvertent shut-downs for maintenance. During the shut-down for the holidays, the corrosion specimens were removed from the flash tanks and stored in a dry atmosphere.

[1]J. E. Harrar, R. D. McCright and A. Goldberg, Materials Evaluation for Geothermal Applications: Plant Materials. Transactions Geothermal Resources Council, May 1977, p. 129.

TABLE 1. SCHEDULE OF CORROSION TESTS IN FLASH TANK SYSTEM

December 1977:

Segment I of Corrosion Test
36 hours of unmodified brine (pH 5.8)
196 hours of acidified brine (pH 4)

January-February 1978:

Segment II of Corrosion Test
4 hours of unmodified brine (pH 5.8)
530 hours of acidified brine (pH 4)

Acidification of the brine was accomplished by adding 1.5 N HCl as shown in Figure 1. The pH of the acidified brine was monitored hourly throughout the duration of the exposure test. Samples were drawn from four locations in the system as shown in Figure 1. The pH was determined on a Beckman Select-Mate pH Meter which was calibrated frequently against standard buffer solutions. The pH varied during the course of the run, due to a number of factors. The most important of these factors was variation in the incoming brine chemistry. Variation in the pH from the desired value of pH could be compensated by adjustment of the acid flow rate.

The corrosion penetration rate was calculated from the weight loss of the specimens. The conventional way to express corrosion rates is in mils/year (mpy). The data, shown in Table 2, were obtained from the formula:

$$mpy = 534\ w/DAt$$

where w is the weight loss in milligrams, D is the density of the alloy in grams/$cm^3$, A is the specimen area in $in^2$ and t is the exposure time in hours.

The results in Table 2 are the average obtained from three replicate specimens placed in the five locations indicated in Figure 1. Precision between the individual results was within 20%. The results indicate that the corrosion rates generally decrease as the temperature decreases. The worst case occurs in the steam phase at 150°C.

The alloy steels performed significantly better than the carbon steels at all locations. Surprisingly, the alloy containing only 0.5% molybdenum performed nearly as well as the alloys with higher chromium and molybdenum contents. The carbon, silicon, manganese and other minor constituent composition varied from one alloy steel to another so that we cannot properly ascribe the improvement solely to the major elements. However, molybdenum additions to stainless steel are beneficial in chloride environments and under reducing conditions. On the other hand, chronium additions improve performance of steel and stainless steel in oxidizing environments. In this sense the two elements are complementary.

Although corrosion rates of 30-50 mpy for carbon steel (the pipe steel in the GLEF is ASTM A106 Grade B) are not catastrophic, plant acidification over a long period of time may require choosing other construction materials. Corrosion rates determined by linear polarization resistance (LPR) agreed generally with weight loss measurements after the LPR probes had been exposed to the brine for at least four days. The LPR probes showed much higher rates for shorter times. The chief advantage of the LPR technique is the much shorter time

TABLE 2. CORROSION PENETRATION RATES OF CARBON AND ALLOY STEELS AS DETERMINED BY THE WEIGHT LOSS TECHNIQUE. BRINE ACIDIFIED TO pH 4.

| | CORROSION PENETRATION RATES (mils/year) | | | | | | |
|---|---|---|---|---|---|---|---|
| | CARBON STEELS | | ALLOY STEELS | | | | |
| | AISI 1009 | ASTM A106B | 1/2 Mo | 1 Cr 1/2 Mo | 2 1/4 Cr 1 Mo | 5 1/2 Cr 1 Mo | 9 Cr 1 Mo |
| 2nd Stage Top Steam, 150°C | 31 | 51 | 8 | 19 | 17 | 9 | 7 |
| 2nd Stage Bottom Brine, 150°C | 27 | 38 | 16 | 17 | 13 | 11 | 10 |
| 3rd Stage Top Steam, 125°C | 16 | 15 | 6 | 7 | 4 | 5 | 3 |
| 3rd Stage Bottom Brine, 125°C | 15 | 15 | 8 | 8 | 7 | 6 | 6 |
| 4th Stage Brine, 110°C | 24 | 16 | 4 | 5 | 4 | 4 | 4 |

Reference:

1. J. E. Harrar, R. D. McCright and A. Goldberg, Materials Evaluation for Geothermal Applications: Plant Materials. Transactions Geothermal Resources Council, May 1977, p. 129.

required to obtain information. Visual examination of the exposed carbon and alloy steel specimens showed surface roughening but no apparent pitting corrosion susceptibility.

Results of further corrosion tests are shown in Tables 3 and 4. The numbers express the general corrosion rates determined by the weight loss in a 30-day exposure period. Each corrosion rate represents the average from four or five specimens of the alloy in each location. The alloy listed as ½ Mo is specified as ASTM A 204 Grade B. Similarly alloy 1 Cr - ½ Mo is A 387 Grade 12; 2¼ Cr - 1 Mo, A 387 Grade 22; 5½ Cr - ½ Mo, A 387 Grade 5; 9 Cr - 1 Mo, A 387 Grade 9. The indication "nil" means the co-rosion rate is less than 0.5 mils/year.

Tables 5, 6 and 7 indicate the corrosion attack morphology for the different alloys according to location. The carbon and alloy steels all showed general corrosion and pitting attack. "Pitting" means localized corrosion was observed on the exposed area of the specimen, while "crevice" means the localized attack was observed under the Teflon washer used in conjunction with the fastener. All of the austenitic stainless steels and nickel-base alloys showed general corrosion rates of less than 2 mils/year. Note that MC-20 (23 Cr, 8 Ni) is a duplex austenitic-ferritic stainless steel (austenite as the major phase) from Uddeholm Steel Corporation, AL 6X (20 Cr - 24 Ni - 6.5 Mo) is produced by Allegheny-Ludlum Steel and USS 18 Cr - 8 Ni - 4 Si is produced by US Steel. The other alloys should be familiar to most readers and their compositions can be found in such sources as the ASM Metal Progress Databook.

The pit depth data shown in Figure 2 were obtained by focusing the microscope at the pit bottom and at the plane specimen surface and taking the difference between the two readings. The

TABLE 3

## CORROSION PENETRATION RATES (mils/year), pH 4 BRINE CARBON AND ALLOY STEELS

| | AISI 1009 | A106B | 1/2 Mo | 1 Cr 1/2 Mo | 2 1/4 Cr 1 Mo | 5 1/2 Cr 1/2 Mo | 9 Cr 1 Mo |
|---|---|---|---|---|---|---|---|
| 2nd Stage top steam, 150°C | 31 | 51 | 8 | 19 | 17 | 9 | 7 |
| 2nd Stage bottom brine, 150°C | 27 | 38 | 16 | 17 | 13 | 11 | 10 |
| 3rd Stage top steam, 125°C | 16 | 15 | 6 | 7 | 4 | 5 | 3 |
| 3rd Stage bottom brine, 125°C | 15 | 15 | 8 | 8 | 7 | 6 | 6 |
| 4th Stage brine, 110°C | 24 | 16 | 4 | 5 | 4 | 4 | 4 |

TABLE 4

## CORROSION PENETRATION RATES (mils/year), pH 4 BRINE FERRITIC/MARTENSITIC ALLOYS

| | 9 Cr 1 Mo | Type 410 | Type 403 | Type 430 | 18 Cr–2 Mo | 26 Cr–1 Mo | 29 Cr–4 Mo | Si Cast Iron |
|---|---|---|---|---|---|---|---|---|
| 2nd Stage top steam, 150°C | 7 | 5 | 6 | 2 | 1 | 1 | Nil | 4 |
| 2nd Stage bottom brine, 150°C | 10 | 6 | 6 | 3 | 1 | 2 | 1 | 6 |
| 3rd Stage top steam, 125°C | 3 | 3 | 4 | 2 | 2 | 1 | 2 | 3 |
| 3rd Stage bottom brine, 125°C | 7 | 4 | 2 | 2 | 1 | 1 | 1 | 1 |
| 4th Stage brine, 110°C | 4 | 4 | 3 | 1 | 1 | 1 | 2 | Nil |

TABLE 5

## LOCALIZED CORROSION TENDENCY pH 4 BRINE

Ferritic/Martensitic Stainless Steels

| Alloy | 2nd Stage top steam, 150°C | 2nd Stage bottom brine, 150°C | 3rd Stage top steam, 125°C | 3rd Stage bottom brine, 125°C | 4th Stage brine, 110°C |
|---|---|---|---|---|---|
| Type 410 | Pitting attack | | | General to pitting attack | |
| Type 430 | Pitting | | | | |
| 18 Cr–2 Mo | Pitting | | | | |
| 26 Cr–1 Mo | Pitting | | | | Slight pitting |
| 29 Cr–4 Mo | No attack | | | | |
| 29 Cr–4 Mo–2 Ni | No attack | | | | |

TABLE 6

## LOCALIZED CORROSION TENDENCY pH 4 BRINE Austenitic Stainless Steels

| Alloy | 2nd Stage top steam, 150°C | 2nd Stage bottom brine, 150°C | 3rd Stage top steam, 125°C | 3rd Stage bottom brine, 125°C | 4th Stage brine, 110°C |
|---|---|---|---|---|---|
| Type 316 | Pitting/crevice | | No attack | | |
| Type 317LM | No attack | | | | |
| USS 18 Cr 8 Ni-4 Si | No attack | | | | |
| MC-20 | No attack | Pitting | No attack | Pitting | No attack |
| 20 Cb 3 | Crevice | No attack | | | |
| AL 6X | No attack | | | | |

TABLE 7

## LOCALIZED CORROSION TENDENCY pH 4 BRINE Nickel-Base and Other Alloys

| Alloy | 2nd Stage top steam, 150°C | 2nd Stage bottom brine, 150°C | 3rd Stage top steam, 125°C | 3rd Stage bottom brine, 125°C | 4th Stage brine, 110°C |
|---|---|---|---|---|---|
| Inconel 600 | No attack | | | | |
| Hastelloy B | No attack | | | | |
| Hastelloy C-276 | No attack | | | | |
| MP 35 N | Crevice | No attack | | | |
| Mo | No attack | | | | |
| Zr | No attack | | | | |
| Ti CP 50 | Crevice | | | | |
| Ti-6 Al-4 V | Crevice | | | | |
| Ti-Code 12 | Crevice | | | | No attack |

FIGURE 2

# AVERAGE "TEN DEEPEST PITS" VERSUS ALLOY CONTENT EXPOSED 150°C, pH 4 GEOTHERMAL BRINE, 720 HOURS

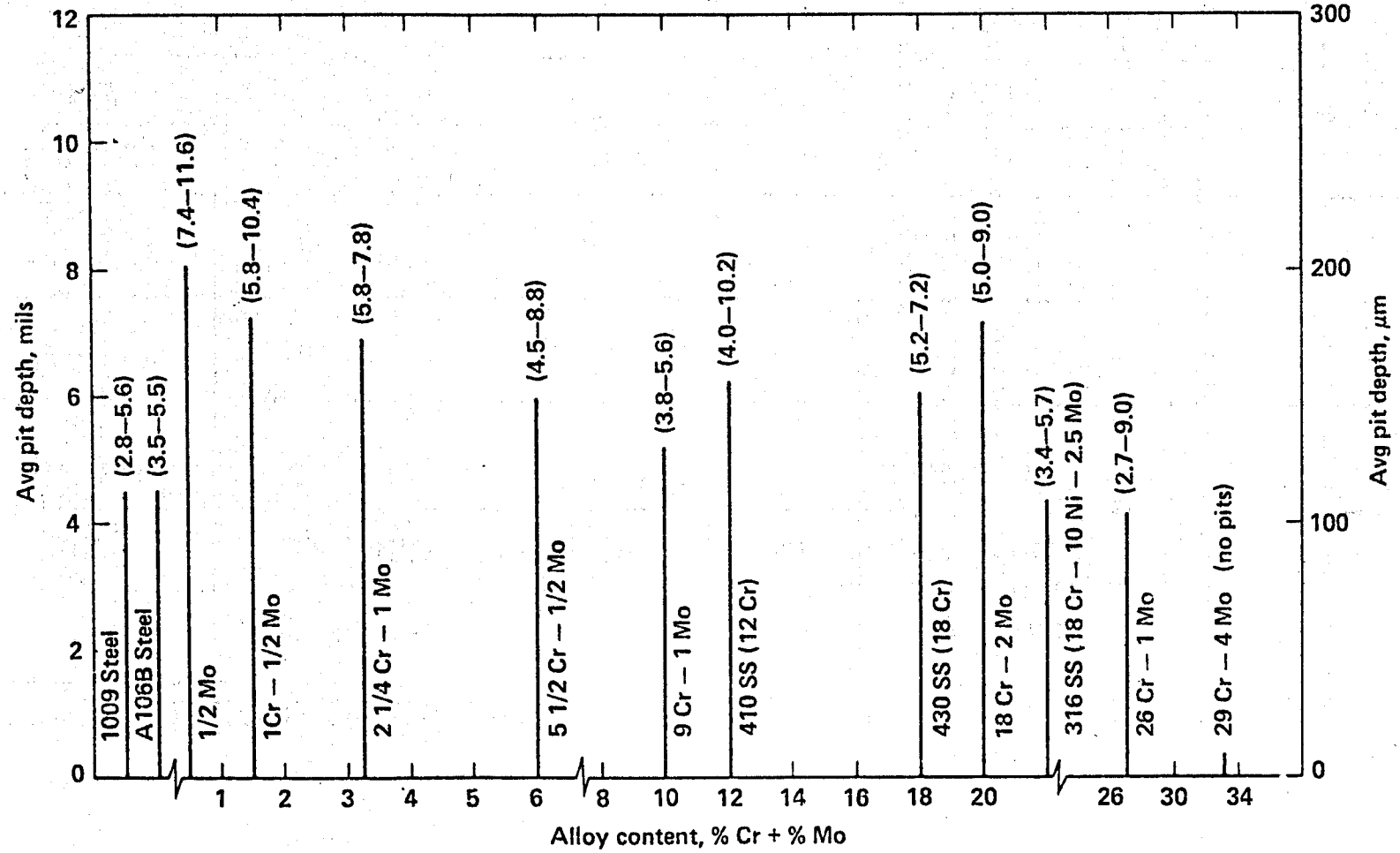

data were analyzed according to ASTM G-46 (Section 7.3.1). The other numbers on this figure indicate the range of pit depth values obtained.

The curves to the left of Figure 3 indicate the variation of the corrosion rate determined by the LPR technique as a function of time. The numbers to the right indicate the corrosion rates experienced by the four selected alloys over the 30-day test period, i.e., the mild steel corroded at the rate of 27 mils/year; the 2¼ Cr - 1 Mo alloy steel, 3 mpy; Type 410 stainless steel, 6 mpy; and Hastelloy B, 1 mpy. These weight loss corrosion rate data correlate reasonably well with the LPR results obtained after 100-120 hours.

FIGURE 3

## COMPARISON OF CORROSION RATES DETERMINED BY LINEAR POLARIZATION RESISTANCE (LPR) AND WEIGHT LOSS METHODS

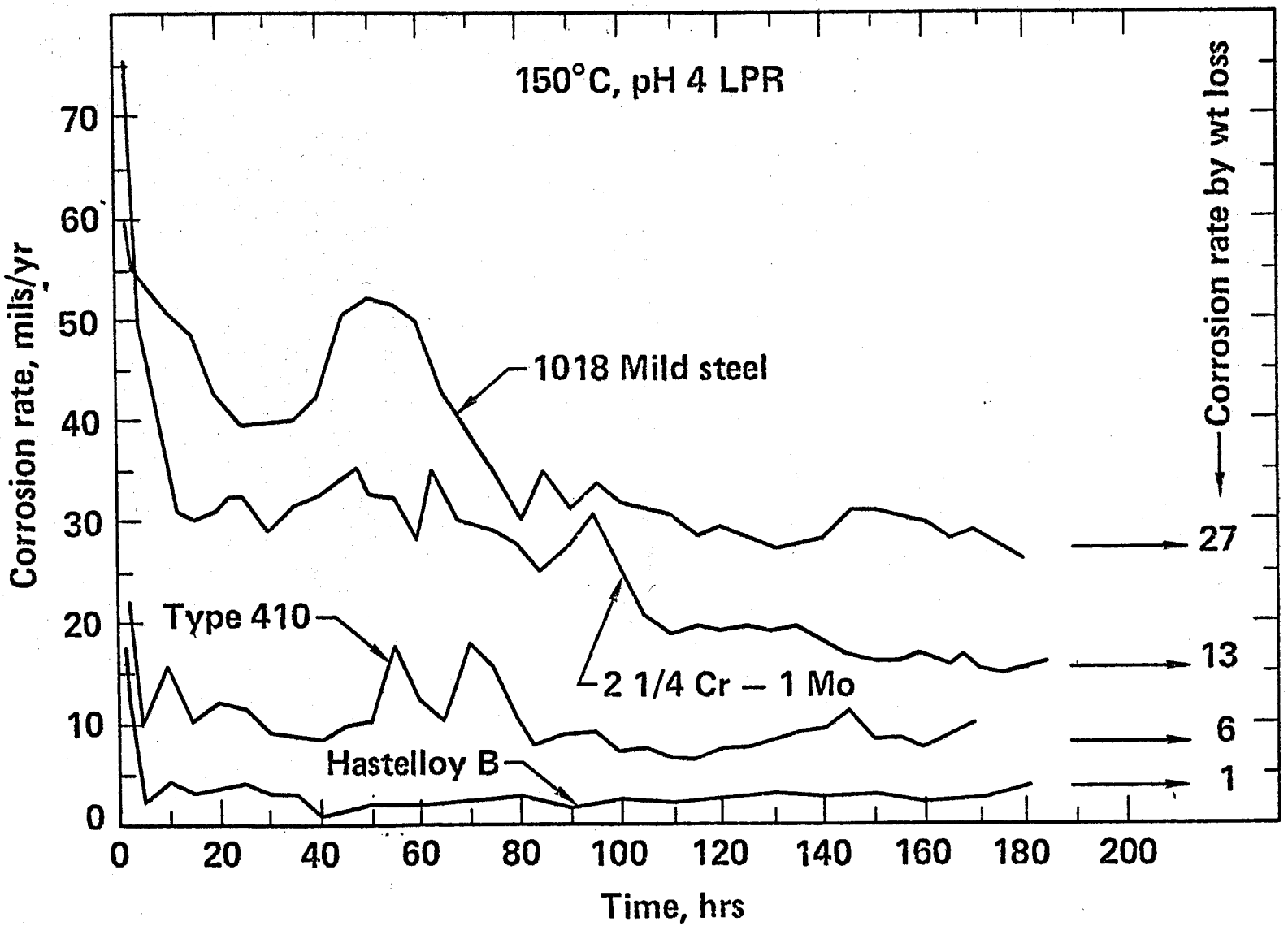

# HYDROGEN SULFIDE STRESS CORROSION CRACKING IN MATERIALS FOR GEOTHERMAL POWER

by

A.R. Troiano and R.F. Hehemann

Presented at

The Geothermal Power Workshop
May 23-25, 1978 at Austin, Texas

Sponsored by DOE
Division of Geothermal Energy
under Contract EY-76-5-02-2602.000
in the Department of Metallurgy at
Case Western Reserve University
Cleveland, Ohio
and in cooperation with
ARMCO, Inc., Middletown, Ohio.

# HYDROGEN SULFIDE STRESS CORROSION CRACKING IN MATERIALS FOR GEOTHERMAL POWER

## Introduction

Catastrophic, brittle delayed failure can occur in many environments, some of which may not appear to be very aggressive from a classical corrosion point of view. This type of environmentally induced failure, often occurring well below conservative design stresses, has generally been termed stress corrosion cracking (SCC) or sulphide stress cracking (SSC) when $H_2S$ is involved. It is well-recognized that, in many instances, hydrogen is involved as an embrittling agent leading to this type of failure and constituting a definite limitation on the use of available materials.

The sour well problem was first encountered by the petroleum industry about 30 years ago. The ultimate success of a greatly expanded source of geothermal power may depend on solutions to these same problems. Indeed, a major limitation in the growing energy economy resides in materials to contain, process, and generally handle the various aggressive environments that are encountered (1-6).

Experience in the petroleum industry has demonstrated that relatively high strength constructional steels will crack in "sour" environments. Such an environment has been characterized as one that contains damaging amounts of $H_2S$ which can be as low as 3 ppm in solution. This is based on the susceptibility to cracking of normally employed oil well casing and tubing steels in the 80,000 psi yield strength range and above (7-12). Indeed, as little as 0.1 ppm of hydrogen sulfide produced failure in laboratory tests. The hydrogen sulfide acts as a cathodic poison, greatly increasing the amount of hydrogen absorbed from the environment (13). In many wells, substantial $CO_2$ contents result in acidification and pH levels of 3 to 4 are not uncommon.

In geothermal holes much the same type and even more aggressive environments are often encountered (14) and the associated failures have been recognized for many years in some of the older geothermal fields. As far back as 1960, wells in New Zealand experienced brittle delayed failure in well casing at 80,000 psi yield strength and below (15, 16). At this same time it also was indicated that a form of erosion and thermal or corrosion fatigue was encountered due to the "unclean" nature of geothermal steam, particularly damaging to pumps, turbines, and ancillary equipment.

Other experience with geothermal wells indicated that 55,000 psi yield strength was the maximum safe strength allowable in terms of hydrogen sulfide induced failures. However, at these low strengths, tubing collapse was encountered and limited the strength of the joints required to compensate for non-axial loading, thermal stresses, etc. In fact, thermal stresses alone can exceed 60,000 psi (17).

Even at the strength levels generally considered to be safe, greater reliability would be most valuable and help alleviate the drill pipe, casing, and tubing problems. The consistency of performance depends not only on material strength level but also on environmental factors, some of which may change with time or the manner in which a well is operated. Reliability at higher strength is imperative in much of the ancillary equipment such as well head fittings, valves, pump, and turbine components, etc. Indeed, similar limitations on useful strength level exist even in the higher alloyed classes of materials including stainless steels, Inconel, Monel, and others. However, in these alloys, the specificity of the environment with regard to temperature range for sensitivity or influence of chloride concentration generally is different than that for the constructional steels.

Since it is generally accepted that cracking in sour environments involves hydrogen embrittlement, particularly for the constructional steels, it may be of value to outline some of the parallelism of behavior between SSC and brittle delayed failure induced by cathodically charged hydrogen (18-21). Both will exhibit an incubation time for crack initiation, discontinuous crack propagation, preferred crack nucleation at crevices, notches, or pits, similar temperature ranges of sensitivity, similar fracture appearance, a critical threshold stress for failure, a generally low stress intensity factor ($K_{I_{SCC}}$) and increased sensitivity to failure as the yield strength is raised (22-23).

Of particular interest in these applications are the temperature range of sensitivity and the threshold stress. The temperature range is generally considered to span the region from approximately minus 50°F to several hundred °F for the constructional type alloys. Of course, this range is also sensitive to many other parameters such as the environment and strength level (24-26). The critical temperature limits correspond with those at which hydrogen can be mobile and yet not so high as to preclude the accumulation of a critical concentration of hydrogen at the notch root (27). Also of significance is the relation between the threshold stress for failure and the Y.S. This threshold stress rises as the Y.S. is reduced until eventually it becomes equal to the Y.S. Below this strength, brittle delayed failure will not occur. This, of course, accounts for the present limitations of 80,000-100,000 psi yield strength at ambient temperatures. This threshold stress is also sensitive to temperature and increases as the temperature is raised (28).

The incubation time is of some relevance to the behavior of geothermal materials, especially for above-ground components. The incubation time marks the line between reversible and permanent damage and as such provides the basis for dehydrogenation cycles for equipment involving hydrogeneous environments.

Proposed solutions to this problem can take many different directions. Obviously one approach is to systematically establish the limits of confidence in terms of strength level, temperature and environmental conditions for established or recently developed alloys. Clearly another approach involves attempts to develop materials with higher threshold stress values for the specific environmental conditions related to geothermal systems.

The development of materials resistant at higher yield strengths and thus higher threshold stress values is of prime concern. There is an increasing awareness of the role of metallurgical structure. It is now generally appreciated that fine structures with uniform carbide distributions such as tempered martensite are more resistant to hydrogeneous environments than the more coarse structures such as ferrite-pearlite mixtures (normalized structures) in constructional-type steels, all other things equal (29-31).

For the available constructional steels, the behavior in sour oil well and similar environments has been quite thoroughly

explored. Although there are many similarities of environment in oil or gas and geothermal wells, potential geothermal sources present a much wider spectrum of variation in the environment; for example, the broad range of chloride contents and of pH in some of these environments.

Many different types of materials are necessary to meet the requirements of a complete geothermal power system. For the most part, steels suitable for casing, tubing, etc., may not serve for much of the rest of the installation, such as well head fittings, valves, pumps, bolts and ancilliary equipment. Often, more highly alloyed and corrosion resistant materials are employed. In terms of the available alloys, particularly the age hardenable and corrosion resistant types such as austenitic stainless steel, Inconel, Stellites, K-Monel, A-286, MP35N, etc., the limits of confidence in terms of heat treatment (e.g. overaging), threshold stress, maximum safe strength level, etc., have not been systematically determined particularly with respect to the relevant geothermal environments. Indeed, recent studies, largely unpublished, have indicated unexpected failure behavior in some of these alloys which are currently under intense study (32-33).

## Methods and Materials

### Types of Tests:

Three different types of tests have been employed thus far in this program. A two point type bend specimen, loaded to approximately 100% of the design yield strength, is used for much of the study, providing a simple early screening test (34). Aside from the advantage of low cost and simplicity, there is virtually no crevice corrosion. However, extreme care must be exercized in loading, since any plastic flow will reduce the calculated applied stress. Figure 1a shows an example of a no-fail and a fail result.

Since a substantial portion of this study involves materials for casing, tubing and other down hole applications. A C-ring type test, widely employed in the petroleum industry, has been adopted (10, 35). Here, a series of rings cut from commercially heat treated casing and tubing were examined, stressed to approximately 100% of their yield strength. Fig. 2, illustrates how the C-ring is loaded and the stress calculated by the deflection method. With the use of caliphers an accuracy of approximately one percent in the stress is attainable.

The loading bolts, nuts, washers, etc., must be protected from the solution which was accomplished by the use of RTV102 silicone rubber.

Most recently smooth tensile bar testing has been initiated. This has recently (July 1977) been adopted as a NACE standard for testing in sour environments (36). A copy of this test standard is appended to this report. Fig. 1b shows the type of test unit we employ for this study. The stress is applied by loading a calibrated proof ring. The container surrounding the tensile specimen will allow the continuous flow of gas and/or liquid test environment through inlet and outlet parts.

### Environments:

The primary test environment employed the standard NACE solution for sour environments which is a deaerated aqueous solution of 5% NaCl, 0.5% acetic acid saturated with a continuous flow of $H_2S$ (36). This solution has been widely used for evaluating materials in sour environments and thus there is a vast storehouse of information on almost all commercially

available alloys with standard treatments. On the other hand, geothermal environments vary widely and no one solution can serve for total evaluation. Thus, the NACE solution was modified to encompass chloride concentrations of 0, 1, 5 and 20%, pH levels from 3 to 7 and temperatures up to 425°F.

In the early phases of the program the recommended tentative procedure of continuous purging with $H_2S$ for the full 30-day test duration was adopted (36). However, later it was observed that specimens that failed at ambient temperature did so within the first 10-12 days. Thus, except for the most promising materials, tests were generally terminated after this test period. This was done for the constructional type steels only. For the higher temperatures employing a pressure vessel, continuous purging with $H_2S$ was not possible. However, this does not pose a problem, since it is a closed system, previously deaerated and substantial concentration of $H_2S$ is evident in the environment after 30 days. Dessicators were employed to contain the solution for tests at ambient temperature and autoclaves for tests at 212°F and higher.

The available tank $H_2S$ has approximately 300 ppm of oxygen. Where a continuous flow of $H_2S$ was employed, the influence of this oxygen was quite apparent in the relatively low but definite corrosion in the 30-day tests at ambient temperature and seriously affected tests near the boiling temperature of the solution. Consequently, tests much above ambient were conducted in autoclaves. The oxygen effect was minimized by prepurging the $H_2S$ through scrap iron in the NACE solution.

Materials:

A wide range of alloys are under examination both with standard commercial treatments and metallurgical structures as well as composition variations which may potentially enhance performance. Their compositions are listed in Tables 1a, b, and c. The bent beam specimen has yielded data for commercial alloys in the standard NACE solution at ambient temperatures that are quite consistent with the literature. For example, steels such as 410, 431, and 440, which represent industry's attempts to achieve improved corrosion resistance with strengths above the present general limits, all failed at the higher strength levels just as they had with

many other types of test specimens, including simple tensile, notch bend, bent tubing, etc. These particular steels will not be further considered here.

The heat treatments were as commercially recommended or reasonably adjusted for the experimental steels, and were conducted in a purified nitrogen atmosphere at controlled temperatures. For the constructional steels in particular, extra precautions were taken to avoid decarburization during both the normalizing and austenitizing treatment. This is vitally important for the bent beam specimens. All constructional steels were quenched for martensite and tempered at the appropriate temperature to attain the desired strength as indicated in the tables. The age-hardenable alloys all required prior cold work to attain their optimum yield strength levels. Generally, these materials were received in the cold worked condition. Our ageing treatments were designed to produce under-aged, fully aged, and over-aged conditions. The stainless steels were examined in both the low strength annealed condition and after strengthening by cold work. The C-ring test specimens were all cut from commercially heat treated casing or tubing. It should be appreciated that not all of these steels were designed for use in sour environments.

## Results and Discussion

### Bent Beam Tests

Constructional Steels:

The superior resistance to SSC of tempered martensite compared with normalized (ferrite-pearlite) structures has placed a premium on hardenability. This is particularly true considering the difficulty of thru quenching long sections of tubing or increased wall thickness at upset joints (37). Thus the Cr/Mo steels for example have become favored over the more economical Mn or Mn/Mo grades. Here, 4130 with its well documented behavior in sour environments has been chosen as a reference material.

Since several thousand tests are involved it is not feasible to tabulate every test item in a series of tables.

Rather, Table 2 indicates the nature of the raw data obtained for a steel of considerable interest. Specifically, Table 2 indicates the manner in which the 0.2% offset yield strength "break-point" is obtained; that is, the highest value of the yield strength which survives the sour environment when loaded to approximately 100% of its yield strength. Also shown is the influence of chloride concentration at the indicated pH values. For example, for this steel, these data would indicate an average "break-point" at a yield strength of approximately 122 ksi, relatively independent of the chloride concentration. Also indicated is the slightly lower pH of the 20% chloride environment which rises about 1 point pH during the run as shown. Tables 3-11 inclusive summarize this type of data.

Table 3 shows the break points for a variety of steels which, with one notable exception (4340), are more or less based on the widely used 4130 analysis. Clearly, the modified 4135 steel exhibits a 10% higher break point than the standard 4130, approximately 122 ksi compared to 110 ksi. The modified analysis varies from the standard primarily in a higher molybdenum content and the addition of columbium. At this time, this appears to be the best commercially available steel in terms of strength level and resistance to chloride containing sour environments. The very low breakpoint for the 4340 steel emphasizes the deleterious influence of nickel in constructional steels exposed to sour environments.

The V1397 steel is of rather special interest. This is a vacuum melted high purity steel with the basic analysis of 4130. Although the purity is obviously outside of regular commercial feasibility, the idea was to examine the influence of inclusion content, distribution, etc. as well as sulphur and phosphorus. These are factors known to influence fracture characteristics in normal environments and several studies have indicated some influence in sour environments (38-40). Comparing in Table 3, the standard 4130 with its high, virtually inclusion-free counterpart, it is apparent that the V1397 steel enjoys a substantial advantage and in fact matches the modified 4135 steel. The obvious implication is that at least some of these factors are significant and perhaps may be benefically controlled without the necessity for super purity. Indeed, very low sulphur is most certainly commercially feasible today and modern steel making practice offer opportunities for controlled inclusion types, etc.

V1312 and V1313 are vacuum melted experimental steels more or less designed on the model of the modified 4135 but with lower carbon and sulphur; both of which are known to improve resistance to fracture. Table 3 indicates that these steels are somewhat better than the standard 4130 but do not quite match either the modified 4135 or the high purity analysis. One possible reason may be the lower carbon content. It is interesting to note that the sulphur in these two steels was substantially lower than for the modified 4135 (.004 vs .010%). On the other hand, the Mn, Si and P contents were at normal levels and these elements may play a decisive role in the response of these steels to hydrogeneous environments.

It is quite well established that lower carbon contents enhanced resistance to brittle behavior for the constructional type steels. The 4118 together with the other steels represent an attempt to determine whether the enhanced resistance to brittle fracture under atmospheric conditions carries over to sour environments --- apparently it does not!

At this time, it is instructive to recognize that the lower carbon steels require a lower tempering temperature to attain the same strength level as one of higher carbon. In this connection, there is some evidence to indicate that the tempering temperature per se required to attain a given strength level may be a significant factor in resistance to sour environments (41, 42). In fact, this effect may extend beyond the influence of carbon alone. Specifically, the higher the tempering temperature required to attain a given strength the more resistant the steel, particularly at the strength levels of interest. A comparison of 4118 with 4135 modified clearly illustrates this. At 5% NaCl, 4118 has a break point of less than 110 ksi obtained by tempering at 1075°F. On the other hand, 4135 modified gave a break point value of 122 ksi resulting from tempering at 1275°F. The phenomenon of temper embrittlement may be responsible for this beneficial influence of the higher tempering temperature. The lower tempering temperatures (below $\sim$ 1150°F) are known to promote brittle behavior.

The influence of chloride concentration on cracking in sour environments has been open to some question particularly for the constructional type steels. Examination of Table 4, clearly reveals that the higher chloride concentrations are not detrimental and may even be slightly beneficial. To the extent that the hydrogen pickup results from corrosion, the

inhibitive effect of chlorides above 1% in these steels can account for this behavior (43). This result is particularly relevant to the development of the Imperial Valley, and similar high chloride geothermal resources.

It has long been recognized that the resistance to hydrogen embrittlement in constructional type steels improves substantially as the temperature is raised. The data of Table 5 indicate the substantial improvement in resistance to SSC at higher exposure temperatures. Break points of 140 ksi or slightly higher are apparent and again essentially independent of chloride concentration. The improvement appears also to be independent of the temperature above 215°F. Isolated tests at 325°F were quite consistent with this view.

Although exposure at elevated temperatures does provide improvement, contrary to common belief, there apparently is no complete immunity; there still is a critical yield strength break point which can not be exceeded. In short, this type of data is significant in that it can provide at least semi-quantitative design guidelines to match temperature changes with depth. This phenomenon is merely a manifestation of the influence of temperature on the critical yield strength for hydrogen induced brittle delayed failure (24, 28).

It is well recognized that the threshold stress for failure decreases as the pH is lowered, particularly at pH values less than 4-5 (10), this in turn can limit the yield strength break point as indicated in the introduction. The data of Table 6 illustrates the improvement in the critical yield strength at pH values close to neutral. In Table 3 at ambient temperature and pH values of 2.5-4, yield strength break points of 110 ksi-122 ksi were indicated as compared to approximately 140 ksi at pH 6-7. Solutions initially started at pH 6.0 rather quickly settled at 6.5 as did those initially started at 7.

Here again, contrary to common belief, a near neutral pH does not provide immunity. Indeed, SSC has been observed at pH 12. However, quite similar to the effect of elevated exposure temperatures it does quite substantially raise the critical yield strength for SSC. Just as in the case of higher down hole operating temperatures, this phenomenon provides greater reliability for those steels that may be operating marginally.

## Corrosion Resistant Alloys

### A286

Many of the corrosion resistant alloys are based on face-centered cubic structures and may be expected to exhibit greater susceptibility to SSC at temperatures significantly above ambient. The age-hardenable austenitic stainless steel A-286 behaves in this manner. When fully aged to 190 ksi (16 hrs. - 1200°F) there was no failure at 215°F. On the other hand testing at 325 and 425°F in both 5 and 20% chloride modified NACE solution produced failure. However, the 30 day-215°F exposure did indicate some loss of basic ductility in other tests. At this time, there is no way of knowing whether or not this loss of ductility indicated impending failure at some longer exposure time; a basic problem in any of these accelerated tests.

Overaging (16 hrs.-1300°F) to obtain a Y.S. of 155 ksi did not fail in the 5% NaCl solution. In the 20% NaCl solution only one of three specimens cracked but pitting was evident in all three. This appears to be more than a simple strength level effect since under-aging to similar strength levels exhibited failure in all cases. Although not examined systematically, reference to Table 7 indicates a greater sensitivity to higher chloride concentrations for A286 in contrast to the behavior in constructional type (BCC) steels.

### K Monel

K Monel 500, treated to 140 and 170 ksi yield strengths has resisted cracking in both the 5% and 20% NaCl, $H_2S$ environments (Table 8). This agrees with the rather limited literature on this alloy indicating resistance to SSC in the standard NACE solution. However, there are several unofficially reported service failures in sour wells. Also, there is evidence that this alloy can be subject to hydrogen embrittlement under rather specific conditions (21). Many additional tests, not reported in Table 8, have involved coupling this alloy to steel and exposing to the standard NACE solution. A variety of heat treatments were examined at ambient and 260°F for 30-34 days. No failures were observed.

MP35N

Much attention has been focused recently on a highly corrosion resistant non-ferrous, age-hardenable alloy, MP35N (33, 44). This alloy has not only demonstrated excellent corrosion properties but also resists pitting and until recently was believed to be completely immune to SSC at yield strength levels up to 250 ksi.

It is evident in Table 9 that at the high strength levels SSC can occur at ambient temperatures when coupled with iron; in short, under cathodic charging (32). Indeed aging at almost any temperature below approximately 1300°F will produce failure when coupled to iron or otherwise cathodically charged. Pertinent conferences and a recent comprehensive publication clearly indicate this and extend the phenomenon to some of the Inconels and Hastalloys (33).

The data of Table 9 are consistent with those being compiled in many laboratories. It is apparent that no failures occurred in the 30 day tests in the NACE solutions at all temperatures when not coupled to iron or otherwise cathodically charged. As recent studies have indicated, coupling to iron and testing at ambient temperature in acid or NACE solution produces failure quite readily. However, testing at 215°F, even when coupled, did not yield failure. However, failures at elevated temperatures in these chloride solutions have been observed at longer test durations (45).

Most of the tests were conducted on transverse oriented specimens which usually are a direction of lesser resistance to cracking. However, as expected, it is possible to get failure in the longitudinal orientation; for example, the 50% HCl acid environment tests listed in Table 9. This is probably merely a question of degree and severity of the environment. The concept of the beneficial effect of over-aging with only slight loss of strength as indicated in our studies on A286 (Table 7) shows early promise for the MP35N alloy. A limitation on the maximum aging temperature involves recrystallization following the necessary cold work prior to aging (46). In passing, it is interesting to observe that aging treatments which lead to great sensitivity when exposed, do not show any change in the excellent tensile properties prior to the exposure.

The 300 series austenitic stainless steels are not generally considered to be high strength alloys but can be substantially strengthened by cold work. Table 10 for 304 indicates that in the annealed condition there was no failure at ambient temperature and without chloride. This was true even when given an embrittling treatment at 1200°F. On the other hand, after strengthening by cold work, failure was encountered above 1% NaCl, even at pH 6.5. Also, at all elevated temperatures and all chloride concentrations failure was evident.

The more highly alloyed 310 data are presented in Table 11. At ambient temperature there does appear to be greater resistance to SSC than for 304 in the cold worked condition. Indeed, failure occurred only with the maximum 20% NaCl condition. Just as with 304, failure was observed at all elevated temperatures.

As might be expected, the austenitic stainless steels demonstrated greater sensitivity at the higher chloride concentrations and at the elevated temperatures even in the absence of oxygen. Strengthening by cold work also increased the sensitivity to SSC.

## C-Ring Tests

The results of the C-Ring tests, in the standard NACE solution are given in Table 12. Since the grade numbers indicate a minimum yield strength, the rings were usually loaded to a stress approximately 5 ksi above the indicated minimum; the usual aim for commercial heat treatment. Reference to Table 1c indicates that a majority of the steels examined thus far are of the more economical grades depending upon higher than usual manganese for a measure of hardenability. These steels are not generally recommended for sour environment service except possibly at very low strength levels.

A cursory examination of this table clearly indicates the well-recognized sensitivity of steel to a sour environment above moderate strength levels. As an example, compare steels #1 or #2 with steel #6, all with essentially the same alloy composition, yet the P110 (RC29) failed and the K55(RC19) did not fail. A comparison of steels #4 and #10 also illustrate

the influence of strength level.

Although strength level is a vital factor, an evaluation on this basis alone would constitute a gross oversimplification. Hardenability and its relation to structure exerts a major influence on performance. Hardenability is primarily determined by the alloy content and for a given composition the full use of its potential for hardening will be sensitive to section size and quenching efficiency. The importance of hardenability resides in the fact that fine structures with uniform carbide distributions (i.e. tempered martensite) are more resistant to hydrogeneous environments than the more coarse structures such as ferrite-pearlite mixtures (i.e. normalized structures), all other things equal.

The influence of section size on the attainment of the fine structure (hardenability) is quite evident in a general comparison of the greater resistance to failure of the smaller, thinner wall tubing compared to the heavier casing.

Although, the materials tested to date do not present a great variety of alloy steels, the influence of alloy on hardenability and thus structure can be seen, for example, in a comparison of steels #4 and #5 (See Tables 1c and 12), the compositions are essentially the same, except that steel #4 has .30 percent molybdenum and did not fail while steel #5, without molybdenum, did fail. Molybdenum is a strong promoter of increased hardenability. Steels #13 and 14 essentially 4130 type analyses, also did not fail, despite relatively thick wall sections. Examination of steels 12, 13 and 14 indicate the improved structure (martensite) obtainable by alloy and/or efficient fast quenching.

As indicated earlier in this report, temper embrittlement may be a factor in some cases. Not only tempering at inappropriate temperatures (i.e. ∿1150°F or lower) but slow cooling through this temperature range can induce embrittlement. At the present time no commercially produced casing, tubing or drill pipe is quenched from the tempering temperature. This means relatively slow air cooling particularly for larger diameters and/or wall thicknesses.

The data of Fig. 13, give the results of a brief study to determine if commercially treated casing, tubing, etc. may indeed be subject to temper embrittlement. Note that steel #5, as received did fail, but after being retempered and quenched from the tempering temperature, it did not fail. On the

other hand steel #9 which did not fail in the as received condition, exhibited failure after given a temper embrittling treatment. One must conclude that the potential for temper embrittlement does exist and in some cases may actually limit the performance of the casing or tubing, not to mention other components of a geothermal power system which may employ alloy constructional steels.

## NACE Standard Tensile Tests

The National Association of Corrosion Engineers has recently completed a comprehensive study involving a round robin testing program involving a large number of organizations and various test methods for evaluating steels for sour environment service. This resulted in the adoption of the smooth bar tensile test as indicated earlier in this study. (Also see appendix)

In many cases where substantial corrosion resistance is required with reasonable strength, an evaluation of the threshold stress even if less than the yield strength provides essential design data. The CA6NM alloy presents such a situation. Table 14 indicates that in the standard NACE solution and for the indicated double temper heat treatment, the threshold stress has been bracketed between 75 and 85% of the yield strength. Tests in progress will hopefully narrow this gap. It is interesting to note that this is substantially better than the 410 type alloy which has a threshold value of only 20% of the yield strength and nevertheless is widely employed at the well-head of oil and gas wells (35, 47).

## Summary

1. A high hardenability, modified version of 4130 appears to be the best commercially available steel for down hole service.

2. The lower carbon varieties (below .30%C) of the 41xx type steels do not appear to be as resistant to SSC as their somewhat higher carbon counterparts. This is contrary to expectations in view of the greater toughness of low carbon steels.

3. The SSC resistance is improved, the higher the tempering temperature necessary to achieve a given yield strength.

4. The resistance to SSC is essentially independent of the chloride concentration. In fact, there appears to be a slight improvement at the higher concentrations.

5. The yield strength "break point" is raised by elevated temperature service. However, a definite critical yield strength does exist which can not be exceeded. In short, there is no complete immunity.

6. The influence of pH is quite analogous to that of temperature. Increasing values of pH up to 7 raise the useable yield strength. Again, there is no immunity only a higher yield strength "break point."

7. Overaging of A286 stainless steel appeared to be beneficial at a still respectable strength level. Underaging to the same approximate strength was not effective. Increased chloride concentration increased sensitivity to failure.

8. K Monel 500 resisted SSC at both 170 ksi and 140 ksi at 5 and 20% NaCl.

9. No failures were encountered in MP35N at ambient up to 425°F. However, when coupled to iron failure occurred at ambient temperature but not at an elevated temperature, consistent with data being accumulated by others.

10. No failure was observed in 304 in the annealed condition at ambient temperature; but when cold worked, chloride concentrations above 1% increased sensitivity. At elevated temperatures, failure was encountered at all chloride concentrations. In the cold worked condition, 310 displayed the usual sensitivity to chloride concentration and to elevated temperatures.

11. C-ring tests of commercially heat treated casing and tubing indicated the influence of strength and the superior properties of quenched and tempered structures based on martensite.

12. Temper embrittlement can be a serious problem in limiting the performance of casing, tubing, and drill pipe.

13. The NACE adopted tensile test has shown a corrosion resistant alloy CA6NM to be quite superior to its counterpart currently in use.

## Acknowledgement

This study is sponsored by the DOE, Division of Geothermal Energy. The authors have received cooperation from so many people it is not possible to name them all. However, we wish to acknowledge the assistance of Exxon and Shell Oil Co., Climax Molybdenum Corporation, Latrobe, Republic and Timken Steel Companies and particularly ARMCO Steel Corporation, which is directly involved in this program.

## References

1. R.N. Tuttle, "Deep Drilling-A Materials Engineering Challenge", Shell Development Comp., Bellair Research Center. Publication #BRC-EP-630, Houston, Texas, 1973. See also Materials Performance, February, 1974.

2. T. Marshall and A. Tombs, "Delayed Fracture of Geothermal Bore Casing Steels", Aus. Corros. En'g., 13, 9, 2-8, 1969.

3. Basil Wood, "Basis of Selection of Materials for Geothermal Schemes," UNESCO, Geothermal Energy, Paris, 1973.

4. D. Dominguez and F. Vital, "Repair and Control of Geothermal Wells at Cerro Prieto, Boja, Calif., Mexico", Second United Nations Symposium on Development and Uses of Geothermal Resources, Vol. 2, p. 1495, 1975.

5. K.C. Youngblut, "Materials Selection-Coal Gasification Pilot Plant", Materials Protection and Performance, p. 33, Dec. 1973.

6. C.N. Bowers, W.J. McGuire and A.E. Wiehe, "Stress Corrosion Cracking of Steel Under Sulphide Conditions," Corrosion, Vol. 8, p. 333, 1952.

7. R.S. Treseder and T.M. Swanson, "Factors in Sulphide Corrosion Cracking", Corrosion, 24, 31, 1968.

8. J. F. Bates, "Sulphide Cracking of High Yield Strength Steels in Sour Crude Oils," Materials Protection, p. 33, Jan. 1969.

9. E.H. Phelps, "Stress Corrosion Behavior of High Yield Strength Steels," Proc. 7th World Petroleum Congress, Elsevier Publishing Company, Ltd., p. 201, 1967.

10. C.M. Hudgins, R.L. McGlasson, P. Mehdizadeh and W.M. Roseborough, "Hydrogen Sulphide Cracking of Carbon and Alloy Steels," Corrosion, Vol. 22, p. 238, 1966.

11. J.L. Battle, T.V. Miller and M.E. True, "Resistance of Commercially Available High Strength Tubular Goods to Sulphide Stress Cracking," Materials Performance, June, 1975.

12. D.S. Burns, "Laboratory Test for Evaluating Alloys for $H_2S$ Service," Materials Performance, Jan. 1976.

13. P. Bastien and Amiot, "Mechanism of the Effect of Ionized Solutions of $H_2S$ on Iron and Steel," Compte Rendue, Vol. 235, p. 1031, 1952.

14. H.C. Helgeson, "Geologic and Thermodynamic Characteristics of the Salton Sea Geothermal System," Amer. Journal of Science, 266, p. 129, 1968.

15. J.H. Smith, "Casing Failures in Geothermal Bores at Wairakei," Geothermal Energy, Vol. 3, U.N. Conf., p. 254, 1961.

16. P.K. Forster, T. Marshall and A. Tombs, U.N. Conf. on New Sources of Energy, Rome, 1961. See also Aust. Corrosion Eng'g., Vol. 6, p. 306, 1962.

17. A.C.L. Fooks, "The Development of Casings for Geothermal Boreholes," Ibid.

18. A.R. Troiano and J.P. Fidelle, "Hydrogen Embrittlement in Stress Corrosion Cracking," Magistrale Lecture, Intern'l Conf. Hydrogen in Metals. Paris, France, June 1972. See also ART Keynote Lecture, Ref. No. 18.

19. C.F. Barth, E.A. Steigerwald and A.R. Troiano, "Hydrogen Permeability and Delayed Failure of Martensitic Steels," Corrosion, Vol. 25, p. 353, 1969.

20. A.R. Troiano, "Hydrogen in Metals". Proceeding of ASM-CMU International Conference. Vol. 2, ASM Materials/Metal Working Technology series 1974.

21. J. Papp, R.F. Hehemann and A.R. Troiano, "Hydrogen Embrittlement of High Strength FCC Alloys," ASM, CMU Conference, Seven Springs, Penn. Sept. 1973, ASM Conference, Vol. 1973.

22. E.A. Steigerwald, "Delayed Failure of High Strength Steel in Liquid Environments," Proc. Am. Soc. Testing Materials, Vol. 60, p. 750, 1960.

23. L.M. Dvoracek, "Sulphide Stress Corrosion Cracking of Steels," Corrosion, Vol. 26, p. 177, 1970.

24. W. Beck, E.J. Jankowsky and P. Fischer, "Hydrogen Stress Cracking of High Strength Steels," Naval Air Development Center, Rept. No. NADC-MA-7140, 1972.

25. J.B. Greer, "Factors Affecting the Sulphide Cracking of High Strength Steels," Materials Performance, Vol. 14, 11-22, 1975.

26. R.D. Kane and J.B. Greer, Sulphide Stress Cracking of High Strength Steels in Laboratory and Oil Field Environments", Journ. Petroleum Tech., AIME, Oct. 1976. Preprint SPE 6144.

27. A.R. Troiano, "The Role of Hydrogen and Other Interstitials In The Mechanical Behavior of Metals," Edward Demille Campbell Memorial Lecture, Trans. ASM, Vol. 52, p. 54, 1960.

28. M.R. McGuire, A.R. Troiano and R.F. Hehemann, "Stress Corrosion of Ferritic and Martensitic Stainless Steels", Corrosion, Vol. 29, p. 268, 1973.

29. W.M. Cain and A.R. Troiano, "Steel Structure and Hydrogen Embrittlement", Petroleum Eng., Vol. 37, p. 5, May 1965.

30. E. Snape, "Roles of Composition and Microstructure in Sulphide Cracking of Steel", Corrosion, Vol. 24, p. 261, 1968.

31. E. Snape, "Sulphide Stress Corrosion of Some Medium and Low Alloy Steels," Corrosion, Vol. 23, p. 154, 1967.

32. P. Rhodes, Private Communications, Shell Dev. Co., Houston, Texas, R.D. Kane, EXXON Production Research Co., Houston Texas, and A. Simkovich, Latrobe Steel Co., Latrobe, PA.

33. R.D. Kane, M. Watkins, D.J. Jacobs and G.L. Hancock, "Factors Influencing the Embrittlement of Cold Worked High Alloy Materials in $H_2S$ Environments", Corrak, 33(9) 309-320, 1977.

34. ASTM, Designation: G39-73, "Preparation and Use of Bent-Beam Stress Corrosion Specimens", p. 692, 1973.

35. R.D. Kane, M. Watkins and J.B. Greer, "The Improvement of SCC REsistance of 12% Chromium Stainless Steels through Heat Treatment." Corres. 33,(7), p. 231, 1977.

36. "Testing of Metals for Resistance to SSC at Ambient Temperatures". NACE Standard TM-01-77.

37. J.A. Noerager and J.B. Greer, "An Investigation of Coupled Tubing Joints for Sour Service," Materials Performance, Feb. 1977.

38. T. Ohki, M. Tanimura, K. Kinoshita and G. Tenmyo, "The Effect of Inclusions on Sulphide Stress Cracking", Report, Nippon Kohan Kabushiki Kaisha.

39. E. Miyoshi, T. Tanaka, F. Terasaki and I. Takeda. "Hydrogen-Induced Cracking of Steels under Wet $H_2S$ Environment", Paper #75-Pet-2, ASME, 1976.

40. A. Ikeda, S. Nagata, T. Tsumura, Y. Nara and M. Kowaka, "Development of High Strength Oil Country Tubular Goods Highly Resistant to Sulphide Stress Corrosion Cracking," Sumitomo Metal Industries, Ltd., Osaka, Japan, API Standarization Conference, June 1977.

41. J.B. Grobner, D.L. Sponseller and W.W. Cias, "Development of Higher Strength $H_2S$ Resistant Steels for Oil Field Applications," Materials Performance, June 1975.

42. L.M. Dvoracek, "High Strength Steels for $H_2S$ Service," Materials Performance, May 1976.

43. D.W. Shannon and J.E. Boggs, "Factors Affecting the Corrosion of Steel by Oil-Brine-Hydrogen Sulphide Mixtures", Corrosion, p. 299t, June 1959.

44. J.P. Stroup, A.H. Bauman and A. Simkovich, "Multi-phase MP35N-An Alloy for Deep Sour Well Service," Materials Performance, June 1976.

45. R.D. Kane, Private communication, EXXON Corp., Houston, Texas.

46. T. Mohr, Private communication, Timken Steel Co., Canton, Ohio.

47. F.J. Grobner, "Sulphide Stress Cracking Resistance of CA-6-NM Steel". Climax Molybdenum Co., Report J-4135-02, June 1977.

# TABLE 1A
## ANALYSES*
## CONSTRUCTIONAL STEELS

| STEEL | C | MN | P | S | SI | CR | MO | CB | V | NI |
|---|---|---|---|---|---|---|---|---|---|---|
| 4118 | .20 | .80 | .008 | .012 | .27 | .51 | .11 | -- | -- | -- |
| 4123 | .23 | .84 | .036 | .016 | .36 | .93 | .20 | -- | -- | -- |
| 4130 | .33 | .53 | .015 | .029 | .27 | .91 | .21 | -- | -- | -- |
| 4135 MOD | .34 | .86 | .013 | .010 | .28 | 1.08 | .83 | .054 | -- | -- |
| 4340 | .35 | .76 | .007 | .011 | .25 | .82 | .25 | -- | -- | 1.79 |
| V1397 | .35 | -- | -- | -- | -- | 1.40 | .20 | -- | -- | -- |
| V1312 | .26 | .50 | .010 | .005 | .21 | 1.01 | .78 | .04 | -- | -- |
| V1313 | .26 | .52 | .010 | .004 | .22 | 1.01 | .78 | -- | .06 | -- |

* ELEMENTS NOT LISTED ARE IN RESIDUAL AMOUNTS EXCEPT FOR V1397 WHICH IS A SUPER PURE VACUUM MELTED HEAT.

## TABLE 1B

## CORROSION RESISTANT ALLOYS
### NOMINAL COMPOSITION

| | Ni | Cr | Ti | Mn | Mo | V |
|---|---|---|---|---|---|---|
| A-286 | 25 | 15 | 2 | 1.5 | 1.3 | 0.3 |

| | Ni | Cu | Al | Fe | Ti | Mn |
|---|---|---|---|---|---|---|
| K MONEL | 65 | 30 | 3 | 1.0 | 0.50 | 0.50 |

| | Ni | Co | Cr | Mo |
|---|---|---|---|---|
| MP35N | 35 | 35 | 20 | 10 |

| | C | Mn | Cr | Ni |
|---|---|---|---|---|
| 304 | .08 | 1.5 | 19 | 9 |
| 310 | .08 | 1.5 | 25 | 20 |

| | C | Mn | P | S | Si | Cr | Ni | Mo |
|---|---|---|---|---|---|---|---|---|
| CA6NM | .01 | .38 | .023 | .007 | .03 | 12.92 | 3.89 | .51 |

## TABLE 1c - ANALYSES

### C-RINGS

| STEEL | C | MN | P | S | SI | CR | MO | V |
|---|---|---|---|---|---|---|---|---|
| 1 | .26 | 1.47 | .013 | .015 | .20 | -- | -- | -- |
| 2 | .25 | 1.53 | .011 | .018 | .19 | -- | -- | -- |
| 3 | .35 | 1.58 | .009 | .015 | .18 | -- | .17 | .06 |
| 4 | .24 | 1.62 | .011 | .012 | .22 | -- | .30 | -- |
| 5 | .25 | 1.40 | .010 | .014 | .19 | -- | -- | -- |
| 6 | .43 | 1.24 | .013 | .017 | .19 | -- | -- | -- |
| 7 | .43 | 1.16 | .015 | .016 | .21 | -- | -- | -- |
| 8 | .37 | 1.58 | .017 | .014 | .20 | -- | .14 | .06 |
| 9 | .26 | 1.42 | .008 | .017 | .08 | -- | -- | -- |
| 10 | .23 | 1.61 | .015 | .011 | .14 | -- | .33 | .06 |
| 11 | .26 | 1.54 | .013 | .019 | .18 | -- | -- | -- |
| 12 | .13 | .45 | .010 | .007 | .51 | 9.0 | .95 | -- |
| 13 | .32 | .54 | .008 | .014 | .29 | .97 | .22 | -- |
| 14 | .32 | .53 | .008 | .023 | .27 | 1.1 | .29 | -- |

## TABLE 2

## SULPHIDE STRESS CRACKING OF MODIFIED 4135 STEEL

### AMBIENT TEMPERATURE

| RC | Y.S. MPa (KSI) | No. Failed / No. Tested |
|---|---|---|
| | 5% NaCl pH 3.5-4.0 | |
| 30 | 883 (128) | 2/2 |
| 29 | 869 (126) | 3/3 |
| 28 | 848 (123) | 2/5 |
| 27 | 827 (120) | 0/1 |
| 26 | 800 (116) | 0/3 |
| 24 | 759 (110) | 0/4 |
| | 20% NaCl pH 2.5-3.5 | |
| 33 | 952 (138) | 4/4 |
| 31 | 903 (131) | 4/4 |
| 30 | 883 (128) | 2/5 |
| 29 | 869 (126) | 1/2 |
| 28 | 848 (123) | 0/3 |
| 27 | 827 (120) | 0/2 |
| 26 | 807 (117) | 0/2 |
| 24 | 759 (110) | 0/1 |

## TABLE 3

### YIELD STRENGTH BREAK-POINTS FOR DIFFERENT STEELS EXAMINED IN THE STANDARD NACE SOLUTION

| MATERIAL | Y.S. (MPA) KSI |
|---|---|
| STANDARD 4130 | 759 (110) |
| 4135 MODIFIED | 841 (122) |
| V1397 (4130 HIGH PURITY) | 841 (122) |
| V1312 | 814 (118) |
| V1313 | 814 (118) |
| 4123 (COMMERCIAL PIPE) | 772 (112) |
| 4118 (COMMERCIAL CARBURIZING GRADE) | <759 (110) |
| 4340 | <744 (108) |

## TABLE 4

### YIELD STRENGTH BREAK-POINTS FOR SEVERAL STEELS EXAMINED AT VARIOUS CHLORIDE CONCENTRATIONS

| CHLORIDE CONCENTRATION | Y.S. MPa (KSI) |
|---|---|
| **STANDARD 4130** | |
| 0% | 780 (113) |
| 1% | 759 (110) |
| 5% | 759 (110) |
| 20% | 814 (118) |
| **4135 MODIFIED** | |
| 0% | 827 (120) |
| 1% | 855 (124) |
| 5% | 841 (122) |
| 20% | 855 (124) |
| **V1397 (4130 HIGH PURITY)** | |
| 0% | 855 (124) |
| 1% | 848 (123) |
| 5% | 841 (122) |
| 20% | 855 (124) |

## TABLE 5

### THE INFLUENCE OF TEMPERATURE ON THE YIELD STRENGTH BREAK-POINTS IN THE STANDARD NACE SOLUTION.

| MATERIAL | TEMPERATURE °C (°F) | Y.S. BREAK-POINT MPa (KSI) |
|---|---|---|
| STANDARD 4130 | AMBIENT | 759 (110) |
| | 102 (215) | 965 (140) |
| | 218 (425) | 965 (140) |
| MODIFIED 4135 | AMBIENT | 841 (122) |
| | 102 (215) | 952 (138) |
| | 218 (425) | 952 (138) |
| V1397 | AMBIENT | 841 (122) |
| | 102 (215) | 986 (143) |
| V1313 | AMBIENT | 814 (118) |
| | 102 (215) | 952 (138) |

## TABLE 6

THE INFLUENCE OF pH 6-7 ON THE YIELD STRENGTH BREAK-POINTS AT AMBIENT TEMPERATURE AND 5% NaCl

| STEEL | Y.S. MPa (KSI) |
|---|---|
| 4130 STANDARD | 965 (140) |
| 4135 MODIFIED | 965 (140) |
| V1397 HIGH PURITY | 979 (142) |
| V1312 | 965 (140) |
| V1313 | 979 (142) |

# TABLE 7

## SULPHIDE CRACKING OF A286 STAINLESS STEEL IN STANDARD NACE SOLUTION

| TEST TEMPERATURE °C (°F) | AGEING TREATMENT TEMPERATURES °C (°F) | Y.S. MPA (KSI) | NO. FAILED NO. TESTED |
|---|---|---|---|
| | 5% NACL | | |
| 102 (215) | 649 (1200)-16 HRS. | 1310 (190) | 0/1 |
| 163 (325) | 649 (1200)-16 HRS. | 1310 (190) | 1/1 |
| 163 (325) | 704 (1300)-16 HRS. | 1062 (155) | 0/1 |
| | 20% NACL | | |
| 218 (425) | 621 (1150)-1 HR. | 1138 (165) | 1/1 |
| 218 (425) | 649 (1200)-1 HR. | 1165 (170) | 1/1 |
| 218 (425) | 649 (1200)-4 HRS. | 1199 (175) | 1/1 |
| 218 (425) | 649 (1200)-16 HRS. | 1310 (190) | 3/3 |
| 218 (425) | 704 (1300)-16 HRS. | 1062 (155) | 1/3 |

## TABLE 8

### SULPHIDE STRESS CRACKING OF K MONEL

| TEST TEMPERATURE | HEAT TREATMENT | Y.S. MPA (KSI) | NO. FAILED / NO. TESTED |
|---|---|---|---|
| | 5% NaCl | | |
| AMBIENT | 8 HRS., 538°C (1000°F) F.C. TO 482°C (900°F) W.Q. | 1165 (170) | 0/1 |
| 163°C (325°F) | 16 HRS. 593°C (1100°F) F.C. TO 482°C (900°F) A.C. | 965 (140) | 0/1 |
| 218°C (425°F) | SAME AS ABOVE. | 965 (140) | 0/2 |
| | 20% NaCl | | |
| 218°C (425°F) | 8 HRS., 538°C (1000°F) F.C. TO 482°C (900°F) W.Q. | 1165 (170) | 0/1 |
| 218°C (425°F) | 16 HRS. 593°C (1100°F) F.C. TO 482°C (900°F) A.C. | 965 (140) | 0/2 |

## TABLE 9

### SULPHIDE STRESS CRACKING OF MP35N*
### NOT COUPLED TO IRON

| HEAT TREATMENT | TEST TEMPERATURE | NO. FAILED / NO. TESTED |
|---|---|---|
| 593°C (1100°F)-4 HRS. | AMBIENT | 0/5 |
| 704°C (1300°F)-4 HRS. | AMBIENT | 0/1 |
| 538°C (1000°F)-1 HR. | 102°C (215°F) | 0/1 |
| 593°C (1100°F)-4 HRS. | 163°C (325°F) | 0/1 |
| 593°C (1100°F)-4 HRS. | 218°C (425°F) | 0/5 |

### COUPLED TO IRON

| | | |
|---|---|---|
| 593°C (1100°F)-4 HRS. 288°C (550°F)-20 DAYS | AMBIENT | 2/2 |
| 593°C (1100°F) + 354°C (670°F)- 16 HRS. | AMBIENT | 1/2 |
| 354°C (670°F)- 16 HRS. | AMBIENT | 2/2 |
| 538°C (1000°F)- 1.5 HRS. | AMBIENT | 2/2 |
| 593°C (1100°F) - 4 HRS. 288°C (550°F) - 20 DAYS | 102°C (215°F) | 0/2 |

* THESE DATA INCLUDE BOTH 5 AND 20% CHLORIDE SOLUTIONS WITH NO SIGNIFICANT DIFFERENCE.

### ACID HYDROGENATION
### COUPLED TO IRON IN 50% HCL

| | | |
|---|---|---|
| 1000°F-1 HR. | AMBIENT | 2/2 |

## TABLE 10

SULPHIDE STRESS CRACKING OF 30% COLD WORKED 304 STAINLESS STEEL AT 1379 MPA (200 KSI).

| CHLORIDE PERCENT | pH | TEST TEMPERATURE °C (°F) | NO. FAILED NO. TESTED |
|---|---|---|---|
| 0 | 3.5 | AMBIENT | 1/5 |
| 1 | 3.5 | " | 0/2 |
| 5 | 3.5 | " | 5/5 |
| 5 | 6.5 | " | 2/2 |
| 20 | 2.5 | " | 3/3 |
| 1 | 3.5 | 102 (215) | 1/1 |
| 20 | 2.5 | 102 (215) | 1/1 |
| 1 | 3.5 | 163 (325) | 1/1 |
| 20 | 2.5 | 218 (425) | 1/1 |

IN THE ANNEALED CONDITION, NO FAILURES WERE ENCOUNTERED IN 4 TESTS IN 0 PERCENT CHLORIDE.

# TABLE 11

## SULPHIDE STRESS CRACKING OF 310 AUSTENITIC STAINLESS STEEL COLD WORKED 30 PERCENT FOR 1241 MPA (180 KSI)

| CHLORIDE PERCENT | pH | TEST TEMPERATURE °C (°F) | NO. FAILED NO. TESTED |
|---|---|---|---|
| 1 | 3.5 | AMBIENT | 0/1 |
| 5 | 3.5 | " | 0/2 |
| 5 | 6.5 | " | 0/2 |
| 20 | 2.5 | " | 2/2 |
| 1 | 3.5 | 102 (215) | 1/1 |
| 20 | 2.5 | 102 (215) | 1/1 |
| 1 | 3.5 | 163 (325) | 1/1 |
| 1 | 3.5 | 218 (425) | 1/1 |

TABLE 12

C-RING TESTS

| STEEL | SIZE | *GRADE | **HEAT TREATMENT | RC | WALL, IN. | FAIL-NO FAIL |
|---|---|---|---|---|---|---|
| 1 | 7" CASING | P110 | QUENCH + TEMPER | 29 | .46 INCHES | 2 FAILED |
| 2 | 7" CASING | P110 | QUENCH + TEMPER | 29 | .34 INCHES | 2 FAILED |
| 3 | 7" CASING | N80 | NORMALIZED | 19 | .36 INCHES | 1 NO FAIL |
| 4 | 7" CASING | L80 | QUENCH + TEMPER | 21 | .28 INCHES | 2 NO FAIL |
| 5 | 7" CASING | N80 | QUENCH + TEMPER | 23 | .27 INCHES | 2 FAILED |
| 6 | 7" CASING | K55 | HOT ROLLED | 19 | .26 INCHES | 2 NO FAIL |
| 7 | 2-7/8" TUBING | J55 | NORMALIZED | 19 | .19 INCHES | 2 NO FAIL |
| 8 | 2-7/8" TUBING | N80 | NORMALIZED | 20 | .17 INCHES | 4 NO FAIL |
| 9 | 2-7/8" TUBING | N80 | QUENCH + TEMPER | 25 | .18 INCHES | 2 NO FAIL |
| 10 | 2-7/8" TUBING | P105 | QUENCH + TEMPER | 32 | .16 INCHES | 2 FAILED |
| 11 | 7" CASING | P110 | QUENCH + TEMPER | 30 | .50 INCHES | 2 FAILED |
| 12 | 2-3/4" TUBING | N80 | NORMALIZE + TEMPER | 21 | .48 INCHES | 2 NO FAIL |
| 13 | 3-3/4" TUBING | C80 | QUENCH + TEMPER | 21 | .40 INCHES | 2 NO FAIL |
| 14 | 5-1/2" TUBING | C90 | BORE QUENCH + TEMPER | 20 | .42 INCHES | 2 NO FAIL |

* MINIMUM YIELD STRENGTH, KSI

** OUTSIDE ONLY WATER QUENCH UNLESS OTHERWISE NOTED.

TABLE 13

C-RING TESTS

TEMPER EMBRITTLEMENT

| STEEL | HEAT TREATMENT | HARDNESS | FAIL/NO FAIL |
|---|---|---|---|
| STEEL #5<br>N80 Q + T | AS RECEIVED. | RC23 | 2 FAILED |
| | 1200°F- 1 HR.<br>WATER QUENCH. | RC22 | 2 NO FAIL |
| STEEL #9<br>2-7/8" TUBING<br>N80 Q + T | AS RECEIVED. | RC25 | 2 NO FAIL |
| | STEP-COOLED,<br>1125°F TO 950°F<br>IN 25°-1/2 HR.<br>INCREMENTS. | RC25 | 2 FAIL |

TABLE 14

NACE STANDARD TENSILE TEST
FOR SULPHIDE ENVIRONMENTS
TM-01-77

| STEEL | HEAT TREATMENT | Y.S. AND RC | APPLIED STRESS (% Y.S.) | FAIL/NO FAIL |
|---|---|---|---|---|
| CA6NM | 1925°F-AIR | 531 MPA | 100% | FAIL |
| | DOUBLE TEMPER | 77 KSI | 90% | FAIL |
| | 1250°F-AIR | RC-21 | 85% | FAIL |
| | 1125°F-AIR | | 75% | NO FAIL |

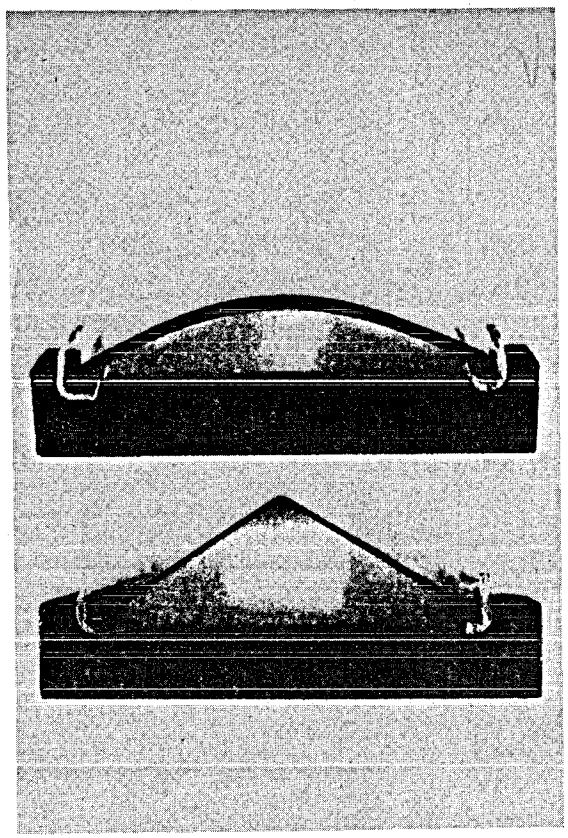

Fig. 1a: Bent Beam type specimen showing example of no-fail vs. fail.

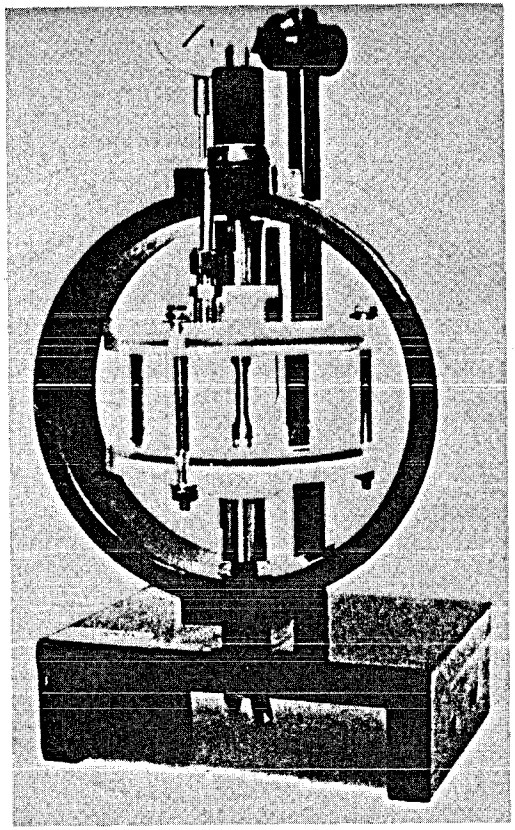

Fig. 1b: Test unit for standard NACE tensile test evaluation in sour environment.

Figure 2

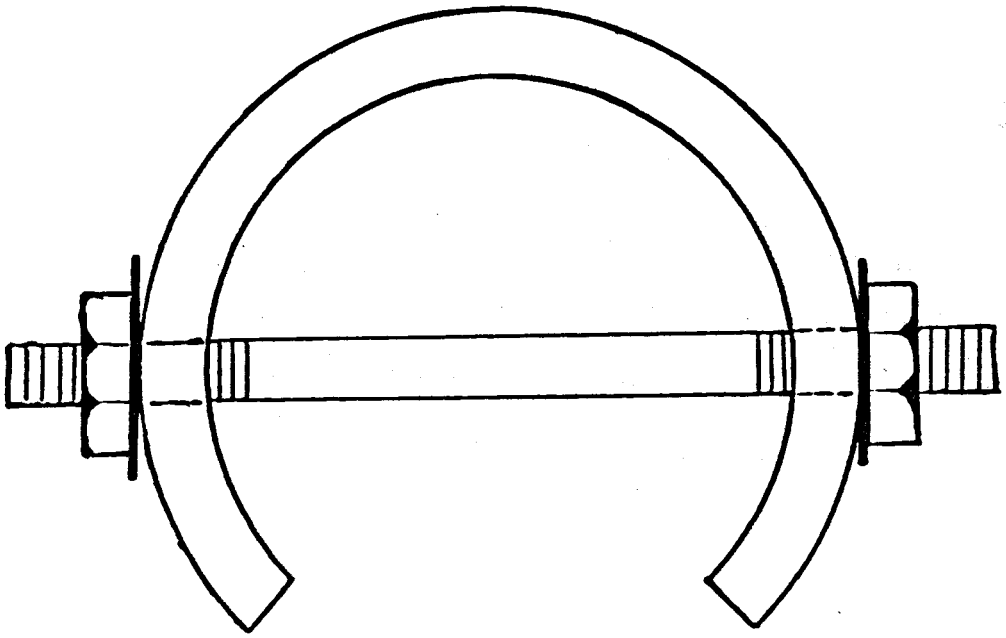

C-Ring Equation for Stress

$$\delta = 2000\,\sigma \left[\frac{\pi R r_2}{4E}\right] \left[\frac{12R^2}{6tR^2 + Rt^2 - r_2 t^2}\right]$$

where:

$\delta$ = diametrical deflection, inches
$E$ = young's modulus
$\sigma$ = stress, ksi
$t$ = ring thickness, inches
$OD$ = ring outer diameter, inches
$r_2 = OD/2$ ; $D = (OD - t)$ ; $R = D/2$

NATIONAL ASSOCIATION OF CORROSION ENGINEERS

# Test Method

# Testing of Metals for Resistance to Sulfide Stress Cracking at Ambient Temperatures



**Approved July, 1977**
**National Association of Corrosion Engineers**

The National Association of Corrosion Engineers issues this Standard in conformity to the best current technology regarding the specific subject. This Standard represents minimum requirements and should in no way be interpreted as a restriction on the use of better procedures or materials. Neither is this Standard intended to apply in any and all cases relating to the subject. Unpredictable circumstances may negate the usefulness of this Standard in specific instances.

The National Association of Corrosion Engineers assumes no responsibility for the interpretation or use of this Standard.

Nothing contained in this standard of the National Association of Corrosion Engineers is to be construed as granting any right, by implication or otherwise, for manufacture, sale, or use in connection with any method, apparatus, or product covered by Letters Patent, nor as indemnifying or protecting anyone against liability for infringement of Letters Patent.

## Foreword

Sulfide stress cracking (SSC) failures of metals exposed to hydrogen sulfide containing oil field environments have been recognized as a problem for almost 25 years. Both laboratory and field data have shown that concentrations of a few parts per million of hydrogen sulfide may be sufficient to lead to SSC failures. Laboratory and field experiences have allowed engineers to select materials having minimum susceptibility to SSC. Though the remainder of this Standard will be focused on SSC failures, other failure modes such as corrosion fatigue, general corrosion, etc., can be the cause of failure in sulfide environments.

During the last few years, the need for better understanding of the variables and better correlation of data have become apparent for several reasons. New design requirements call for higher strength alloys, which in general are more susceptible to SSC than the lower strength alloys. These design requirements resulted in extensive developmental programs to obtain more resistant alloys and/or heat treatments. At the same time, users in the petroleum industry are pushing present materials much closer to their physical limits. Attempts to use higher strength steels in other industries have occasionally resulted in SSC failures.

SSC failures are generally thought to result from hydrogen embrittlement. When hydrogen atoms are cathodically evolved on the surface of a metal (as by corrosion or cathodic charging), the presence of hydrogen sulfide (and a few other compounds containing cyanides, arsenic, etc.) tends to cause hydrogen atoms to enter the metal rather than form hydrogen molecules which do not enter the metal. In the metal, hydrogen atoms diffuse to regions of high triaxial tensile stress or some microstructural configurations where they become trapped and increase the brittleness of the metal. Though there are several kinds of hydrogen damage to metals, delayed brittle fracture of metals due to the combined action of corrosion in a sulfide environment and tensile stresses (which may be well below the yield stress) is the phenomenon that is known as sulfide stress cracking.

These and other considerations led NACE Unit Committee T-1F on Metallurgy of Oil Field Equipment to establish Task Group T-1F-9 (Metals Testing Techniques for Sulfide Corrosion Cracking) with the assignment to prepare a NACE Test Method Standard pertaining to testing of metals for resistance to sulfide stress cracking. Task Group T-1F-13 was established to verify that the T-1F-9 Test Method was reproducible between different laboratories. Originally, this Test Method contained a notched beam as well as the smooth tensile specimen. Task Group T-1F-13 recommended standardization of the tensile test but not the notched beam test. Further work is indicated with different types of beam and fracture mechanics specimens for possible inclusion at a later date. Task Group T-1F-17 has been established to accumulate data of interest to NACE conducted with the tensile test as described in this Standard.

This Test Method, issued by the NACE Group Committee on Corrosion Control in Petroleum Production (T-1), is directed toward testing of metals for resistance to cracking failure in aqueous environments containing hydrogen sulfide. It must be emphasized that the sole purpose of the Test Method is to facilitate conformity in testing so that data may be accumulated from different sources and compared on an equal basis. Evaluation of the data requires judgment on several difficult points which must remain a matter for the individual user or other specific groups and situations. It has been noted that stress corrosion testing is a difficult task. This Test Method is generally conceded to be a severe, accelerated test for SSC, making the evaluation of the data extremely difficult. In testing the reproducibility of this Test Method among different laboratories, several undesirable side effects, natural with any accelerated test, were noted:

1. The test environment may cause failure by hydrogen blistering as well as SSC. This is especially true for lower strength steels not usually subject to SSC. The presence of a blistering form of failure may be detected by metallographic observation.

2. The test environment may cause corrosion for some alloys which normally do not corrode in actual field service and thereby induce SSC failures in alloys which ordinarily do not fail by SSC. This problem is especially acute with stainless steels.

In summary, this Test Method is an accelerated test for SSC and may also produce failures by other modes. It should not be used as a single criterion for evaluating an alloy for use where hydrogen sulfide or other hydrogen charging situations occur. Attention should be paid to the other factors which may strongly influence SSC such as pH, temperature, $H_2S$ concentration, corrosion potential, stress level, manufacturing considerations, bimetallic effects, etc., as well as prior field experience and safety considerations when attempting to judge the suitability of a metal for use in a specific situation.

## Section 1: General

1.1 This Test Method is concerned with the ambient temperature testing of metals subjected to tensile stresses for resistance to cracking failure in low pH aqueous environments containing hydrogen sulfide.

1.2 This Test Method gives recommendations on the reagents to be used, describes the test specimens and equipment to be used, discusses base material and specimen properties, and gives the test procedures to be followed. Reporting of the test results is also discussed. The test procedure can be summarized as follows: Stressed specimens are immersed in acidified sodium chloride solution saturated with hydrogen sulfide at ambient pressure and temperature. Applied stresses at convenient increments of the yield strength can be used to obtain sulfide stress cracking data. Time-to-failure at a fixed stress is an important parameter for experimental correlation purposes. A 30 day test period is considered sufficient to reveal failures in materials susceptible to sulfide stress cracking. In borderline cases, longer test periods may be desirable.

1.3 Safety Precautions: *Hydrogen sulfide is an extremely toxic gas which must be handled with care.* See discussion in Appendix 1 for safety considerations and toxicity of this gas.

## Section 2: Reagents

2.1 Reagent Purity.

2.1.1 The gases, sodium chloride, acetic acid, and solvents shall be reagent or chemically pure (99.5% minimum purity) grade chemicals.

2.1.2 The water shall be distilled or deionized; tap water shall not be used (Appendix 2).

2.2 Preparation of Solution

2.2.1 Fifty grams of sodium chloride and 5 grams of glacial acetic acid (4.8 ml) are dissolved in 945 grams of water. The initial pH should be approximately 3. During the test, the pH may increase but not exceed 4.5

## Section 3: Test Specimens

3.1 The selection of the test specimens that can be used is often restricted by the size and shape of the material available for testing and by technical considerations or stress analysis, etc. The orientation of the specimen can affect the results and should be noted.

3.2 Tension Specimen (Figure 1)

3.2.1 The gage section of the tension specimen shall be 0.250 inch (6.4 mm) in diameter and 1 inch (25.4 mm) long (ASTM-A-370). A subsize specimen with gage of 0.100 inch (2.54 mm) in diameter by 1 inch (25.4 mm) long is acceptable.

3.2.2 The radius of curvature to the large diameter portion shall be at least 0.25 inch (0.64 cm) to minimize stress concentrations.

3.2.3 Ends of the specimen must be long enough to accommodate seals for the test container and to make connections to the stressing fixture.

3.2.4 Machining of the specimens must be done carefully to avoid overheating and cold working in the gage section. The final two passes should remove about 0.002 inch (0.05 mm) metal total.

3.2.5 The specimen is finished to a surface roughness of 32 microinch (0.81 $\mu$m) or better.

3.3 Cleaning of Specimens

3.3.1 The specimens should be degreased with tetrachloroethylene or a similar solvent, rinsed with acetone, and stored in a desiccator until ready for use.

3.3.2 Specimens must be handled only with clean tongs, polyethylene or cotton gloves after cleaning. Under no circumstances are the cleaned specimens to be handled with bare hands.

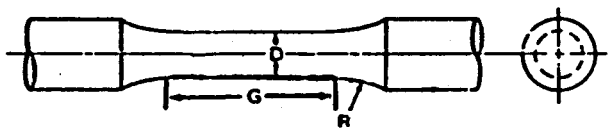


| Dimension | D | G | R (min) |
|---|---|---|---|
| Standard | 0.250 ± 0.005 inch (6.4 ± 0.13 mm) | 1.00 inch (25.4 mm) | 0.25 inch (6.4 mm) |
| Subsize | 0.100 ± 0.002 inch (2.54 ± .005 mm) | 1.00 inch (25.4 mm) | 0.25 inch (6.4 mm) |

**FIGURE 1 – Dimensions of the tension specimen.**

## Section 4: Test Equipment

4.1 Many types of stress jigs and test containers used for stress corrosion testing are acceptable for sulfide stress cracking testing. Consequently, the discussion in this section is intended to emphasize the required characteristics of the euipment to permit selection of suitable items and procedures.

4.2 Tension tests should be performed with constant load or sustained load devices.

4.3 Testing with constant or sustained load devices insures that susceptible materials will fail completely, eliminating the chance that a small crack will be overlooked in visual and microscopic examination of the test specimens.

4.4 Dead weight testers or hydraulic equipment, capable of maintaining constant pressure on a hydraulic cell, can be used for constant load testing.

4.5 Sustained load tests can be conducted with spring type devices and proving rings where relaxation in the fixtures or specimen will result in only a small percentage decrease in the applied load.

4.6 Because the test container will probably jacket the gage section of the specimen and possibly some of the thicker portion but not the stressing fixture itself, the specimen must be electrically isolated from any other metals in contact with the test solution.

4.6.1 The seals around the specimen must be electrically insulating and air tight but allow movement of the specimen with negligible friction.

4.6.2 In cases where it is feasible to immerse the complete test fixture in the test solution, the specimen must be electrically isolated from the stressing fixture, with the fixture made of a material that is not susceptible to SSC. A susceptible fixture must be coated completely with a nonconducting impermeable coating.

4.7 Test Vessels

4.7.1 The size, shape, and entry ports of the test vessel will be determined by the actual test fixtures used to stress the specimens.

4.7.2 Vessels shall be capable of being purged to remove oxygen before the test is begun and also capable of keeping air out during the test. The use of a small outlet trap on the hydrogen sulfide effluent line to maintain 1 inch (2.54 cm) of water back pressure on the test vessel will prevent oxygen entry through small leaks or by diffusion up the vent line (Appendix 2, Reasons for Exclusion of Oxygen).

4.7.3 The test vessel shall be of a size that the solution volume can be maintained between 20 and 100 ml per square centimeter of specimen to standardize the drift of pH with time due to the consumption of the acetic acid.

4.7.4 The fixture, cell, etc., shall be essentially inert.

4.8 Temperature Control

4.8.1 The test solution shall be maintained at 75 ± 5 F (24 ± 2.8 C).

## Section 5: Material Properties

5.1 Tensile testing shall be used for determining base material properties. Two or more specimens shall be pulled and averaged to determine the yield and ultimate strengths, percent elongation, and reduction of area for the material. It is desirable to machine a standard tension test specimen and the tension type stress corrosion test specimen from adjacent lengths of the item to be tested so that any minor variations in properties which normally occur from bar to bar can be minimized.

5.2 Some uncertainty still exists as to the fundamental material properties which correlate to the susceptibility to

TABLE 1 – Suggested Data Reporting Forms for SSC Testing
(Artificial Data for Example Purposes Only)

Table A – Alloy Data

| Alloy | Chemical Composition C | Mn | S | P | Mo | Cr | Ni | Si | Heat Treatment | YS | TS | HRC |
|---|---|---|---|---|---|---|---|---|---|---|---|---|
| N-80-A | 0.46 | 1.00 | 0.036 | 0.020 | 0.020 | – | – | – | Q,T 1200 F (649 C) | 120 | 130 | 27 |
| N-80-B | | | Same | | | | | | Q,T 1000 F (538 C) | 134 | 147 | 32 |
| N-80-C | 0.42 | 1.13 | 0.028 | 0.020 | 0.018 | – | – | – | N 1600 F (871 C), T 800 F (427 C) | 94 | 122 | 24 |
| 4340-A | 0.43 | 0.77 | 0.01 | 0.020 | 0.26 | 0.81 | 1.21 | – | Q,T 1200 F (649 C) | 116 | 127 | 27 |
| 9Cr-A | 0.15 | 0.83 | 0.01 | 0.016 | 0.96 | 8.1 | – | – | N 1700 F (927 C), T 1000 F (538 C) | 120 | 152 | 36 |

Note: Q = Quenched, T = Tempered, YS = Yield Strength, and TS = Tensile Strength.

Table B – Test Results

| Alloy | YS | Time-to-Failure, Hours Applied Stress, 100 psi (6.89 MPa) 40 | 60 | 75 | 80 | 85 | 90 | 95 | 100 | 120 |
|---|---|---|---|---|---|---|---|---|---|---|
| N-80-A | 120 | NF | NF | NF | 200 | 72 | – | – | 15 | 3 |
| N-80-B | 134 | 13 | 1.9 | – | 0.7 | – | – | – | 0.4 | 0.3 |
| N-80-C | 94 | NF | NF | – | NF | – | NF | NF | 62 | 15 |
| 4340-A | 116 | NF | NF | NF | F | – | – | – | F | F |
| 9Cr-A | 120 | NF | – | – | F | – | – | – | F | F |

Note: NF = No Failure, F = Failure During Test (32 days), and – = No Test.

SSC. Consequently, all pertinent data on chemical composition, mechanical properties, heat treatment, and mechanical (such as percent cold reduction or prestrain) histories shall be determined and reported (Table 1) in addition to the tensile test data. It is emphasized that each different heat treatment, microstructure, etc., of a metal of fixed chemical composition shall be tested as though it were a different metal.

5.3 Before testing, hardness measurements shall be taken on the thick portion of each specimen.

## Section 6: Test Procedures

6.1 Specimen Loading and Test Initiation

6.1.1 A variety of fixtures can be used to stress the specimens if the fixtures have the following important features:

6.1.1.1 Electrical isolation of the specimen from the fixture.

6.1.1.2 Ease of making precision load measurements.

6.1.1.3 Stable load behavior.

6.1.1.4 Proper environmental control.

6.1.2 Testing Sequence

6.1.2.1 A clean specimen is placed in the test cell and the necessary seals made.

6.1.2.2 The stressing fixture is placed in the test container, and then the test cell is purged with inert gas.

6.1.2.3 After the cell is purged, the load is applied carefully not to exceed the desired level of loading.

6.1.2.4 The test cell is filled immediately with deaerated solution and then saturated with hydrogen sulfide at a moderate flow rate (100 to 200 ml per minute) for 10 to 15 minutes.

6.1.2.5 It is necessary to maintain a continuous flow of hydrogen sulfide through the test container and outlet trap for the duration of the test at a low flow rate (a few bubbles per minute). This maintains the hydrogen sulfide concentration and a slight positive pressure to prevent air from entering the test container through small leaks.

6.1.2.6 With some highly alloyed corrosion resistant materials, it may be necessary to follow an alternate loading sequence such as 6.1.2.1, 6.1.2.4, 6.1.2.3 to prevent reformation of a protective film (if used, this alternate sequence shall be reported).

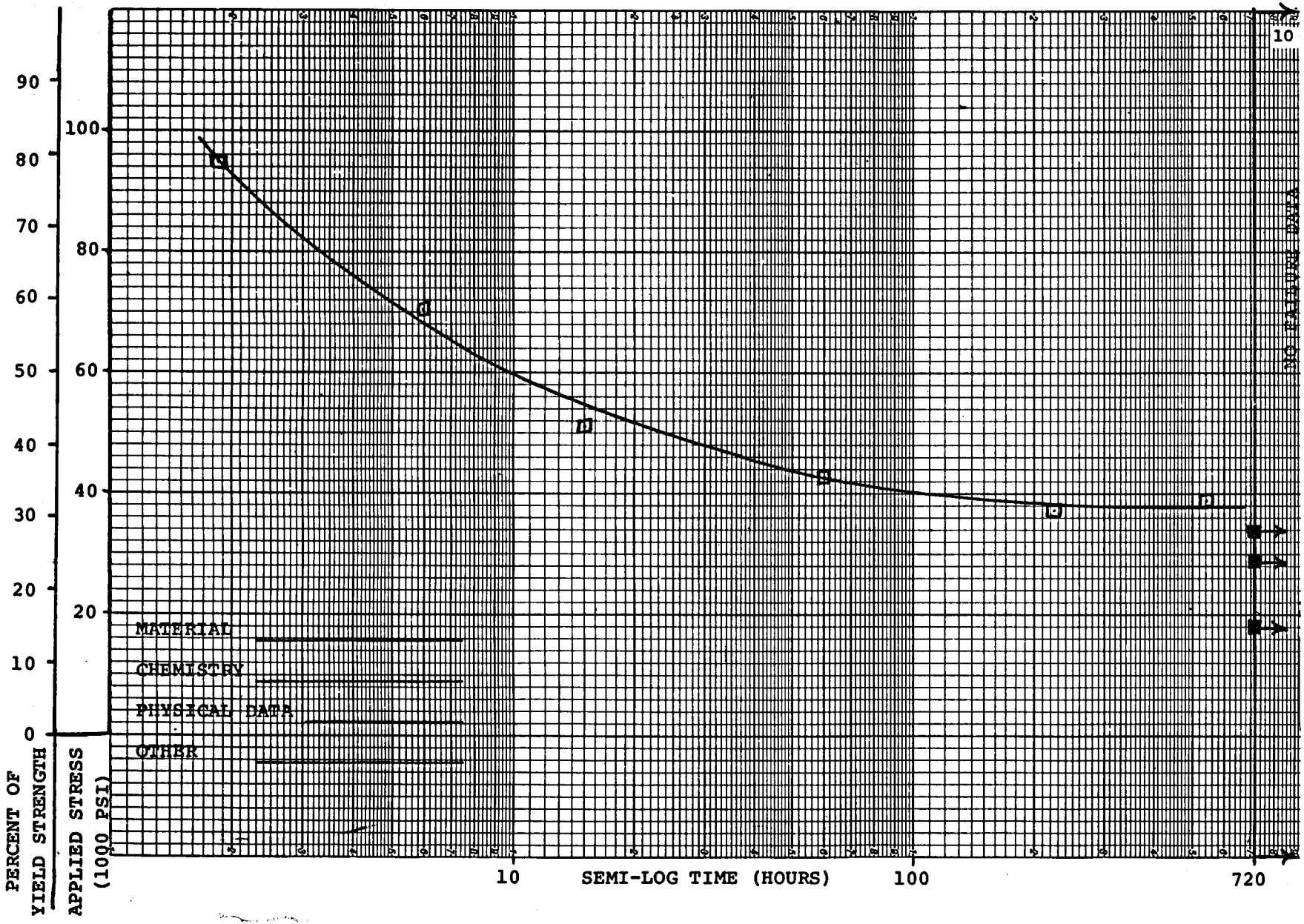


FIGURE 2 — Presentation of data by semilog graph.

6.2 Failure Detection

6.2.1 Time-to-failure shall be recorded using electrical timers and microswitches.

6.2.2 Tension specimens may be stressed at convenient increments of the yield strength.

6.2.3 Additional specimens shall be tested to closely define the fail/no fail stress.

## Section 7: Reporting of Test Results

7.1 Time-to-failure and no failure data are reported for each stress level.

7.2 Table 1 shows a suggested format for reporting the data. Presentation of the data may also be shown on semilog graph paper (Figure 2).

7.3 All chemical compositions, heat treatment, physical property, and other data taken shall be reported.

## Appendix 1

## Safety Considerations in Handling Hydrogen Sulfide

### Toxicity

Hydrogen sulfide is perhaps responsible for more industrial poisoning accidents than any other single chemical. A number of these accidents have been fatal. Hydrogen sulfide shall be handled with caution and any experiments using it planned carefully. The maximum allowable OSHA[1] concentration in the air for an 8 hour work day is 20 parts per million (ppm), well above the level detectable by smell. However, the olfactory nerves can become deadened to the odor after exposure of 2 to 15 minutes, dependent on concentration, so that odor is not a completely reliable alarm system.

Briefly, the following are some of the human physiological reactions to various concentrations of hydrogen sulfide. Exposure to concentrations in the range of 150 to 200 ppm for prolonged periods may cause edema of the lungs. Nausea, stomach distress, belching, coughing, headache, dizziness, and blistering are signs and symptoms of poisoning in this range of concentration. Pulmonary complications, such as pneumonia, are strong possibilities from such subacute exposure. At 500 ppm, unconsciousness usually results within 30 minutes and results in acute toxic reactions. In the 700 to 1000 ppm range, unconsciousness may occur in less than 15 minutes and death occur within 30 minutes. At concentrations above 1000 ppm, a single lungfull may result in instantaneous unconsciousness, with death quickly following due to complete respiratory failure and cardiac arrest.

Additional information on the toxicity of hydrogen sulfide can be obtained from the *Chemical Safety Data Sheet SD-36*, adopted January, 1950, available from the Manufacturing Chemists Association, 1825 Connecticut Ave., N. W., Washington, D. C. 20009, and from *Dangerous Properties of Industrial Materials* by N. Irving Sax, published in 1968, by Reinhold Book Corp., New York, New York; American Conference of Governmental Industries Hygenists – 1969.

### Fire and Explosion Hazards

Hydrogen sulfide is a flammable gas, yielding poisonous sulfur dioxide as a combustion product. In addition, its explosive limits range from 4 to 46% in air. Appropriate precautions should be taken to prevent these hazards from developing.

### Experimental Suggestions

All tests should be performed in a hood with adequate ventilation to exhaust all the $H_2S$. The $H_2S$ flow rates should be kept low to minimize the quantity exhausted. A 10% caustic absorbent solution for effluent gas can be used to further minimize the quantity of $H_2S$ gas exhausted. This solution will need periodic replenishment. Provision should be made to prevent backflow of the caustic solution into the test vessel if the $H_2S$ flow is interrupted. Suitable safety equipment should be used when working with $H_2S$.

Particular attention should be given to the output pressure on the pressure regulators as the downstream pressure frequently will rise as corrosion product, debris, etc., and interfere with regulation at low flow rates. Gas cylinders should be securely fastened to prevent tipping and breakage of the cylinder head. Because hydrogen sulfide is in liquid form in the cylinders, the high pressure gage should be checked frequently, as relatively little time will elapse after the last liquid evaporates until the pressure drops from 250 psi (1.7 MPa) to atmospheric pressure. The cylinder should be replaced by the time it reaches 75 to 100 psi (0.5 to 0.7 MPa) because the regulator control may become erratic. Flow should not be allowed to stop without closing a valve or disconnecting the tubing at the test vessel because the solution will continue to absorb $H_2S$ and move upstream into the flowline, regulator, and even the cylinder. A check valve in the line should prevent the problem if the valve works properly. However, if such an accident occurs, the

remaining hydrogen sulfide should be vented as rapidly and safely as possible and the manufacturer notified so that the cylinder can receive special attention.

## Reference

1. OSHA Rules and Regulations (Federal Register, Vol. 37, No. 202, Part II, dated October 18, 1972).

# Appendix 2

## Explanatory Notes on Test Method

### Reasons for Reagent Purity (Section 2)

Water impurities of major concern are alkaline or acid buffering constituents which would alter the pH of the test solution and organic and inorganic compounds which could change the nature of the corrosion reaction. Oxidizing agents could also convert part of the hydrogen sulfide to soluble products such as polysulfides and polythionic acids, which may also affect the corrosion process.

Alkaline materials (magnesium carbonate, sodium silica aluminate, etc.) are often added to (or not removed from) commercial grades of sodium chloride to assure free flowing characteristics and can greatly affect the pH.

Trace oxygen impurities in the purge gas would be much more critical if the nitrogen (or other inert gas) were to be continuously mixed with the hydrogen sulfide in order to obtain a lower partial pressure of hydrogen sulfide in the gas and hence a lower hydrogen sulfide concentration in solution. Oxidation products could accumulate resulting in changes in corrosion rate and/or hydrogen entry rate (Appendix 2, Reasons for Exclusion of Oxygen).

### Preparation of Tensile Specimen (Section 3)

It should be emphasized that all machining operations should be performed carefully and slowly so that overheating, excessive gouging, and cold work, etc., do not alter critical physical properties of the material. Surface smoothness is critical in unnotched specimens.

### Reasons for Exclusion of Oxygen

Obtaining and maintaining an environment with minimum dissolved oxygen contamination is considered very important because of significant effects noted in field and laboratory studies.

1. Oxygen contamination in brines containing $H_2S$ can result in drastic increases in corrosion rates by as much as two orders of magnitude. Generally, the oxygen can also reduce hydrogen evolution and entry into the metal. Systematic studies of the parameters affecting these phenomena (as they apply to SSC) have not been reported in the literature.

2. Small amounts of oxygen or ammonium polysulfide are sometimes added to aqueous refinery streams in conjunction with careful pH control near 8 to minimize both corrosion and hydrogen blistering. The effectiveness is attributed to an alteration of the corrosion product.

In the absence of sufficient data to define and clarify the effects of these phenomena on SSC, it is thought that all reasonable precautions to exclude oxygen should be taken. The precautions cited in this Test Method will minimize the effects of oxygen with little increase in cost, difficulty, or complexity.

# EAST MESA GEOTHERMAL COMPONENT TEST FACILITY

by

K. L. Newman
WESTEC Services, Inc.
1520 State Street
San Diego, California 92101

The U.S. Department of Energy (DOE) in its program of promoting the more rapid commercialization of geothermal energy recognizes the need for the development of new technology to adapt new and old energy conversion systems to geothermal energy. DOE has established a facility to test new and old technologies in actual application with geothermal fluids in a laboratory atmosphere. The Geothermal Component Test Facility (GCTF) is the only one of its kind in the United States. Other test facilities have been designed for specialized applications of specific systems for specific "hot water" reservoirs, but none are openly available to geothermal investigators for experimentation on generally applicable technologies.

The operation and maintenance of the GCTF is funded by DOE. Fluids from three production wells are available for experimentation. Also available are: cooling water, instrument air, utility water and electricity at 110, 220 and 440 VAC. Physical area available to experimenters in on one of four adjacent 40 foot by 80 foot concrete test stations. Support facilities located on site include a machine, welding and electrical shop, an extensive tool crib and inventory of hardware, a complete chemical laboratory, and office space with desk and telephone. Personnel assigned to the Facility include personnel trained for the operation of the Facility, a staff chemist, and skilled craftsmen each extensively experienced in each of their respective fields. Technical

and scheduling responsibilities are handled by the speaker at WESTEC Services' corporate headquarters in San Diego, California. Applications for use of the Facility are made through the DOE San Francisco Operations Office in Oakland, California.

EAST MESA TEST SITE WELL DATA

| Well | Temp (°F) | Temp (°C) | Press. (psig) | Flow (gpm) | TDS mg/l |
|---|---|---|---|---|---|
| Mesa 5-1 | 315 | 157 | -- | -- | 2,390 |
| Mesa 6-1 | 331 | 166 | 95 | 90 | 26,000 |
| Mesa 6-2 | 338 | 170 | 140 | 85 | 5,000 |
| Mesa 8-1 | 306 | 152 | 100 | 45 | 1,600 |
| Mesa 31-1 | 309 | 154 | -- | -- | 2,900 |

NOTE: Mesa 5-1 is used as an injection well, and Mesa 31-1 is not presently in use. All data gathered in June, 1976, for 100 percent liquid flow (not pumped).

# MATERIALS FOR USE IN CORROSIVE GEOTHERMAL BRINE ENVIRONMENTS

by

F. X. McCawley, J. P. Carter,
and
S. D. Cramer
Avondale Metallurgy Research Center
U.S. Department of the Interior
Bureau of Mines
College Park, Maryland 20740

The U.S. Department of the Interior, Bureau of Mines, is conducting field and laboratory corrosion studies to determine the optimum materials of construction for use in geothermal resource recovery facilities. These studies support the Bureau's goal of minimizing requirements for mineral and metal commodities through conservation and substitution.

The Imperial Valley of California, where the field studies have been conducted, is one of the largest liquid-dominated geothermal resource areas in the United States. This known geothermal resource area (KGRA) comprises six distinct geothermal fields that contain brines that not only have the highest heat contents, but also high mineral concentrations. Although the Bureau is primarily interested in the recovery of minerals, development of both the mineral and energy resources will depend to a great extent on the solution of major problems stemming from a lack of technology in certain areas. This includes reservoir engineering, brine processing, and information on materials to withstand the severe corrosion and scaling phenomena that occur in these brines.

The Bureau's geothermal materials corrosion program is divided into four interrelated phases: (1) laboratory studies to determine the basic brine corrosion mechanisms and to aid

in the screening of materials for field studies,[1] (2) studies on gas solubilities in geothermal brines and their relationship to brine corrosion processes,[2] (3) field testing of selected materials in typical geothermal process environments,[3] and (4) an investigation of the geothermal brine chemistry to aid in evaluation of field corrosion tests. This paper will present some of the laboratory and field corrosion tests conducted in both low- and high-salinity brines. It will also discuss some of the equipment failures due to corrosion and scaling that occurred during laboratory and field tests.

Laboratory studies included weight-loss, crevice, and pitting corrosion, stress-corrosion cracking, linear-polarization measurements, and corrosion attack of welded materials. The laboratory work was conducted in autoclaves using high-salinity brines at a temperature of 232°C and a pressure of 450 psig. Materials were evaluated in both deaerated brines and in brines which contained $O_2$, $CH_4$, and $CO_2$ gases. Materials evaluated include 1020, 4130, COR-TEN[4] and Mariner steels; 316 L, 430, and E-Brite 26-1 stainless steels; commercially pure titanium, TiCode-12, Ti-0.2%Pd, Inconel 625, and Hastelloy C-276.

Field corrosion tests were conducted on brine from the East Mesa (low salinity) and Salton Sea (high salinity) Imperial Valley geothermal fields. The work was carried out in

---

[1]Carter, J. P. and S. D. Cramer. Corrosion Resistance of Some Commercially Available Metals and Alloys to Geothermal Brines. Transaction Electrochem. Soc. Corrosion Problems in Energy Conversion and Generation. October 1974, pp. 240-250.
[2]Cramer, S. C. The Solubility of Oxygen in Geothermal Brines. Transaction Electrochem. Soc., October 1974, pp. 251-262.
[3]Carter, J. P. and F. X. McCawley. In Situ Corrosion Tests in Salton Sea Geothermal Brine Environments. Jour. Metals, v. 30, No. 3, March 1978, pp. 11-15.
[4]References to specific trade names does not imply endorsement by the Bureau of Mines.

materials testing facilities (MTF), such as depicted in Figure 1, which were designed to simulate several of the process streams of a typical geothermal resource recovery plant. Materials studied include 1020 and 4130 steels; 316 L, E-Brite 26-1, alloys 6X and 29-4 stainless steels; Inconel 625 and Hastelloys S, G, and C-276; and Ti-1.5%Ni. The nickel-based alloys and stainless alloy 29-4 were found to be the most corrosion resistant and exhibited corrosion rates of less than 1 mil per year (mpy). Mild steel had the least resistance to corrosion and exhibited corrosion rates up to 70 mpy in the high-salinity brines. The high alloy steels had good resistance to general corrosion (1 to 5 mpy) but were extremely susceptible to localized corrosion such as pitting (Figure 2) and crevice corrosion. Type 316 L stainless steel exhibited intergranular corrosion (Figure 3) and developed transgranular microcracks and macrocracks on the surface (Figure 4). It was also susceptible to stress-corrosion cracking.

Field electrochemical studies using a linear polarization technique were conducted in the high-temperature, high-salinity brines of the Salton Sea KGRA. Corrosion rates obtained by this technique, when corrected for scale deposition, established the upper corrosion rate limit and were found to be in good agreement with the in situ weight-loss corrosion rates obtained in (1) input brine from the well, (2) brine after two stages of separation, and (3) steam after one stage of separation.

During corrosion tests both in the laboratory and at the Bureau's field test facility, several mechanical-corrosion failures of the test equipment occurred. Thermocouple wells (Figure 5) in the stainless steel autoclaves failed by stress-corrosion cracking in 4 to 6 days when exposed to brines con-

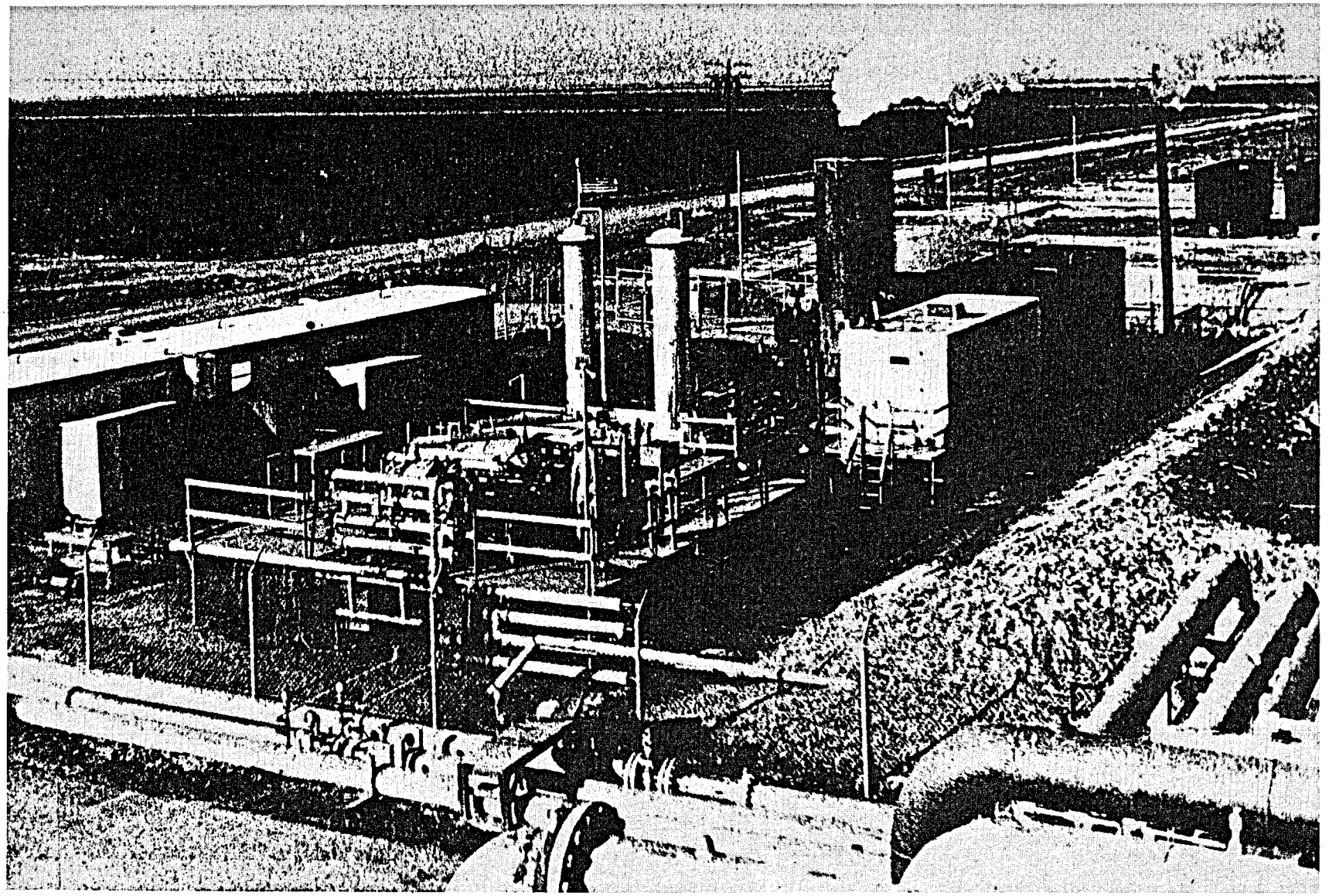

Figure 1. Bureau of Mines Geothermal Test Facility showing Materials Testing Facility in foreground, mobile chemistry laboratory, atmospheric flash tower, equipment van, and Baker holding tanks.

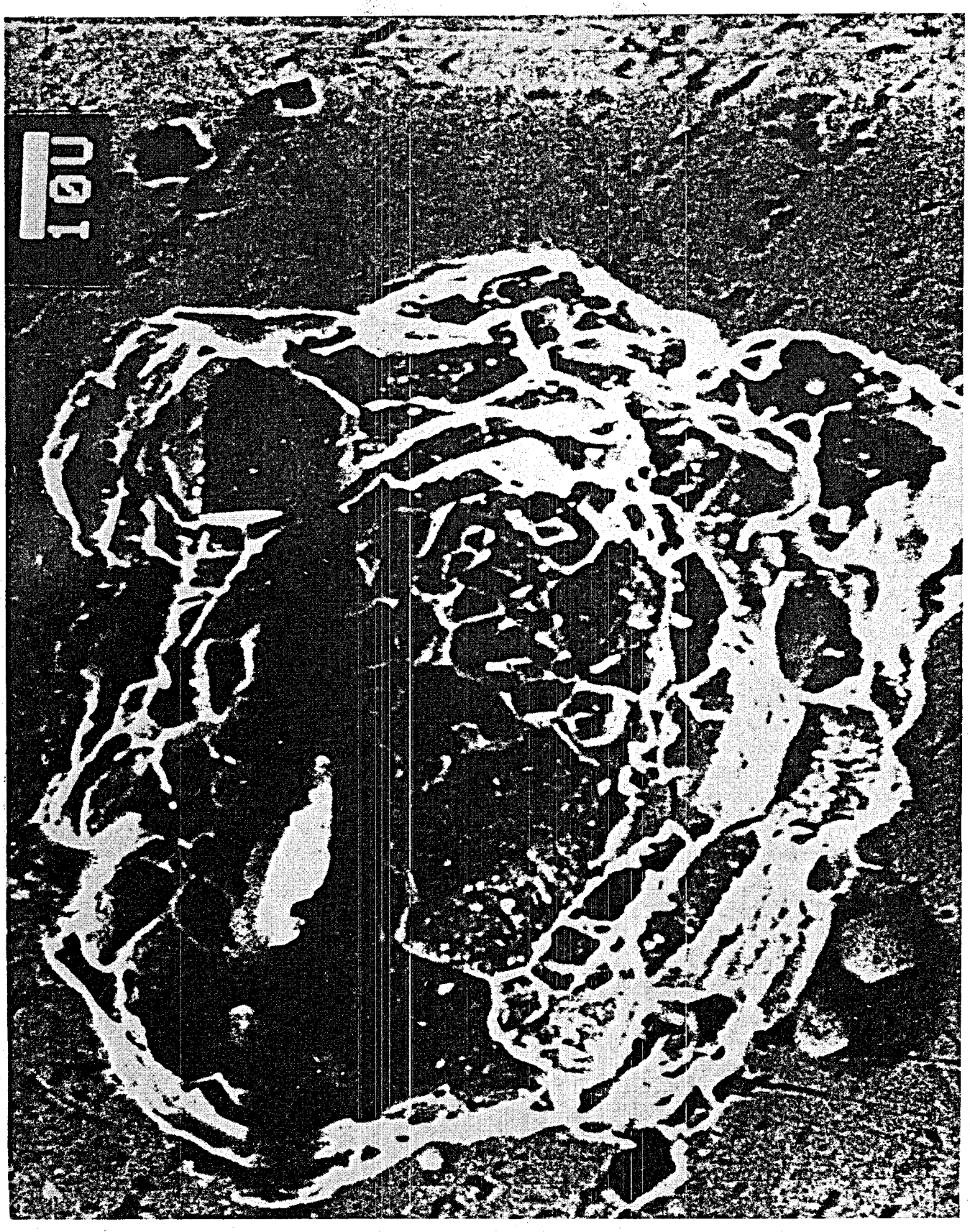


Figure 2. SEM photograph of pit formed on 430 stainless steel.

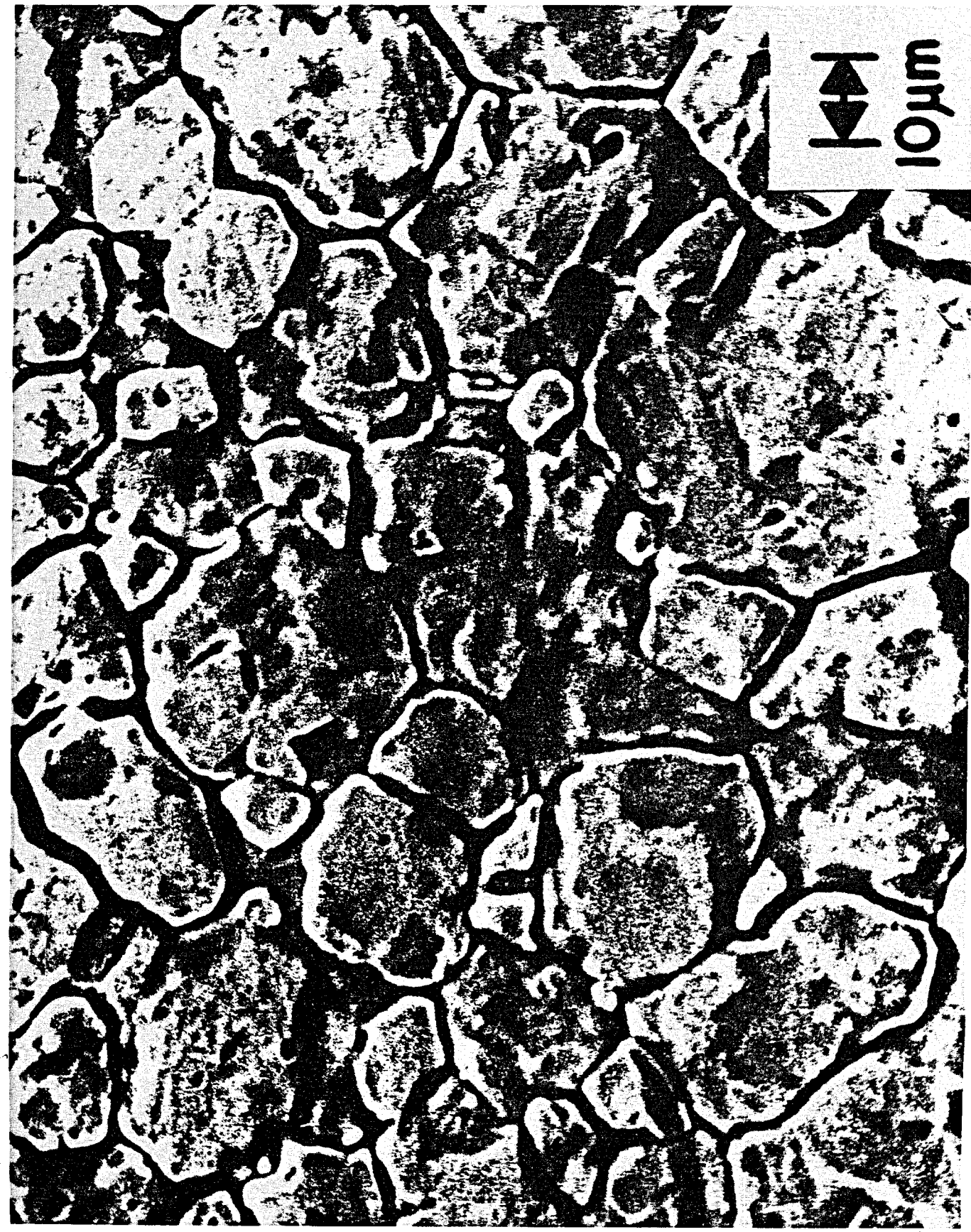


Figure 3. SEM photograph of 316 L stainless steel showing intergranular corrosion.

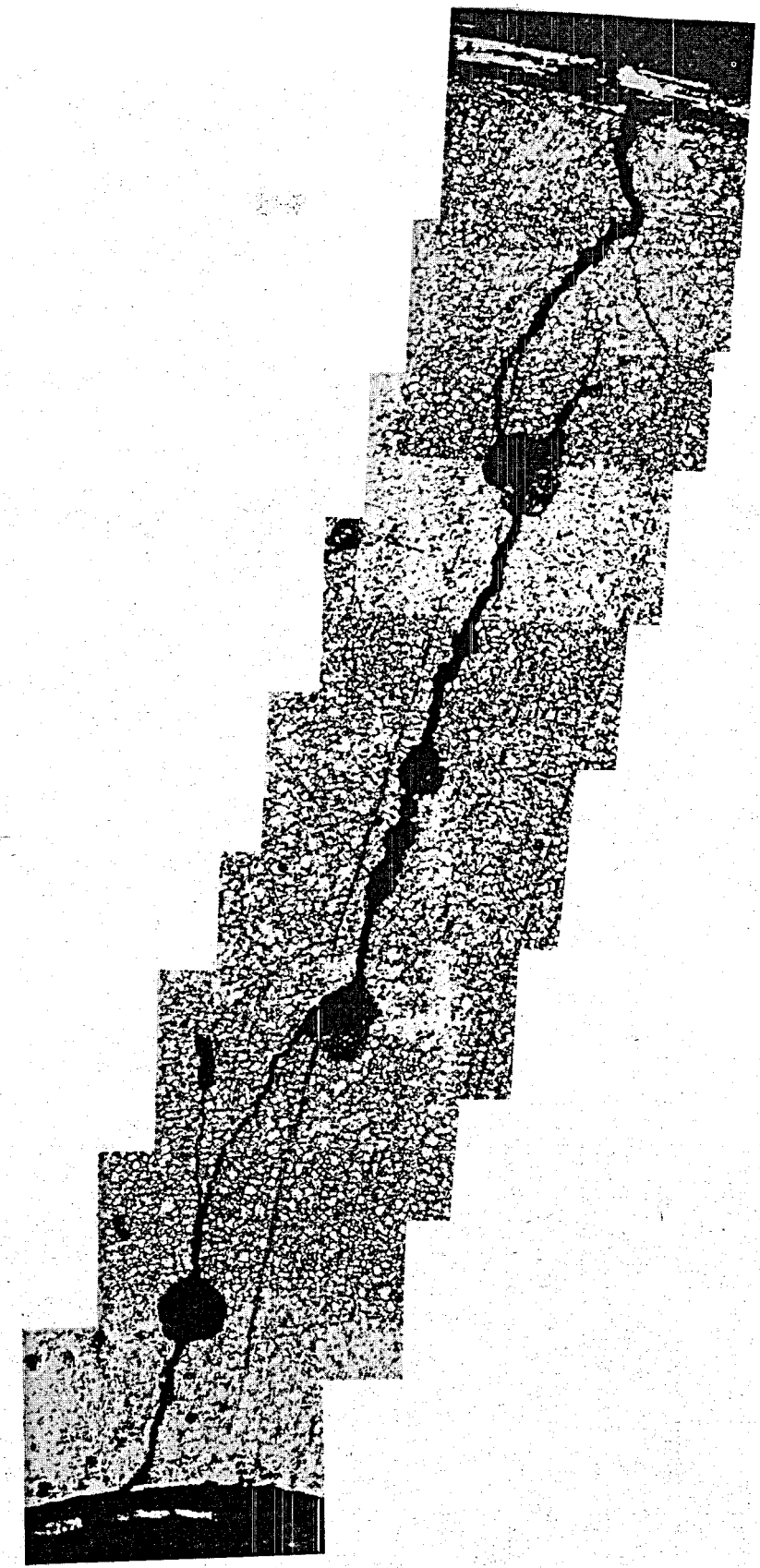

Figure 4. Composite photograph of 316 L stainless steel exposed for 30 days in brine after first stage separator, showing macrocrack through test sample from edge to mounting hole (original magnification X 50).

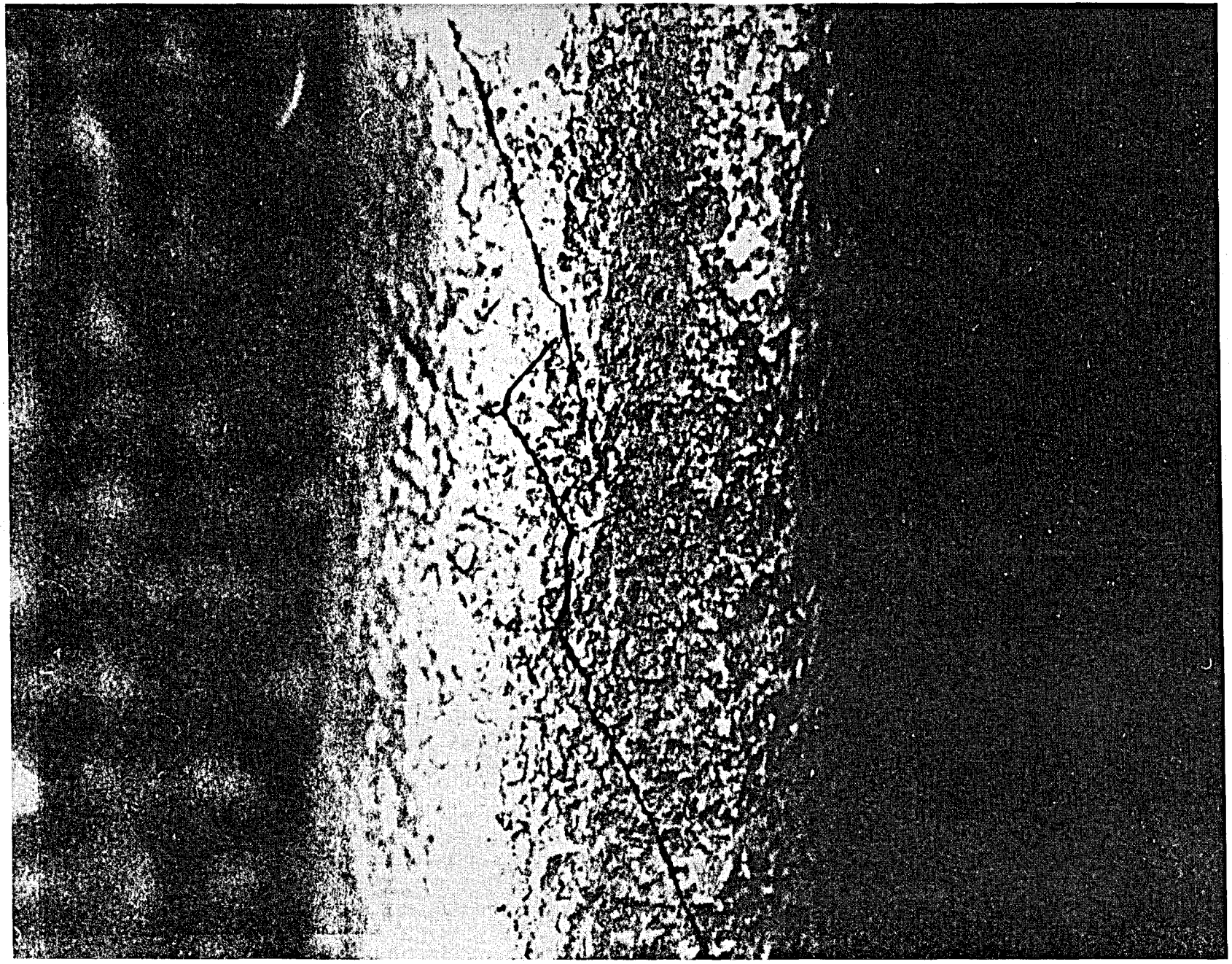

Figure 5. One-half-inch-diameter stainless steel thermocouple well after 5 days use in oxygenated geothermal brine at 232°C and 430 psig.

taining 100 ppm $O_2$. In the field, weld joints and pipe elbows failed due to corrosion fatigue, general corrosion, or other erosion/corrosion processes. Figures 6a and 6b show a 3-inch elbow that failed after only 2 weeks of operation. Failure was caused by brine flashing to steam in a control valve about 10 inches upstream.

Results obtained to date have shown (1) the necessity for a strong emphasis on in situ field corrosion studies, and (2) that selection of construction materials for each plant will have to be made on the demonstrated characteristics and evaluation of the particular geothermal reservoir from which the plant will operate.

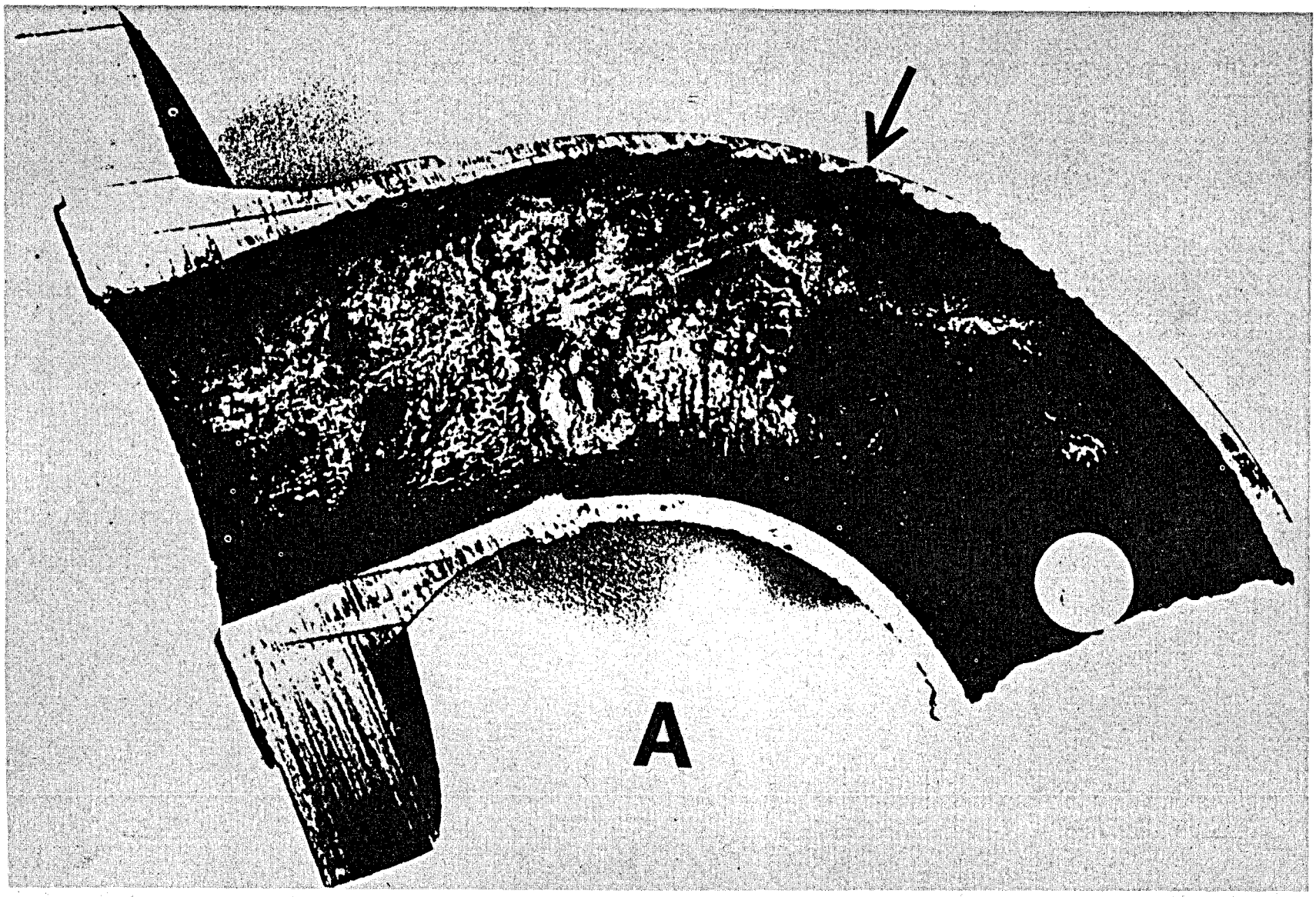


Figure 6A. Schedule-40 3-inch steel pipe elbow that failed after 2 weeks of operation in the FTF. View of the entire elbow.

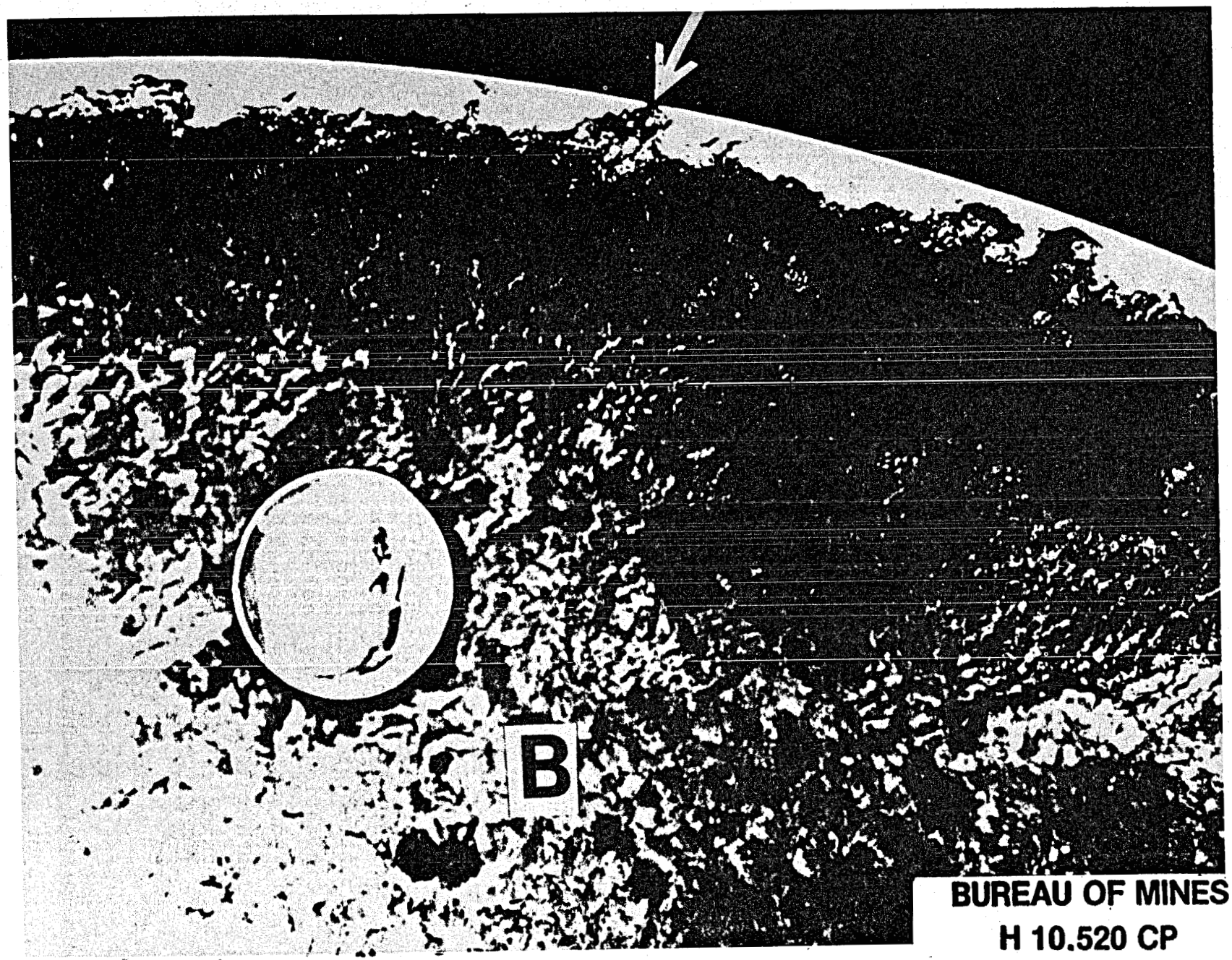


Figure 6B. Closeup view of the pit.

# IN-SITU PROTECTION OF METALS AGAINST CORROSION AND SCALING IN HOT BRINES

by

S. B. Brummer
EIC Corporation
55 Chapel Street
Newton, Massachusetts 02158

The timely development of geothermal energy as a national resource requires the resolution of a number of institutional and technical problems. Two of the most significant amongst the latter are metallic corrosion and scale formation.

Hot brines are widely acknowledged to be intensely corrosive media. One way of working with them will involve the use of specialty alloys which have adequate corrosion resistance. This is a costly approach and may involve relatively scarce alloying metals such as nickel or chromium. In addition, the low thermal grade of some geothermal resources precludes the high capital cost of a plant built with specialty materials.

A more intrinsic difficulty arises from scale formation when the energy is extracted from the brine. As the brine cools, it becomes supersaturated in solids, notably the salt content of the brine and such minor components as silica. Precipitation of these solids on the surface of heat exchangers is potentially disastrous for the efficient operation of a geothermal energy plant, as it grossly diminishes heat exchanger efficiency and raises capital cost.

A method to overcome both of these problems simultaneously is presented. It involves deposition of a thin (<1 mil) layer of polymer onto the surface of the metal. Ideally, such a layer should have the following properties:

- adhesive and adherent, without pinholes
- chemically, thermally, and mechanically resistant to the severe environment
- minimal effect on the thermal conductivity of the heat exchanger, i.e., < 5%
- can be deposited onto complex shapes, e.g., the inside of a heat exchanger tube
- can be repaired from time-to-time in situ.

A polymer whose formation from a dissolved monomer is electrochemically initiated onto the surface of the metal can fulfill these requirements.

Because of their mode of formation, such films are intrinsically pinhole-free and coherent. They are also readily deposited onto the surface of complex shapes and, because of their electrical resistance, they control the "throwing power" of the medium for their own formation. Consequently, a protective polymer layer can be progressively applied along an extended and complex surface. Essentially a wave of surface polymerization proceeds from the point nearest to the auxiliary negative electrode along the heat exchanger surface. Pinholes are automatically self-repairing. The layer can be repaired from time-to-time by repolymerization from a dilute monomer solution. Such repair is economical because polymerization takes place essentially only at uncovered areas of the metal substrate.

Clearly, such plastic films will protect the metal against the most serious corrosion potential of the brines. "Holidays" in the film can be inexpensively and efficiently protected cathodically, because of the small area exposed.

Preliminary experiments have been carried out with the polymer films formed from phenols and certain aromatic amines on copper, various steels and cupronickel. Several of these, for example the films formed on copper by polymerizing metaphenylenediamine (MPD) were found to be adherent and temperature resistant. Particular indexes of the films' integrity were the small (and decreasing-with-time) polymerization currents and their ability to retard calcium sulfate scaling.

An example of the current-time transient during polymerization of MPD on CU is shown in Figure 1. The Cu, held at 0.5V vs. the saturated calomel electrode (SCE), soon becomes covered with a layer of protective plastic. Within 2 min, the polymerization rate is $\sim 2\ \mu A/cm^2$, compared with an initial rate $\sim 50\ \mu A/cm^2$. The current falls subsequently and in the steady state is $\ll 1\ \mu A/cm^2$. This is indicative of a well-formed, pinhole-free layer.

Scaling was studied in two ways: In one case, a polymer-coated plate was heated to 277 °F and contacted with a solution of 187 °F.* In another, a polymer-coated tube separated two solutions at 199 and 266 °F. Brine was pumped through the tubes to simulate a heat exchanger flow of 4 ft/sec. Films were effective in both instances in retarding scale essentially completely. On stainless steel, both the 0.5- and 1-hour formed films were not visible. The 1-hour film was completely effective in inhibiting scaling. The 0.5-hour film was 98% effective. Thicker films were visible and colored. Invisible films on cupronickel (1-hour) completely suppressed scaling.

The layers thus formed were thermally and chemically very stable. They were stable at temperature for at least 60 hours

*$CaSO_4$ has an inverse solubility-temperature relationship.

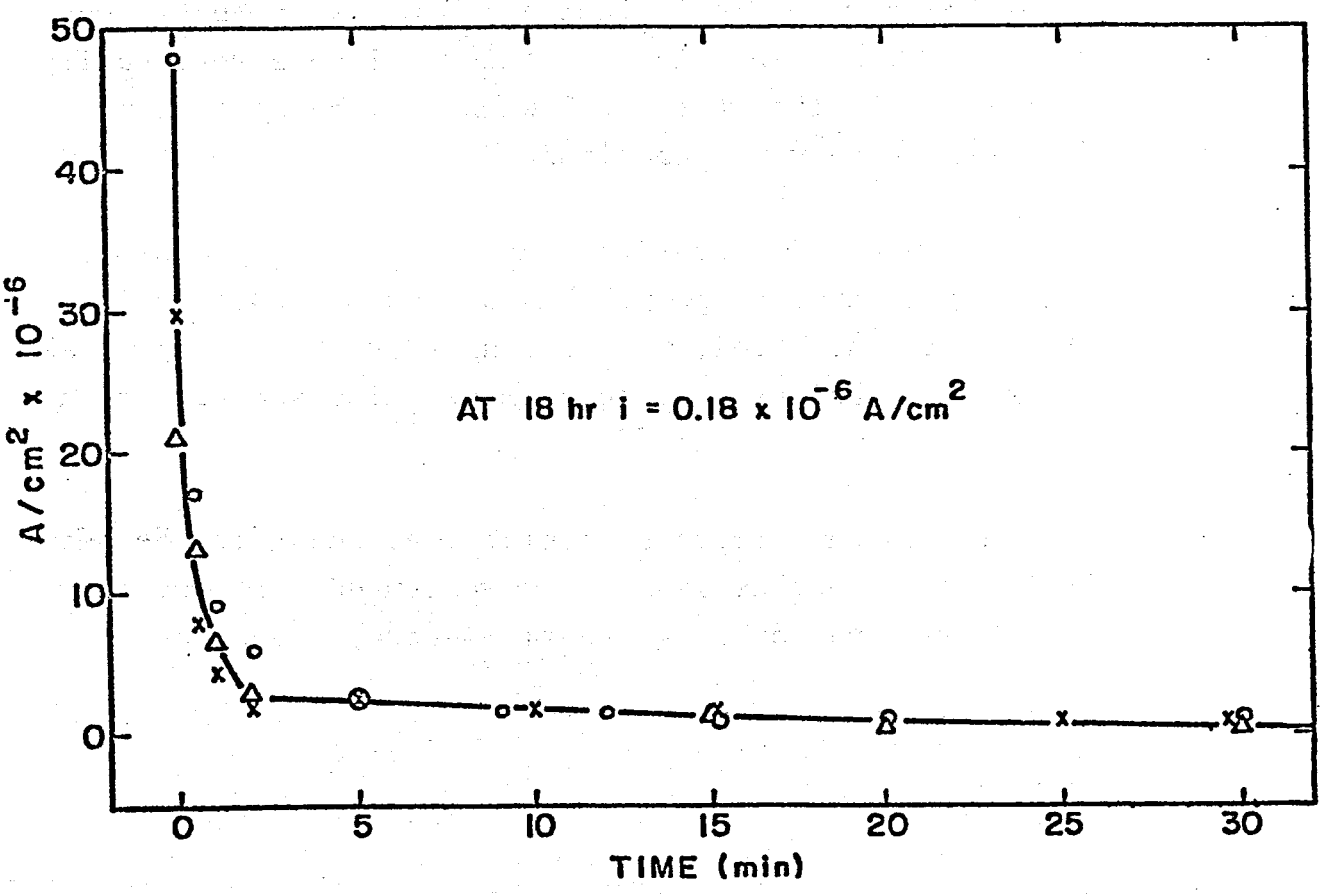


Fig. 1: Current-time characteristics during the formation of polymeric coatings by electropolymerization at 0.5 V (SCE) on copper at ambient temperature in $10^{-2}$M m-phenylenediamine solution of pH 10.2

without degradation (as judged by continued ability to retard scaling). They resisted aqua regia, ether, chloroform, hot (80°C) acetic acid and dimethylformamide. They could be removed by soaking for 20 min in fuming 85% $H_2SO_4$, probably due to their sulfonation. The visible, thicker layers were easily removed mechanically from the metal when wet, but the thin, invisible layers were very tenacious.

A relatively brief survey was carried out using ambient temperature application of phenol and o- and m-phenylenediamine on Pt, stainless steel, Cu, Ni and 70/30 cupronickel. All were satisfactory, but m-phenylenediamine films appeared to be the best.

The procedure thus appears feasible, at least in the short term. Longer term testing is clearly warranted. Methodology for practical application in geothermal energy loops must be developed.

BNL-24214

*GEOTHERMAL MATERIALS SYMPOSIUM, PROCEEDINGS, MAY 1978*

# POLYMER CONCRETE MATERIALS FOR USE IN GEOTHERMAL ENERGY PROCESSES

Lawrence E. Kukacka
Process Sciences Division
Department of Energy and Environment
Brookhaven National Laboratory
Upton, New York 11973

# POLYMER CONCRETE MATERIALS FOR USE IN GEOTHERMAL ENERGY PROCESSES*

by

Lawrence E. Kukacka

Department of Energy and Environment

Brookhaven National Laboratory

Upton, New York 11973

## SYNOPSIS

The feasibility of using polymer concretes as materials of construction in geothermal processes has been demonstrated and tests to determine the practicability are in progress. High temperature polymer concrete systems have been formulated and laboratory and field tests are being performed in brine, flashing brine, and steam at temperatures up to 500°F (260°C). Results are available from field exposures of up to 18 months in four geothermal environments. Good durability at temperatures > 392°F (200°C) is obtained with samples containing portland cement-silica sand aggregate. Based upon these results, potential applications for polymer concrete in geothermal processes have been identified and the effects of its use on the cost of electric power generation have been estimated. Reductions in the cost of power delivered to the distribution system of ∿ 10% were calculated. Redesign

of the plants for the optimum utilization of polymer concrete would be expected to result in greater savings.

KEY WORDS

acid, aggregate, applications, brine, cement, durability, economics, geothermal, initiators, high temperature, monomers, polymerization, polymers, polymer concrete, promoters

## INTRODUCTION

The availability of durable and economic materials of construction for handling hot brine and steam is a serious problem in the development of geothermal energy. To date, corrosion and scale incrustations have been encountered in all geothermal plants, and to various degrees, adversely affected plant life times and power outputs.[1]

As produced, geothermal brines are generally characterized by their high salt contents, low pH, dissolved carbon dioxide and hydrogen sulfide, and substantial amounts of calcium sulfate, calcium carbonate and silica. These materials, dissolved in water at elevated temperatures, render the brine quite corrosive to many materials of construction and to the deposition of solids when the temperature is lowered.

A review of the effect of geothermal brines on common materials of construction such as carbon steel, shows that the rate of corrosion is a function of pH and temperature. Corrosion is highest at pH values in the acid and highly alkaline regions, and minimal in the pH 5 to pH 12 region. At the predicted pH of 4.9 for oxygen-free brines of the type generally present in the Salton Sea area of California, and a temperature of 122°F (50°C), a service life of less than 15 years is estimated.[1] At a pH of 4, the estimated service life is 2 years.

General guidelines to materials selection for oxygen-free geothermal systems have been published by Shannon.[1] At a temperature of 248°F (120°C) and pH < 6, the use of expensive materials such as titanium, zirconium and Hastalloy C is suggested.

Concrete polymer materials are a series of composite materials which have strength and durability characteristics far superior to those of portland cement concrete. As a result, these materials are beginning to be utilized throughout the world in applications where portland cement cannot be used or where severe maintenance problems occur. Recent results from laboratory and field tests indicate that the composites may be applicable to many parts of geothermal processes.

The feasibility of using concrete polymer composites as materials of construction for handling hot brine and steam was demonstrated in 1972.[2] As part of this work the concrete liner on a vertical tube evaporator at the Office of Saline Water Desalting Facility in Freeport, Texas was partially impregnated to a depth of approximately 0.25 in. (6.3 mm). The results from these tests indicated that the materials had long-term stability in seawater at 350°F (177°C) and in acid solutions. Based upon these results, research to develop the materials for use in geothermal systems was started in 1974. To date, high temperature polymer concrete systems have been formulated, and laboratory and field tests performed in brine, flashing brine, and steam at temperatures up to 500°F (260°C). Results are available from laboratory and field exposures of up to 760 days. The results from these studies are summarized below.

## PRODUCTION METHODS

Polymer concrete (PC) consists of an aggregate mixed with a monomer which is subsequently polymerized in place. The techniques used for mixing and placement are similar to those used for portland cement concrete, and after curing a high strength durable material is produced. The most important process variables are monomer and aggregate composition and the aggregate particle size distribution. Specimens can be produced with compressive strengths of 30,000 psi (207 MPa). Full strength is attained immediately after the polymerization reaction is completed. Polymerization can be accomplished using polymerization initiators in conjunction with heat or at ambient temperature using initiators and promoters. Depending upon the concentrations of the promoter and initiator and the temperature, the cure time can be varied from a few minutes to 4 hr.

### Monomer Formulations

Several polymer systems that can be used in high temperature PC formulations have been developed and work to extend the operating temperature to higher limits is in progress.

Long-term test data are available for two monomer formulations, 60 wt% styrene-40 wt% trimethylolpropane trimethacrylate (TMPTMA) and 50 wt% styrene-33 wt% acrylonitrile-17 wt% TMPTMA. Both systems can be polymerized using chemical initiators and heat or by chemical initiators and promoters. The styrene-TMPTMA mixture appears suitable for temperatures up to 300°F (∿ 150°C) while the latter has given good results up to 460°F (238°C).[3]

Other monomer systems that have been or are currently being evaluated in the laboratory include styrene-triallyl cyanurate-polyphenylene oxide, isobornyl methacrylate-methyl methacrylate-ethylthioethyl methacrylate, styrene-acrylonitrile-acrylamide, and styrene-acrylonitrile-methacrylamide. Preliminary tests indicate that the latter two systems yield PC with the best high temperature and chemical resistance obtained to date. The development of these systems is currently being emphasized. Results to date[4] indicate that the use of a 12 wt% concentration of a 55 wt% styrene-35 wt% acrylonitrile-5 wt% acrylamide-5 wt% TMPTMA monomer mixture in conjunction with 88 wt% of a 70 wt% silica sand-30 wt% portland cement aggregate produces a composite with a compressive strength at 68°F (20°C) in the range 25,000 to 30,000 psi (170 to 270 MPa). The PC is thermally stable to ∿ 464°F (240°C).

Aggregate Selection

The durability of PC to geothermal fluids is highly dependent upon the composition of the aggregate. Materials such as quartz, silica, flyash, and portland cement have been investigated. All of the aggregates have been used successfully in materials at temperatures less than 425°F (218°C). Above this temperature, only PC materials containing an aggregate consisting of silica sand and portland cement have been durable to brine and steam. This is illustrated in Figure 1.

Experiments to determine the cause of the effect of portland cement on the durability are in progress. In these tests, Type III portland cement and each of its chemical constituents ($SiO_2$, $Al_2O_3$, $Fe_2O_3$, CaO, and MgO) are being combined with silica sand and vinyl-type

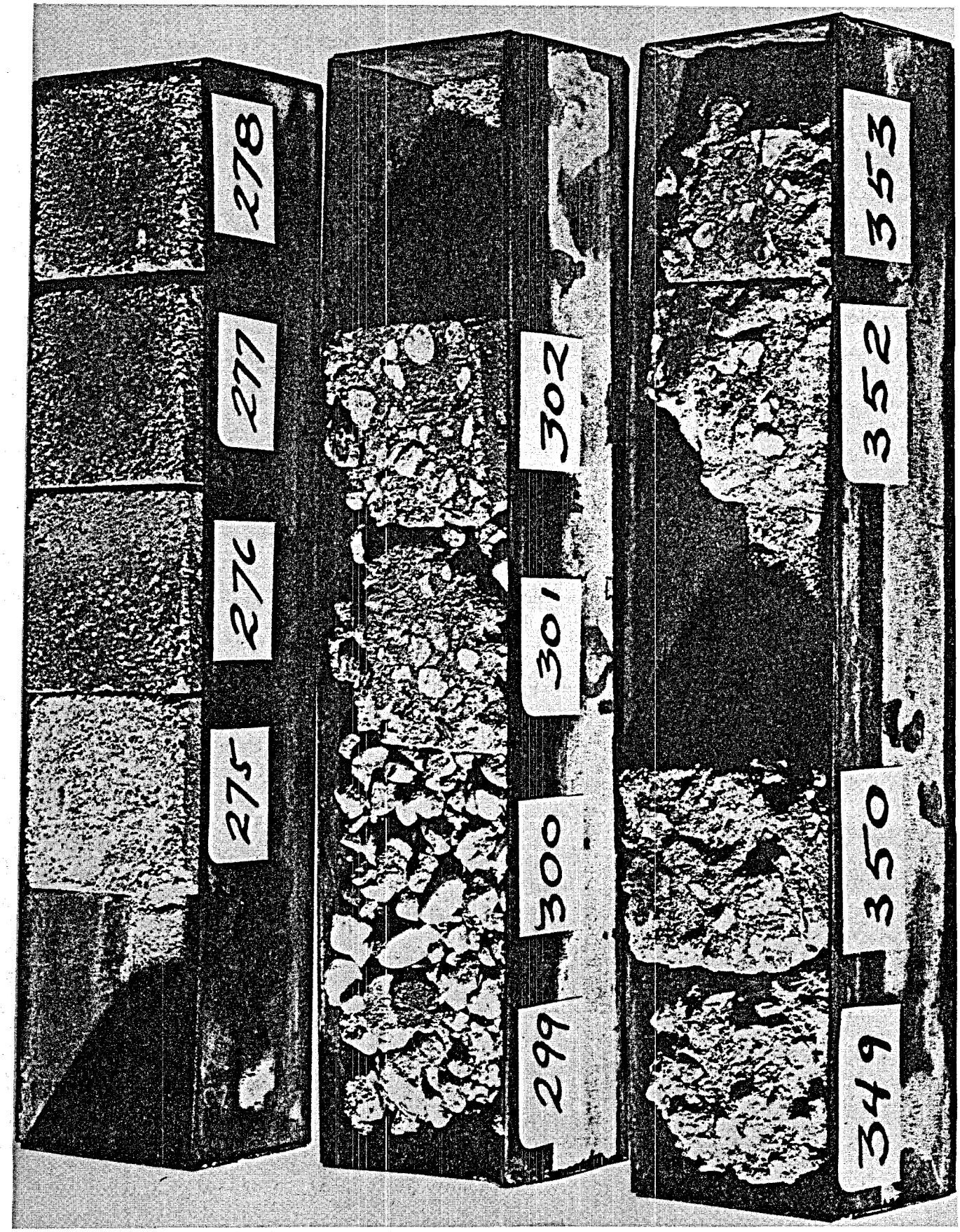


Figure 1

monomers such as methyl methacrylate, styrene and TMPTMA to form PC. Infra-red studies are performed on the samples before and after exposure to brine and air at 460°F (238°C) for 30 days.

The initial results from these tests indicate that the improved durability is due to chemical bonding between the CaO and the $-CH_2$ groups in the vinyl monomers. However, there is no evidence whether the reaction is caused by free CaO or the calcium ion.[5]

Studies to determine the optimum ratio of sand to cement in the aggregate used to produce PC for high temperature applications are also being performed.[4] The results from studies performed using a monomer system consisting of 55 wt% styrene-35 wt% acrylonitrile-5 wt% acrylamide-5 wt% TMPTMA indicated that increases in cement content from 10 to 30% resulted in increases in compressive strength from 20,000 to 25,000 psi (138 to 170 MPa). The water absorption remained essentially constant (< 0.6%) over this range. Further increases in cement content reduced the strength and increased the water absorption.

Similar trends have been noted with PC containing other monomer systems but to date optimizations have not been completed. Based upon partial results, aggregate compositions containing 65 to 80 wt% silica sand and 20 to 35 wt% cement appear to yield durable PC materials.

Mixing, Placement, and Curing

The monomers are mixed and the polymerization initiator is added and dissolved. If acrylamide or methacrylamide is to be included in the formulation, the mixture is heated to 122°F (50°C) prior to the addition of initiator (azobisisobutironitrile) to dissolve these

monomers which are solids. The formulation is mixed conventionally with the sand-cement aggregate and placed in forms which are coated with a release agent. Vibration is used to compact the PC. The specimens are then placed in an oven for curing. The curing cycle is determined by the monomer formulation being used. For example, curing of PC containing 60 wt% styrene-40 wt% TMPTMA with benzoyl peroxide initiator is performed by heating at ∿ 180°F (82°C) for 4 hr. Samples containing 55 wt% styrene-35 wt% acrylonitrile-5 wt% acrylamide-5 wt% TMPTMA and the initiator azobisiobutironitrile are first heated at 140°F (60°C) for 16 hr. The temperature is then raised to 185°F (85°C) for 2 hr. After cooling, the samples can be removed from the forms.

## PROPERTIES

### Laboratory Tests

Tests to measure the mechanical and chemical resistance properties of PC are being performed. The tests are conducted in autoclaves at conditions simulating geothermal environments. The test facility consists of ten autoclaves which were designed for continuous operation with brine or steam at 428°F (220°C) and two other vessels rated at 536°F (280°C).

Testing of two PC formulations, 60 wt% styrene-40 wt% TMPTMA and 50 wt% styrene-33 wt% acrylonitrile-17 wt% TMPTMA, in a 25% brine solution at 350°F (177°C) has been in progress for 760 days. The PC mixes which were selected prior to the performance of the aggregate optimization tests described above, consist of 12 wt% of the monomer mixture and 88 wt% of a 90 wt% silica sand-10 wt% portland cement aggregate. Polymerization was initiated using 2% benzoyl peroxide by weight of monomer and heating to 176°F (80°C).

The results of compressive strength measurements made on the specimens as a function of time are given in Table 1. As noted, both series exhibited initial reductions in strength, probably due to the decomposition of low molecular weight fractions of the polymer or an insufficient amount of portland cement in the aggregate. Strengths measured after 466 days were essentially the same as those measured after 63 days. Visual inspection after 760 days has indicated no cracking or other signs of deterioration.

Only short-term data (30 days) are available for specimens containing optimized sand-cement aggregate ratios. Specimens containing a 12 wt% concentration of 50 wt% styrene-37.5 wt% acrylonitrile-5 wt% acrylamide-7.5 wt% divinyl benzene in conjunction with a 70 wt% silica sand-30 wt% portland cement aggregate did not lose strength after exposure for 30 days to a 25% brine solution at 460°F (238°C). The compressive strength and water absorption of the samples were 29,900 psi (206 MPa) and 0.5%, respectively.

Sections of PC pipe representative of materials being field tested as potential materials for use in low temperature < 300°F (∿ 150°C) direct utilization processes are being evaluated. One section (shown in Figure 2) containing a 60 wt% styrene-40 wt% TMPTMA mixture and an aggregate containing 90 wt% silica sand-10 wt% portland cement has been exposed to a 400 ppm brine solution at 300°F (∿ 150°C) for 312 days. With the exception of slight discoloration, no evidence of deterioration is apparent. This test is being continued.

Tests are also being performed to determine the feasibility of using PC materials in high temperature-low pH environments. If the

Table 1

Compressive Strength of PC After Exposure

to 25% Brine at 350°F (177°C)

| Exposure time, days | PC No. 1 Compressive strength, psi (MPa) | PC No. 2 Compressive strength, psi (MPa) |
|---|---|---|
| 0 | 9600(66) | 10900(75) |
| 63 | 4450(31) | 7000(48) |
| 142 | 3900(27) | 6100(42) |
| 280 | 4352(30) | 7567(52) |
| 466 | 4355(30) | 7511 (52) |

PC No. 1, 60 wt% styrene-40 wt% TMPTMA.

PC No. 2, 50 wt% styrene-33 wt% acrylonitrile-17 wt% TMPTMA.

Aggregate, 90 wt% sand-10 wt% portland cement.

Specimen size, 0.75-in.-diam x 1.5-in.-long (19 x 38 mm).

Strengths measured at 68°F (20°C).

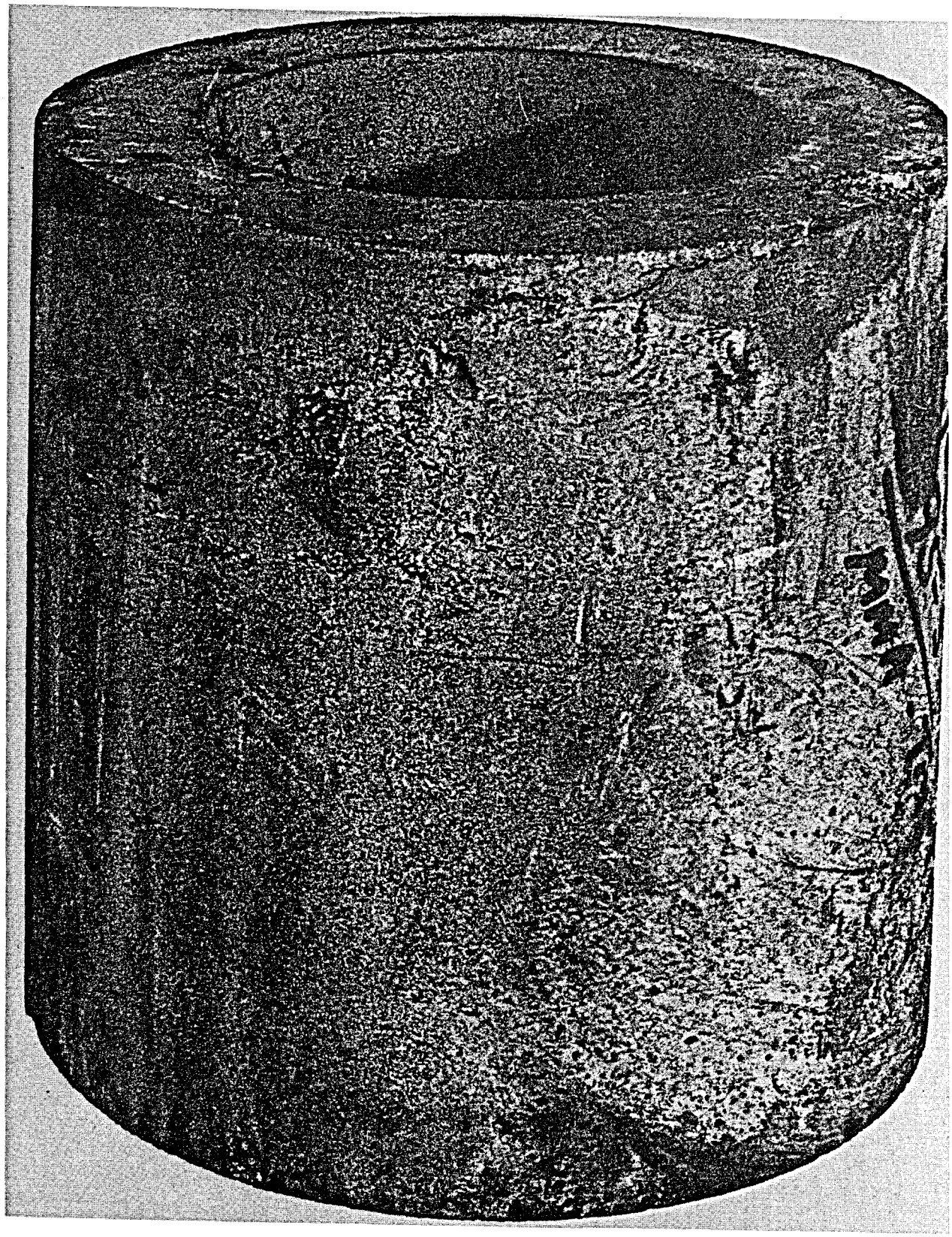

Figure 2

PC is durable, applications in acid injection systems possibly needed for scale control, may be feasible.

In one test, PC samples are being exposed to a pH 1 hydrochloric acid (HCl) solution at 194°F (90°C). After 440 days in test, no evidence of attack on the PC as determined by the pH and weight change measurements has been detected.

Tests in pH 1 HCl at 392°F (200°C) are also being performed. Monomer systems being evaluated include 60 wt% styrene-40 wt% TMPTMA, 55 wt% styrene-36 wt% acrylonitrile-9 wt% TMPTMA and 50 wt% styrene-33 wt% acrylonitrile-17 wt% TMPTMA. Two types of aggregate, limestone and mixtures containing 90 wt% silica sand-10 wt% portland cement, were used in conjunction with the monomer formulations. The samples containing limestone cracked after 24 days in test. Samples containing sand-cement are in good condition after 170 days. These samples are shown in Figure 3.

Field Tests

Due to the great difficulty in simulating geothermal environments in the laboratory and the "site-specific" nature of the fluids, field tests are being performed at several locations where geothermal development is in progress. The fluids being utilized in these tests vary from 90°F (32°C) water with a salt content of 800 ppm to the hypersaline (250,000 ppm) brines of the type present in the Salton Sea region of California at temperatures up to 500°F (260°C). Tests are also being performed in dry and flashing steam reservoirs. The tests are being performed with the cooperation of governmental agencies and private companies. In some cases due to the proprietary nature of the work,

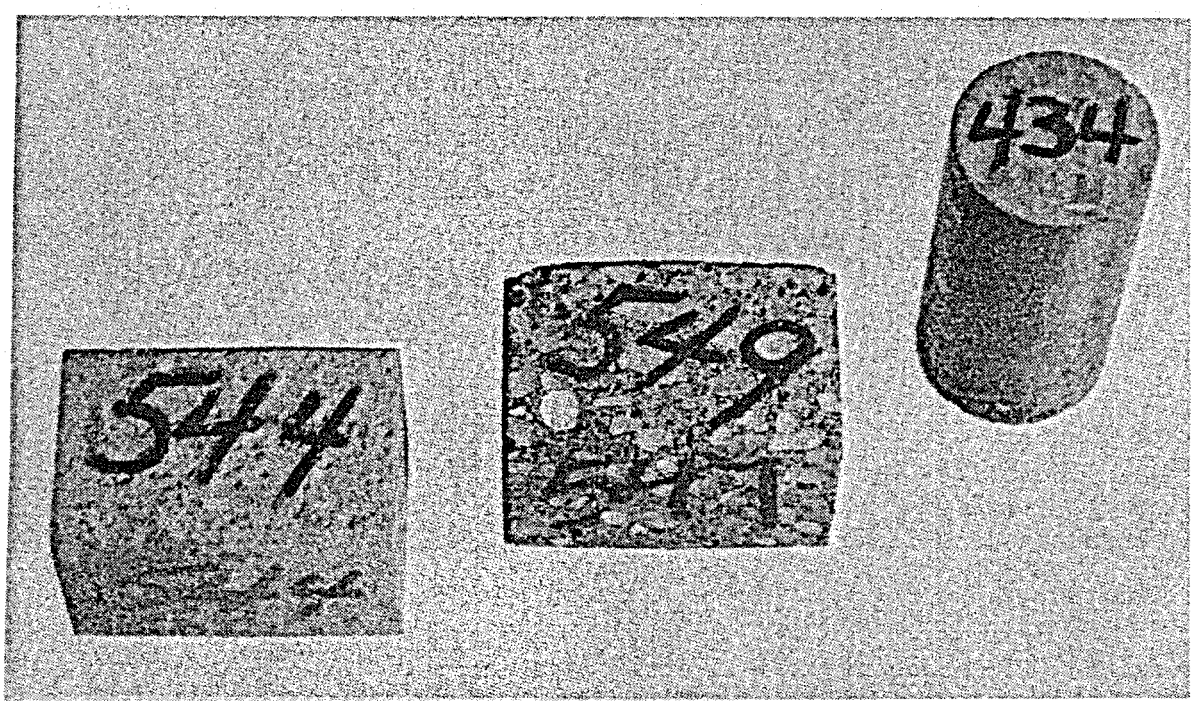


**Figure 3**

the characteristics of the geothermal fluids have not been fully revealed to BNL. The tests are on-going and in several cases only the results from visual inspections are available. Field test results obtained to date are summarized below.

Dry Steam

Two series of tests have been performed in which samples of PC were exposed in a well-head chamber to dry steam at a temperature of 460°F (238°C). A third series of samples is in test.

To date, data for a 50 wt% styrene-33 wt% acrylonitrile-17 wt% TMPTMA monomer formulation are available. The results from a preliminary 90 day test indicated that the samples maintained high strength and low permeability. Based upon these data, a two year exposure test was started. Aggregate composition was one of the variables in this test series.

Samples have been evaluated after exposure times up to 540 days. All samples containing an aggregate consisting of 90 wt% silica sand-10 wt% portland cement have shown reasonably good durability but strength reductions have been noted. Composites containing other aggregates such as silica sand or limestone failed. This is shown in Figure 1.

Samples polymerized using 1.5 wt% benzoyl peroxide were examined after 90 and 365 day exposures. Compared to a control strength of 8,000 psi (55 MPa) compressive strengths of 4,900 and 4,200 psi (34 and 29 MPa) were measured.

Samples polymerized using initiators and promoters were examined after exposure for 180 and 540 days. Compared to a control strength

of 12,000 psi (82 MPa), an average strength of 2,400 psi (16 MPa) was measured after 180 days. No further deterioration was noted by the strength of 2,600 psi (18 MPa) after 540 days. In both cases, the strengths leveled off at values greater than that needed (1000 psi) (7 MPa) for use as a geothermal well cementing material. It is believed that the strength reductions were due to decomposition of low molecular weight fractions of polymer. Increased cement content will also result in improved stability.

Samples containing mixtures of styrene-acrylonitrile-acrylamide-TMPTMA, styrene-polyphenylene oxide-TMPTMA, and styrene-triallyl cyanurate-polyphenylene oxide are currently in test but results are not yet available. Based upon laboratory tests, these systems are expected to yield further improvements.

Flashing Brine

Samples of PC have been exposed in a well-head chamber to flashing brine at a temperature of 320°F (160°C) for 180 days.

The test series consisted of two monomer mixtures, 60 wt% styrene-40 wt% TMPTMA and 50 wt% styrene-33 wt% acrylonitrile-17 wt% TMPTMA, mixed with an aggregate consisting of 90 wt% silica sand and 10 wt% portland cement. Three different polymerization methods were utilized.

The specimens were found to be in good conditions after the 180 day test. Two samples (No. 5 and No. 29 in Figure 4) which contained the 60 wt% styrene-40 wt% TMPTMA mixture polymerized using benzoyl peroxide as an initiator and dimethyl aniline as a promoter, were slightly cracked. All of the other materials were crack free.

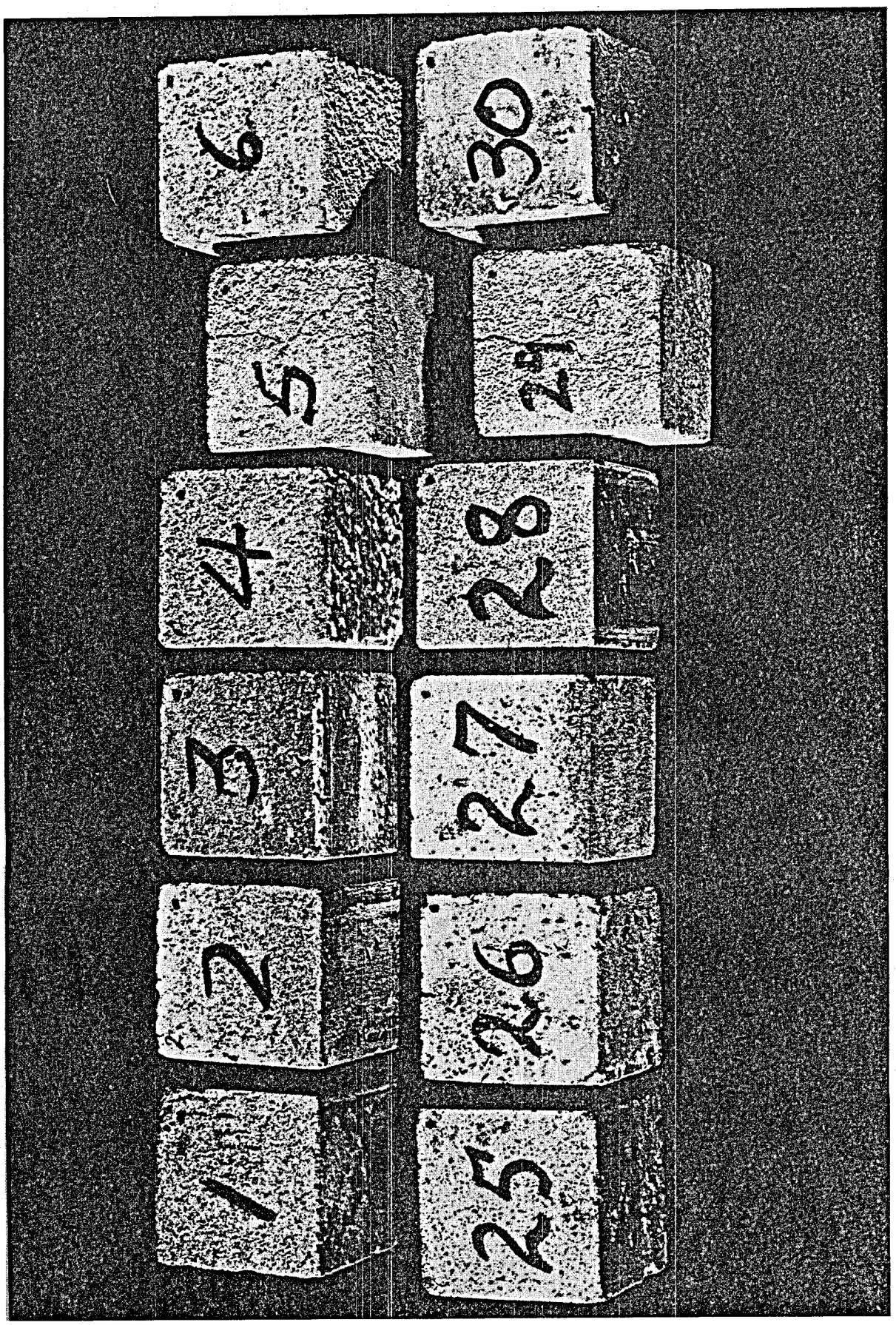


Figure 4

Tests performed on the samples included dimensional stability, weight change, water absorption, and compressive strength. Little if any changes in the dimensions and weight were detected. Compared to the controls, all of the samples containing styrene-TMPTMA had strengths which were essentially unaffected by the exposure. The samples containing styrene-acrylonitrile-TMPTMA polymerized by promoters and initiators were also unaffected. The other samples exhibited slight strength reductions and increases in absorption. These strengths were in the same order as those obtained after 180 day exposures in dry steam at 460°F (238°C).

Low Temperature-Low Salinity Fluids

PC samples containing 60 wt% styrene-40 wt% TMPTMA were exposed to low temperature geothermal fluids of the type currently being utilized in Klamath Falls, Oregon for space heating and process heat applications. Samples were placed in six wells with temperatures ranging between 90° and 210°F (32° and 99°C). The pH of the fluids was between 7.1 and 8.2 and the total solids content was ∿ 800 ppm. Evaluations were performed after exposures for 90, 180, and 360 days.

All of the specimens were found to be crack free. The results from compressive strength and water absorption tests indicated that both properties were independent of the exposure temperature. The absorptions remained constant throughout the test. Reductions in compressive strength ranging between 14 to 18% were noted for samples exposed for 180 days. Beyond that time, the strengths remained essentially constant.

High Temperature-High Salinity Brine

Tests have recently been initiated in the Imperial Valley of California. Most of the geothermal reservoirs in the USA that are suitable for electric power generation are located in this region. To date, small PC test specimens and sections of PC-lined pipe have been placed in test. Only limited data are available.

In one test, hollow PC cylinders were exposed to flowing brine containing 26,000 ppm salt at 320°F (160°C). PC formulations containing two monomer mixtures, 50 wt% styrene-33 wt% acrylonitrile-17 wt% TMPTMA, in conjunction with 4/1 and 1/1 ratios of sand and portland cement aggregate, were exposed to the fluid.

After 60 days in test, no apparent deterioration as determined by visual inspection was apparent. A small amount of scale which could be easily brushed off was found on the specimens. The results from crushing strength tests indicated no changes in strength due to the brine exposure.

An 8-ft (∿ 2.4 m) section of PC-lined 3-in. Sch 40 (∿ 7.6 cm) steel pipe is currently being exposed to the same brine. The PC liner is 0.5-in. (∿ 13 mm) thick and is composed of a 60 wt% styrene-40 wt% TMPTMA monomer mixture. The aggregate contains 70 wt% sand-30 wt% Type III portland cement.

Visual inspection of the unit was made after exposure for 70 days to 320°F (160°C) brine flowing at a rate of ∿ 70 gal/min (265 $dm^3$/min.). No deterioration or scale accumulation was apparent. Scale build-up on the connecting steel pipe was observed.

Tests are also in progress in brine containing ∿ 250,000 ppm salt at temperatures up to 500°F (260°C). Test cylinders and a section of PC-lined pipe are being exposed. These tests were started in January 1978 and results are not yet available.

## POTENTIAL APPLICATIONS

Based upon the test data obtained to date, several applications in geothermal processes appear feasible. These include the use of PC-lined components as replacements for stainless steel or other expensive metals in brine supply and condensate piping systems, reinjection lines and steam separators. Uses in cooling towers, power transmission towers, electrical insulators and to protect concrete surfaces also appear promising.

The potential economic impact of the use of PC materials in geothermal electric generation processes has been studied.[6] In this work, conceptual designs for 50 MWe power plants at Heber and Niland, California[7] were reviewed to determine the potential savings in capital and operating costs resulting from the use of PC in applicable portions of the plants. The results indicated that savings can be accrued in the capital cost of both plants. These savings result in reductions in the cost of electric power of 2.7 mills/KWH. Additionally, the use of PC should markedly reduce corrosion problems in the plants. It was estimated that on-stream availability will increase by 4% and that electric power cost will be reduced by an additional 3.4 mills/KWH. The total savings of 6.1 mills/KWH represents a reduction in the cost of power delivered to the distribution system of 9.7%.

## SUMMARY AND CONCLUSIONS

The feasibility of using PC as a material of construction in geothermal processes has been demonstrated.

PC formulations containing 60 wt% styrene-40 wt% TMPTMA and 50 wt% styrene-33 wt% acrylonitrile-17 wt% TMPTMA have exhibited good durability after long-term exposures to steam and hot brine. The former system appears suitable for use at temperatures up to 300°F (∿ 150°C) while the latter has given good results up to 462°F (240°C). Laboratory test results indicate that the addition of acrylamide or methacrylamide to styrene-acrylonitrile-TMPTMA mixtures results in further increases in the maximum operating temperature. Field testing of these systems is in progress but data are not yet available.

Aggregate selection is very important in the production of PC that is durable to geothermal environments. Only PC's containing silica sand-portland cement mixtures have exhibited durability at temperatures > 425°F (> 218°C). At lower temperatures, quartz, silica and flyash have given good results.

Laboratory tests have been performed in several synthetic geothermal brines which simulate compositions at field test locations. Tests in HCl solutions at temperatures up to 392°F (200°C) have also been performed. Good durability is indicated.

Field test programs are in progress at several sites. Small PC cylinders and cubes have generally been exposed but recently sections of PC-lined pipe were installed. In general good durability has been obtained and the results are in agreement with laboratory data.

Economic studies to identify potential applications for PC in geothermal processes are being made. Applications in condensate piping systems, acid handling systems, reinjection lines, cooling towers, district heating systems, and to protect concrete surfaces appear cost effective.

Studies to determine the potential economic impact of the use of PC in geothermal electric generating processes have been made. Reductions can be accrued in capital and operating costs. The total savings ($\sim$ 6.1 mills/KWH) represents a reduction in power cost of $\sim$ 10%. Further reductions would be expected if the plants were designed to optimize the utilization of PC.

## REFERENCES



1. Shannon, D. W., Economic Impact of Corrosion and Scaling Problems in Geothermal Energy Systems, Battelle Northwest Laboratories, BNWL-1866 UC-4, Jan. 1975.
2. DePuy, G. W. and Kukacka, L. E., Editors, Concrete Polymer Materials, Fifth Topical Report, Brookhaven National Laboratory, BNL 50390 and REC-ERC-73-12, Dec. 1973.
3. Kukacka, L. E. et al., Alternate Materials of Construction for Geothermal Applications, Progress Report No. 14, Brookhaven National Laboratory, BNL 50751, Sept. 1977.
4. Zeldin, A., Kukacka, L. E., and Carciello, N., Polymer Concrete Materials for Geothermal Applications, to be presented at American Institute of Chemical Engineers, Philadelphia, June 1978, in press.
5. Kukacka, L. E. et al., Cementing of Geothermal Wells, Progress Report No. 6, Brookhaven National Laboratory, BNL 50738, Sept. 1977.
6. Economic Assessment of Polymer Concrete Usage in Geothermal Power Plants, Burns and Roe Industrial Services Corporation, Brookhaven National Laboratory Report BNL 50777, November 1977.
7. Conceptual Design of Commercial 50 MWe(Net) Geothermal Power Plants at Heber and Niland, California, Energy Research and Development Administration, SAN-1124-1, Oct. 1976.

## FIGURE CAPTIONS

Figure 1. PC samples after exposure at The Geysers to dry steam at 460°F (238°C) for 1 yr. Samples 275-278 contain aggregate consisting of 90% silica sand-10% cement. All others contain only sand.

Figure 2. PC pipe after exposure to 400 ppm brine at 300°F (∿ 150°C) for 312 days.

Figure 3. PC samples after exposure to pH 1 HCl at 392°F (200°C) for 170 days.

Figure 4. PC samples after exposure to flashing brine at 320°F (160°C) for 180 days.

# CORROSION PROBLEMS IN KLAMATH FALLS, OREGON

by

Gene Culver
Geo-Heat Utilization Center
Oregon Institute of Technology
Klamath Falls, Oregon 97601

There are approximately 450 geothermal wells in Klamath Falls, used primarily for space heating of 500-550 homes. Most of the home heating wells have downhole heat exchangers installed, (Figure 1) the first one being installed in about 1930.

Other applications include seven schools, a hospital and nursing home, the Oregon Institute of Technology college campus, several small business and office buildings and a few industrial applications. Three of the schools also utilize downhole heat exchangers. Two schools and the hospital have shell and tube exchangers and most of the remainder, including the Oregon Institute of Technology campus, use geothermal water directly in the heating system.

Plate heat exchangers are just beginning to be utilized with three presently on-line and several more planned for completion within a year.

Until very recently, corrosion has not been considered a major problem and no formal studies were made. Local plumbers and heating contractors handled problems.

The average useful life of a black iron pipe downhole heat exchanger is approximately 14 years, although lives ranging from as few as three years to over 30 years have been noted. Total replacement cost of the average downhole heat exchanger is about $600 but many are repaired for considerably less. Since this is the only major cost for operation and maintenance of the systems

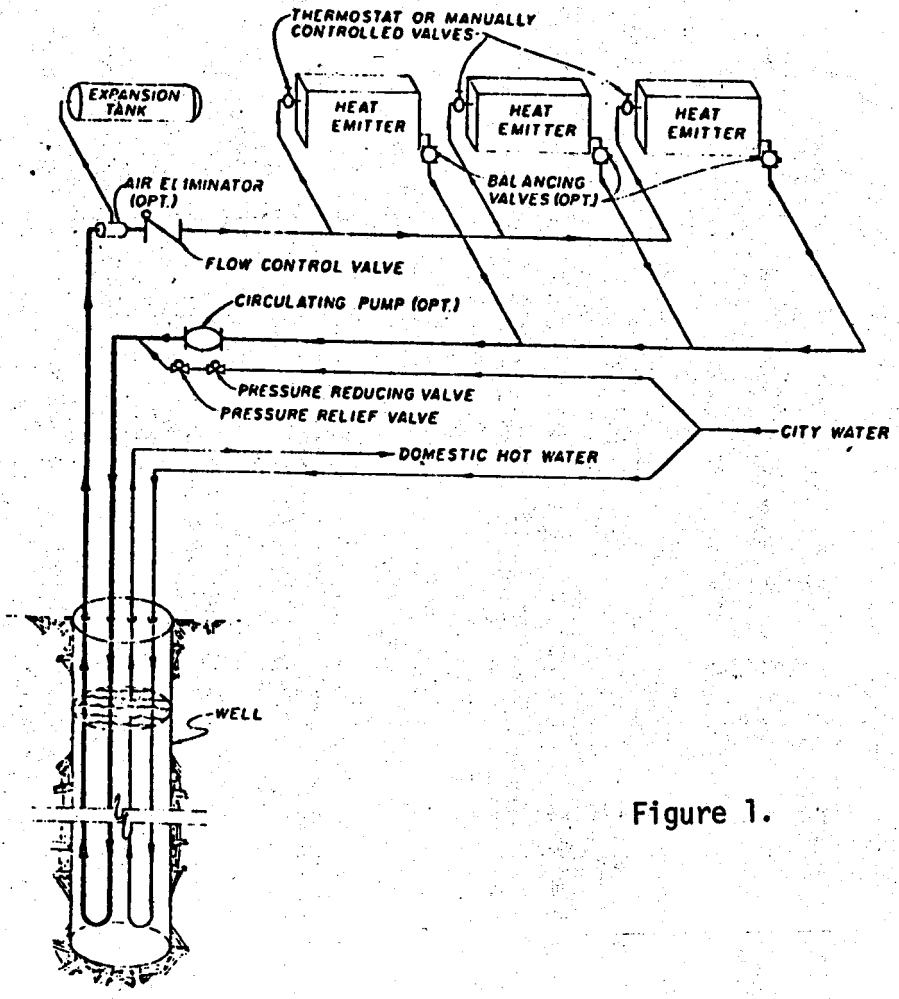
THERMOSTAT OR MANUALLY CONTROLLED VALVES
EXPANSION TANK
HEAT EMITTER
HEAT EMITTER
HEAT EMITTER
AIR ELIMINATOR (OPT.)
BALANCING VALVES (OPT.)
FLOW CONTROL VALVE
CIRCULATING PUMP (OPT.)
PRESSURE REDUCING VALVE
PRESSURE RELIEF VALVE
CITY WATER
DOMESTIC HOT WATER
WELL

Figure 1.

they were generally considered very economical after the initial cost of drilling and installation.

Because of the wide range of useful life and the fact that a few wells consistently had short lived downhole heat exchangers, a study was initiated in 1976. (Corrosion of Downhole Heat Exchangers; Lund et.al., Geo-Heat Utilization Center, Oregon Institute of Technology.) The results of the study were inconclusive in that the reasons for the variations in life were not pinpointed, however stray electrical currents are suggested. The source and nature of these currents is unknown. Further analysis and cross correlation of the data gathered during that study may provide more information.

There have been no major problems with the tube and shell exchangers, either with corrosion or sealing although the installations are all less than 20 years old. Exchangers are designed to carry geothermal waters in naval brass or bronze, straight through tubes and the tubes are rodded for cleaning about every three years. Little scale build-up is noted and as far as is known no tubes have been replaced.

Previous to 1964 most of the systems using geothermal water in the heating systems, used iron or steel in the plumbing and radiating devices, either cast iron radiators or steel finned tubes or fan coil units. Although problems were encountered with non-ferrous valves, and occassionally in radiators or fan coil unit heaters, the systems were still generally considered more economical than conventional fuels. Most failures were considered to be associated with air leaks somewhere in the system.

In 1964, the major direct use application, the Oregon Institute of Technology campus, went on-line with predominately steel

piping and copper tube fan coil units. Although some problems were noted with automatic valves scaling and seizing, no major problems were noted for several years.

Although there had been some failures in fan coil units on the campus this did not become a major concern until the last year when fan coil failures became more frequent and larger coil units failed, and there were distribution pipeline failures.

During the past year, several distribution lines have failed; predominately at changes in direction. The lines are steel pipe field insulated with foam glass sections wrapped with an asphaltic and cloth mesh material. It appears (although still inconclusive) that failure is due to external corrosion where thermal expansion has caused failure of the covering allowing ground water to come into contact with the hot steel piping. Sections of distribution line that have been removed where the insulation and asphaltic material have remained intact showed no evidence of external or internal corrosion and about 1-1/16 inch or less of a modular scale build-up. We presently believe that internal corrosion of the steel distribution lines is not a major problem.

Leaks in the copper tube fan coil units have been predominately at or near solder joints and where copper tubes connect to iron headers although a few failures have occurred in the body of the coils. At this time the cause of failures is not known and a study is under way to determine the exact cause and to suggest remedies.

Unfortunately (or perhaps fortunately from an investigative point of view) two systems were designed after the Oregon Institute of Technology system, but before problems with the OIT system were noted. These systems both utilize geothermal water

directly in the heating system and both use individual small copper tube fan coil units in apartments. Both are relatively low-temperature applications and utilize coils originally designed for cooling applications where the tubes are made of thinner material. Failures in these systems appeared in two-three years again at solder joints and where tubes are connected to heaters. One of these systems has been converted to use a plate type heat exchanger between the geothermal water and heating system water, the other is being studied in an attempt to determine the exact cause of failure but no progress can be reported at this time.

## WORKSHOP SUMMARIES

- Corrosion
- Failure Analysis
- Fluid Chemistry
- Materials Selection
- Non-Metallic Materials

# CORROSION WORKSHOP

Dr. R. L. Miller, Discussion Leader

## Introduction

Four sessions were held during the course of the conference to assess the present knowledge concerning materials for geothermal service, to define the areas requiring further study, and to make recommendations for research and development in this field. This report is a summary of the discussions held during these four sessions.

Corrosion of metals in contact with geothermal fluid is one of the major problems that must be resolved for the successful utilization of geothermal fluids. Typical chemical process industry corrosion control practices involve a combination of materials selection and chemical inhibition. The volumes of water involved in geothermal applications are generally too large for chemical inhibitors to be economically effective. Further, one must anticipate that any chemical added to the geothermal fluid for corrosion control will have to be removed to satisfy environmental requirements. Thus, materials selection appears to be the most profitable route to corrosion control when large volumes of geothermal fluids are involved.

The two general areas of geothermal fluid usage are electric power production and direct applications such as space heating, agricultural stimulation and process heat. Water used in power plants may then be reused for direct applications (secondary use). Of the two areas, direct applications offer greater opportunities for intrusion of oxygen (from the atmosphere) into the fluid. This would result in greater corrosion attack, (Legaut, et al, 1971).

## Available Data

Conferees noted that efforts directed towards an understanding of the corrosion problems have been limited to site-specific applications rather than a broad study to create a data base for materials selection and application to a wide spectrum of geothermal environments. The following citations are offered as sources of data; no attempt is made here to provide a thorough literature search and critique of available data. This will be provided in a materials handbook prepared by Radian Corporation (Austin) and published by DOE (U.S. Department of Energy). Banning and Oden (1973) provided a good summary of available data on metals response in hot brines, including geothermal fluids. Marshall and Braithwaite (1973) have also reviewed the literature up to about 1973 with special reference to New Zealand experience.

Considerable interest was expressed in a concerted effort to gather data on a systematic basis and as a function of several variables. The parameters considered to be most important are temperature, salinity, pH, and content of active gases such as oxygen or hydrogen sulfide. Carbon dioxide is a mild oxidizing agent which in geothermal fluids influences the solubility of calcium carbonate. The precipitation of calcium carbonate scales on metal surfaces will generally retard corrosion; this effect of carbon dioxide is probably more important than its act as an oxidizing agent. The predominant dissolved solid in geothermal fluids is the chloride ion. The tendency of this species to depolarize metals and to form stable metal/chloride coordination compounds leads to rapid corrosion of many metals. Many other dissolved species result in accelerated corrosion. Oxygen is particularly aggressive, especially in the presence of chloride. Butler and Mercer (1975) noted that dissolved silica may retard corrosion, but this has not been verified in geothermal systems.

Sulfides, even when present in trace amounts, are very deleterious towards copper/nickel alloys and bronzes containing nickel alloy additions (Fernelias, 1975 and Miller, 1977). In this respect, one needs to use data from seawater and desalination service with care, since these applications are free of sulfides and materials that have performed well in these services have not responded well to geothermal fluids.

More needs to be said about the sulfur problem. The sulfide ion is very aggressive and the oil and gas industry has expended considerable time and effort to understand the nature of and means of controlling sulfide attack. In the presence of oxygen, the sulfide is oxidized to polysulfide ($-S-S-\ldots-S_n$) which is also aggressive. Mention was made of corrosion rates of several inches per year in transmission lines. This attack is attributed to both hydrogen sulfide and polysulfide. The corrosion rate increases with time, indicating that the process is autocatalytic.

Further oxidation of the hydrogen sulfide and polysulfides yields elemental sulfur, which is a weaker oxidizing agent than its precursors. However, elemental sulfur is aggressive in oil and gas environments and should be considered to be potentially so in geothermal systems. Oxidation of the sulfur by oxygen or by sulfur oxidizing bacteria, such as Thiobacillus thiooxidans, results in the formation of sulfuric acid and other products such as thiosulfate, polythionates, etc. Such action was said to result in depression of pH to values as low as 3.5. The consequence of such low pH is accelerated corrosion. Thiobacillus bacteria are frequently found in significant amounts in wastewater and in cooling towers.

This listing of dissolved species presents only the more obvious variables and chemical species that need to be considered

in selecting materials for geothermal applications. Since no concerted study of these factors has been conducted, such a program was recommended by nearly all participants in the discussion group. The principal parameters appear to be temperature and salinity. These two variables could form the basis of an in-depth study of materials response with modifications from other factors such as pH and concentrations of oxygen and hydrogen sulfide. Such a study would be very helpful in making materials selections and predicting the response of materials to geothermal environments. A dividend from such a study could be a preliminary mathematical model for selecting materials.

## Technology Transfer

The potential for technology transfer from other disciplines was noted by several conferees. The three general areas that seem to be most important are seawater applications, desalination technology, and experience in oil and gas service. Experience in seawater and desalination usage is of marginal value since those systems typically contain dissolved oxygen and are therefore in a potential-pH region that is somewhat different from the reducing conditions found in most geothermal fluids.

Fluids produced from oil and gas wells are similar to geothermal fluids in several respects. They are saline, contain hydrocarbons and usually, hydrogen sulfide. They are therefore reducing, as are most geothermal fluids. Oil and gas corrosion data may be more applicable than either seawater or desalination experience. The dissolved solids in geothermal fluids are primarily silica and chlorides; oil well brines are similar but frequently contain greater amounts of sulfates than geothermal fluids. Cowin and Weintritt (1976) have compiled a great deal of data on scales in oil well systems. These data should be of some assistance in geothermal applications. The hydrogen sulfide concentra-

tions of most geothermal fluids are somewhat less than those found in oil brines. The temperatures of oil wells reach as high as 558 K, while geothermal fluids may reach as high as 643 K. The number and distribution of medium and low temperature geothermal resources suggests that these have the greatest potential for making a contribution to the national energy situation; thus, the temperature range found in oil and gas wells is of the proper magnitude for consideration of corrosion problems. Geothermal fluids frequently contain traces of hydrocarbons, whereas fluids from oil and gas wells must contain substantial amounts of hydrocarbons to be economically viable. The hydrocarbon concentration may represent the greatest disparity between oil and gas fluids and geothermal brines.

The brief comparison of geothermal fluids with those from oil and gas wells suggests that a detailed literature review be conducted, a bibliography be prepared, and geothermal fluids be critically compared with those from oil and gas brines in order to compare corrosion (and scaling) experience in these two areas. Data sources would include the Society of Petroleum Engineers of the American Institute of Mining, Metallurgical and Petroleum Engineers (Dallas, Texas) and the National Association of Corrosion Engineers (Houston, Texas). The international publications of the corrosion engineering community would have to be examined for data. A handbook for materials selection is being prepared for DOE by Radian Corporation of Austin, Texas. This book will contain much of the available data on geothermal corrosion and tentative recommendations for materials selection for these environments. Other data collections are usually too general to have much value in the present context.

Equilibrium thermodynamics of corrosion systems are frequently represented in terms of potential (Eh) as a function

of pH. Pourbaix (1966, 1971, 1973) has pioneered in this area; graphs of Eh vs pH are frequently termed Pourbaix diagrams. These diagrams represent a theoretical approach to understanding corrosion. The vast majority of this work has been conducted at normal temperature and pressure, (298 K, one atmosphere). Work at higher temperatures has been conducted and will materially aid our understanding of corrosion. Mathematical models have been developed which can be used on high speed computers for generation of a number of correlations.

## Corrosion Testing

Means of evaluating materials prior to selection for plant construction are required to provide a rational basis for materials selection. Once a plant has been built, monitoring is required to estimate the corrosion rate in various plant units. Corrosion testing procedures for the chemical process industries are available from ASTM and NACE and are applicable to materials testing in geothermal environments. The development of new or alternate procedures may be desirable for certain forms of corrosion; for example, neither of these organizations has recommended procedures for crevice corrosion. Stress corrosion cracking is another area that may require some adaptation to assure that sufficient time is allowed for an induction period. Conferees were of the opinion that the NACE stress corrosion test was preferred to the ASTM procedures.

Conferees were particularly concerned that any tests conducted to simulate conditions in a system be designed to duplicate hydrodynamic conditions. Other variables would include water chemistry, temperature and pressure. The NACE procedure for conducting velocity effects tests is not applicable to operations at high temperatures or under pressure; new test procedures are required in this area. In the area of velocity effects testing,

a lower boundary, i.e., zero velocity, exists and would occur when the system is put into wet layup. Zero velocity is generally considered to be a very undesirable condition and needs to be studied as a function of temperature.

Atlantic Richfield (ARCO, Ponca City, Oklahoma) engineers have developed a "Rocker Test" for evaluating materials for gas and oil applications. One conferee recommended that this system be studied for possible use in testing materials in geothermal environments. Too few details were available to describe the system here.

Conferees were of the opinion that water chemistry simulation is very difficult and laboratory tests in simulated geothermal fluids need to be verified by testing under field conditions. There are well-to-well variations in a geothermal resource in addition to distinct water chemistry variations among geothermal resources. Further complications arise from subtle changes in water chemistry as a function of time or rate of production. Participants noted that development of standard solutions for laboratory testing should be considered. Such solutions would permit comparison of materials between laboratory and field studies as well as comparison of test results between laboratories.

It has been hoped that electrochemical testing would permit accurate materials selection from rapid and easy test procedures; these hopes are still unrealized. Conferees were of the opinion that electrochemical testing needs to be applied carefully, with the results given through evaluation. The consensus was that linear polarization techniques will be useful in monitoring geothermal systems but of limited value for materials selection in the near term. Any time-dependent studies must consider a wide range of frequencies and be followed by careful data analysis.

Electrochemical tests are, therefore, of uncertain value; immersion tests, on the other hand, are virtually guaranteed to provide useful data.

As ASTM, NACE, or other test procedures are verified for geothermal applications, some ancillary but useful standards need to be included. For example, standard reporting formats would be useful in making interlaboratory data comparisons. A second concern presented by conferees was for a standard coupon configuration. Typically, corrosion coupons are selected according to availability, however, some effort should be made to obtain materials in the welded configuration. Welds should be made using the same materials and procedures as will be used in the actual weldment being simulated.

Although the actual coupon shape may not be critical, hydrodynamics will vary between round, square, rectangular and tubular configurations. The mounting assembly may be relatively unimportant; ASTM Standard G 4 shows one recommended mounting procedure. Another mounting system, developed for testing at Raft River, provides an insulator that permits electrical coupling of coupons for galvanic corrosion tests and has a varying crevice to promote crevice corrosion (Miller, 1977). Wicking action of gasket materials may promote crevice corrosion; gaskets should be tested to evaluate their tendency toward supporting this kind of attack.

Test duration and scheduling has not been uniform in the tests conducted to date. This reflects the individual preferences of the engineers and scientists involved. Some uniformity would assist in interpretation of the results by independent workers. As a guideline the relationship

$$2000/\text{corrosion rate (mpy)} = \text{minimum test time (hrs)}$$

has been suggested (Fontana and Green, 1967). Scheduling of coupon changeout may be done in such a way as to improve the overall value of the test data. The "planned interval" method developed by Wachter and Treaseder (1947) is recommended. (See also Fontana and Green, 1967). Interpretation of data from this method of scheduling results in corrosion rate as a function of time, as usual, and in addition indicates changes in the resistance of the materials being tested and in the corrosiveness of the environment. In view of water chemistry variations with time, information regarding its aggressiveness would be of particular value in materials selection or for predicting the life of a plant system.

Conferees suggested that selected materials be run in all tests to provide a baseline for comparing overall materials performance between laboratories and between geothermal fields. Such materials would normally include those having high, low, and moderate corrosion rates. Data from such a testing program would reflect responses to minor variations in test conditions.

Sample cleaning procedures outlined by ASTM are not entirely satisfactory and are not uniformly applied. One participant has successfully used mechanical abrasion by means of a sand blaster (using 25-micron particles) to remove corrosion products and deposited minerals. Care must be exercised in cleaning to avoid destruction of surface features that would aid in interpretation of the modes of corrosion attack.

General agreement was not reached as to who should pay for materials testing in geothermal applications. One school of thought is that DOE/DGE (Division of Geothermal Energy) should take a leading role in this activity. Some industrial representatives did not support this view. Alloy manufacturers were of the opinion that as much data as possible should be available to

permit well reasoned materials selection. There was no objection to DOE taking a leading role in gathering and correlating available data and making this available to all geothermal users. There was a consensus that DOE should provide a means of distributing corrosion data within their department and to other agencies such as the U.S. Bureau of Mines.

Corrosion data from geothermal testing and plant experience will be useful in other fields where natural waters contact construction materials.

## Corrosion Prevention and Control

Conferees noted that plant design and materials selection appear to be among the most effective means of controlling corrosion. The most critical components require the greatest care in the materials selection process. For example, pumps require more careful consideration than pipe lines. Within any component the most sensitive parts should be fabricated from the more noble materials than the less critical parts to avoid galvanic contributions to the overall attack. Erosion damage to elbows can be reduced to a considerable extent by using blind tees. In common with the chemical process and oil and gas industries, geothermal plant designs should have a minimum of crevices that will promote crevice corrosion. Systems maintained under pressure will have less tendency to cavitate in pumps than liquids that are near their saturation pressure.

Participants were of the opinion that two or three classes of alloys will require special justification before they can be used. High-strength steels are to be avoided in the presence of hydrogen sulfide to avoid hydrogen damage and stress corrosion cracking that may result in catastrophic failure. Low alloy

steels having more than about 0.2% nickel show excessive corrosion rates and should not be used. Combinations of copper and nickel have a tendency to suffer severe general corrosion and selective leaching in the presence of hydrogen sulfide and should not be used if even traces of this gas are present. The consensus of the conferees was that development of specialized alloys for geothermal applications would probably not be economical.

Materials selection was noted earlier as appearing to be the most profitable route to corrosion control in geothermal environments. In this context alternate materials, such as polymers, need to be examined. Fiber reinforced plastics (FRP) have a history of corrosion resistance for specialized applications and environments. These materials are more expensive than many alloys. The principal problems involved in application of FRP's, plastic-lined pipe, etc., is the rapid decrease in tensile properties with increase in temperature. The application of polymers that can be repaired without major disassembly of a system is of considerable interest to the geothermal community and should be studied in depth.

DOE has supported development of a polymer system by the Brookhaven National Laboratory. These "polymer concretes" have been under test at a number of geothermal sites. Sulfurcrete was mentioned as a useful material in the chemical process industries; however, little hope was expressed that extensive use could be made of this material in geothermal applications.

Three factors mitigate against the use of corrosion inhibitors in geothermal fluids. The volumes of fluids involved are usually too large for economical application of chemical inhibitors. The temperatures involved are typically too high for polymer inhibitors to be stable. Finally, the Environmental Protection Agency requires that any corrosion inhibitors be removed

from wastewater before disposal of the fluid. This latter factor includes both cooled geothermal fluid and cooling tower blowdown. One solution for this overall problem is to find an inhibitor system that can be recovered and recycled economically.

Conferees have noted that cathodic protection has been applied to oil wells to reduce well casing corrosion. Such protection procedures require careful analysis, installation, and monitoring to avoid hydrogen embrittlement as promoted by sulfides. Electrochemical corrosion is accelerated by a number of factors that increase potential differences. For example, the temperature differences that occur in a system as heat is abstracted may result in accelerated corrosion. Further, potentials may reverse with a change in temperature. Conferees suggested that another source of potential difference is the streaming potential of a flowing electrolyte, both in pipes and in the geological formation. The motion of the electrolyte could also generate magnetic fields, though the effect of such a field on corrosion properties of a material is likely to be very small.

## Conclusions and Recommendations

A need for corrosion data for a wide range of temperatures and geothermal environments was noted. This need was identified from the following considerations. Studies of materials response to geothermal environments have been site-specific, and usually for rather restricted applications. Technology transfer from the seemingly closely related environments of seawater and desalination service has not been successful. Corrosion data from oil and gas technology have not been examined closely for their relevance to geothermal fluid applications.

A carefully planned study of materials for geothermal service was recommended. Materials to be studied include a wide range of alloys, structural plastics, polymer-coated steels and elastomers. The materials should be studied over a wide temperature range and in a broad spectrum of environments.

Development of a corrosion data base for geothermal environments will require careful attention to testing procedures. Methods recommended by ASTM and NACE should be applicable to geothermal environments but this assumption needs to be verified by laboratory and field testing. Procedures need to be developed for in situ testing where ASTM or NACE procedures are not available or may not be applicable to high temperature, high pressure systems. For example, crevice corrosion, controlled velocity effects, erosion-corrosion, hydrogen embrittlement and stress corrosion cracking were specific areas suggested for procedure development.

Plant design and materials selection appear to be the most effective means of controlling corrosion for geothermal applications. Three specific alloy systems were noted as being especially prone to corrosive attack in geothermal fluids. In each case even trace amounts of hydrogen sulfide in the fluid appeared to be the cause of material degradation. The materials in question are combinations of copper and nickel, low-alloy steels having more than about 0.2% nickel, and high-strength steels. Plastics and fiber-reinforced plastics are largely untried in the medium and high temperature regimes of geothermal fluids. Elastomers for seals in geothermal environments are an area of concern; data on the response of these materials is required for development of, for example, down-hole pumps.

References

Banning, L. H. and Oden, L. L., 1973, "Corrosion Resistance of Metals in Hot Brines: A Literature Review," U.S. Bur. Mines, Inf. Circ. 8601.

Butler, G. and Mercer, A. D., August 28, 1975, "Effect of Glass Dissolution on Corrosion Measurements," Nature, 256, pp 719-720.

Cowan, J. C. and Weintritt, D. J., 1976, Water Formed Scale Deposits, Gulf Publishing Co., Houstin, TX., p. 596.

Ferneliu, W. A., 1975, "Production of Fresh Water by Desalting Geothermal Brines - A Pilot Desalting Program at the East Mesa Geothermal Field, Imperial Valley, California," Proceedings, Second United Nations Symposium on Development and Use of Geothermal Resources, San Francisco, CA, May 20-29, 1975, pp 2201-2208.

Fontana, M. G. and Greene, N. D., 1967, Corrosion Engineering, McGraw-Hill Book Co., New York, p 391.

Legault, R. A., Mori, S., and Leckie, H. P., 1971, "An Electrochemical-Statistical Study of Mild Steel Corrosion Inhibition in Oxygen Containing Environments," Corrosion, 27, pp 418-423.

Marshall, T. and Braithwaite, W. R., 1973, "Corrosion Control in Geothermal Systems," Geothermal Energy (Earth Sciences, 12), UNESCO, pp 151-160.

Miller, R. L., 1977, Results of Short-Term Corrosion Evaluation Tests at Raft River, USDOE Rept. TREE-1176.

Pourbaix, M., 1966, Atlas of Electrochemical Equilibria in Aqueous Solution, Pergamon Press, New York.

Pourbiax, M., 1971, "Potential-pH Diagrams and Metallic Corrosion," Handbook on Corrosion Testing and Evaluation, W. H. Ailor, ed., John Wiley and Sons, Inc., New York, pp 661-687.

Pourbaix, M., 1973, Lectures on Electrochemical Corrosion, Plenum Press, New York.

Wachter, A. and Treseder, R. S., 1974, "Evaluation of Metals for Press Equipment," Chem. Eng. Prog., 43, pp 315-326.

# FAILURE ANALYSIS WORKSHOP

Dr. A. D. Thomas, Discussion Leader

A definition concerning the scope of these discussions was necessary as failure analysis is not an end in itself. Thus the discussion was limited to the role of failure analysis in the prevention of similar occurences in pilot or operating plants. This meant that topics of pre-emergency planning, fault free analysis of system design, quality assurance and inspection, and data base management were regarded as equally important to the analysis of service failures.

There were two distinct purposes for wanting the failure related data. Dr. Reeber expressed an interest in the knowledge of specific system component failures to the end that DOE research could be quickly aimed at filling gaps to insure that at least one of every component necessary for a geothermal system was available. The geothermal contractors or users wanted a reliable data base for design, operation, and maintenance purposes. The latter requires a continuous, more extensive data base management system.

## Data Base Management System

The key to successful use of failure analysis may be a well planned data base management system. Several of these have been generated for other government funded materials programs, and the suggestions were to examine these and modify them as needed for geothermal needs.

## Operating Data

An effort should be made to obtain data from all operating plants, both U.S. and foreign, for the data base. Any requests

for proposals (RFP's) for government-funded geothermal programs should have a requirement to report operating data and failures. Certain operating procedures should be developed, such as EPA has done for various pollutants, for parameters of interest. Until that time, measuring techniques should be reported along with the data.

## Data Reporting

A document similar to the ERDA Newsletter, "Materials and Components in Fossil Energy Applications," should be published for the geothermal community. It was suggested that a list of geothermal contracts with the name of the technical project director be listed for ease in information transfer. Many attendees felt that reports remain too long in the publication process.

## Specifications

There are several specifications and standards applicable to geothermal electrical generation facilities. These include ANSI, ASME Boiler and Pressure Vessel Code, API, etc., and should be fully utilized in design of geothermal components. These should be reviewed for adequacy in geothermal usage. Purchase orders can then carry additions to the present standards to insure proper quality.

## Failure Analysis

All failures resulting in 24 hours downtime or resulting in Remove and Replace procedures should be reported to the manager of the data base management system. The reporting forms should be simple but meaningful.

## Inspection Procedures

Inspection procedures have been set up in many industries to check safe operation, and to plan maintenance shutdowns. Problem areas in geothermal electric generating plants should have specific inspection procedures written and followed to minimize forced outages.

## Training Courses

Because of the problems involving geothermal fluids in power generation, special courses should be set up for plant operators.

# FLUID CHEMISTRY WORKSHOP

Dr. D. W. Shannon, Discussion Leader

Fluid chemistry is the environment that affects many aspects of materials performance in geothermal systems. Geothermal brines have aptly been called "rock soup" and literally contain all naturally occurring elements at some concentration. A major problem arises in determining what concentrations are significant. The fluid chemistry discussion groups concentrated on answering the question, "What chemical species need to be measured, and why?".

Corrosion and scaling in geothermal systems are two major problems directly related to the chemistry of the geothermal brine. Scale deposition has occurred in exploration and production wells, silencers, cyclone separators, drains, water pipes, and turbine blades. The degree of deposition is dependent on temperature, pH, and saturation of the geothermal brine. Deposition occurs when hot, saturated brine becomes supersaturated as part of the water flashes to steam and the brine temperature drops as a result of the phase change.

The following areas were considered important in determining the fluid chemistry of geothermal brines.

## Gases

Commonly measured gases include $CO_2$, $H_2S$, $NH_3$, $CH_x$, Ar, $H_2$, and $SO_2$. They are usually measured in terms of weight percent of geothermal fluid. Gases play a major role in scale deposition and corrosion because they control the pH of the brine. Some gases themselves affect component materials (e.g. brittleness and cracking caused by $H_2S$), and thus affect turbine/condenser design.

## Environment

The U.S. Environmental Protection Agency (EPA) requires environmental quality data on heavy metal ions contained in geothermal brines. Varying concentrations of arsenic, mercury, lead, boron and radon are commonly found in geothermal fluids. Criteria pollutants, such as $H_2S$, must also be monitored.

## Corrosion- and Scale-Causing Elements

The following elements have been found to contribute to corrosion and scaling of geothermal materials: dissolved oxygen, barium, calcium, silicon, mercury, zinc, lead, antimony, iron, manganese, silver, copper, thallium, arsenic, strontium, and vanadium. Geothermal brines vary in composition, depending upon the mineral content of the strata through which they flow. The brines in the Imperial Valley of California, for example, are much more saline than those of Cerro Prieto, Mexico. Sub-surface mineral deposits in the brine's area of origin may often provide information as to the composition of the brine.

## Mineral Recovery

In some instances, it may be profitable to extract valuable metals from spent geothermal brine. Elements which may be of value include: potassium, mercury, silver, copper, cobalt, molybdenum, manganese, chromium, tungsten, tantalum, columbium, lead, eithium, iron, magnesium, uranium, and nickel.

## Other Considerations

Other aspects of fluid chemistry which may affect geothermal materials performance include molecular species (measurement of metal complexes may indicate the chemical activity of

various ions), hydrocarbons and organic acids, anions ($Cl^-$, $F^-$, borates, $SO_4^{-2}$, $HCO_3^-$ $S^{-2}$, $HS^-$), and species important to exploration and reservoirs (the above anions plus rubidium, cesium, and various isotopes). Total dissolved solids (TDS) are commonly measured, but are of less importance than the dissolved gases and individual minor components.

The following methods and equipment were suggested as needed ways to obtain fluid chemistry data:

- A continuous scaling rate meter;
- In-line instruments for measuring pH, sulfide concentration, redox potential, conducturity, $CO_2$, in-line corrosion;
- Down-hole samplers;
- A way to insert and retrieve coupons without system shutdown;
- A reliable two-phase sampling system;
- One or more "standard" (NACE-type) geothermal test solutions for laboratory tests.

# MATERIALS SELECTION WORKSHOP

Dr. R. R. Reeber, Discussion Leader

Discussion in the Materials Selection Workshop centered around materials needs, testing criteria, and technology transfer. Recommendations and suggestions made are summarized below.

## Materials Needs

New materials needs are continually developing. There is a great need for information on materials chemistry. Research and development needs differ as to what materials should be used in various applications (e.g. materials specifications are not the same for electricity generation and heat utilization).

There was much discussion regarding materials testing procedures. The suggestion was made that initial testing should be done in small installations rather than large ones. For example, more site-specific information can be obtained from 25 small plants than five large plants, for about the same cost.

Several problems with this approach were discussed. Many small installations cannot afford to test several different materials at once. Geographical location of the site must also be considered; in some areas, testing at large facilities may be as economical as testing at smaller installations.

Some standardized tests are already in use in low temperature applications. It was felt that it can be dangerous and expensive to depend heavily on short-term materials corrosion tests for major plant materials decisions. Longer-term standardized tests should be developed and implemented. This is especially true for materials and/or new environments.

Building codes and standards were also discussed. It was felt that the U.S. Bureau of Standards should become more heavily involved in standards development. It was mentioned that the better standards are concensus standards promulgated through joint ventures between industry and government. Representatives from the U.S. Environmental Protection Agency (EPA) and the U.S. Geological Survey (USGS), as well as DOE and industry should be involved in standards development.

The American Society for Testing Materials (ASTM) cooperates with the International Standards Organization in developing standards. International promulgation of standards would be an effective way to standardize materials specifications and promote cooperation between countries with geothermal resources. Some international cooperation already exists; for example, West Germany is collaborating with the United States on a hot dry rock project at Los Alamos.

Miscellaneous materials concerns included the following:

- A standard format should be developed for reporting materials data.
- More emphasis should be given to lower salinity resources.
- A schedule of periodic inspections might be a viable way to obtain failure analysis data. Often such data are difficult to obtain for new systems because of operators' desires to minimize downtime. Periodic inspection could potentially reduce downtime by detecting possible faulty equipment.

## Technology Transfer

Communication and information transfer were important topics to most of the participants in the materials selection discussion group. The need for better ways of technology transfer were stressed many times. Symposia and seminars were considered the most economical and effective means of communication.

The ASTM and the National Association of Corrosion Engineers (NACE) need to get involved in the technology transfer process. These groups have several committees whose functions overlap. It was suggested that a joint committee be formed with representatives from these and other professional organizations interested in materials science. Some joint work is already being done by the ASTM and the American Institute of Mining, Metallurgical, and Petroleum Engineers (AIME). ASTM and AIME will hold a joint conference in New Orleans, Louisiana in February 1979. A DOE-sponsored seminar was suggested as a way to bring the professional and industrial associations together.

Other ways of information transfer included:

- A liason officer whose job would be to attend meetings of professional, industrial, and governmental groups and keep each sector up-to-date on materials science developments.
- A geothermal materials-oriented newsletter. This publication would contain reviews of government and industrial research and development, and information on conferences, contracts, and patents of interest to the geothermal industry.

# NON-METALLIC MATERIALS WORKSHOP

Dr. Patrick Cassidy, Discussion Leader

In four discussion groups, the topic of non-metallic materials was broken down into four items of discussion as given below. The first item was to identify the areas of application for non-metallic materials in the recovery of geothermal energy. The second problem was to list all types of materials which are being used, have been used, or are considered or being tested for use in geothermal wells or surface equipment. The third topic of discussion was to outline some of the problems as presently defined; and the fourth and final item was simply to list other comments, questions, or concerns which people have concerning non-metallic materials.

## Applications of Non-Metallic Materials

- Packers - To seal between the central drill pipe and the casing of the well
- "O" Rings/Reed Ovals - To seal lubricants in drill bits
- Lubricants - For sealed drill bits
- Pipes - For transporting fluids on the surface
- Gaskets - For surface equipment
- Pipe protectors (centralizers) - To fit between the drill pipe and the well casing
- Coatings - To impart corrosion or erosion resistance to equipment or to prevent the buildup of scale or to ease the removal of scale once formed
- Valve packings

- Pump packings
- Face seals
- Scale release surfaces
- Logging equipment (cable insulation, cable connector encapsulation, cable connector boot, and down hole probes) - For short-term exposure during data collection
- Bearings for down hole turbines
- Impeller coatings for generator turbine blades
- Electrodes/Detectors - For surface data collection
- Surface probes
- Muds
- Mounting pads - For large surface equipment
- Well cements - For outside the casings
- Separators - For surface fluid processing
- Cooling towers
- Electrical insulators
- Seals - For flat plate heat exchangers

<u>Types of Materials Which Have Been Applied to or Considered for the Above Needs</u>

- Viton - A fluorinated, high-termperature elastomer
- EPDM - A hydrocarbon rubber
- Buna-N - A hydrocarbon-nitrile rubber
- Kalrez - A fluorinated-polyether, high-temperature elastomer

- Teflon (polytetrafluoroethylene - PTFE)
- Polyurethane (for low temperature application)
- Asbestos
- Graphite fiber (as gasket material)
- Fiberglass pipe (as fluid return line, 130°F) - An epoxy fiberglass composite
- Transite (cement and asbestos composite) - For pipes for transporting geothermal fluid
- Braided Teflon (valve packing)
- Silicon carbide - For face seals
- Boron carbide
- Diamondized graphite - For face seals
- Polymer concrete
- Impreglon - A thin fluorinated polymer coating deposited from vapor or plasma
- Kevlar (a polyimide)
- Ryton and graphitized Ryton (polyphenylene sulfide)
- Epoxy resins
- Wood or wood-polymer composite
- Silicon nitride
- Sulfur concrete ("Sulfurcrete")
- Alumina
- Zirconia
- Bentonite clay - As a base for lubricants
- Polyamines and polyphenols - As corrosion resistant coatings

- Buna-N lined fiberglass - For containers or pipes as erosion- and corrosion-resistant materials
- Vinylpolymers other than those mentioned above - styrene, acrylonitrile, acrylamide, divinylbenzene, TMPTMA (trimethylpropane trimethacrylate) vinyl chloride and methylmethacrylate
- Siloxane - styrene copolymer - As a resin for polymer concrete

Problems With the Above Materials

- Adhesion of packer to casing. The adhesion of the packer to the casing is not a desirable phenomenon. This problem can occur with normal packers or when packers are cured or processed in place.
- Brittleness of ceramic face seal materials. In some cases this brittleness or low impact in fracture resistance can be overcome by design changes. That is, in some pieces the ceramic can be made self-supporting.
- Blistering of well logging cable, cable connectors, and boot. This problem is seen when the components of the logging equipment are not well vulcanized or bonded. Since this application can be a short-term one and since it can be attacked by present day technology, it is not considered serious.

- Resistance of fiberglass to fluids. Although fiberglass pipes and vessels are corrosion resistant, they do have temperature limitations not experienced by metals. They are also somewhat susceptible to erosion.
- Extrusion of Teflon and Kalrez. These materials will flow easily at high temperatures and pressures. Therefore, they must be retained with metal seals under very close tolerances.
- Coatings.
  (1) There is presently no way to inspect coatings for lack of voids and good bonding in inaccessible areas.
  (2) If or when the coating failure fails, this failure cannot be of the type that the entire coating strips off permitting the removal of large pieces. These large pieces can then move downstream and cause further more serious equipment problems.
  (3) Reliability of coatings is always a question.
  (4) Abrasion resistance of coatings is sometimes less than desirable.
  (5) Coatings must be able to be repaired in the field.
  (6) The non-destructive testing of coatings is not possible. It would be desirable to be able to quickly test the adhesion, lack of voids, completeness of cure of the coating, etc., before use of the piece in the field.

- Adhesion of casing to supporting cement. When thermal changes occur in the well, a casing movement is a serious problem unless special design considerations are made (such as a slip spool). Good adhesion of the casing is important for this reason as well as for sealing the well.
- Degradation of packer seal. Present seal materials have been tested and found sufficient only to about 260° for 24 hours in a geothermal environment.
- Bit seals. A great advantage could be had by sealing drilling bits and thereby retaining lubricants in the bearing area and excluding the by-products of drilling. However, at this point, no seal materials are available which can withstand the requirements of temperature (in excess of the bottom-hole temperature due to friction), a confining pressure (2500 psi), differential pressure (50-100 psi), friction forces, and chemical resistance to the geothermal environment and to the lubricant being retained by the seal.
- A system is needed to prevent loss of mud circulation during drilling.
- Coefficients of expansion for dissimilar materials. In order to maintain coatings, adhesion, and good seals, similar coefficients of expansion are necessary for materials in close contact and for which contact is to remain. This, of course, is due to the variable temperature in geothermal processes.

- Packer design. A packer is needed which can be inserted in a small diameter and which then can be enlarged to fulfill this packing requirement.
- Realism of test methods and requirements. Some of the methods which may now be used to test non-metallic materials for geothermal applications may not provide realistic data. Furthermore, they may provide misleading information regarding the ability of the material to withstand a geothermal environment. For example, essentially all polymers have been tested by thermogravimetric analysis (TGA), differential thermal analysis (DTA), and differential scanning calorimetry (DSC) in air or nitrogen. These techniques have arisen from the past twenty years' work in attempting to qualify these materials for aerospace applications. However, these kinds of data have little or no value when considering the conditions of geothermal processes: high temperature, water, carbon dioxide, hydrogen sulfide, and salt.
- Polymer concrete processes. The production of polymer concrete composites must be carefully controlled and parameters affecting this production must be well known - such as cure schedule (time and temperature), toxicity, environmental considerations (volatility and odor of impregnating monomer), permeability of the final product and filler effects.

Other Comments and Suggestions

- For air drilling, a drill bit life of 100 hours would be exceptional. The average life time now is approximately 12 hours with occasional very good results being as much as 20 hours. This is the maximum life time to be expected for bit seals. Bit seals are critical for improving drilling technology and costs. For example, it will take approximately 6 hours work to replace a bit from 5000 feet.
- For most non-metallic materials, a 24-hour test is sufficient for screening. However, short-term data can be considered only superficial screening since many materials need a much longer life time and, therefore, a much longer test. For example, packers will be expected to exist and function for 1 to 2 years. For applications which are not so stressful as geothermal systems, accelerated tests can be devised by increasing temperature and pressure. However, accelerated tests for geothermal applications may be impossible or at least very difficult because the use conditions are presently at the operating limit of the non-metallic material. A long-term screening and testing program needs to be established for all materials under various conditions which they experience in geothermal energy production. For these non-metallics, a matrix of materials versus test conditions is very much needed.

- An elastomer of graded hardness would be very helpful. For example, in seals a soft elastomer on the stationary side would provide a seal but, on the side of the seal where friction is developed, a lubricated hard surface is desirable.
- A Viton bonding agent has proved valuable for holding ceramics on carriers at 350°F.
- Logging equipment must withstand 2 to 8 hours down hole. However, it is possible to use this type of equipment for only a short period (approximately 30 minutes). Therefore, perhaps materials problems for this application are not critical.
- Long-term real life condition exposure tests are necessary for all materials in a simulated design.
- Asbestos is an unacceptable packer because it allows aeration of the fluid with subsequent corrosion of metals.
- There are applications for fiberglass composites which have yet to be realized in some installations; for example, silencer chimmneys, transport of corrosive media, etc.
- An incentive is needed for private industry to test their commercial materials for geothermal applications. Many large suppliers of specialty polymers do not have data which relate the value of their materials to their use in the geothermal environment. This is due to the fact that geothermal uses are a very small market.

- In testing and designing materials, perhaps the general requirements have been set too high. That is, one seeks the worst case conditions to which a non-metallic material must be subjected when, in fact, many installations can use materials with less stringent properties and requirements.
- There is a need to develop valid test methods and scan all commercially available materials to establish some basic stability relationships for geothermal conditions. As mentioned earlier, much of the thermal stability data for polymers have been derived from aerospace technology. These data do not consider high temperature, high pressure and hydrolitic stability. Many polymers which have been useful in oxidative media degrade very rapidly in the reductive, hydrolitic chemical stresses which are experienced in geothermal wells and processing equipment. The resistance of functional groups (in organic polymers) to high temperature, high pressure and hydrolysis in the presence of $CO_2$, $H_2S$ and salt has not been studied or established.
- New materials, compositions, and effects of mixtures of materials are greatly needed.

# GEOTHERMAL SYMPOSIUM ATTENDEES
Lakeway Inn
Austin, Texas
May 22 - 25, 1978

Stan Allen
Wellhead Systems, Inc.
P. O. Box 1095
Shreveport, Louisiana 71163

John C. Bond
Barber-Nichols Engr. Co.
6325 West 55th Avenue
Arvada, Colorado 80002

S. Barry Brummer
EIC Corporation
Chapel Street
Newton, Massachusetts 02158

Joseph A. Cameron
Elliott Company
Division of Carrier Corp.
Jeannette, Pennsylvania 15644

Dan D. Carda
SDSM&T
E & M Expt. Station
Rapid City, South Dakota 57701

Lawrence Casper
Idaho National Engr. Lab.
Box 1625
Idaho Falls, Idaho 83401

Patrick E. Cassidy
Texas Research Institute
5902 W. Bee Cave Road
Austin, Texas 78746

John M. Cieslewicz
AMPCO Metal Division
AMPCO-Pittsburg Corp.
P. O. Box 2004
Milwaukee, Wisconsin 53201

Shelton Clark
Radian Corporation
P. O. Box 9948
Austin, Texas 78766

Marshall Conover
Radian Corporation
P. O. Box 9948
Austin, Texas 78766

Raymond Cedillo
Southern California Edison
P. O. Box 8000
Rosemead, California 91770

C. J. Cron
Union Oil Co. of California
P. O. Box 76
Brea, California 92621

Gene Culver
Oregon Institute of Technology
Klamath Falls, Oregon 97601

David DeBerry
Radian Corporation
P. O. Box 9948
Austin, Texas 78766

Earl Dumitru
University of Texas at Austin
Austin, Texas 78712

Peter F. Ellis
Radian Corporation
P. O. Box 9948
Austin, Texas 78766

Don Fowler
McEvoy Oil Field Equipment Co.
P. O. Box 3127
Houston, Texas 77001

Edwin R. Fuller, Jr.
National Bureau of Standards
Building 223, Room A355
Washington, D.C. 20234

GEOTHERMAL SYMPOSIUM ATTENDEES

Elizabeth D. Gibson
Radian Corporation
P. O. Box 9948
Austin, Texas 78766

Jim Goodson
Regal Tool & Rubber Company
Box 1237
Corsicana, Texas 75110

D. H. Gurinsky
Brookhaven National Lab.
Upton, New York 11973

Robert F. Hehemann
Case Western Reserve Univ.
University Circle
Cleveland, Ohio 44106

Robert R. Hendrickson
Terra Tek, Inc.
Salt Lake City, Utah

Alan Hirasuna
L'Garde, Inc.
1555 Placentia Avenue
Newport Beach, California 92663

A. A. Hochrein, Jr.
Daedalean Associates, Inc.
Woodbine, Maryland

Stanley M. Howard
S. D. School of Mines and
Technology
Rapid City, South Dakota 57701

Hank Janney
Daedalean Associates, Inc.
Woodbine, Maryland

Walt Jasionowski
Institute of Gas Technology
3424 South State Street
Chicago, Illinois 60616

Peggy Jeffcoat
Radian Corporation
P. O. Box 9948
Austin, Texas 78766

Donald R. Johnson
Sandia Laboratories
Division 5737
P. O. Box 5800
Albuquerque, New Mexico 87185

W. Neal Kocurek
Radian Corporation
P. O. Box 9948
Austin, Texas 78766

Henry Kuc
Peerless Pump
1200 Sycamore Street
Montebello, California 90640

Barbara Lee
Radian Corporation
P. O. Box 9948
Austin, Texas 78766

William Lee
Atomics International
8900 DeSoto Avenue
Canoga Park, California 91304

Digby D. MacDonald
SRI International
Menlo Park, California

Charles Madsen
Bechtel National
P. O. Box 3965
San Francisco, California 94119

GEOTHERMAL SYMPOSIUM ATTENDEES

Roland Marchand
U. S. Department of Energy
Las Vegas, Nevada

H. B. Matthews
Sperry Rand Corporation
Sudbury, Massachusetts

Frank X. McCawley
U. S. Bureau of Mines
College Park, Maryland 20740

Daniel McCright
Lawrence Livermore Lab.
Box 808
Livermore, California 94550

D. M. McStravik
Baker Packers
P. O. Box 3048
Houston, Texas 77001

Alfredo Mañón Mercado
Comision Federal de Electridad
Mexicali, Mexico

Richard L. Miller
Idaho National Engr. Lab.
P. O. Box 1625
Idaho Falls, Idaho 83401

David G. Newell
San Diego Gas & Electric Co.
P. O. Box 1831
San Diego, California 92112

Kenneth L. Newman
WESTEC Services, Inc.
1520 State Street
San Diego, California 92101

Terry B. Parsons
Radian Corporation
P. O. Box 9948
Austin, Texas 78766

J. A. Peterson
ARMCO Steel Corporation
Research and Technology
Middletown, Ohio 45043

F. B. Pippert
UTEX Industries, Inc.
5200 Clinton Drive
Houston, Texas 77020

Robert R. Reeber
U. S. Department of Energy
Washington, D.C.

Jacob M. Rudisill
Thermal Power Company
601 California Street
San Francisco, California 94108

Jerry W. Russell
AMF/Tuboscope
P. O. Box 808
Houston, Texas 77001

Donald W. Shannon
Battelle-Northwest
P. O. Box 999
Richland, Washington 99352

Terry Shinn
McEvoy Oil Field Equipment Co.
Tyler, Texas

Meyer Steinberg
Brookhaven National Lab.
Upton, New York 11973

GEOTHERMAL SYMPOSIUM ATTENDEES

A. D. Thomas
Radian Corporation
P. O. Box 9948
Austin, Texas 78766

A. R. Troiano
Case Western Reserve Univ.
Cleveland, Ohio 44106

Daniel Van Rooyen
Brookhaven National Lab.
Upton, New York 11973

Larry Vyvial
W-K-M Valve
P. O. Box 2117
Houston, Texas 77001

Richard W. Winzenried
Terra Tek, Inc.
Salt Lake City, Utah

L. L. Yeager
Daedalean Associates, Inc.
Woodbine, Maryland



☆U.S. GOVERNMENT PRINTING OFFICE: 1980-640-258/55